

ARIZONA DEPARTMENT OF TRANSPORTATION

REPORT NUMBER: FHWA-AZ87-254

RATIONAL CHARACTERIZATION OF PAVEMENT STRUCTURES USING DEFLECTION ANALYSIS

Volume I - Research Results & Findings

Final Report

Prepared by:

Michael S. Mamlouk

William N. Houston

Sandra L. Houston

John P. Zaniewski

Center for Advanced Research in Transportation, and
Department of Civil Engineering
College of Engineering & Applied Sciences
Arizona State University
Tempe, Arizona 85287

December 1988

Prepared for:

Arizona Department of Transportation

206 South 17th Avenue

Phoenix, Arizona 85007

in cooperation with

U.S. Department of Transportation

Federal Highway Administration

The contents of this report reflect the views of the authors who are responsible for the facts and the accuracy of the data presented herein. The contents do not necessarily reflect the official views or policies of the Arizona Department of Transportation or the Federal Highways Administration. This report does not constitute a standard, specification, or regulation. Trade or manufacturer's names which may appear herein are cited only because they are considered essential to the objectives of the report. The U.S. Government and the State of Arizona do not endorse products or manufacturers.

Technical Report Documentation Page

| | | | |
|---|------------------------------------|--|--|
| 1. Report No. FHWA-AZ88-254, I | 2. Government Accession No. | 3. Recipient's Catalog No. | |
| 4. Title and Subtitle RATIONAL CHARACTERIZATION OF PAVEMENT STRUCTURES USING DEFLECTION ANALYSIS | | 5. Report Date December, 1988 | 6. Performing Organization Code |
| | | 8. Performing Organization Report No. CART-88-101 | |
| 7. Author(s) Michael S. Mamlouk, William N. Houston, Sandra L. Houston, John P. Zaniewski | | 10. Work Unit No. | |
| 9. Performing Organization Name and Address Center for Advanced Research in Transportation Arizona State University Tempe, AZ 85287-6306 | | 11. Contact or Grant No. HPR-PL-1(31) Item 254 | |
| | | 13. Type of Report & Period Covered Vol I-Final Rept 8/86-12/88 | |
| 12. Sponsoring Agency Name and Address ARIZONA DEPARTMENT OF TRANSPORTATION 206 S. 17TH AVENUE PHOENIX, ARIZONA 85007 | | 14. Sponsoring Agency Code | |
| | | 15. Supplementary Notes <p style="text-align: center;">Prepared in cooperation with the U.S. Department of Transportation, Federal Highway Administration</p> | |
| 16. Abstract <p>In this study, a rational overlay design method for flexible pavements in Arizona has been developed which includes roughness, fatigue and plastic deformation models. The method is incorporated in a microcomputer program which is also capable of analyzing the economics of other rehabilitation alternatives.</p> <p>During the development of the method, twenty in-service pavement sites were selected from Arizona highways covering various geographical and environmental regions, soil types, pavement conditions and traffic volumes. Nondestructive tests (NDT) were performed on these sites using the Falling Weight Deflectometer at three stress levels as well as the Dynaflect. The pavement layers and subgrade moduli were backcalculated from NDT data using both static and dynamic analyses. The moduli of asphaltic layers were further adjusted for temperature. Statistical analysis was performed and the stress sensitivity was found to be small. Cone penetration tests were further performed to verify the subgrade moduli.</p> <p>Asphalt concrete cores, base and subbase samples and undisturbed subgrade samples were collected from the selected sites. Resilient modulus tests were performed in the lab on asphalt concrete cores at three temperatures and on subgrade materials. In addition, base and subbase gradation as well as soil classification and Atterberg limits were obtained. The study expanded the data base for material properties in Arizona.</p> <p>This volume is the first in a three volume set. Volume II provides field testing procedure and workstation development and Volume III is a computer user guide.</p> | | | |
| 17. Key Words Overlay Design, Flexible Pavement, Roughness, Fatigue, Plastic Deformation, Nondestructive Testing, Deflection, Resilient Modulus, Dynamic Analysis, Backcalculation, Stress Sensitivity, Economic Analysis | | 18. Distribution Statement Document is available to the U.S. public through the National Technical Information Service, Springfield, Virginia 22161 | |
| 19. Security Classification (of this report) Unclassified | | 20. Security Classification (of this page) Unclassified | 21. No. of Pages 234 |
| 22. Price | | 23. Registrant's Seal  | |

ACKNOWLEDGEMENTS

The authors would like to thank many people who contributed to the success of this project. Special thanks go to the ADOT personnel who provided valuable input and assistance during the course of the project. These people include:

Mr. Frank R. McCullaugh
Mr. Larry Scofield
Mr. Richard Power
Mr. Steven L. Tritsch
Dr. Subodh Kumar
Mr. George B. Way
Mr. James Delton
Mr. Gary L. Cooper
Mr. John F. Eisenberg
Mr. John E. Lawson

The authors appreciate the cooperation and important input from all of the ADOT personnel.

The principal investigator of this project is Dr. Michael S. Mamlouk and the co-principal investigators are Drs. William N. Houston, Sandra L. Houston and John P. Zaniewski. Two research assistants participated in this project especially in the laboratory testing, data collection and data analysis. These research assistants are Messrs. Rohan W. S. Perera and Tim Anderson. The field sample collection and cone penetration testing were performed by Foree and Vann, Inc. The nondestruction testing was performed by ADOT personnel and ERES Consultants, Inc. R-value tests were performed by ADOT.

VOLUME I

TABLE OF CONTENTS

| | Page |
|---|------|
| LIST OF TABLES | vi |
| LIST OF FIGURES. | ix |
| TECHNICAL SUMMARY | xii |
| CONVERSION FACTORS, U.S. CUSTOMARY TO METRIC (SI) UNITS OF MEASUREMENTS | xv |
| CHAPTER 1. INTRODUCTION | 1 |
| 1.1 Problem Statement | 1 |
| 1.2 Objectives and Scope of Work | 2 |
| CHAPTER 2. LITERATURE REVIEW | 5 |
| 2.1 Basic Overlay Design Approaches | 5 |
| 2.1.1 Engineering Judgement | 5 |
| 2.1.2 Standard Thickness | 5 |
| 2.1.3 Empirical | 5 |
| 2.1.4 Mechanistic or Mechanistic-Empirical. | 5 |
| 2.2 Factors Considered in Overlay Design | 8 |
| 2.3 Concepts of Dynamic Analysis | 9 |
| 2.3.1 Single Degree of Freedom (SDOF) System | 9 |
| 2.3.2 Multidegree of Freedom System. | 9 |
| 2.4 Material and System Properties | 13 |
| 2.4.1 Layer Moduli | 13 |
| 2.4.2 Material Damping | 15 |
| 2.4.3 Geometric Damping. | 15 |
| 2.4.4 Out-of-Phase Response. | 15 |
| 2.4.5 Nonlinearity and Stress Sensitivity. | 17 |
| CHAPTER 3. SITE SELECTION | 18 |
| CHAPTER 4. FIELD WORK | 31 |
| 4.1 Nondestructive Testing | 31 |
| 4.2 Sample Collection | 34 |
| 4.2.1 Description of Site Configuration | 34 |
| 4.2.2 Boring and Sample Equipment | 34 |
| 4.2.3 Sampling Procedures | 34 |
| 4.3 Cone Penetration Testing. | 35 |
| 4.3.1 Determination of Subsurface Profile | 35 |
| 4.3.2 Correlation between CPT Data and Modulus. | 35 |

| | |
|--|-----|
| CHAPTER 5. LABORATORY TESTING | 40 |
| 5.1 Asphalt Concrete | 40 |
| 5.1.1 Materials and Equipment | 40 |
| 5.1.2 Test Procedure. | 40 |
| 5.1.3 Test Results. | 42 |
| 5.2 Base and Subbase | 47 |
| 5.3 Subgrade Material | 47 |
| 5.3.1 Equipment | 47 |
| 5.3.2 Calibration | 52 |
| 5.3.3 Testing Procedure | 52 |
| 5.3.4 Resilient Modulus Test Results. | 56 |
| CHAPTER 6. THEORETICAL ANALYSIS | 60 |
| 6.1 Statistical Analysis of NDT data | 60 |
| 6.1.1 FWD Data | 60 |
| 6.1.2 Dynaflect Data | 60 |
| 6.2 Nonlinearity and Stress Sensitivity | 60 |
| 6.2.1 A Study of Nonlinearity Using NDT Data | 72 |
| 6.2.2 Comparison of Site Variability to Nonlinearity Effects | 75 |
| 6.2.3 Stress Sensitivity-Laboratory Tests | 75 |
| 6.3 Backcalculation of Layer Moduli | 76 |
| 6.3.1 Background | 76 |
| 6.3.2 Research-Phase Backcalculation Studies. | 76 |
| 6.3.3 Backcalculation Procedure for the CART Overlay Method | 77 |
| 6.4 Correlations among Variables | 84 |
| 6.4.1 Comparison between Static and Dynamic Results . . . | 84 |
| 6.4.2 Comparison between Laboratory and Backcalculated Moduli | 86 |
| 6.4.3 Comparison between Laboratory Moduli and R-Values . . | 106 |
| CHAPTER 7. DEVELOPMENT OF OVERLAY DESIGN METHODOLOGY | 108 |
| 7.1 Overview of Overlay Design | 108 |
| 7.2 Roughness Models | 111 |
| 7.2.1 Change in Roughness Due to Overlay | 112 |
| 7.2.2 Rate of Change in Roughness. | 118 |
| 7.2.3 Use of the Roughness Model | 122 |
| 7.3 Fatigue Model. | 122 |
| 7.3.1 Background | 122 |
| 7.3.2 Model Development | 125 |
| 7.4 Plastic Deformation Model | 131 |
| 7.4.1 Introduction | 131 |
| 7.4.2 Objective | 133 |
| 7.4.3 General Description of Design Procedure | 133 |

| | |
|---|-----|
| CHAPTER 8. CART OVERLAY DESIGN METHOD FOR ARIZONA. | 137 |
| 8.1 Overlay Design | 137 |
| 8.1.1 Roughness Criterion | 138 |
| 8.1.2 Fatigue Criterion | 138 |
| 8.1.3 Plastic Deformation Criterion | 140 |
| 8.1.4 Comparison with SODA Method. | 144 |
| 8.2 Remaining Life Analysis | 144 |
| 8.3 Life of a User Specified Overlay. | 146 |
| 8.4 Economic Analysis | 146 |
| CHAPTER 9. SUMMARY, CONCLUSIONS, AND RECOMMENDATIONS | 149 |
| 9.1 Summary and Conclusions | 149 |
| 9.1.1 Site Variability/Stress Sensitivity from NDT Data. | 149 |
| 9.1.2 Layer Thickness and Material Types | 149 |
| 9.1.3 Dynamic Analysis vs. Static Analysis | 149 |
| 9.1.4 Estimation of Layer Moduli | 150 |
| 9.1.5 Laboratory Testing | 150 |
| 9.1.6 Comparison between Backcalculated and Lab Moduli | 151 |
| 9.1.7 Comparison Between Lab Moduli and R-Values | 152 |
| 9.1.8 Modes of Pavement Failure. | 152 |
| 9.1.9 Economic Analysis. | 153 |
| 9.1.10 CART Overlay Design for Arizona (CODA) | 153 |
| 9.2 Recommendations | 154 |
| REFERENCES. | 156 |
| APPENDIX A. SUMMARY OF NDT DATA | A-1 |
| APPENDIX B. SAMPLING EQUIPMENT. | B-1 |
| APPENDIX C. LABORATORY RESILIENT MODULUS DATA OF ASPHALT CONCRETE CORES | C-1 |
| APPENDIX D. LABORATORY RESILIENT MODULUS DATA OF SUBGRADE MATERIALS . . | D-1 |
| APPENDIX E. DESCRIPTION OF STRESS STATE | E-1 |

LIST OF TABLES

| | | |
|------------|--|----|
| Table 3-1. | Location of test sites and climatic zones | 22 |
| Table 3-2. | Cracking of the selected sites as recorded in the ADOT pavement management system data base | 23 |
| Table 3-3. | Roughness of the selected sites as recorded in the ADOT pavement management system data base | 24 |
| Table 3-4. | Friction numbers of the selected sections as recorded in the ADOT pavement management system data base | 25 |
| Table 3-5. | Information of traffic, maintenance, and the most recent construction project as recorded in the ADOT pavement management system data base | 26 |
| Table 3-6. | Historical data for sites | 27 |
| Table 3-7. | Abbreviations used for material types | 29 |
| Table 5-1. | Summary of density and average resilient moduli of asphalt concrete samples at 41F | 44 |
| Table 5-2. | Summary of density and average moduli of asphalt concrete samples at 77F | 45 |
| Table 5-3. | Summary of density and average resilient moduli of asphalt concrete samples at 104F | 46 |
| Table 5-4. | Gradation of aggregate and select materials at various sites | 48 |
| Table 5-5. | Summary of average resilient moduli of soil samples | 57 |
| Table 5-6. | Atterberg Limits of subgrade materials | 58 |
| Table 5-7. | Subgrade properties as reported by ADOT | 59 |
| Table 6-1. | Descriptive statistics of FWD data | 61 |
| Table 6-2. | Coefficient of variation of FWD data within each site (%) | 66 |
| Table 6-3. | Coefficient of variation of FWD for station 1 (%) - 9000 lb drop | 67 |
| Table 6-4. | Descriptive statistics of Dynaflect data | 68 |
| Table 6-5. | Coefficient of variation of Dynaflect data within each site (%) | 71 |
| Table 6-6. | Summary of coefficients of determination, R^2 , for FWD data stress-deflection | 74 |

| | | |
|-------------|---|-----|
| Table 6-7. | Material types and layer thicknesses at different sites . . . | 78 |
| Table 6-8. | Backcalculated moduli and thickness of uncompacted subgrade using static analysis for FWD data (Asphalt moduli are adjusted to 77F) | 79 |
| Table 6-9. | Backcalculated moduli and thickness of uncompacted subgrade using dynamic analysis of FWD data (Asphalt moduli are adjusted to 77F) | 80 |
| Table 6-10. | Backcalculated moduli and thickness of uncompacted subgrade using static analysis of Dynaflect data (Asphalt moduli are adjusted to 77F) | 81 |
| Table 6-11. | Backcalculated moduli and thickness of uncompacted subgrade using dynamic analysis of Dynaflect data (Asphalt moduli are adjusted to 77F) | 82 |
| Table 6-12. | Comparison between laboratory and backcalculated asphalt concrete moduli (at 77F) using static analysis of FWD data. | 87 |
| Table 6-13. | Comparison between laboratory and backcalculated asphalt concrete moduli (at 77F) using dynamic analysis of FWD data. | 88 |
| Table 6-14. | Comparison between laboratory and backcalculated asphalt concrete moduli (at 77F) using static analysis of Dynaflect data | 89 |
| Table 6-15. | Comparison between laboratory and backcalculated asphalt concrete moduli (at 77F) using dynamic analysis of Dynaflect data | 90 |
| Table 6-16. | Comparison between laboratory and backcalculated soil moduli using static analysis of FWD data | 97 |
| Table 6-18. | Comparison between laboratory and backcalculated soil moduli using static analysis of Dynaflect data | 98 |
| Table 6-19. | Comparison between laboratory and backcalculated soil moduli using dynamic analysis of Dynaflect data | 100 |
| Table 7-1. | Frequency distribution of roughness after overlay | 117 |
| Table 7-2. | Distribution of the rate of change of roughness (projects overlaid between 1974 and 1981) | 121 |
| Table 7-3. | Cumulative ESAL and tensile strain at bottom of AC | 126 |
| Table 7-4. | Axle loads for different probabilities | 135 |
| Table 7-5. | Typical data used in model development | 136 |
| Table 8-1. | Comparison of SODA and CODA overlay designs for study sites | 145 |

Tables C-1 to C-3. Laboratory resilient moduli of asphalt concrete
samples at 41F, 77F and 104F C-1 - C-3

Table D-1. Laboratory resilient modulus data of subgrade materials . . D-1

LIST OF FIGURES

Figure 1-1. Deflection measurements of five NDT devices on a flexible pavement normalized to 1000-lb force level (1) 3

Figure 1-2. Comparison of different measurement methods on different road structures, with deflections normalized to 11, 250-lb load (2). 3

Figure 2-1. Typical multi-layered pavement system subjected to dynamic load11

Figure 2-2. Definition of resilient modulus14

Figure 2-3. Definition of dynamic modulus14

Figure 2-4. Deflection measured by the Dynaflect16

Figure 2-5. Typical load deflection diagram from repetitive plate load testing (54)16

Figure 3-1. Selected sites19

Figure 3-2. Map of climatological zones in Arizona.21

Figure 4-1. Dynaflect32

Figure 4-2. Location of loading wheels and geophones of the Dynaflect . . 32

Figure 4-3. Dynatest FWD33

Figure 4-4. FWD: Sensor Locations33

Figure 4-5. Typical plot of cone resistance vs. depth (Site 1, Station 1, shoulder)36

Figure 4-6. Typical plot of cone resistance vs. depth (Site 1, Station 4) .36

Figure 4-7. Example of moisture content variation with depth (Site 3, Station 1)37

Figure 4-8. Example of moisture content variation with depth (Site 7, Station 1)37

Figure 4-9. Example plot of E/E_{min} vs. depth39

Figure 5-1. Resilient modulus machine for asphalt concrete testing.41

Figure 5-2. Typical load and horizontal deformation obtained during the resilient modulus testing43

Figure 5-3. Triaxial resilient modulus apparatus for subgrade material testing50

| | |
|--|-----|
| Figure 6-1. FWD data at 9000 lb. drop for site 2 | .65 |
| Figure 6-2. Typical plot of Dynaflect data, site 1, station 1-10 | .70 |
| Figure 6-3. Equivalent 9000-lb deflections, site 9, station 10. | .73 |
| Figure 6-4. Comparison between laboratory and backcalculated asphalt concrete moduli (at 77F) using static analysis of FWD data. | .91 |
| Figure 6-5. Comparison between laboratory and backcalculated asphalt concrete moduli (at 77F) using dynamic analysis of FWD data | .92 |
| Figure 6-6. Comparison between laboratory and backcalculated asphalt concrete moduli (at 77F) using static analysis of Dynaflect data | .93 |
| Figure 6-7. Comparison between laboratory and backcalculated asphalt concrete moduli (at 77F) using dynamic analysis of Dynaflect data | .94 |
| Figure 6-8. Comparison between laboratory and backcalculated soil moduli using static analysis of FWD data | 101 |
| Figure 6-9. Comparison between laboratory and backcalculated soil moduli using dynamic analysis of FWD data | 102 |
| Figure 6-10. Comparison between laboratory and backcalculated soil moduli using static analysis of Dynaflect data | 103 |
| Figure 6-11. Comparison between laboratory and backcalculated soil moduli using dynamic analysis of Dynaflect dynamic data | 104 |
| Figure 6-12. Laboratory resilient moduli vs. R-value used for the correlation evaluation | 107 |
| Figure 7-1. Overview of the overlay design process | 109 |
| Figure 7-2. Flow chart of the overlay design procedure | 110 |
| Figure 7-3. Reduction in roughness due to overlay vs. roughness before overlay for interstate highways | 113 |
| Figure 7-4. Reduction in roughness due to overlay vs. roughness before overlay for U.S. routes | 113 |
| Figure 7-5. Reduction in roughness due to overlay vs. roughness before overlay for state routes. | 114 |
| Figure 7-6. Reduction in roughness due to overlay vs. overlay thickness for interstate highways | 115 |
| Figure 7-7. Reduction in roughness due to overlay vs. overlay thickness for U.S. routes | 115 |

Figure 7-8. Reduction in roughness due to overlay vs. overlay thickness for state routes 116

Figure 7-9. Typical rate of change of roughness vs. time for interstate highways 119

Figure 7-10. Typical rate of change of roughness vs. time for U.S. routes. 119

Figure 7-11. Typical rate of change of roughness vs. time for state routes 120

Figure 7-12. Some fatigue relations including results of laboratory testing, wheel-tracking tests, and efforts to represent field conditions (64) 124

Figure 7-13. Asphalt concrete tensile strain vs. strain repetitions for all 20 sites 130

Figure 7-14. Nonlinearity of subgrade materials 132

Figure 7-15. Definition of F_{NL} 132

Figure 8-1. Relationship between critical strain and overlay thickness with a reduction in the existing surface modulus for various conditions. 141

Figures A-1 to A-20. FWD data at 9000 lb drop for sites 1 to 20 . .A-2 to A-11

Figures A-21 to A-34. Dynaflect data for sites 1 to 13 and 15. . . A-13 to A-19

Figures A-35 to A-76. Equivalent 9000 lb FWD deflections for sites 1 to 13 and 15 A-21 to A-41

Figure E-1.E-3

Figure E-2.E-4

Figure E-3.E-5

Figure E-4.E-6

Figure E-6.E-7

TECHNICAL SUMMARY

A large percentage of highway budget in Arizona is being devoted to upgrading and maintaining existing roads. A mechanistically-based overlay design method was needed in order for the rehabilitation process to be performed in a more optimal manner. In this study, a rational overlay design method for flexible pavements in Arizona has been developed which considers roughness, fatigue and plastic deformation failure criteria. The method is also capable of analyzing the economics of overlay projects and other rehabilitation alternatives.

During the development of the method, twenty in-service pavement sites were selected from various locations in Arizona for detailed evaluation and data collection. Several factors were considered during the selection of these sites including the availability of historical records and the representation of various geographical and environmental regions, soil types, pavement conditions and traffic volumes. At each site a total of 10 stations were established at a spacing of 10 ft apart. These stations were located in the right-hand wheel track of the right lane. Station 1 was set at a distance of 1 ft ahead of the milepost marker corresponding to the site.

Nondestructive tests (NDT) were performed using the Dynaflect and the Falling Weight Deflectometer (FWD) at the ten stations at each site. The FWD was operated at 3 stress levels (6, 9 and 12 kips) at stations 1, 5 and 10 at each site, while one stress level at 9 kips was used at the other stations. All 20 sites were tested with the FWD, while sites 1 through 13 and 15 were tested using the Dynaflect.

In order to more accurately determine the subsurface profile, and to detect layering, cone penetration testing (CPT) was performed at three locations at each test site. In general, these locations correspond to station 1, the shoulder adjacent to station 1 and station 4. The CPT followed the ASTM D3441-86 procedure to depths of 25 ft or refusal.

Asphalt concrete cores, base and subbase samples and undisturbed subgrade samples were collected from the 20 test sites. Unless otherwise noted, the boring locations were at stations 1, 4 and 7 at each site. Resilient modulus tests were performed in the lab on asphalt concrete cores at three temperatures according to ASTM D4123-82 procedure. In addition, resilient modulus tests were performed in the lab on the undisturbed subgrade materials according to AASHTO T274-82 procedure with some minor modifications. Moreover, base and subbase gradation as well as subgrade soil classification and Atterberg limits were obtained. One cement treated base sample was also tested for resilient modulus.

The study concluded that the variability of NDT data across a 90 ft span can be attributed primarily to spacial variability in material properties. It was also found that within the stress range of the FWD tests (6 to 12 kips), the effect of material nonlinearity was less significant than the effect of spacial variability in material properties. However, at stress levels associated with the Dynaflect, there may be a more significant effect of material nonlinearity when compared with FWD stress levels.

The CPT results showed that there is a large number of distinct layers within the subgrade resulting in a wide variation in subgrade stiffnesses in the first 25 ft.

The layer moduli were manually backcalculated using both Dynaflect and FWD data. Both static and dynamic analyses were used for this purpose. The asphalt concrete modulus was further adjusted to a reference temperature of 77°F for the purpose of comparison with the lab moduli and to 70°F for the purpose of developing the overlay design method. The difference between the results of static and dynamic analyses was found to be moderately small. Although the dynamic analysis results (considering the inertial forces) are considered to be more accurate, the differences are too small to justify the greater complexities and time requirements of dynamic analyses for routine design computations. An automated computerized backcalculation procedure using static analysis has been developed for use in design.

The backcalculated moduli were compared with lab-measured moduli. On the average, the lab-measured asphalt concrete moduli were about three times as high as the backcalculated values, with significant deviations from the average. However, the backcalculated subgrade moduli were about 50 percent higher than the lab values, with significant deviations from the average. A number of factors which might contribute to these differences were presented and discussed. It was concluded that the major contributor to these differences is that the lab moduli represent only the small specimens on which the tests were performed, while the backcalculated moduli from NDT are weighted-average values representing relatively large volumes of material. For most overlay design procedures, the NDT values would be more useful.

For the purpose of developing an overlay design procedure, three failure criteria were used; roughness, fatigue and plastic deformation. The roughness model was developed using the ADOT data base. The Maysmeter roughness before overlay was correlated with the roughness after overlay. Also, the rate of change of roughness was found to be well correlated with time, but it was poorly correlated with overlay thickness, layer moduli, traffic loading and regional factor. Thus, knowing the roughness before overlay the time before reaching the roughness failure level can be computed.

The fatigue model was developed through consideration of fatigue curves from the literature and from data from Arizona highways. The fatigue model is based on the cumulative damage concept (Minor's law). It relates the number of load applications to the tensile strain at the bottom of AC layer. The fatigue curve selected for Arizona pavements indicates that they are somewhat more resistant to fatigue failure than other pavements. Using the fatigue model the overlay thickness required to protect the pavement from fatigue cracking during the design period can be computed.

The plastic deformation model was developed to insure that the overlay thickness is adequate for protection against excessive plastic deformation. The model is based on FWD testing at different stress levels.

The three pavement failure criteria (roughness, fatigue and plastic deformation) were incorporated in an integrated CART (Center for Advanced Research in Transportation) Overlay Design for Arizona (CODA). A

microcomputer program CODA was also developed to compute the required overlay thickness as well as performing economic analysis for various rehabilitation procedures. The CODA procedure is recommended for implementation by ADOT for future overlay designs.

CONVERSION FACTORS, U. S. CUSTOMARY TO METRIC (SI)
UNITS OF MEASUREMENT

U. S. customary units of measurement used in this report can be converted to metric (SI) units as follows:

| Multiply | By | To Obtain |
|--------------------------------|-----------|--------------------------------|
| inches | 2.54 | centimetres |
| feet | 0.3048 | metres |
| miles (U. S. statute) | 1.609344 | kilometres |
| pounds (mass) | 0.4535924 | kilograms |
| pounds (force) | 4.448222 | newtons |
| pounds (mass) per cubic foot | 16.0185 | kilograms per cubic metre |
| pounds (force) per square inch | 6894.757 | pascals |
| kip (force) | 4448.222 | newtons |
| kip (force) per square inch | 6.894757 | megapascals |
| Fahrenheit degrees | 5/9 | Celsius degrees or Kelvins* |

* To obtain Celsius (C) temperature readings from Fahrenheit (F) readings, use the following formula: $C = (5/9)(F - 32)$. To obtain Kelvin (K) readings, use: $K = (5/9)(F - 32) + 273.15$.

CHAPTER 1. INTRODUCTION

1.1. PROBLEM STATEMENT

For a variety of reasons, the number of new highway construction projects is steadily decreasing. As a consequence, a higher percentage of resources is being devoted to upgrading and maintaining existing highways. Thus, overlay design has moved into the forefront of highway engineering.

The primary goal in overlay design is to provide a section which can withstand the applied traffic loads throughout the design life without pavement failure such as excessive cracking, rutting or loss in serviceability. Fundamental engineering decisions include assessing which sections of highway require overlaying and how much overlay is needed.

The lack of basic research in the pavement area for the past few decades has hampered the development of new knowledge on pavement behavior. New mechanistically-based design methods should be developed to close the gap between theory and practice and to upgrade the performance of the existing highway system. As a part of this study, detailed consideration has been given to basing overlay design on a more rational analysis of nondestructive testing data as well as on typical pavement performance in Arizona.

The loads applied by traffic and by most deflection measurement devices on pavement structures are dynamic in nature. When truck wheels impact the pavement, it is subjected to a series of half sine waves. The duration of the wave pulse could be dependent on the speed of the moving wheel and the depth in the pavement system at which the response is analyzed.

Deflection measurement devices have been extensively used in the past few decades to evaluate the load-deformation response and the overlay design of highway and airfield pavement systems. One of the earliest devices developed for this purpose was the Benkelman Beam. Because of the static loading condition, generation of creep in the pavement, and the slow operating rate, the Benkelman Beam is outdated. Vibratory deflection measurement devices such as the Dynaflect, Road Rater and the 16-kip Vibrator developed by the U.S. Army Waterways Experiment Station, were developed for better characterization of pavement properties. The vibratory devices apply dynamic loads, and surface deflections are measured at several lateral distances, however, these devices do not accurately simulate loads applied by moving vehicles. More sophisticated deflection measurement devices were developed, such as the Falling Weight Deflectometer (FWD) and the FHWA Thumper, that better simulate moving wheel loads. Currently, highway and airfield agencies are moving towards using the FWD and reducing dependence on other devices.

The technology is available to utilize nondestructive measurement devices that accurately simulate actual traffic conditions. The missing link, however, is an acceptable method of analyzing the data. Analysis of data obtained from actual traffic loading and from dynamic loading devices has previously been based on either empirical approaches or static (elasto-static and viscoelasto-static) models. Empirical correlations are restricted to conditions similar to those from which they were originally developed, while static analyses neglect the inertia of the pavement. Most computer programs currently used in analyzing pavement response are based on static analyses.

In other words, it is assumed that the dynamic response of pavement structures is not different from the static response. In fact, the static and dynamic responses of pavements may be significantly different. Field data show that pavement response is dependent on mode of loading and/or load frequency, a condition which cannot be interpreted using any static analysis. For example, Figures 1-1 and 1-2 show that deflection devices with different modes of loading generate slightly different responses on the same pavement sections, even after the data are normalized to the same force level. These differences are no doubt due in part to differences in dynamic response and in part to stress level sensitivity.

In addition, the subgrade moduli obtained through analysis of deflection measurements have not been verified under different loading conditions, especially in Arizona. Since the deflections at the pavement surface are sensitive to various layer moduli, any improvement in the accuracy of the subgrade modulus would increase the confidence in the remaining moduli. Therefore, independent methods of modulus measurement such as lab testing and cone penetration testing, when compared to the calculated moduli from deflection measurements, may provide some new insight into the best method for evaluating the subgrade modulus. If a substantial improvement in measuring moduli can be made, then a corresponding improvement in overlay design procedures can be made.

1.2. OBJECTIVES AND SCOPE OF WORK

The overall objective of this study is to improve pavement overlay design procedures for the Arizona Department of Transportation.

The overall objective has been pursued by accomplishing a series of intermediate objectives as follows:

1. Improved material characterization by
 - a) Developing better techniques for analyzing NDT data. This was accomplished by developing an improved backcalculation procedure and evaluating the importance of the dynamic response of pavements under various loading conditions, as compared to static.
 - b) Adding to the existing material characterization data base by performing laboratory triaxial resilient modulus testing on subgrade materials from Arizona pavements
 - c) Adding to existing material characterization data base by performing laboratory resilient modulus testing on asphalt concrete cores from Arizona pavements.
 - d) Adding to existing material characterization data base by performing cone penetration testing on subgrade materials from Arizona pavements.
2. Evaluation of non-linear subgrade response on overlay design parameters.
3. Assessing variability in pavement section properties across a particular pavement "site." This was accomplished by evaluating

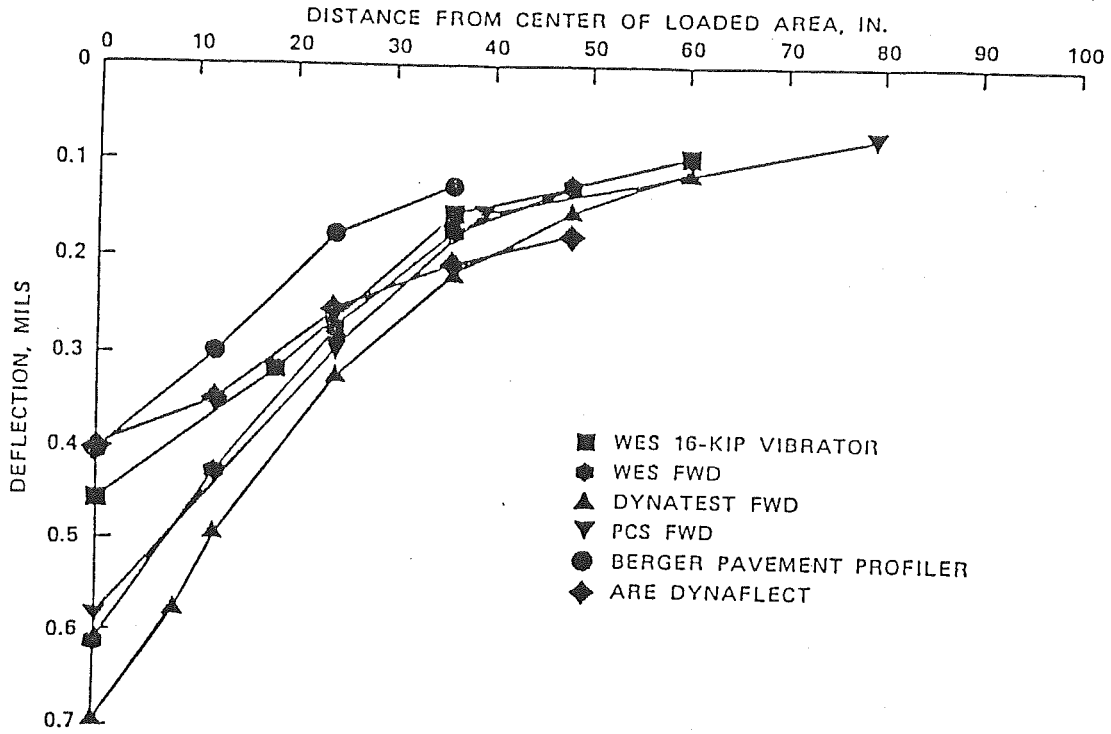


FIGURE 1-1. DEFLECTION MEASUREMENTS OF FIVE NDT DEVICES ON A FLEXIBLE PAVEMENT NORMALIZED TO 1000-LB FORCE LEVEL (1)

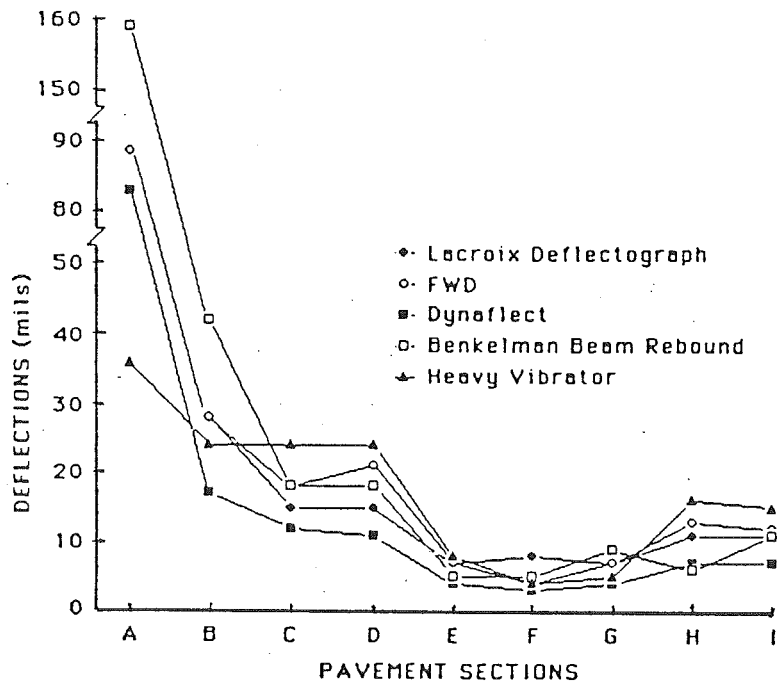


FIGURE 1-2. COMPARISON OF DIFFERENT MEASUREMENT METHODS ON DIFFERENT ROAD STRUCTURES, WITH DEFLECTIONS NORMALIZED TO 11,250-LB LOAD (2)

the means, standard deviations, and coefficients of variation for surface deflection measurements taken over a 90 ft stretch of highway.

4. Evaluating the performance of Arizona pavements using the available pavement management data base, and developing a rational overlay design method for Arizona. Three design models were developed; roughness, fatigue and plastic deformation.
5. Developing an economic analysis technique to compare the costs of several rehabilitation options such as overlay only, milling plus overlay, milling, recycling plus overlay, and reconstruction. The results of these accomplishments are presented in this final report.

CHAPTER 2. LITERATURE REVIEW

2.1. BASIC OVERLAY DESIGN APPROACHES

The most commonly used overlay design procedures are: a) engineering judgment b) standard thicknesses c) empirical and d) mechanistic or mechanistic-empirical. A brief description of these procedures is discussed in the following paragraphs (3).

2.1.1. Engineering Judgment - This approach is based on previous experience; in many ways, it is still a part of most current overlay design procedures. The advantage of this procedure is the direct tie between the design and the experience of the engineer, which usually guarantees the design will not be grossly inconsistent with experience. The disadvantage is that the experience available may not cover the design requirement at hand. Furthermore, methods based almost entirely on engineering judgment may not be sufficiently sophisticated and detailed to account for variations in the numerous factors which influence overlaid pavement performance.

2.1.2. Standard Thicknesses - Some agencies use this procedure, either formally through policies, or informally. For a given existing pavement type, traffic level, pavement thickness and other factors, a standard overlay thickness is prescribed.

2.1.3. Empirical - The degree of empiricism varies from one design method to another. Basically, relationships are developed between performance of overlay thicknesses and known data such as age, traffic, construction, structural section, and environmental factors. Regression techniques are normally used to develop such relationships. Deflection measurements are commonly used to characterize the structural adequacy of the pavement sections before overlay. The basic concept of these deflection-based analyses is that similar pavements with higher deflections will fail more quickly than those with lower deflections under the same loading. This approach has gained wide acceptance and is currently used by many states.

2.1.4. Mechanistic or Mechanistic-Empirical - Mechanistic design procedures differ from others in that they are used to characterize the response of the pavement to a load in terms of basic parameters such as strains or stresses. On the other hand, failure is normally defined in terms of specific mechanisms such as fatigue cracking and/or rutting. For the system to be fully mechanistic, fracture mechanics should be used to determine the relation between strain or stress and cracking, and basic mechanical and theoretical concepts should be used to determine the relation between stresses and permanent deformation. Also, the response of the pavement to dynamic loading should be correctly analyzed, using an appropriate method of analysis.

Currently, no completely mechanistically-based overlay design method exists. All mechanistically-based methods depend in part on empirical relations between pavement parameters and the number of load applications the pavement can support before failure. For example, the strain at the bottom of the existing asphalt layer is normally correlated to fatigue damage to develop a fatigue failure criterion. In some instances, the stress or strain at the

top of the subgrade has also been correlated to rutting resulting in a permanent deformation failure criterion.

All existing mechanistically-based methods of overlay design use static analyses to determine the dynamic response of the pavement structure. Recent studies (4-16) indicate the dynamic response of pavements may be different from the static response. Therefore, if the available static multilayer elastic computer programs (such as Chevron, ELSYM5, BISAR, VESYS, BISTRO, ILLI-PAV, etc.) are used to predict the response of pavements, the results may be misleading due to the inability of these programs to model the dynamic characteristics of pavement loading. On the other hand, if the dynamic analysis does not significantly affect the required overlay thickness, a simpler static analysis would be preferred. Thus, both advantages and disadvantages of the dynamic analysis need to be evaluated and a decision has to be made as to which type of analysis to consider in the overlay design process.

In addition, when a condition survey or other considerations indicate a need for an overlay, a set of deflection measurements would be taken at enough locations to statistically characterize the section to be overlaid. The deflections imposed would be less than or equal to the maximum deflection previously imposed thousands of times by traffic. Thus, the strains imposed during the surface deflection measurements would be expected to be essentially elastic, due to the conditioning of the pavement layers and subgrade by the traffic.

Although the strains imposed by loading, for measurement purposes, would be expected to be elastic, they may be non-linear. Indications from the literature review are that there may be some nonlinearity in the response of pavement materials (17-21). The effect of material nonlinearity is not taken into account in most of the available multi-layer elastic computer programs. If the non-linearity is significant, then moduli back-calculated from light vibrators, such as the Dynaflect, could be significantly different from those obtained from a heavy load device, such as the Falling Weight Deflectometer.

The major advantage of the mechanistically-based approach, even when empirical relations between calculated strain or stress and number of applications to failure are used, is that the overlay requirements can be determined for any pavement for which the strain and stress can be calculated. Users are not limited to pavements with which they have extensive experience; instead, they can analyze the expected performance of new designs and the influence of new materials. Another significant advantage of this approach is that past and projected damage can be calculated more accurately. In some environments, there are significantly different subgrade support conditions throughout the year, affecting the stress or strain in the pavement. A mechanistic procedure will allow damage in various seasons of the year to be calculated and used in the analysis.

The Arizona Department of Transportation (ADOT) is actively engaged in the design and construction of pavement overlays. ADOT reports (22,23) describe a recently developed overlay design procedure called Structural Overlay Design for Arizona (SODA). The first version of the method is essentially deflection-based utilizing the Dynaflect (a light vibrator) measurements. The procedure was developed from both theoretical analyses and

considerable field data. It is based heavily on data from actual Arizona pavement materials and it employs most of the parameters that regression analyses indicate are important to performance such as traffic load regional factor, roughness, spreadability index, and the number 5 Dynaflect sensor reading. Other parameters such as layer thicknesses and moduli were not included in the SODA equation since regression analyses proved that they are insignificant.

The SODA method uses as input values:

- 1) Total traffic loads expected over the design period (18 kip equivalentents).
 - 2) Road roughness (Mays-meter value)
 - 3) Regional Factor
 - 4) Spreadability Index = ((sum of the 5 sensor readings)/(5x#1 sensor)) x 100 based on Dynaflect tests.
 - 5) Dynaflect #5 sensor readings
- The equation for thickness is:

$$T = \frac{\text{Log } L + 0.104 \times R + 0.000578 \times P_o - 0.0653 \times \text{SIB}}{0.0587 \times (2.6 + 32.0 \times D_5)^{0.333}}$$

Where:

L = 18k loads in 1000's
R = Regional Factor
Po = Roughness, inches/mile
SIB = Spreadability index before Overlay
D5 = #5 Dynaflect sensor reading.

The overlay thickness should be determined at each test location and the mean value of thickness for all test locations in a design section is then used as the overlay thickness. No statistical manipulations are needed as they were incorporated into the development of the method. Any individual test location results less than zero are assigned a value of zero, and any results over 6 inches are assigned a value of 6 inches.

The developers of the method state that the method still needs some improvements. One potential shortcoming is that it is based on small deflections from a light vibrator. Thus, if FWD data are incorporated in the design procedure, the method can be improved. Also, if dynamic analyses and material non-linearities have a significant impact on overlay design, some modification to SODA may be warranted. Furthermore, incorporating more of the material properties parameters such as the layer moduli or providing better estimation of critical stresses or strains in the pavement structure might improve the method.

The SODA method was later modified by ADOT to use FWD measurements. The modification was essentially performed using regression analyses between Dynaflect and FWD data. It should be noted that the use of regression analysis in the original development of the method is associated with a certain degree of error. Further use of regression analysis to transfer from

Dynalect data to FWD data increases the error associated with the use of the method.

The research performed herein is aimed at developing a rational overlay design procedure considering roughness, fatigue and plastic deformation criteria. The significance of dynamic analysis and the effect of nonlinearity are evaluated. Finally, a comparison between the results of the new overlay method and the SODA method is to be evaluated.

2.2. FACTORS CONSIDERED IN OVERLAY DESIGN

The literature includes a number of overlay design methods based on deflection measurements (24). Most of these methods have common features and take into consideration the following factors:

1. The season in which testing is performed.
2. The location on the pavement where tests are made.
3. The frequency of testing along the pavement.
4. The need for taking cores and performing laboratory tests.
5. The NDT device(s) that are or may be used.
6. The measurements that are made with the NDT devices, such as single deflection under the load, peak-to-peak deflections, or deflection basin.
7. The other measurements made in addition to NDT, such as air temperature, pavement temperature, etc.
8. The corrections made either to the NDT measurements or to the calculated pavement properties to consider the temperature and seasonal differences between measurement conditions and design conditions.
9. The properties of the pavement or layers calculated or inferred from the NDT measurements. These properties can be either qualitative ratings, representative basin properties, representative structural properties, or layer moduli.
10. The methods used to distinguish between sections of pavement that require different thicknesses of overlay.
11. Empirical relations used to convert the NDT measurements to design parameters. These conversions may be:
 - a. Correlations between the deflections measured with NDT device and those produced by a design load,
 - b. Correlations between layer materials properties corresponding to the load level applied by the NDT device and the same material properties at design load level, or
 - c. Correlations between an NDT deflection and a design strain at a critical point in the pavement structure.
12. Empirical design relationships that convert the measurement at design load into the number of load applications that the pavement can support.

Specific details about individual overlay design methods are presented in Refs. (25-43).

2.3. CONCEPTS OF DYNAMIC ANALYSIS

The load applied by traffic and most NDT devices is dynamic in nature. When a dynamic load is applied to pavements, the inertia of the vehicle and/or the pavement system may play an important role in the resulting deflections.

When a dynamic load is applied at the surface of a homogeneous media, the energy is transmitted to the ground by a combination of primary (compression), secondary (shear), and surface (Rayleigh) waves. In a layered half-space system such as a pavement structure, multiple wave reflection and refraction occur. The problem is more difficult to analyze than a homogeneous half-space system. Although not seen by eye, the surface waves developed when an impulse load is applied on the pavement are similar to the waves developed on a smooth surface of water when a rock is dropped into it. These waves propagate away from the source of excitation and eventually die due to the damping of the pavement system.

Up to the present, analyses of data (obtained from dynamic loading) which are based on mechanistic approaches use static models. Several multilayer elastic computer programs (such as Chevron, ELSYM5, BISAR, VESYS, BISTRO, ILLI-PAVE, etc.), which are based on static analyses are currently used in analyzing the dynamic response of pavement. Pavement response to dynamic loading may be dependent on the mode of loading and/or frequency. The dynamics of the pavement system can be represented using either single or multiple degree of freedom modeling systems.

2.3.1. Single Degree of Freedom (SDOF) System - In this approach the pavement system is represented by a combination of masses, springs and dashpots (44). Although SDOF models take into account inertial effects, one of their major shortcomings is the assumption that loads, deflections, stresses and strains are applied in one direction; i.e., the vertical direction. In fact, when a vertical load is applied, stresses and strains are developed in all directions throughout the pavement structure. Thus, the SDOF model cannot represent the three dimensional nature of the pavement response. Deflections at points away from the load (at various geophone locations) cannot be predicted.

2.3.2. Multidegree of Freedom System - In this method both the inertial effect and the three-dimensional nature of the pavement structure are considered. Although the effect of inertia has been recognized for a long time, no three-dimensional dynamic solution was available for multilayer elastic systems until 1982, due to the complicated nature of the problem.

The load applied by the moving wheels of trucks and airplanes on pavements can be represented by a series of half sine waves. The magnitude and duration of such waves depend mainly on the magnitude of the applied load, the speed of the vehicle and the depth in the pavement system at which the effect is considered. To simplify the analysis, the wave (transient) mode of loading can be represented by a series of harmonic loadings having different frequencies and magnitudes. The transformation from transient to harmonic loadings can be easily performed using Fourier transformation. Therefore, once the pavement response to harmonic loading, as a function of frequency and magnitude, is evaluated, the response to any wave (transient) mode of loading can be obtained.

The governing equation for steady-state (harmonic) elastodynamics is the Helmholtz equation (45), written in a tensor form as:

$$\mu u_{i,jj} + (\lambda + \mu) u_{j,ij} + \rho \omega^2 u_i = 0 \quad (2-1)$$

in which λ, μ = Lamé's constants; ρ = mass density; ω = circular frequency of excitation; and u_i = i -th cartesian component of the displacement vector. In Equation 2-1, cartesian indicial notation is used in which the subscripts range from 1-3, addition is implied over repeated subscripts, and a comma denotes differentiation with respect to the space variable, i.e., $u_{i,j} = \partial u_i / \partial x_j$. Thus, this tensor form differential equation is a short representation of a number of regular differential equations. The displacement is also assumed to be time harmonic.

The dynamic analysis currently used employ the assumption that the pavement system consists of several layers which are unbounded laterally, but are underlain by a rigid bedrock layer at a finite depth. Full interface bonding (no slip) condition is assumed at the layer interfaces. Materials are assumed to be homogeneous and isotropic, and exhibit either linear elastic or viscoelastic response. A uniformly distributed harmonic circular load is considered to be applied to the pavement surface. A typical multilayered pavement system subjected to dynamic loading is illustrated in Figure 2-1, where each layer is characterized by thickness H , modulus E , Poisson's ratio ν , density ρ , and damping β .

Displacement Computation - The solution of Equation 2-1 for a point load on a half-space is available. However, no closed form solution is available for excitation of layered systems. Therefore, solutions must be obtained by numerical means. Kausel and Peek (46) have recently proposed a numerical technique which renders the elasto-dynamic problem of multilayered systems tractable. The solution is based on the assumption that the displacement field is linear in the direction of layering between adjacent interfaces. Thus, sufficiently thin layers must be specified to ensure the validity of this representation. In practice, artificial sublayers may be introduced in order to satisfy this requirement.

Finally, the response of the pavement system to the wave (transient) mode of loading can be obtained by adding the responses due to a number of harmonic loadings using Fourier transformation as indicated earlier. Using this procedure, the in-phase and out-of-phase deflections in the vertical, radial and tangential directions at any point in the pavement system can be computed.

Stress and Strain Computation - Once the deformations in the vertical, radial and tangential directions are determined, the normal strains can be calculated using the theory of elasticity as follows.

$$\epsilon_z = \frac{\partial w}{\partial z}$$

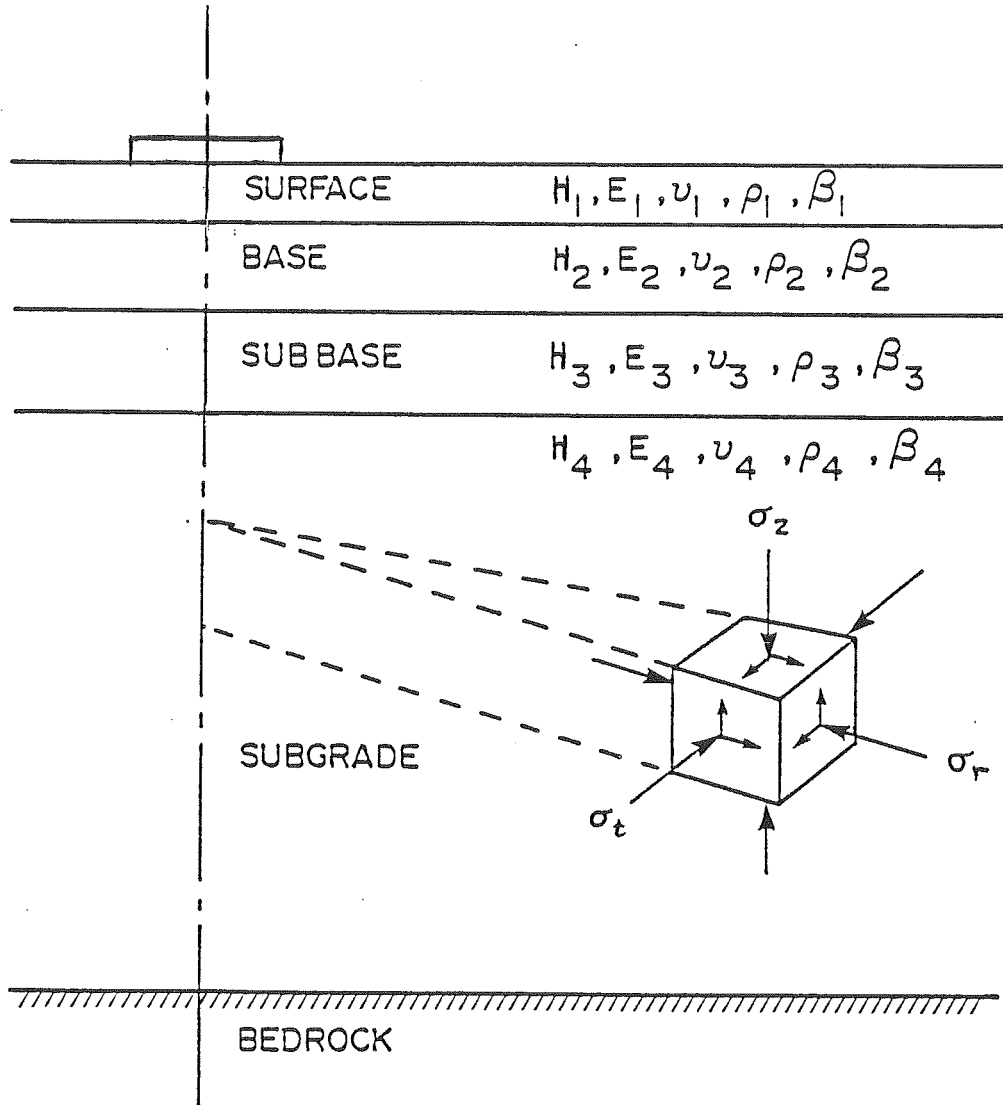


FIGURE 2-1. TYPICAL MULTILAYERED PAVEMENT SYSTEM SUBJECTED TO DYNAMIC LOAD

$$\epsilon_r = \frac{\partial u}{\partial r}$$

$$\epsilon_t = \frac{u}{r} + \frac{\partial v}{\partial \theta} \quad (2-2)$$

where ϵ_z , ϵ_r , and ϵ_t are the vertical, radial, and tangential strains, respectively; w , u , and v are the vertical, radial, and tangential displacements, respectively; and z , r , and θ are the vertical, radial, and angular coordinates, respectively.

The displacements can not be obtained using a closed form solution. The differentiation can be carried out using a numerical approach, such as the finite difference solution. In addition to the normal strains, the shear strains can also be computed using similar procedures. The normal and shear stresses can then be computed from the theory of elasticity using the generalized Hooke's law. Further details about the theory of dynamic analysis are presented in Reference 11.

It should be noted that the subject of dynamic analysis can be divided into two areas. The first area, which can be referred to as vehicle dynamics, deals with analyzing the dynamic loading of vehicles due to pavement roughness and the truck suspension system (14-16). The second area, which can be referred to as pavement dynamics, deals with analyzing the dynamic response of pavements due to vehicle dynamic loading (4-13). The two areas are complimentary. The ultimate goal is to study the interaction between vehicle dynamic loading and the pavement dynamic response. Up to the present time, this interaction effect has not been reported in the literature.

Results from experimental research performed on in-service pavements (1,2,47-49) indicate some differences in pavement response under various modes of loading (static, harmonic and transient) and under various frequencies of harmonic loading.

The dynamic solution of multi-layered elastic systems was incorporated in a computer program by Kausel (46). This version of the dynamic program is capable of computing the in-phase and out-of-phase vertical, radial, and tangential displacements at any point in the multi-layer system (due to harmonic loading). The program was further modified by Sebaaly (11) to compute stresses and strains, in addition to displacements, caused by harmonic and impulsive loadings. The currently available programs are:

1. DYNAMIC1, which computes the response of multi-layered systems to harmonic loading
2. DYNAMIC2, which computes the response of multi-layered systems to impulsive loading
3. DYNAMIC3, which back-calculates the layer moduli of multi-layer systems if the deflections due to harmonic loading are known.

The DYNAMIC1 and DYNAMIC2 programs are capable of handling pavements with any number of layers within the capability of the computer memory. The static response can also be obtained by assuming a loading frequency of zero in DYNAMIC1 or a very long load duration in DYNAMIC2. The static response was

checked against Chevron program for similar conditions and loading, and identical results were obtained.

The DYNAMIC3 program was developed in this study in order to backcalculate the layer moduli, given deflections due to harmonic loading. During the development of this program, the concepts of DYNAMIC1 and CHEVDEF (50) programs were used. The program is capable of handling up to 4 layers, including the subgrade.

The current version of DYNAMIC1, DYNAMIC2 and DYNAMIC3 programs are used with the VAX-VMS mainframe computers. Their operation requires several minutes of running time, depending on the number of layers and the number of output parameters required. No microcomputer version of these programs is currently available. The DYNAMIC1, DYNAMIC2 AND DYNAMIC3 programs, together with flow charts and user's guides, were previously submitted to ADOT.

2.4. MATERIAL AND SYSTEM PROPERTIES

Material properties used in the mechanistic analysis of a multilayer pavement system are elastic moduli (Young's moduli, shear moduli, etc.), Poisson's ratios, mass densities, and material damping ratio. A brief discussion of some of the material and pavement system properties as they relate to dynamic analysis are presented below.

2.4.1. Layer Moduli - The stress-strain relations of isotropic elastic materials are, in classical formulations, expressed in terms of fundamental material parameters, e.g., Young's modulus, and Poisson's ratio. For flexible pavement materials, however, it has become common to define state dependent parameters such as the resilient modulus and the dynamic modulus. These parameters are often used to interpret the nonlinear and time-dependent response of pavement materials. The resilient modulus is obtained by subjecting a specimen to repeated stresses and measuring the recoverable strain after a number of load applications, as shown in Figure 2-2. The resilient modulus, therefore, is the Young's modulus of the material after many load repetitions, i.e., the "shake-down modulus" of the material, which is normally different from the initial value. On the other hand, the dynamic modulus is obtained by subjecting a finite specimen to harmonic loading and determining the ratio of the stress amplitude to the corresponding strain amplitude, as illustrated by Figure 2-3.

Clearly, the resilient modulus is relevant to the analyses of pavement deflections since field deflection data reflect the current stiffness of pavements. The dynamic modulus, however, can be used only if the phase lag between load and deformation is also considered (complex modulus). Laboratory measured values of complex moduli obtained from the dynamic modulus test can yield valuable information on the fundamental material parameters such as stiffness and internal damping, provided that these tests are properly interpreted. Such data, combined with a rigorous elastodynamic analysis of the pavement structure, offer the greatest promise for progress in evaluating the response of pavements to moving loads.

The "inverse" problem of determining moduli from the response of the pavement structure to surface loading (from NDT devices) has not been fully resolved. No direct theoretical solution is available in the literature to

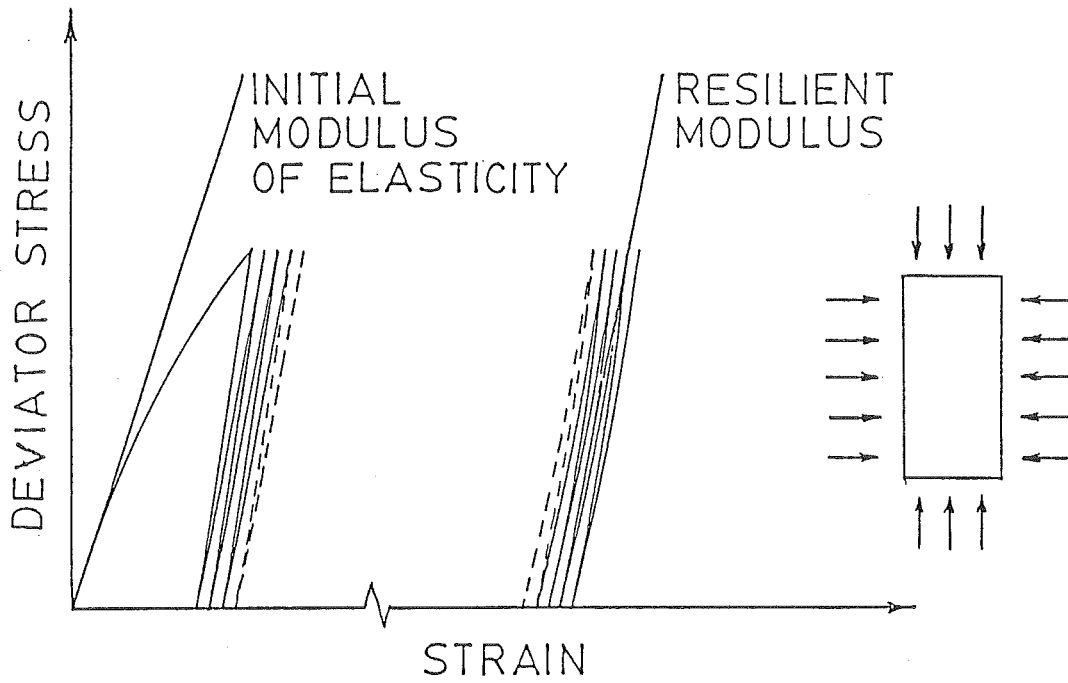


FIGURE 2-2. DEFINITION OF RESILIENT MODULUS

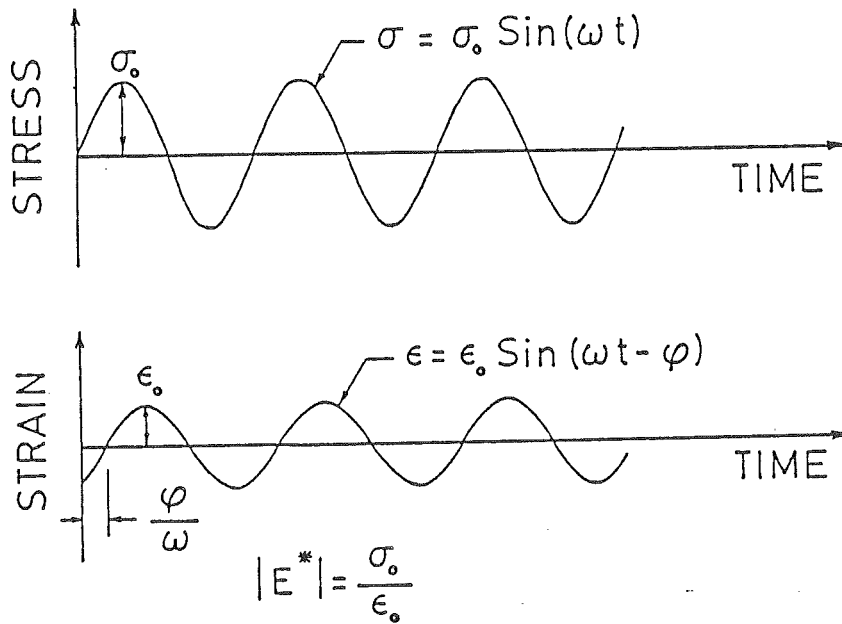


FIGURE 2-3. DEFINITION OF DYNAMIC MODULUS

determine the moduli of a multi-layered system where the surface deflections and layer thicknesses are known. Therefore, it is necessary to employ iterative schemes, that make use of the fact that surface deflections remote from the loaded area are governed primarily by the stiffness of the deeper layers. The predicted moduli are very sensitive to minor changes in surface deflections. Thus, proper procedure has to be followed in order to increase the accuracy of the predicted moduli.

2.4.2. Material Damping - Material damping refers to the internal energy dissipation which occurs in real materials subjected to dynamic loading. Granular pavement materials (gravels, etc.) exhibit hysteretic damping behavior, manifested by a frequency invariant damping ratio with typical values ranging from 2 to 10% (51,52). Using the principle of viscoelasticity, material damping can easily be incorporated into the analysis by replacing Young's modulus by its complex counterpart, i.e.:

$$E^* = E(1 + 2i\beta) \quad (2-3)$$

where

E^* = complex modulus
 E = Young's modulus

i = $\sqrt{-1}$
 β = damping ratio

2.4.3. Geometric Damping - When a dynamic load is applied at the surface of a homogenous half-space, the energy imparted to the ground is transmitted away by a combination of waves. These waves encounter an increasingly larger volume of material as they travel outward; thus, the energy density in each wave decreases with distance from the source. This decrease in energy density or decrease in displacement amplitude is called geometric (radiation) damping (51). In a layered half-space system, such as a pavement system, multiple wave reflection and refraction may occur.

The major component, by far, of energy dissipation in pavements results from geometric damping - the dispersion of energy from the source of excitation to the far field - rather than material damping.

2.4.4. Out-of-Phase Response - If a static load is applied to the pavement system, the pavement response will be in-phase with the load. However, if a dynamic load is applied, the instantaneous pavement response will generally be out-of-phase with the load, due to both geometric and material dampings. In fact, the pavement surface takes a wave form propagating away from the load. Using the Dynaflect sensors, only peak-to-peak surface deflections are recorded and no information is obtained regarding the instantaneous pavement response or the out-of-phase condition as illustrated in Figure 2-4. The dynamic response of the pavement can be represented by a complex number in which the real part represents the in-phase response, while the imaginary part represents the 90° out-of-phase response.

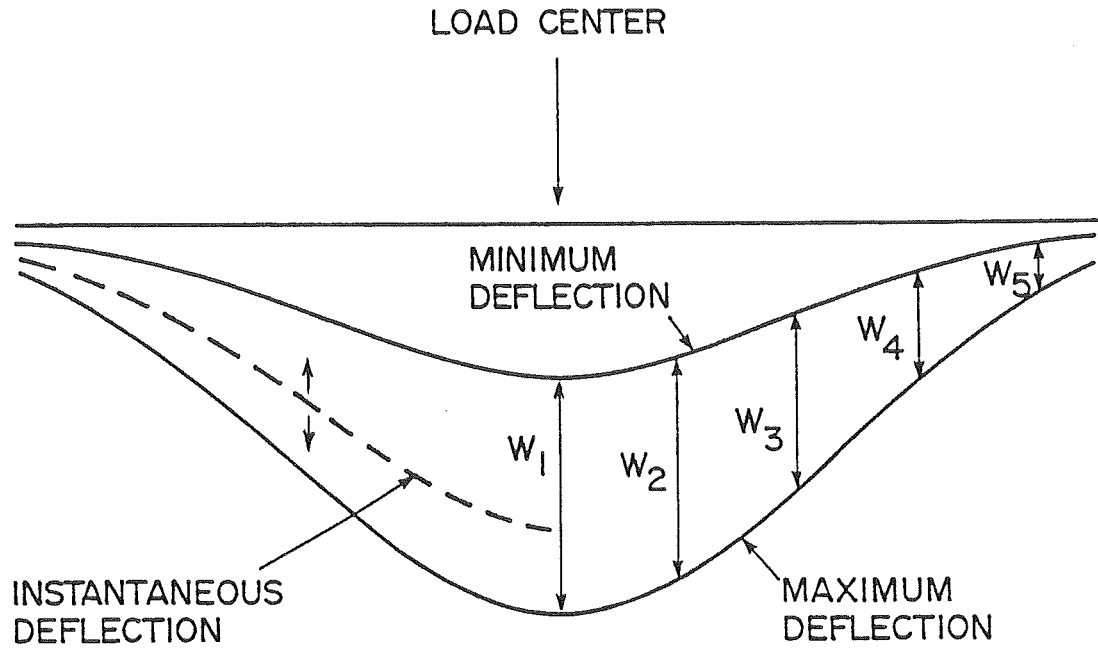


FIGURE 2-4. DEFLECTIONS MEASURED BY THE DYNAFLECT

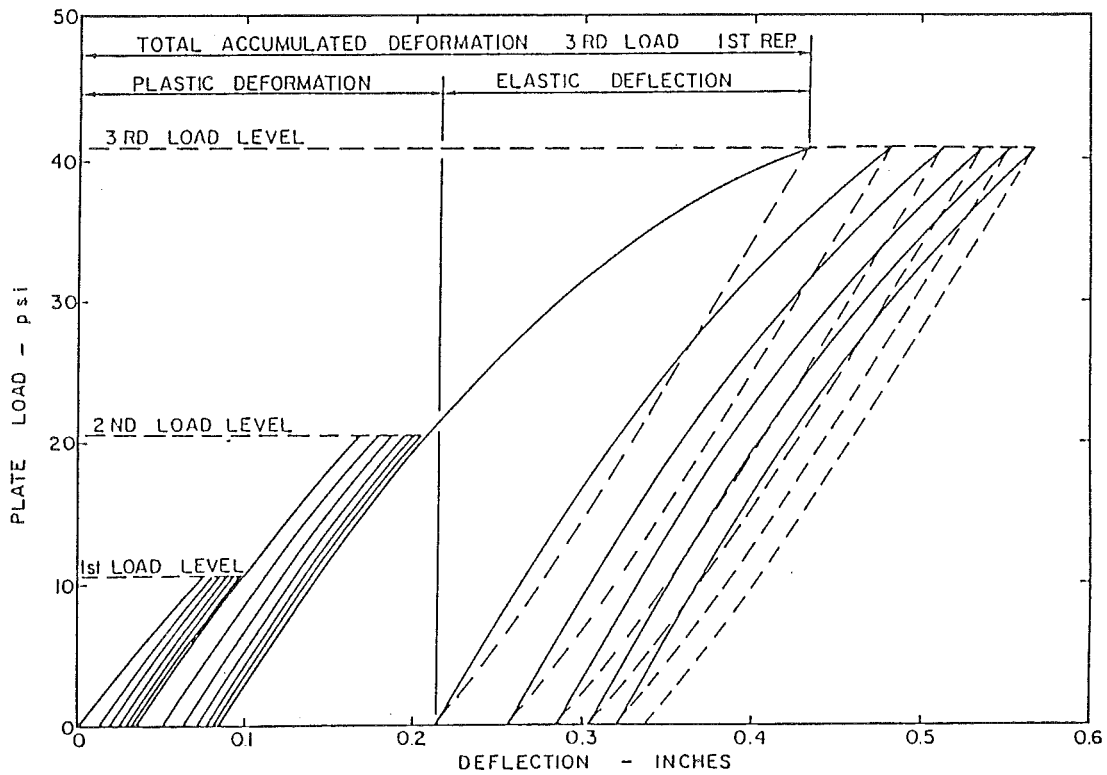


FIGURE 2-5. TYPICAL LOAD DEFLECTION DIAGRAM FROM REPETITIVE PLATE LOAD TESTING (54)

Resonance occurs when the response of the pavement system is 90° out-of-phase with the applied load and, consequently, the applied load is exactly balanced by the damping force (53). The resonant response of the pavement system occurs when the frequency of the applied load equals a natural vibration frequency of the pavement system.

2.4.5. Nonlinearity and Stress Sensitivity - It has long been known that subgrade materials have a nonlinear response to load. However, if the load is repeated several times the effect of nonlinearity is reduced. For example, Figure 2-2 shows a typical stress strain relationship for a soil specimen subjected to a triaxial state of stress where the axial stress is varied in a pulsating form while the confining pressure is kept constant. The nonlinearity is vpry large when the load is applied for the first time. After many applications the response is still somewhat nonlinear, but much less so.

The modulus is affected by the state of stress of the material. For example, the material properties predicted by the light load of the Dynaflect may not be the same as those predicted by a heavy axle load, even if the difference in the mode of loading is considered. As discussed above, the effect of stress sensitivity is reduced when the load is applied several times. Figure 2-5 shows a typical stress-deflection diagram from repetitive plate load testing on a subgrade material according to ASTM test procedure D1195 (54). This figure shows that the peak stress divided by the corresponding recoverable deflection is almost constant regardless of the applied stress level. However, some variation in the tangent moduli still persists after several load applications.

CHAPTER 3. SITE SELECTION

The overall objective of the project is to improve pavement overlay design procedures for ADOT. Pursuant to this objective is the need to improve the materials characterization process and improve performance models. To support this objective 15 pavement sites were originally selected for detailed evaluation during the project, and later they were increased to 20.

The goal of improving pavement performance models required the researchers to concentrate the search for test sites on pavements with good historical records. The Department had performed an evaluation of "Environmental Factor Determination From In-place Temperature and Moisture Measurements Under Arizona Pavements," (55) in 1980. During this study, 37 sites were monitored for five years for temperature, moisture, and deflection. In addition, detailed material sampling and testing were performed. These sites contain the best set of historical data on pavement condition and material properties and therefore, they served as a starting point in the search for test sites for this project.

Given this set of sites, the researchers identified a set of criteria for selection of the 20 sites to be studied as a part of this research:

1. availability of traffic and nondestructive test (NDT) data.
2. availability of material properties such as R-value.
3. overlay history of the site.
4. current pavement condition.
5. geographical distribution.
6. materials in the pavement structure.

All of the 37 sites studied by ADOT met the first two criteria. However, the traffic data for the sites were limited to the data routinely collected by the Department. The available traffic data includes the current annual volume of 18k equivalent single axle loads (ADL or ESAL) and a growth factor. The growth factor is the percent change between the current ADL and the preceding count. When the rate of traffic growth is nonlinear over time, the data maintained by the Department does not provide an accurate count of the total truck traffic.

Since one objective of the evaluation of the pavement sites was to permit the evaluation or development of performance models for overlaid pavements, criteria number 3 was very important. The most desirable pavement site would be one that had been overlaid one time and the overlay was near the end of its service life. Sites which meet this criteria would provide direct data on the service life of overlaid pavements in Arizona. Unfortunately, only two of the 37 pavements in the data base met this criteria.

Since an insufficient number of sites met the above criteria, the criteria for the present condition of the pavements were established. Distressed pavement sites were sought from pavement sections other than those studied in Reference 55. Unless the pavements were showing distress, the life of the pavements could not be established. The locations of the 20 selected sites are shown in Figure 3-1.

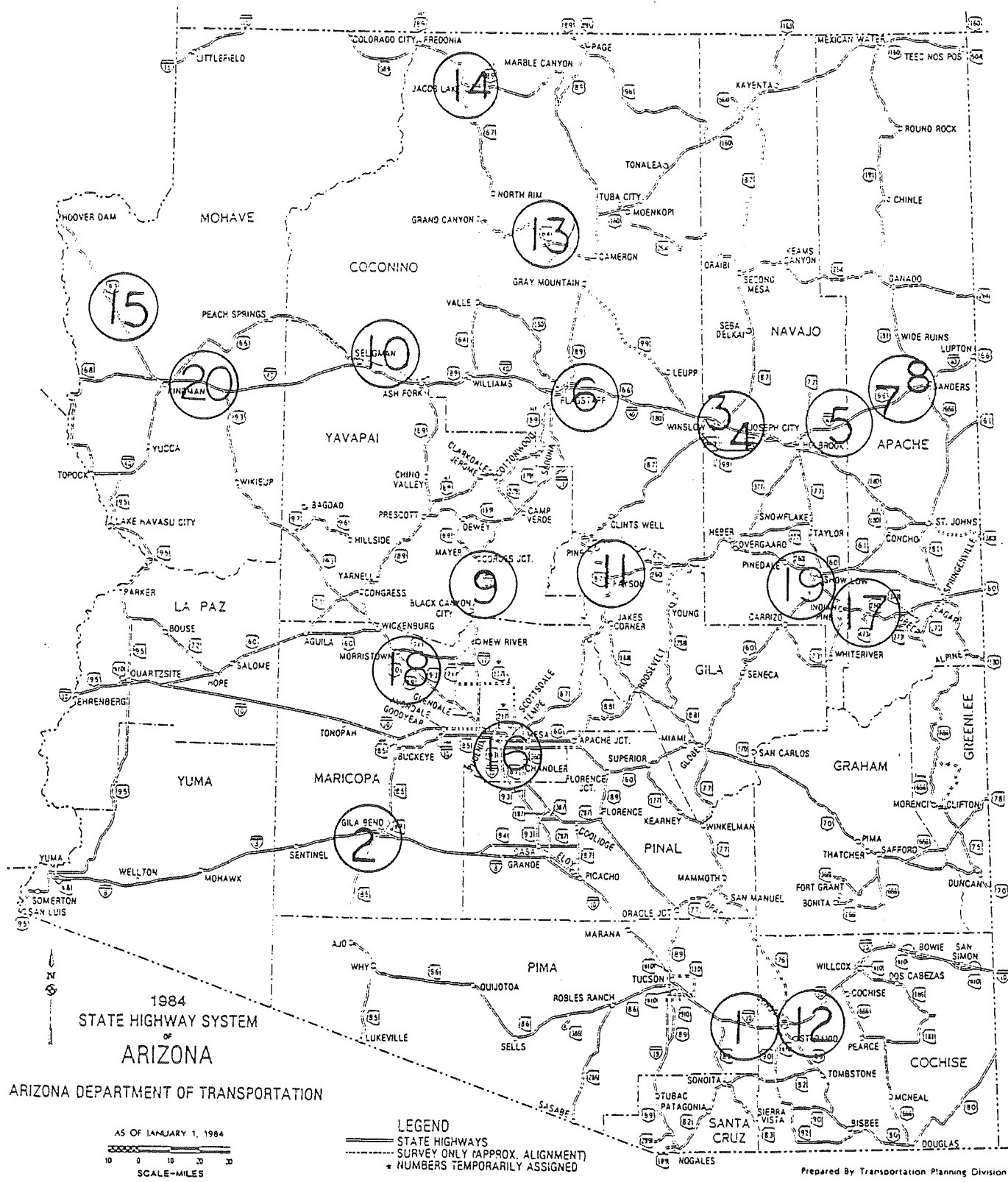


FIGURE 3-1. SELECTED SITES

During the selection process, geographical distribution was an important concern for ensuring the entire range of geographical and climatic conditions were included in the data base. Previous work by the Department identified nine climatic zones in the state as shown in Figure 3-2. Sites were located in eight of the nine climatic zones; zone 5 was not represented. Due to other considerations, various climatic zones were not equally represented. The location of the sites and the climatic zones are given in Table 3-1.

It should be noted that the search for sites did not identify 20 sites which completely matched the criteria, therefore, as will be subsequently discussed, the selection was based on satisfying most of the criteria.

The performance of the sites, as listed in the ADOT pavement management data base, are given in Tables 3-2, 3-3, and 3-4 for cracking, roughness, and friction number respectively. Table 3-5 presents the traffic data, annual truck loads, the traffic growth factor, the maintenance cost in 1986, and the most recent construction project. The data in these tables are for the milepost closest to the site rather than for the actual pavement site.

Review of Table 3-1 shows the sites selected for the research are predominantly on the interstate system. There are two state routes and six U.S. highways, the remaining twelve sites are interstate highways.

Table 3-2 shows ten of the sites had cracking in 1987. Site 15 has the most cracking, 35 percent. Ten of the sites do not have cracking as of the 1987 survey.

Table 3-3 shows the sites have a wide range of roughness. In the ADOT pavement management system roughness less than 165 is considered good and more than 265 is unacceptable. Thirteen of the sites are in the good range, and the remaining sites are in the intermediate category as of 1987. Three sites are close to the unacceptable limit for roughness.

The friction numbers are fairly uniform between the sites, with the exception of Site 9 which has a friction number of 36 as of 1985.

Table 3-5 shows the sites have a wide range of traffic loadings. The ADL ranges from 14 to 2,830 where site 13 has the lowest truck loadings. Table 3-5 also shows site 9 has gone the longest time since a construction project, 1969. The most recent project was on site 5 in 1984. The 1986 maintenance cost data vary widely from zero expenditures on three pavement sites to \$22,227 on site 7.

Table 3-6 shows historical construction data for the selected sites, while the abbreviations used are defined in Table 3-7. As shown in Table 3-6, a wide range of material types and layer thicknesses has been represented.

Four of the sites have asphalt-rubber membranes as part of the overlay treatment.

The original surface designs show three sites with a 4" or greater surface thickness, eight sites with an AC layer of less than 4" and nine sites where the original surface was a bituminous stabilized layer. In addition, 2

TABLE 3-1. LOCATION OF TEST SITES AND CLIMATIC ZONES

| Site Number | Approximate Location | Route | Milepost | Climatic Zone |
|-------------|----------------------|--------|----------|---------------|
| 1 | Benson | I10W | 300.07 | 3 |
| 2 | Gila Bend | I8E | 112.80 | 1 |
| 3 | Winslow | I40E | 260.21 | 4 |
| 4 | Minnelonka | I40E | 261.78 | 4 |
| 5 | Dead River | I40E | 317.06 | 4 |
| 6 | Flagstaff | I17N | 337.0 | 8 |
| 7 | Crazy Creek #1 | I40E | 322.72 | 4 |
| 8 | Crazy Creek #2 | I40E | 323.78 | 4 |
| 9 | Sunset Point | I17N | 251.41 | 6 |
| 10 | Seligman | I40W | 131.71 | 6 |
| 11 | Expo Hill | S87S | 249.00 | 8 |
| 12 | Benson East | I10W | 303.00 | 3 |
| 13 | Camron West | S64E | 273.00 | 4 |
| 14 | Jacob Lake | US89AN | 578.00 | 7 |
| 15 | Mohave | US93S | 44.00 | 2 |
| 16 | Tempe | US60E | 191.00 | 1 |
| 17 | Show Low | US60E | 330.00 | 9 |
| 18 | Morristown | US60W | 120.00 | 1 |
| 19 | McNary | US260E | 369.00 | 9 |
| 20 | Kingman | I-40E | 59.00 | 2 |

Table 3-2. Cracking of the Selected Sites as Recorded in the ADOT Pavement Management System Data Base

| SITE | Year | | | | | | | | |
|------|------|----|----|----|----|----|----|----|----|
| | 79 | 80 | 81 | 82 | 83 | 84 | 85 | 86 | 87 |
| 1 | 0 | 0 | 0 | 0 | 1 | 1 | 2 | 3 | 3 |
| 2 | 0 | 0 | 0 | 0 | 1 | 3 | 4 | 6 | 5 |
| 3 | 0 | 0 | 0 | 0 | 0 | 0 | 0 | 0 | 0 |
| 4 | 0 | 0 | 0 | 0 | 0 | 0 | 0 | 0 | 0 |
| 5 | 0 | 0 | 0 | 0 | 0 | 0 | 0 | 0 | 0 |
| 6 | 0 | 1 | 0 | 0 | 0 | 0 | 0 | 1 | 1 |
| 7 | 0 | 0 | 0 | 0 | 0 | 0 | 0 | 0 | 0 |
| 8 | 0 | 0 | 0 | 0 | 0 | 0 | 0 | 0 | 0 |
| 9 | 5 | 12 | 20 | 20 | 25 | 35 | 30 | 30 | 0 |
| 10 | 0 | 50 | 0 | 0 | 0 | 0 | 0 | 0 | 1 |
| 11 | 0 | 0 | 0 | 0 | 0 | 0 | 1 | 2 | 5 |
| 12 | 0 | 0 | 0 | 0 | 1 | 1 | 2 | 3 | 5 |
| 13 | 0 | 0 | 0 | 0 | 0 | 0 | 0 | 0 | 0 |
| 14 | 0 | 0 | 12 | 15 | 0 | 0 | 0 | 1 | 0 |
| 15 | 1 | 0 | 0 | 4 | 4 | 5 | 7 | 15 | 35 |
| 16 | 0 | 0 | 0 | 0 | 0 | 00 | 0 | 6 | 7 |
| 17 | 0 | 0 | 0 | 0 | 0 | 0 | 0 | 0 | 0 |
| 18 | 0 | 30 | 1 | 2 | 0 | 0 | 0 | 2 | 4 |
| 19 | 0 | 0 | 0 | 0 | 0 | 0 | 1 | 0 | 0 |
| 20 | 20 | 35 | 0 | 0 | 0 | 0 | 0 | 1 | 1 |

TABLE 3-3. ROUGHNESS OF THE SELECTED SITES AS RECORDED IN THE ADOT PAVEMENT MANAGEMENT SYSTEM DATA BASE

| SITE | YEAR | | | | | | | | | | | | | | | |
|------|------|-----|-----|-----|-----|-----|-----|-----|-----|-----|-----|-----|-----|-----|-----|-----|
| | 72 | 73 | 74 | 75 | 76 | 77 | 78 | 79 | 80 | 81 | 82 | 83 | 84 | 85 | 86 | 87 |
| 1 | 39 | 43 | 36 | 52 | 55 | 48 | 39 | 28 | 72 | 79 | 47 | 77 | 83 | 110 | 103 | 110 |
| 2 | 33 | 49 | 53 | 65 | 66 | 38 | 80 | 59 | 96 | 100 | 73 | 86 | 80 | 109 | 96 | 90 |
| 3 | 41 | 64 | 71 | 103 | 161 | 185 | 168 | 97 | 49 | 81 | 82 | 97 | 99 | 139 | 114 | 143 |
| 4 | 30 | 56 | 62 | 102 | 144 | 157 | 192 | 103 | 54 | 96 | 91 | 82 | 95 | 118 | 134 | 131 |
| 5 | 180 | 211 | 35 | 39 | 57 | 116 | 84 | 89 | 92 | 117 | 97 | 132 | 78 | 90 | 100 | 114 |
| 6 | 61 | 92 | 54 | 91 | 112 | 132 | 142 | 149 | 182 | 64 | 72 | 74 | 67 | 109 | 126 | 101 |
| 7 | 228 | 269 | 324 | 49 | 62 | 112 | 82 | 93 | 107 | 179 | 153 | 210 | 200 | 219 | 233 | 220 |
| 8 | 198 | 234 | 263 | 28 | 45 | 99 | 57 | 54 | 77 | 101 | 75 | 112 | 85 | 127 | 110 | 137 |
| 9 | 27 | 47 | 75 | 72 | 105 | 96 | 108 | 132 | 142 | 174 | 166 | 187 | 201 | 209 | 210 | 90 |
| 10 | 36 | 62 | 53 | 77 | 124 | 127 | 180 | 198 | 256 | 99 | 77 | 96 | 91 | 126 | 134 | 226 |
| 11 | 208 | 203 | 231 | 211 | 200 | 230 | 0 | 0 | 172 | 190 | 166 | 197 | 168 | 177 | 197 | 167 |
| 12 | 121 | 0 | 48 | 67 | 80 | 77 | 88 | 113 | 129 | 149 | 173 | 152 | 139 | 170 | 169 | 204 |
| 13 | 219 | 253 | 278 | 315 | 320 | 333 | 359 | 197 | 208 | 242 | 235 | 232 | 238 | 218 | 226 | 221 |
| 14 | 160 | 187 | 106 | 129 | 147 | 148 | 176 | 126 | 138 | 134 | 143 | 172 | 177 | 171 | 205 | 180 |
| 15 | 79 | 109 | 107 | 151 | 163 | 102 | 122 | 121 | 120 | 133 | 138 | 140 | 157 | 138 | 175 | 171 |
| 16 | 65 | 70 | 47 | 64 | 71 | 86 | 131 | 0 | 96 | 110 | 94 | 94 | 101 | 103 | 89 | 80 |
| 17 | 0 | 280 | 166 | 143 | 161 | 185 | 175 | 161 | 49 | 69 | 64 | 91 | 94 | 134 | 106 | 95 |
| 18 | 29 | 51 | 63 | 72 | 78 | 130 | 103 | 99 | 98 | 134 | 97 | 128 | 138 | 133 | 119 | 120 |
| 19 | 109 | 215 | 128 | 139 | 191 | 244 | 259 | 93 | 109 | 141 | 139 | 89 | 101 | 119 | 117 | 123 |
| 20 | 35 | 37 | 44 | 46 | 59 | 34 | 70 | 81 | 103 | 53 | 55 | 63 | 59 | 104 | 112 | 91 |

TABLE 3-4. FRICTION NUMBERS OF THE SELECTED SECTIONS AS RECORDED IN THE ADOT PAVEMENT MANAGEMENT SYSTEM DATA BASE

| SITE | YEAR | | | | | |
|------|------|----|----|----|----|----|
| | 80 | 81 | 82 | 83 | 84 | 85 |
| 1 | 68 | 77 | 62 | 57 | 66 | 70 |
| 2 | 66 | 73 | 64 | 64 | 59 | 67 |
| 3 | 79 | 88 | 54 | 49 | 53 | 60 |
| 4 | 80 | 88 | 66 | 49 | 46 | 55 |
| 5 | 30 | 35 | 24 | 16 | 71 | 69 |
| 6 | 24 | 71 | 67 | 75 | 72 | 74 |
| 7 | 77 | 73 | 62 | 39 | 63 | 64 |
| 8 | 74 | 77 | 64 | 33 | 62 | 62 |
| 9 | 50 | 69 | 52 | 49 | 49 | 36 |
| 10 | 76 | 88 | 71 | 88 | 74 | 73 |
| 11 | 64 | | 69 | | 56 | |
| 12 | 78 | 77 | 52 | 50 | 60 | 70 |
| 13 | | 81 | 64 | 71 | 72 | 64 |
| 14 | 83 | 67 | 43 | 47 | 78 | |
| 15 | 40 | 54 | 67 | 43 | 63 | 69 |
| 16 | | 54 | 58 | 0 | 54 | |
| 17 | 73 | 75 | 69 | 66 | 67 | |
| 18 | 71 | 26 | 39 | 0 | 71 | 70 |
| 19 | 79 | 83 | 73 | 67 | 76 | |
| 20 | | 77 | 76 | 77 | 74 | |

TABLE 3-5. INFORMATION OF TRAFFIC, MAINTENANCE, AND THE MOST RECENT CONSTRUCTION PROJECT AS RECORDED IN THE ADOT PAVEMENT MANAGEMENT SYSTEM DATA BASE

| SITE | ADT | ADL | GROWTH FACTOR (%) | MAINT. COST (\$) | MOST RECENT PROJECT | YEA |
|------|--------|-------|----------------------|---------------------|------------------------|-----|
| 1 | 15,592 | 2,830 | 2.2 | 298 | I-10-5-46 | 76 |
| 2 | 5,462 | 1,220 | 0.7 | 70 | I- 8-2-72 | 76 |
| 3 | 13,025 | 2,783 | 4.6 | 261 | IRI-40-4-103 | 79 |
| 4 | 13,025 | 2,783 | 4.6 | 147 | IRI-40-4-103 | 79 |
| 5 | 10,774 | 2,543 | 3.6 | 615 | IR-40-5-66 | 84 |
| 6 | 16,246 | 1,846 | 5.4 | 5,551 | I-17-2-85 | 81 |
| 7 | 10,738 | 2,535 | 3.6 | 22,227 | I-40-5-44 | 75 |
| 8 | 10,738 | 2,535 | 3.6 | 1,438 | I-40-5-44 | 75 |
| 9 | 17,575 | 1,616 | 4.3 | 225 | I-17-1-65 | 69 |
| 10 | 8,115 | 1,382 | 3.7 | 6,283 | I-40-2-86 | 81 |
| 11 | 7,295 | 354 | 4.3 | 0 | DF-F053-1-9 | 77 |
| 12 | 14,095 | 2,544 | 1.1 | 1,100 | IR-10-5-52 | 79 |
| 13 | 2,207 | 14 | 2.3 | 10 | F033-1-505 | 79 |
| 14 | 1,342 | 61 | 3.0 | 7,060 | F037-3-916 | 83 |
| 15 | 5,779 | 348 | 2.9 | 0 | F039-1-908 | 77 |
| 16 | 23,898 | 265 | 0.3 | 226 | F022-5-906 | 79 |
| 17 | 2,451 | 176 | 2.6 | 19 | F026-1-513 | 79 |
| 18 | 7,956 | 290 | 1.9 | 0 | BF022-2-940 | 83 |
| 19 | 1,487 | 65 | 0.0 | 1,963 | F044-1-910 | 82 |
| 20 | 12,902 | 2,225 | 6.2 | 25 | FR11-40-2-89 | 81 |

TABLE 3-6. HISTORICAL DATA FOR SITES

| Site No. | ADOT designation | Date built | RC | AC | SC | RM | ACFC | BS | BTB | CTB | AB | SM | SGS |
|----------|----------------------|------------|------|-----|-----|-----|------|-----|-----|-----|-----|------|------|
| 1 | I-10 WB MP 300.07 | 1942 | | | | | | 2.0 | | | 3.0 | 12.0 | |
| | | 6/1965 | | 4.0 | | | 0.5 | | | | | | |
| | | 9/1975 | | 1.3 | | | 0.5 | | | | | | |
| 2 | I-8 EB MP 112.8 | 5/1955 | | 2.0 | | | | | | | 3.0 | 6.0 | |
| | | 1970 | | 1.3 | | | 0.8 | | | | | | |
| | | 1972 | | | | 0.3 | | | | | | | |
| | | 1976 | | | | | 0.5 | | | | | | |
| 3 | I-40 EB MP 260.21 | 7/1958 | | 3.5 | 0.3 | | | | 3.0 | | | 6.0 | |
| | | 9/1971 | | 1.3 | | | 0.5 | | | | | | |
| | | 6/1975 | | | | 0.3 | | | | | | | |
| | | 12/1979 | | 6.0 | | | 0.5 | | | | | | |
| 4 | I-40 EB MP 261.78 | 7/1958 | | 3.5 | 0.3 | | | | 3.0 | | | 6.0 | |
| | | 9/1971 | | 1.3 | | | 0.5 | | | | | | |
| | | 6/1975 | | | | 0.3 | | | | | | | |
| | | 1979 | | 6.0 | | | 0.5 | | | | | | |
| 5 | I-40 EB MP 317.06 | 7/1960 | | 4.0 | 0.3 | | | | | 6.0 | | 6.0 | |
| | | 11/1973 | | 2.8 | | | 0.5 | | | | | | |
| | | 1984 | | 1.5 | | | 0.5 | | | | | | |
| 6 | I-17 NB MP 337 | 8/1960 | | | 0.3 | | | 1.0 | | | 6.0 | 10.0 | 12.0 |
| | | 9/1966 | | 3.5 | 0.3 | | | | | | | | |
| | | 1970 | | 5.5 | | | | | | | | | |
| | | 1974 | | | | | 0.5 | | | | | | |
| | | 6/1981 | 5.5* | 1.0 | | | | | | | | | |
| 7 | I-40 EB MP 322.72 | 9/1961 | | 4.0 | 0.3 | | | | | 6.0 | | 6.0 | |
| | | 10/1975 | | 2.5 | | 0.3 | 0.5 | | | | | | |
| 8 | I-40 EB MP 323.78 | 9/1961 | | 4.0 | 0.3 | | | | | 6.0 | | 6.0 | |
| | | 10/1975 | | 3.0 | | 0.3 | 0.5 | | | | | | |
| 9 | I-17 NB MP 251.41 | 4/1967 | | 3.5 | | | | 2.0 | | | 2.0 | 17.0 | 6.0 |
| | | 1969 | | | | | 0.5 | | | | | | |
| 10 | I-40 WB MP 131 | 1969 | | 3.5 | | | 0.8 | | | | 6.0 | 22.0 | |
| | | 1981 | 4.0* | 1.5 | | | 0.5 | | | | | | |
| 11 | SR-87 SB MP 249 | 1958 | | | | | | 2.0 | | | | | |
| | | 1968 | | | 0.3 | | | | | | | | |
| | | 1976 | | 2.5 | | 0.3 | 0.5 | | | | | | |

* No new thickness

TABLE 3-6. HISTORICAL DATA FOR SITES (CONT.)

| Site No. | ADOT designation | Date built | RC | AC | SC | RM | ACFC | BS | BTB | CTB | AB | SM | SGS |
|----------|---------------------|------------|----|-----|-----|-----|------|-----|-----|-----|-----|------|-----|
| 12 | I-10 WB MP 303 | 1967 | | 3.5 | | | 0.5 | | | | 6.0 | 15.0 | |
| | | 1979 | | 2.0 | | | 0.5 | | | | | | |
| 13 | SR-64 EB MP 273 | 1936 | | | | | | 2.5 | | | 3.0 | | |
| | | 1979 | | 3.0 | | | | | | | | | |
| 14 | US-89A NB MP 578 | 1938 | | | | | | 1.5 | | | | | |
| | | 1967 | | | | 0.3 | | | | | | | |
| | | 1974 | | | | 0.3 | | | | | | | |
| | | 1978 | | 1.5 | | | | | | | | | |
| | | 1979 | | | | 0.3 | | | | | | | |
| 1983 | | | | 0.3 | | | | | | | | | |
| 15 | US-93 SB MP 44 | 1936 | | | | | | 2.5 | | | 6.0 | | |
| | | 1961 | | 3.0 | | | | | | | | | |
| | | 1975 | | | | 0.3 | | | | | | | |
| | | 1977 | | 3.0 | | | | | | | | | |
| 16 | US-60 EB MP 191 | 10/43 | | | | | | 2 | | | | 9 | |
| | | 9/72 | | | | | 0.5 | | | | | | |
| | | 9/77 | | 3 | | | 0.5 | | | | | | |
| | | 10/79 | | | | | 0.5 | | | | | | |
| 17 | US-60 EB MP 330 | /38 | | | | | | 2 | | | | 6 | |
| | | 8/69 | | | | 0.3 | | | | | | | |
| | | 5/74 | | | | 0.3 | | | | | | | |
| | | 10/79 | | 1.5 | | | 0.5 | | | | | | |
| 18 | US-60 WB MP 120 | /65 | | 3 | 0.3 | | | | | | 4 | 15 | |
| | | 3/74 | | | | 0.3 | | | | | | | |
| | | 6/83 | | | | | 0.5 | | | | | | |
| 19 | US-260 EB MP 369 | /54 | | | | | | 2 | | | 3 | 6 | |
| | | 9/70 | | | | 0.3 | | | | | | | |
| | | 6/78 | | 1.5 | | | | | | | | | |
| | | 10/82 | | | | | 0.5 | | | | | | |
| 20 | I-40 EB MP 59 | 9/67 | | 3.5 | | | 0.5 | | | | 4 | 15 | |
| | | 7/81 | | 2.3 | | | 0.5 | | | | | | |

TABLE 3-7. ABBREVIATIONS USED FOR MATERIAL TYPES

| Abbreviation | Type of layer |
|--------------|------------------------------------|
| RC | Recycled Asphalt Concrete |
| AC | Plant Mixed Asphalt Concrete |
| SC | Seal Coat |
| RM | Rubberized Membrane Seal Coat |
| ACFC | Asphaltic Concrete Friction Course |
| BS | Bituminous Treated Surface |
| BTB | Bituminous Treated Base |
| CTB | Cement Treated Base |
| AB | Aggregate Base |
| SM | Select Material |
| SGS | Subgrade Seal |

sites (sites 6 and 10) have been recycled with a new AC and/or ACFC has been added.

Two sites have a bituminous treated base. Three sites have a cement treated base, and eleven sites have an aggregate base. Four sites do not have a subbase layer. All other sites have select material for the subbase.

CHAPTER 4. FIELD WORK

Data were collected for each of the 20 sites. Three activities were performed at each of the sites; nondestructive testing, coring and sampling the pavement structure and cone penetration.

4.1. NONDESTRUCTIVE TESTING

One of the objectives of the project was to evaluate the ability of nondestructive tests, NDT, to generate the data required for overlay design. In the pavements field, nondestructive testing is synonymous with deflection measurements at the pavement surface. Originally ADOT used the Dynaflect for all NDT testing (Figure 4-1). The Dynaflect generates an oscillating load of 1000 lb transmitted to the pavement through rubber-lined steel wheels. Deflections are measured with five geophones, one between the load wheels and the other four are perpendicular to the load wheel axis spaced at one foot intervals as shown in Figure 4-2.

Due to the light load used to excite the pavement and the vibratory nature of the load, the Dynaflect has been criticized for not representing the stress condition generated by truck traffic. Falling weight deflectometers have been developed to overcome these shortcomings. ADOT purchased the first FWD imported to the United States by Dynatest. This unit was a prototype which generates the load impulse in the same manner as more recent FWD's but was operationally slow due to the need to manually place the deflection sensors and repeat loading the pavement for each sensor location. As a result, ADOT was in the process of upgrading its FWD at the start of the project to the current version manufactured by Dynatest. Since the new equipment was not available when the measurements were required, the services of ERES Consultants, Inc. of Champaign, Illinois were contracted to provide FWD data for sites 1 through 13 and site 15. The ERES Inc. FWD (Figure 4-3) is the same model as the FWD ordered by ADOT. In 1987, ADOT received its new Dynatest FWD which was later used to test sites 14 and 16 through 20.

The FWD is operationally simple. A mass is dropped onto a 11.8-inch plate with a rubber pad generating an impulse load on the pavement which is similar, but not identical to the stress pulse generated by moving trucks. The magnitude of the force on the pavement can be varied by altering either the mass of the drop weight or the drop height. The magnitude of the force generated on the pavement is directly measured with a load cell. Deflections are measured with seven geophones; one is placed at the center of the loaded area. The location of the other six sensors can be varied but are normally placed at one foot intervals as shown in Figure 4-4.

Based on the need to tie the historical deflection records with the new equipment purchased by ADOT, deflection measurements were performed with both the Dynaflect and the Dynatest FWD. The measurements with both instruments were made within a short time period to eliminate environmental factors from influencing the test results. The operational parameters of the Dynaflect are fixed. On the other hand, varying the drop mass and/or the drop height of the FWD provides a direct opportunity to evaluate the stress sensitivity of the materials in the pavement structure. Three force levels were selected to



FIGURE 4-1. DYNAFLECT

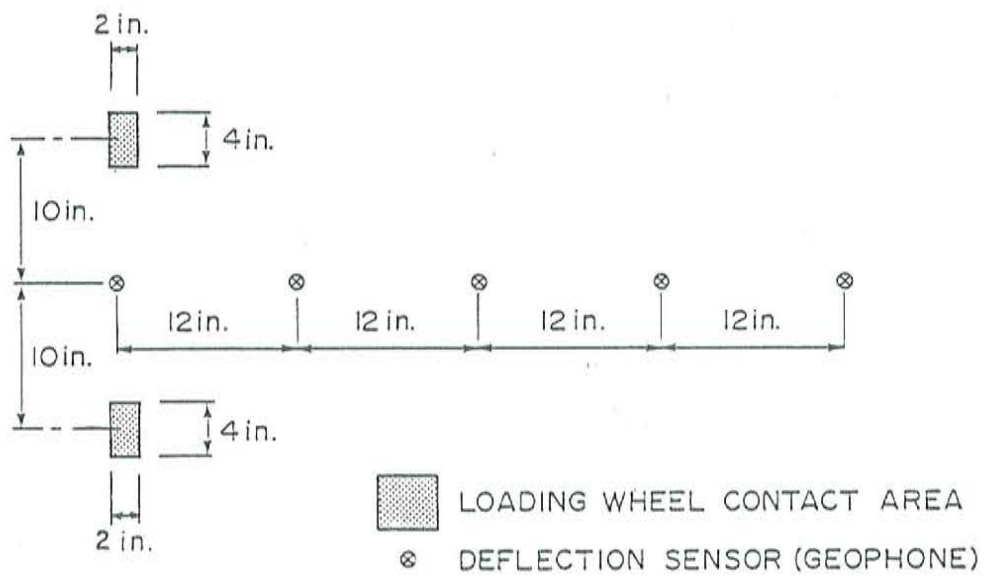


FIGURE 4-2. LOCATION OF LOADING WHEELS AND GEOPHONES OF THE DYNAFLECT



FIGURE 4-3. DYNATEST FWD

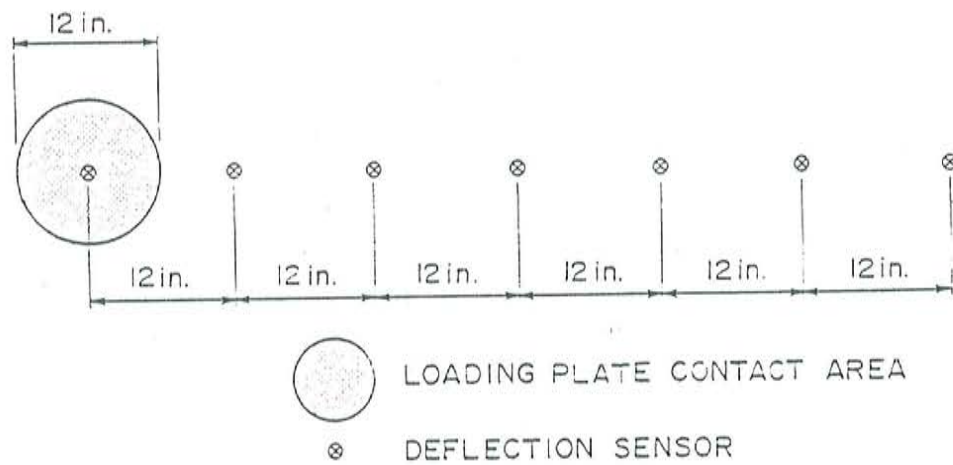


FIGURE 4-4. FWD: SENSOR LOCATIONS

simulate the load of an 18 kip axle, a lighter truck and a heavier truck. The target forces used in the field testing were 6, 9, and 12 kips by varying the drop height. The actual force generated on the pavement varies as a function of the stiffness of the pavement structure.

Deflection measurements were made in the outside wheel track of the pavement using the two devices. Ten stations, at 10 ft intervals within each site were measured on each test site. The pavement surface temperature was measured at the time of the test to allow for subsequent temperature corrections in the computed modulus values for the asphalt concrete layers. The FWD was operated at 3 stress levels (6, 9 and 12 kips) at stations 1, 5 and 10 at each site, while one stress level at 9 kips was used at the other stations. All 20 sites were tested with the FWD, while sites 1 through 13 and 15 were tested using the Dynaflect. A summary of the NDT data is shown in Appendix A.

4.2. SAMPLE COLLECTION

4.2.1. Description of Site Configuration

As mentioned earlier, at each site a total of 10 stations were established at a spacing of 10 ft apart. These stations were located in the right-hand wheel track of the right lane. Station 1 was set at a distance 1 foot ahead of the milepost marker corresponding to the site. Unless otherwise noted, the boring locations were at stations 1, 4 and 7.

4.2.2. Boring and Sample Equipment

Boring and sampling were accomplished through a subcontract with the firm of Foree and Vann. A CME-55 drill rig was used to accomplish sampling. Cores of asphalt concrete were obtained with a small portable electric powered coring device. Running water was used to cool the cutting bit of the 4" I.D. core barrel.

A 4 1/2" O.D. continuous flight auger was used to advance the hole after the asphalt concrete core had been removed. Undisturbed samples of subgrade materials were obtained by pushing 3" O.D., 2.8" I.D. thin-walled stainless steel sample tubes hydraulically with the drill rig.

4.2.3. Sampling Procedures

The procedure followed for this study may be summarized briefly as follows:

At stations 1, 4 and 7 of each site:

- 1) The asphalt concrete was cored, removed, and marked for identification.
- 2) The hole was advanced to the subgrade, using the cuttings to log the hole. Bag samples were obtained for index tests or tests on reconstituted samples.
- 3) A minimum of one thin-walled push tube sample of subgrade was obtained. In a few instances, the tube required driving with the 140 lb drop hammer.

- 4) The hole was backfilled and tamped in stages, and an asphalt cold patch plug approximately equal to the original thickness of the asphalt concrete was tamped into place.

More details on the sampling equipment are presented in Appendix B.

At some sites, it was noted that the layer thicknesses obtained from the boring logs did not exactly match the construction records provided by ADOT prior to sampling, especially site 14. Also, by visual observation of asphalt cores it was not possible in some cases to detect thin layers such as ACFC, SC, etc.

4.3 CONE PENETRATION TESTING

In order to more accurately determine the subsurface profile, and to detect layering, cone penetration testing (CPT) was performed at three locations at each test site. In general, these locations corresponded to station 1, the shoulder adjacent to station 1 (noted 1s) and station 4 (except where noted otherwise). The CPT consisted of advancing an electric friction cone penetrometer attached to a truck mounted CME 55 drill rig unit following ASTM procedure D3441-86 to depths of 25 feet or refusal. On occasion when refusal was met at relatively shallow depth, the cone penetrometer was removed, the hole was augered down to softer material and the cone was then re-advanced in the softer state.

Normal output of the CPT consists of a digital readout of the friction sleeve resistance in tsf and the cone tip resistance in tsf. These values are displayed every 4 in. and are average values over this 4 in. zone. Some typical plots of tip resistance vs. depth, are shown in Figures 4-5 and 4-6.

Although the CPT data consists of friction sleeve resistance along with the tip resistance, the only correlation for modulus which have been attempted are based entirely on soil type and the cone tip resistance (tsf). In addition, the friction sleeve values are somewhat temperature sensitive. Therefore, only the tip resistance was used in estimating modulus variation with depth.

The cone penetrometer data were used basically to determine the following:

1. Accurate subsurface profiling of each site, and
2. Possible correlation with modulus.

4.3.1 Determination of Subsurface Profiles

Friction ratio values were used to a limited extent, along with tip resistance values, the boring logs and the moisture content data in determining the subsurface profile at each site. This was to show the variation of soil type as well as stiffness, and therefore modulus, with depth and also laterally across a particular site. Figures 4-7 and 4-8 are examples of moisture content variations with depth.

4.3.2 Correlation between CPT Data and Modulus

In order to determine a possible correlation of cone tip resistance and modulus, it was first necessary to review the literature. Almost all correlations found in the literature contain a correlation of Young's modulus

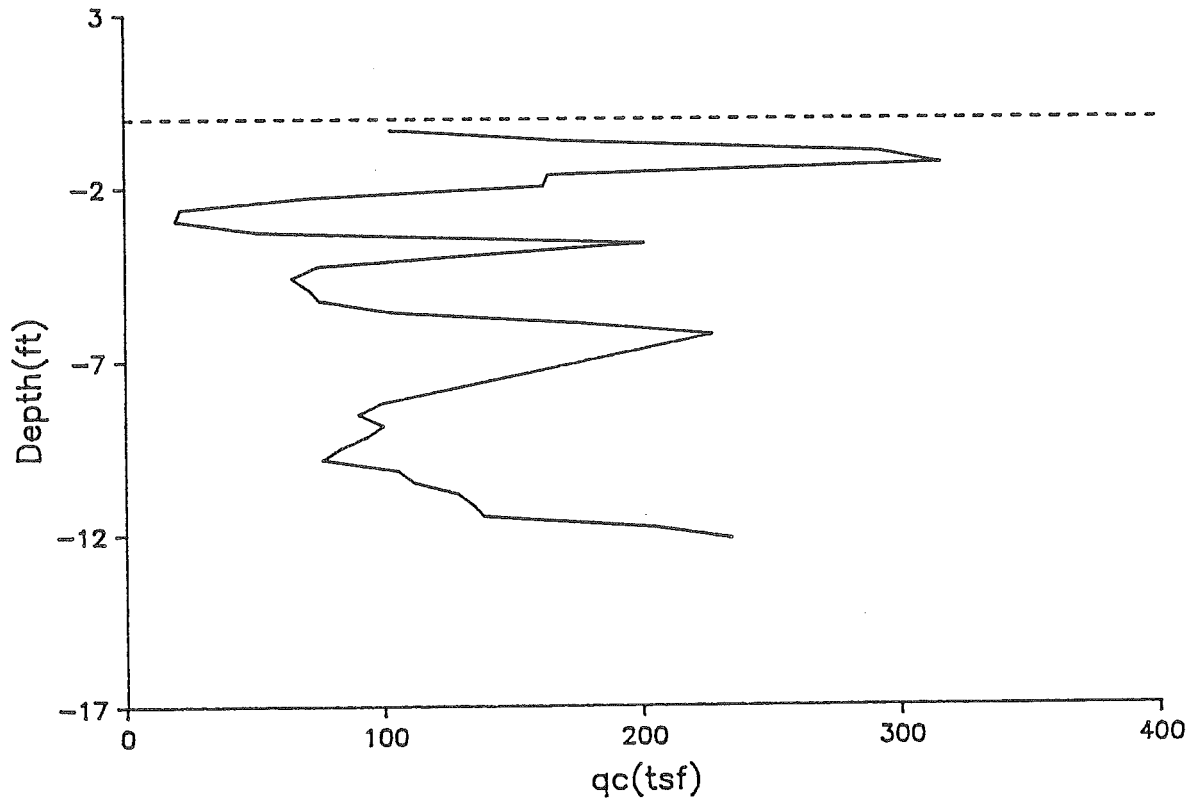


FIGURE 4-5. TYPICAL PLOT OF CONE RESISTANCE VS DEPTH (SITE 1, STATION 1, SHOULDER)

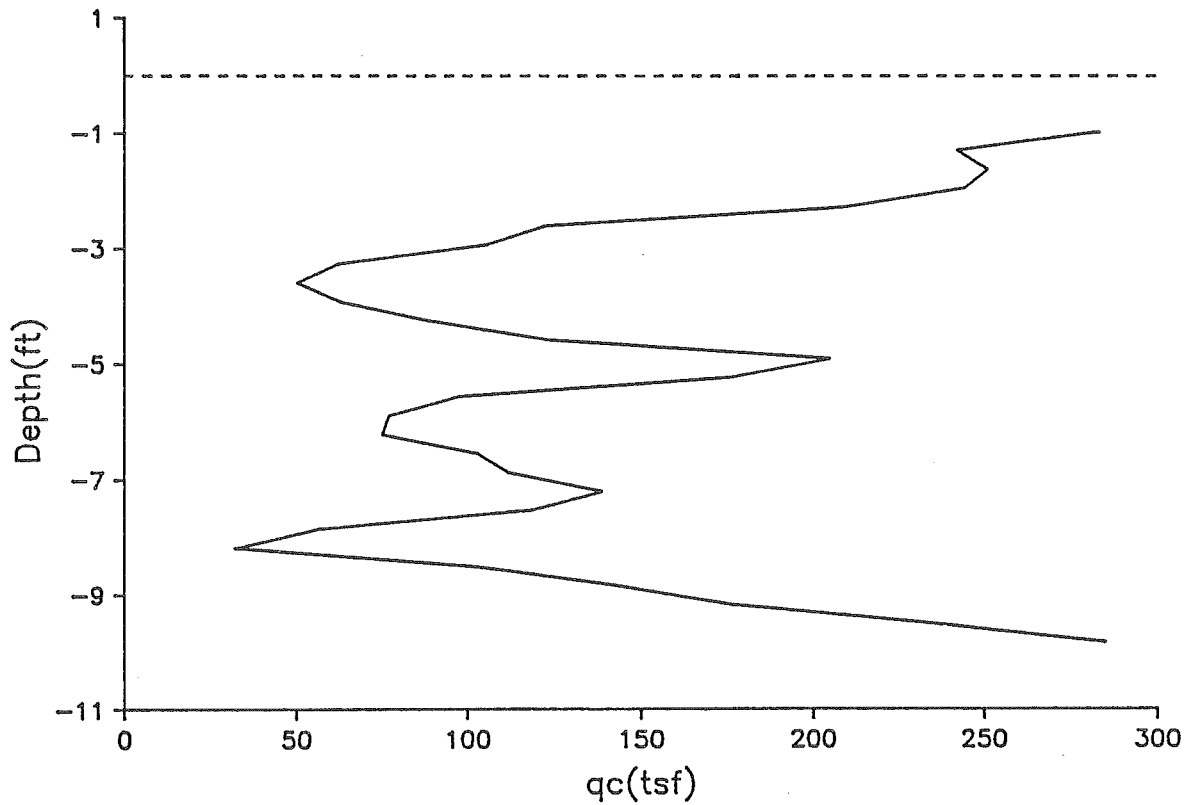


FIGURE 4-6. TYPICAL PLOT OF CONE RESISTANCE VS DEPTH (SITE 1, STATION 4)

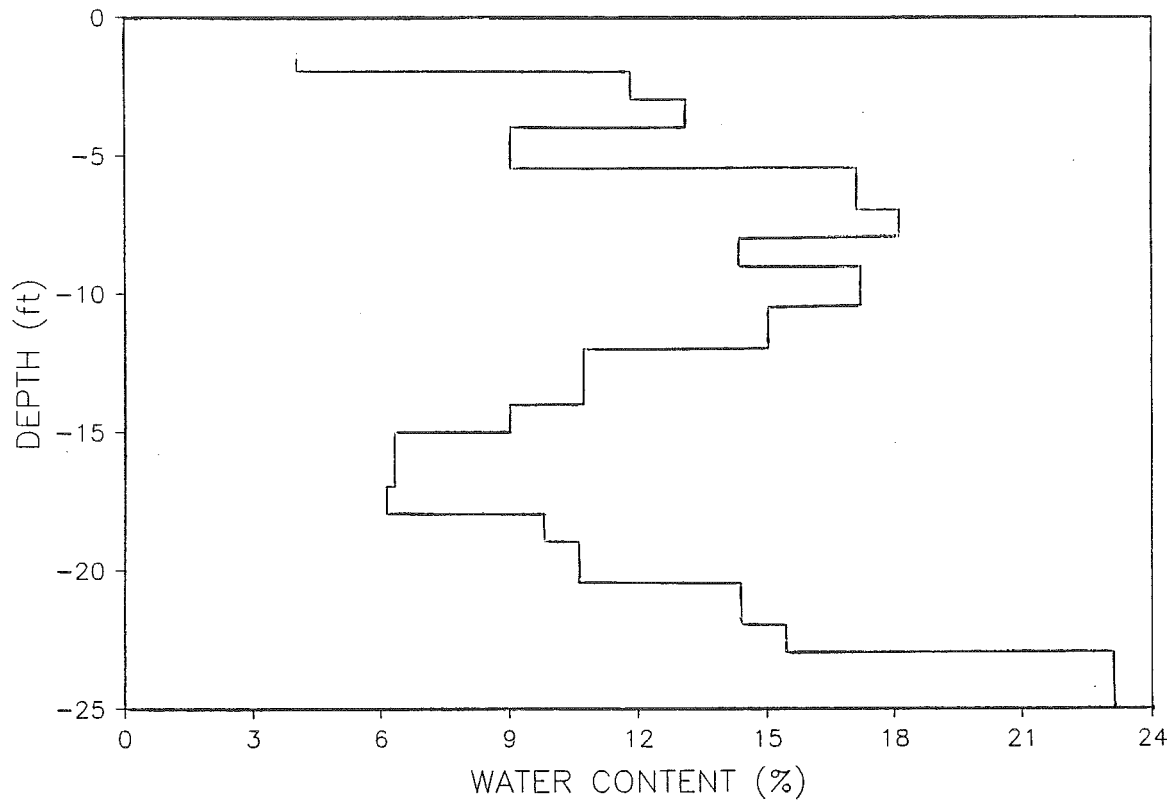


FIGURE 4-7 EXAMPLE OF MOISTURE CONTENT VARIATION WITH DEPTH (SITE 3, STATION 1)

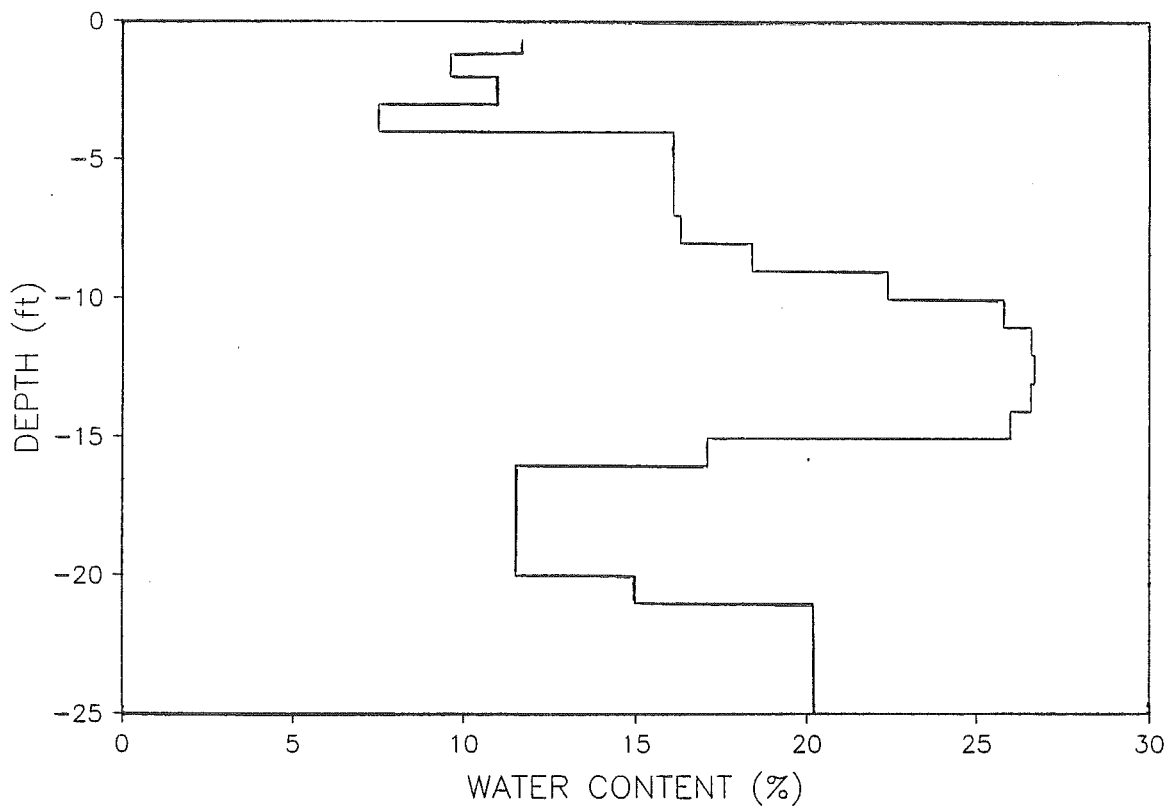


FIGURE 4-8 EXAMPLE OF MOISTURE CONTENT VARIATION WITH DEPTH (SITE 7, STATION 1)

and q_c of the form, $E = \alpha q_c$, with α values varying from 1 to 22. Values from the literature were used, together with our own laboratory data, to select α values. Heavier weight was attached to our laboratory values for this first trial analysis of the data. Accordingly, α were selected as follows:

CL: $\alpha = 50$
CH: $\alpha = 30$

Sands and Gravels: $\alpha = 10$

These α values were then used to develop a layered profile of modulus vs. depth using the concept of a minimum modulus with all other values being multiples thereof. Figure 4-9 shows an example plot of E/E_{min} vs. depth where a remarkable variation of modulus vs. depth is exhibited. This plot, as well as Figures 4-5 and 4-6, which are typical, show that there is pronounced layering and that the q_c and the modulus are definitely not constant with depth. In fact, the modulus and q_c typically vary greatly with depth. It should be noted that previous studies have showed that the cone sleeve resistance is not correlated with the Young's modulus. Therefore, only the cone tip resistance was considered in this study.

Cone penetration resistance values measured in the traffic lane and on the shoulder were compared and it was found that the lateral variation was generally too great to suggest using test values from the shoulder location to represent values in the traffic lane.

Further analysis of the cone penetration data will be made as a part of a master thesis at ASU and a copy of this thesis will be transmitted to ADOT under separate cover.

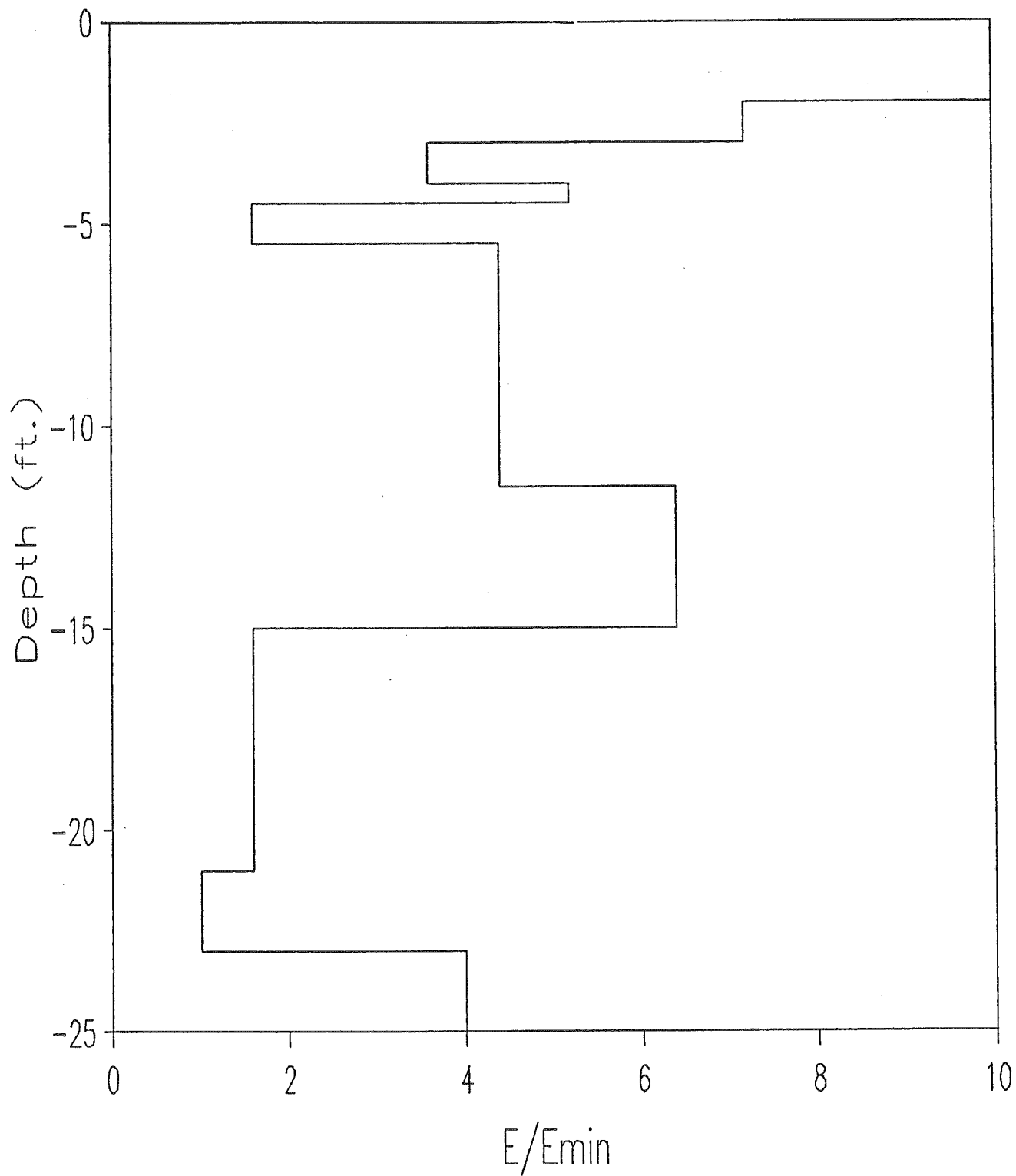


FIGURE 4-9 EXAMPLE PLOT OF E/E_{\min} VS DEPTH

CHAPTER 5. LABORATORY TESTING

5.1. ASPHALT CONCRETE

5.1.1. Materials and Equipment

Asphalt concrete core samples of 4 in. diameter were collected from the 20 sites. By visual observation, it could be seen that some cores had only one distinct asphalt layer while some had two or three clearly defined asphalt layers. These distinct asphalt layers in the cores were most often separated by a seal coat or an asphalt concrete friction course. Samples were cut from these cores in such a way that a sample would be obtained from each distinct layer observed in the core. The thickness of the samples after trimming varied between 2 and 2.5 inches in most cases. However, several samples had a thickness of slightly less than 2 inches. A total of 34 asphalt concrete core samples were tested.

The resilient modulus equipment (Figure 5-1) was designed and fabricated at ASU to ASTM specifications D4123-82. It was similar to the equipment developed by Schmidt (57) with some modifications. It consisted mainly of a compressed air source, solenoid valve, timer, piston, loading frame, measuring devices and a two-channel chart recorder. The laboratory was equipped with a compressed air source which could be controlled by a pressure regulator and a surge tank. A solenoid valve activated by timer was used to provide pulses of compressed air. The compressed air was transmitted to a light pulsating load by means of the piston fixed on top of the loading frame. The load was applied across the vertical diameter of the specimen using two stainless steel loading strips with 0.5 in. width. The loading strips were curved at the interface with the specimen with a radius of 2 in.

The load was measured using a load cell attached to the top loading strip. The output voltage of the load cell was connected to one channel of the chart recorder and was precalibrated using static weights. The horizontal deformation of the specimen was measured using two Linear Variable Differential Transformers (LVDTs) connected to a special frame attached to the specimen. The output voltages of the two LVDT's were merged into one signal and connected to the other channel of the chart recorder. The outputs of the LVDTs were calibrated using a micrometer at temperatures of 41, 77 and 104°F which were used in the test.

The test was conducted inside a large controlled temperature room. A thermometer was buried inside a dummy specimen to indicate the actual temperature of the specimens. It took between 3-4 hours to change the temperature to the required test temperature.

5.1.2. Test Procedure

Before running the resilient modulus test, the saturated surface-dry bulk density of the specimens was determined according to ASTM D2726 procedure. The diametral resilient modulus test was then performed according to ASTM D4123-82 procedure. The following is a brief description of the testing procedure of the resilient modulus test.

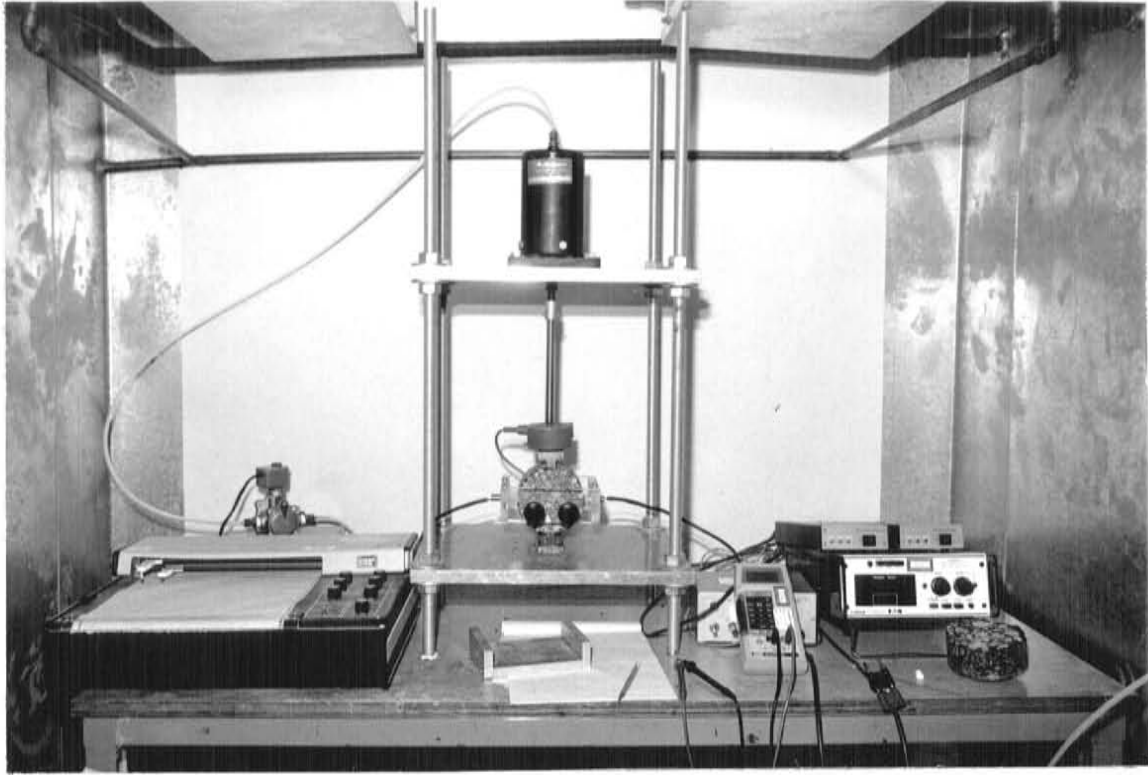


FIGURE 5-1. RESILIENT MODULUS MACHINE FOR ASPHALT CONCRETE TESTING

When the specimen reached the required test temperature it was placed in the resilient modulus test machine. Care was taken to ensure that the specimen was exactly centered between the two loading strips. The frame was then attached to the specimen and the LVDT's were glued to the specimen at its horizontal diametral plane. The output voltages of the LVDT's were adjusted in order that the LVDTs be used within their linear ranges. A pulse load of 30 to 85 lb was then applied across the vertical diameter of the specimen every 2 seconds with a duration of 0.1 second. The load was applied 150 times for conditioning the specimen before the results were recorded. The specimen was rotated 90° and tested again in the new position using the same steps. In order to reduce the permanent deformation in the specimen, testing was sequenced from 41°F then 77 and 104°F.

5.1.3. Test Results

A typical plot of load and horizontal deformation is shown in Figure 5-2. The instantaneous and total resilient moduli were calculated using the following equations.

$$E_{ri} = P(v_{ri} + 0.27)/t \cdot \Delta H_i \quad (5-1)$$

$$E_{rt} = P(v_{rt} + 0.27)/t \cdot \Delta H_t \quad (5-2)$$

where:

- E_{ri} = Instantaneous resilient modulus of elasticity (psi)
- E_{rt} = Total resilient modulus of elasticity (psi)
- v_{ri} = Instantaneous resilient Poisson's ratio
- v_{rt} = Total resilient Poisson's ratio
- P = Repeated load (lb)
- t = Thickness of specimen (in.)
- ΔH_i = Instantaneous recoverable horizontal deformation (in)
- ΔH_t = Total recoverable horizontal deformation (in)

Both instantaneous and total Poisson's ratios were assumed to be 0.3, 0.35 and 0.4 at temperatures of 41, 77 and 104°F, respectively. The modulus is taken as the average of the two values obtained in the two perpendicular positions. Tables 5-1, 5-2 and 5-3 show a summary of the density, instantaneous resilient modulus and total resilient modulus of the specimens at test temperatures of 41, 77 and 104°F, respectively. Detailed resilient modulus data are presented in Appendix C.

The resilient modulus results show that the modulus value decreases when the temperature increases. Also, the instantaneous resilient modulus is typically larger than the total resilient modulus and they are well correlated. The use of the instantaneous resilient modulus is more common than the total resilient modulus since the former represents the "elastic" modulus of the material more than the latter. The instantaneous modulus was used in Chapter 6 for comparison with the back-calculated moduli obtained from the NDT data.

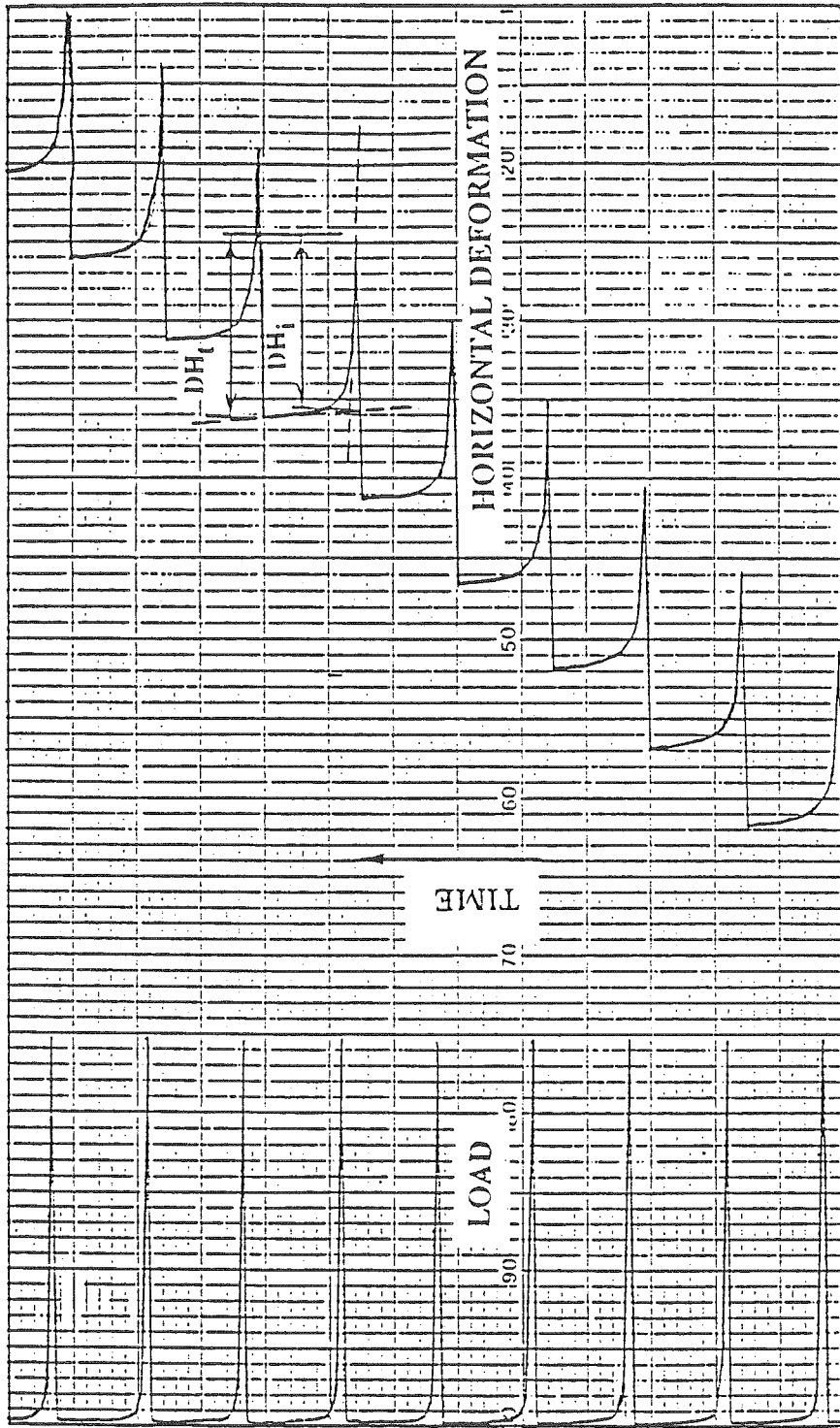


FIGURE 5-2. TYPICAL LOAD AND HORIZONTAL DEFORMATION OBTAINED DURING THE RESILIENT MODULUS TEST

Table 5-1. Summary of density and average resilient moduli of asphalt concrete samples at 41 F

| Site/ Station/ Sample no. | Density (pcf) | Average inst. resilient modulus (ksi) | Average total resilient modulus (ksi) |
|------------------------------------|----------------------|---|---|
| 1/1/1 | 129.4 | 1226 | 1062 |
| 2/1/1 | 148.7 | 3045 | 2131 |
| 2/1/2 | 146.8 | 3111 | 2705 |
| 3/1/1 | 135.2 | 3292 | 2532 |
| 3/1/2 | 145.7 | 1067 | 910 |
| 3/7/1 | 134.7 | 5377 | 4067 |
| 4/1/1 | 132.1 | 3638 | 2430 |
| 4/1/2 | 146.6 | 4016 | 1906 |
| 5/4/1 | 167.5 | 2446 | 1936 |
| 5/4/2 | 145.4 | 1397 | 1194 |
| 6/1/1 | 146.5 | 2133 | 1400 |
| 6/1/2 | 135.2 | 1875 | 804 |
| 6/1/3 | 141.9 | 1376 | 977 |
| 7/4/2 | 153.8 | 2334 | 1794 |
| 8/1/1 | 150.7 | 1075 | 821 |
| 8/1/2 | 141.6 | 1507 | 1162 |
| 9/1/1 | 144.0 | 1858 | 1186 |
| 9/1/2 | 147.7 | 3567 | 2945 |
| 10/4/2 | 153.1 | 2855 | 2217 |
| 11/5/1 | 154.0 | 3776 | 2937 |
| 12/1/1 | 146.8 | 2268 | 1564 |
| 12/1/2 | 146.2 | 4939 | 2573 |
| 13/1/1 | 156.9 | 3778 | 3181 |
| 13/4/1 | 158.2 | 2470 | 2117 |
| 14/4/1 | 140.2 | 1155 | 920 |
| 15/4/1 | 146.7 | 2879 | 1869 |
| 15/4/2 | 152.4 | 2924 | 2215 |
| 16/1/1 | 148.9 | 2993 | 2589 |
| 17/1/1 | 142.3 | 1427 | 1148 |
| 18/1/1 | 147.9 | 2586 | 2277 |
| 19/4/1 | 125.6 | 1315 | 1176 |
| 19/4/2 | 124.3 | 950 | 842 |
| 20/1/1 | 148.3 | 3182 | 2786 |
| 20/1/2 | 145.7 | 4850 | 4021 |

Table 5-2. Summary of density and average modulus of asphalt concrete samples at 77 F

| Site/ Station/ Sample no. | Density (pcf) | Average inst. resilient modulus (ksi) | Average total resilient modulus (ksi) |
|------------------------------------|----------------------|---|---|
| 1/1/1 | 129.4 | 1209 | 1036 |
| 2/1/1 | 148.7 | 999 | 829 |
| 2/1/2 | 146.8 | 541 | 378 |
| 3/1/1 | 135.2 | 814 | 642 |
| 3/1/2 | 145.7 | 675 | 618 |
| 3/7/1 | 134.7 | 1376 | 1173 |
| 4/1/1 | 132.1 | 1319 | 1097 |
| 4/1/2 | 146.6 | 1269 | 1088 |
| 5/4/1 | 167.5 | 987 | 681 |
| 5/4/2 | 145.4 | 411 | 310 |
| 6/1/1 | 146.5 | 549 | 403 |
| 6/1/2 | 135.2 | 892 | 709 |
| 6/1/3 | 141.9 | 487 | 340 |
| 7/4/2 | 153.8 | 1672 | 1430 |
| 8/1/1 | 150.7 | 700 | 539 |
| 8/1/2 | 141.6 | 426 | 374 |
| 9/1/1 | 144.0 | 761 | 599 |
| 9/1/2 | 147.7 | 1557 | 1230 |
| 10/4/2 | 153.1 | 1312 | 992 |
| 11/5/1 | 154.0 | 2191 | 1920 |
| 12/1/1 | 146.8 | 641 | 503 |
| 12/1/2 | 146.2 | 1593 | 1356 |
| 13/1/1 | 156.9 | 954 | 693 |
| 13/4/1 | 158.2 | 1049 | 829 |
| 14/4/1 | 140.2 | 518 | 409 |
| 15/4/1 | 146.7 | 657 | 473 |
| 15/4/2 | 152.4 | 1135 | 860 |
| 16/1/1 | 148.9 | 1569 | 1422 |
| 17/1/1 | 142.3 | 630 | 532 |
| 18/1/1 | 147.9 | 1219 | 1031 |
| 19/4/1 | 125.6 | 741 | 623 |
| 19/4/2 | 124.3 | 645 | 551 |
| 20/1/1 | 148.3 | 1093 | 863 |
| 20/1/2 | 145.7 | 2242 | 1727 |

Table 5-3. Summary of density and average resilient moduli of asphalt concrete samples at 104 F

| Site/ Station/ Sample no. | Density (pcf) | Average inst. resilient modulus (ksi) | Average total resilient modulus (ksi) |
|------------------------------------|----------------------|---|---|
| 1/1/1 | 129.4 | 133 | 110 |
| 2/1/1 | 148.7 | 76 | 66 |
| 2/1/2 | 146.8 | -- | -- |
| 3/1/1 | 135.2 | 398 | 359 |
| 3/1/2 | 145.7 | 329 | 289 |
| 3/7/1 | 134.7 | -- | -- |
| 4/1/1 | 132.1 | 822 | 696 |
| 4/1/2 | 146.6 | 757 | 645 |
| 5/4/1 | 167.5 | 76 | 68 |
| 5/4/2 | 145.4 | 137 | 119 |
| 6/1/1 | 146.5 | 77 | 66 |
| 6/1/2 | 135.2 | 412 | 347 |
| 6/1/3 | 141.9 | -- | -- |
| 7/4/2 | 153.8 | 787 | 661 |
| 8/1/1 | 150.7 | 156 | 141 |
| 8/1/2 | 141.6 | 168 | 131 |
| 9/1/1 | 144.0 | 88 | 66 |
| 9/1/2 | 147.7 | 460 | 372 |
| 10/4/2 | 153.1 | 254 | 205 |
| 11/5/1 | 154.0 | 505 | 423 |
| 12/1/1 | 146.8 | 272 | 226 |
| 12/1/2 | 146.2 | 960 | 886 |
| 13/1/1 | 156.9 | 127 | 107 |
| 13/4/1 | 158.2 | 528 | 457 |
| 14/4/1 | 140.2 | 128 | 102 |
| 15/4/1 | 146.7 | 331 | 259 |
| 15/4/2 | 152.4 | 472 | 403 |
| 16/1/1 | 148.9 | 665 | 522 |
| 17/1/1 | 142.3 | 286 | 231 |
| 18/1/1 | 147.9 | 230 | 201 |
| 19/4/1 | 125.6 | 171 | 146 |
| 19/4/2 | 124.3 | 117 | 99 |
| 20/1/1 | 148.3 | 109 | 84 |
| 20/1/2 | 145.7 | 976 | 841 |

5.2. BASE AND SUBBASE MATERIALS

Samples of base and subbase materials were collected from the 20 sites. The base course material is either bituminous treated, cement treated or unstabilized aggregate as shown in Table 3-6. The subbase material is select material.

Sieve analysis tests were performed on samples of untreated aggregate and select materials at the first 15 sites. The gradation of these materials are shown in Table 5-4.

Bituminous treated bases could not be tested for resilient modulus because the samples did not have smooth surfaces. One CTB sample obtained from site 7 was tested for resilient modulus and the corresponding modulus was 500 ksi. The test proved that the diametral resilient modulus machine can be used for testing CTB samples; however, a large load has to be applied (about 80 lb) in order to get a measurable deformation.

5.3. SUBGRADE MATERIALS

5.3.1. Equipment

An automated microcomputer-controlled triaxial testing system was used to measure the resilient modulus of the subgrade materials in the laboratory. A copy of a photo of the apparatus is shown in Figure 5-3. The system can be described in major components as follows.

(1) Load Frame and Test Chamber

The base of the load frame is a thick anodized aluminum plate which is attached to the upper cross-head beam with 1 1/2" stainless steel threaded rods with nuts. The test chamber is comprised of anodized aluminum bottom and top plates, held together with large ss hex rods. Compressed between the top and bottom cell plates is a 5" I.D., 1/4" wall plexiglass tube, to provide visibility of the specimen. The test chamber is equipped with a very low friction "air bushing" and the piston is guided with two ss Thompson ball bushings. The axial load on the piston was measured with an interface load cell and the vertical displacements were measured with two schaevitz LVDT's. Other transducers available, but not used in this test series, include validyne differential pressure transducers for effective stress, cell pressure, and volume change. However, a regulated back pressure was applied through the specimen base and held constant as an internal pore air pressure and a regulated external air pressure was held constant inside the cell. The difference between these pressures was reported as the confining stress. The axial load on the piston was generated with a 2" I.D. double-acting air piston loader with a 3" stroke. A constant, regulated pressure, called the "steady" pressure, was applied to the lower chamber of the double-acting piston. The pressure applied to the upper chamber was termed the "cyclic" pressure because it was caused to "cycle" by the cyclic loading control unit. The deviator load on the test specimen (which was 2.8" in diameter and

TABLE 5-4. GRADATION OF AGGREGATE AND SELECT MATERIALS AT VARIOUS SITES

| Site | 1 | 2 | 3 | 4 | 5 | 6 | 7 | 8 |
|----------------------|--------|--------|--------|--------|--------|----------------------|--------|--------|
| Sampling Depth (in.) | 12-24 | 8-17 | 15-20 | 13-16 | 13-19 | 9-19 | 14-20 | 18-23 |
| Material Type | Select | Select | Select | Select | Select | Aggregate/ Select | Select | Select |
| % Passing | | | | | | | | |
| No. 4 | 88 | 76 | 97 | 95 | 96 | 65 | 93 | 99 |
| No. 8 | 64 | 62 | 91 | 91 | 92 | 40 | 88 | 96 |
| No. 16 | 45 | 49 | 82 | 83 | 90 | 27 | 81 | 92 |
| No. 30 | 30 | 38 | 60 | 66 | 86 | 20 | 69 | 83 |
| No. 50 | 16 | 26 | 23 | 33 | 72 | 13 | 42 | 51 |
| No. 100 | 4 | 14 | 5 | 11 | 39 | 8 | 14 | 14 |
| No. 200 | 0 | 4 | 2 | 4 | 22 | 4 | 5 | 4 |

TABLE 5-4. GRADATION OF AGGREGATE AND SELECT MATERIALS AT VARIOUS SITES (CONTINUED)

| Site | 9 | 10 | 11 | 12 | 12 | 13 | 14 | 15 |
|------------------------|--------|--------|-------|-----------|--------|-----------|-----------|-----------|
| Sampling Depth(in.) | 10-36 | 12-25 | ----- | 6-12 | 12-30 | 7-11 | 9-13 | 9-14 |
| Material Type | Select | Select | None | Aggregate | Select | Aggregate | Aggregate | Aggregate |
| % Passing | | | | | | | | |
| No. 4 | 78 | 89 | | 63 | 99 | 58 | 46 | 82 |
| No. 8 | 63 | 78 | | 44 | 95 | 43 | 35 | 66 |
| No. 16 | 50 | 68 | | 31 | 86 | 29 | 25 | 50 |
| No. 30 | 38 | 56 | | 19 | 72 | 18 | 17 | 33 |
| No. 50 | 25 | 41 | | 9 | 57 | 11 | 12 | 15 |
| No. 100 | 14 | 24 | | 4 | 36 | 7 | 8 | 6 |
| No. 200 | 7 | 12 | | 2 | 12 | 4 | 4 | 2 |

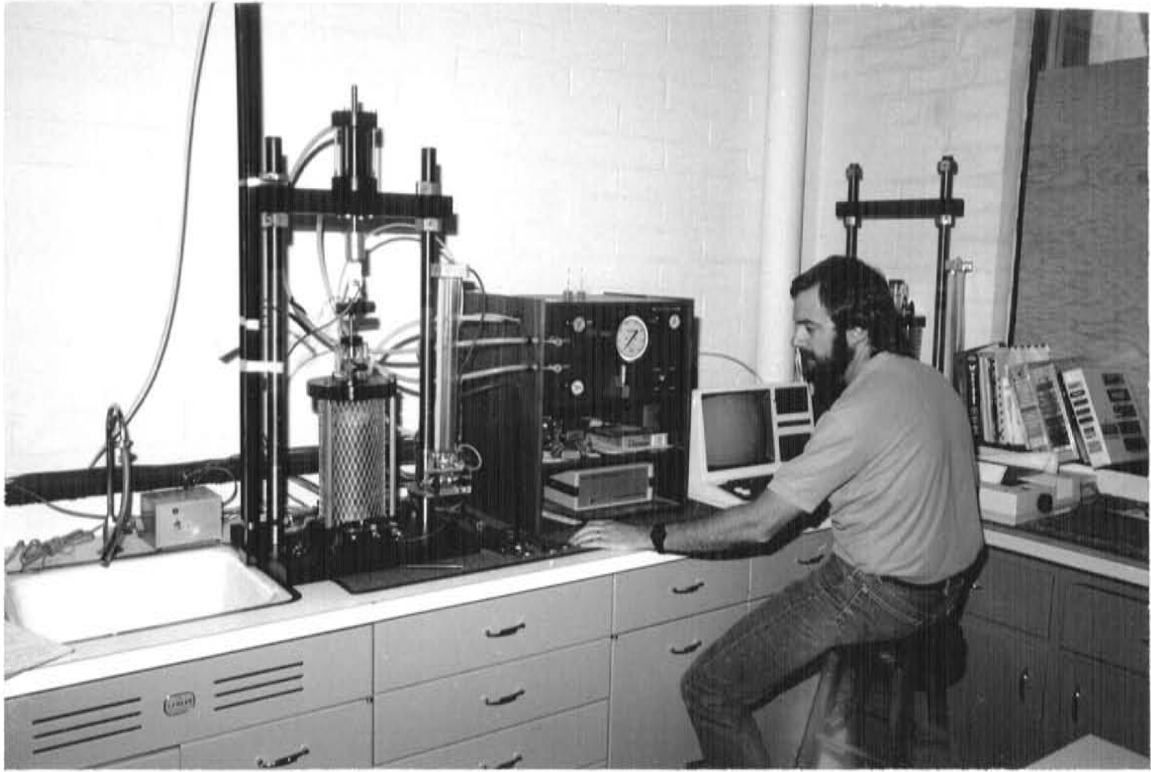


FIGURE 5-3. TRIAXIAL RESILIENT MODULUS APPARATUS FOR SUBGRADE MATERIAL TESTING

about 6.5" to 7" high) corresponded to the amount by which the cyclic pressure exceeded the steady pressure.

(2) Signal conditioning unit

The analog signals from the load cell, LVDT's, and cell pressure transducer were transmitted to a 20-channel Validyne module case, which houses the signal conditioning module for each channel of data. Signal conditioning includes amplification as required so that all signals ranged from 0 to about 10 VDC full scale. Each signal could be displayed one at a time on the digital voltmeter in the Validyne, for checking or calibration. Other signal conditioning included the use of a non-inverting summing amplifier to average the signals from the two LVDT's before transmission to the Validyne.

(3) Process Interface

After amplification to the 0-10 VDC range the signals were transmitted in analog from a Process Interface, a unit manufactured by S and L Instrumentation Co. This unit serves as an interface between the Validyne and the microcomputer. The signals are further conditioned in the process interface, including conversion from analog to digital form, before transmission to the microcomputer.

(4) Microcomputer

A TRS-80 Model 4 microcomputer is used via a series of software packages to collect, reduce, and plot the data. During the test itself, the software package provides closed-loop control of the test. The programs are mostly interactive so the user can specify the desired test conditions, such as stress control vs. strain control, desired rate of load increase, pulse shape for dynamic loading, confining stress, drainage conditions, etc. Test control is accomplished as follows.

- a) Readings from each channel are collected and reduced by the computer.
- b) A comparison is made between the results obtained and the test conditions desired (e.g., for strain rate control, the strain rate obtained is compared with the strain rate requested)
- c) The computer sends a command (in digital form) to the Process Interface, as needed to correct the test condition.
- d) The Process Interface converts the digital command to a voltage and sends the voltage to the electro-pneumatic transducer inside the cyclic loading control unit.
- e) The e/p transducer converts the electrical signal to a pulse of air pressure with the same shape as the electrical signal.
- f) The pulse of air pressure is amplified (boosted) and then transmitted to the "cyclic" chamber of the double-acting loading piston.
- g) The response to this new increment in load is then registered by the transducers and transmitted to the computer, thus "closing the loop." Cell pressure is likewise computer controlled as required.

The microcomputer is also connected to dot-matrix printer which displays data in tabular and/or graphical form.

(5) Cyclic Loading Control Unit

The control unit is a cabinet which houses a variety of components including air filter, e/p transducers, volume boosters, relays, switching valves, pressure gages, and pressure regulators. Some of these components are used to control test conditions manually, such as steady and back pressures, while other components are under computer control.

5.3.2. Calibration

The LVDT's were calibrated individually with the use of a micrometer to determine their personal calibration factor and linear range corresponding to this factor. They were then attached to the triaxial apparatus and wired into the non-inverting summing amplifier to determine the calibration factor of both LVDT's together. This was performed with the aid of an axial dial gage which was also attached to the triaxial cell. The piston was then moved a known distance on the dial gage and the corresponding voltage was recorded from the Validyne signal conditioning unit.

The load cell (Interface - SSM 1000) was calibrated with the aid of a proving ring which had previously been calibrated with Bureau of Standards traceable weights. The static calibration was performed by varying the pressure on the loading system and noting the corresponding proving ring deflection and voltage.

Due to the dynamic loads and the duration of load (0.2 sec), a dynamic calibration of the load cell and the LVDT's was performed using an oscilloscope. The peaks were recorded on the oscilloscope and were then compared to the computer output. This was performed at various different loads and deflections to get an average correction factor. This factor was determined to be 1.042 for the load cell and 1.11 for the LVDT's. The overall correction factor, the load cell factor divided by the LVDT factor, was 0.9387, and this factor was multiplied directly to the calculated modulus values to obtain resilient modulus values corrected for dynamic response.

5.3.3. Testing Procedure

The testing procedure followed in measuring the resilient moduli of the subgrade materials was based generally on the AASHTO-T274-82 procedure. However, it was deemed necessary and desirable to deviate from the AASHTO procedure in a number of aspects which will be discussed in this section. Before discussing these deviations, however, it is necessary to review the definition of the resilient modulus and to make clear what is meant by stress level and stress level sensitivity.

(1) Resilient Modulus

The resilient modulus is defined as the ratio of the repeated stress to the recoverable strain. Therefore, the intent of the pre-conditioning loading phase of the resilient modulus test is to induce any plastic strains which are

prone to occur, so that mostly elastic strains remain when loading to measure resilient modulus occurs later. Ideally, the pre-conditioning loading phase would entail application of stresses comparable to those imposed by traffic loads when the test specimen was in-situ. If the sampling and specimen preparation process were "perfect," i.e., disturbance-free, then reapplication of traffic loads would produce no new plastic strains because plastic strains would have already occurred in-situ. However, the sampling process is not "perfect" and some plastic strains do occur during pre-conditioning. Pre-conditioning is an attempt to erase the effects of disturbance. The degree to which this attempt is generally successful is difficult to assess, but there is no doubt that pre-conditioning loading tends to erase the effects of disturbance.

(2) Stress Level

It is a well-established fact that when stresses on a soil specimen are increased to a level higher than ever applied previously, plastic strains will occur. Therefore, resilient modulus cannot be measured for such a cycle of loading. Stresses may be described broadly as either normal stresses or shear stresses. When discussing stress level it is important to distinguish between normal stress level and shear stress level, because normal and shear stresses produce somewhat differing effects on a soil specimen. When a specimen is "over-stressed" by normal stress, plastic strains occur and bonds between particles are broken. However, they are reformed at higher normal stress and the net effect of having been loaded to a higher normal stress is that the specimen is now denser, stiffer, and stronger than it was. By contrast, when the shear stress is raised to a level higher than ever before, plastic strains result in the breaking of bonds which either do not reform or new bonds which are typically weaker than previous bonds. Therefore, the net effect of increasing the shear stress to a new high is to produce a specimen which is softer and weaker than before. Thus, the effect on modulus of shear stress elevation is opposite to the effect of normal stress elevation. In the laboratory, separation of and distinction between shear and normal stresses is relatively easy. In the field, wheel loads produce both shear and normal stresses, and which effect is likely to predominate varies with the point of consideration within the pavement structure.

(3) Stress Level Sensitivity

In light of the preceding discussion, it is obvious that the measured modulus would be "sensitive" to an increase in either normal or shear stress to levels higher than ever applied before. However, in this case, plastic strains would occur and resilient modulus could not be measured. Thus resilient modulus stress level sensitivity must be quantified only when the following conditions are met:

- a) The stresses applied (both shear and normal) are less than or equal to the maximum level of stress previously applied.
- b) The stress has been applied a sufficient number of times that the strains become essentially entirely recoverable (elastic).

This means that quantification of resilient modulus sensitivity to stress level for this research project corresponds to assessing the extent to which the elastic strains exhibit non-linearity.

With the proceeding background discussion and definitions established, it is now possible to efficiently describe the deviations from the AASHTO Resilient Modulus test procedure.

(4) Deviations from the AASHTO-T274-82 Procedure

After a careful examination of the AASHTO Procedure it was concluded that the following deviations were justified.

- a) Stress State. As part of pre-conditioning the AASHTO Procedure calls for levels of both normal and shear stresses which are in most cases well beyond those estimated to have been applied by in-situ traffic loading. For example, T274 calls for application of shear stresses to triaxial specimens of clayey soils when the confining pressure is zero, a condition which never exists for a subgrade in-situ. Accordingly, a pre-conditioning program for each site was established as follows.
1. The pavement structure geometry was established for each site from the boring logs.
 2. Moduli for the various layers were estimated from available back-calculated values based on NDT data.
 3. Maximum past stress state was estimated using the computer program ELSYM5, together with an assumed axle overload to 22 kips. For this computation the modulus of the asphalt concrete was adjusted in accordance with available pavement temperature data.
 4. The computed stresses were expressed in terms of octahedral shear and normal stresses and formed a "triangle" representing the maximum past stress states for the subgrade at each site. An example of a stress triangle is shown in Appendix E.
 5. A conditioning program and a testing procedure were then established for each test specimen using the load triangle. In general, each specimen was conditioned for 1000 cycles at a low state of stress, 1000 cycles at a medium state of stress, and 2000 cycles at the maximum state of stress, corresponding to the apex of the triangle. The specimen was then loaded for 200 cycles at various lower stress states, to measure the resilient modulus and to check for stress level sensitivity.
- b) Pre-conditioning. The AASHTO Procedure calls for pre-conditioning by cyclic loading to only 200 cycles at each stress state. It was consistently found that cyclic loading to several thousand cycles was needed to remove the plastic strains.
- c) Preparation of Specimen Ends. In order to assure an intimate contact between the specimen ends and the end platens, a layer of Burkestone -- a quick hardening cement -- was placed on the platens and allowed to set-up with the platens in place and the loading piston aligned and screwed into the top cap. If a bonding agent like this were not used, the interfaces between the specimen and the end platens might

be compressible and produce significant error in the measured modulus.

An outline of the sample preparation and the Triaxial Test Sequence used is given in the following sections.

(5) Sample Preparation

The following procedure was used in preparing a sample for resilient modulus testing:

- a) Cut sample tube to size (if necessary) with a hacksaw. Clean inside of tube with a deburrer to ensure smooth surface for extrusion.
- b) Trim sample bottom until flush and smooth.
- c) Place Burkestone (high strength, fast setting cement) on greased cap and place on trimmed sample bottom.
- d) Let cement harden and remove cap.
- e) Mark location of porous stone in the Burkestone and drill a small hole for air communication.
- f) Mark tube and base to assure hole alignment.
- g) Place thin layer of Burkestone on base (around porous stone), line up marks and place on sample bottom.
- h) Place tube in extruding apparatus and apply a small pressure to allow a good bond between two layers of Burkestone. Let set for 15 minutes, or until hard.
- i) Extrude until 7 inches of sample is still in tube.
- j) Trim off excess soil, dig soil down 5mm maximum and make level.

(6) Triaxial Test Sequence

After the specimen has been extruded, weighed, and measured, the following steps are followed to prepare the sample for testing.

- a) Screw the specimen base into the bottom of the triaxial cell.
- b) Screw the loading piston into the specimen cap, place a thin layer of Burkestone on the cap, loosen ram screw, and place entire top of triaxial cell on top of the three tie rods and confirm centering. Ease piston down by hand until Burkestone is in contact with sample top. Vibrate the piston until the entire surface of the specimen top is covered with Burkestone and there are no voids between the cap and the specimen. Let Burkestone set until hard, usually about 15 minutes.
- c) Holding cap by hand, screw out piston and remove entire top assembly. Place membrane in membrane expander and apply a vacuum to the expander to pull membrane out tight. Place membrane over specimen, remove vacuum and pull membrane away from expander.
- d) Place o-rings on o-ring expander and place one on the base and then one on the cap over the membrane.
- e) Assemble entire cell including plastic chamber, screw piston into cap, tighten down top of cell and then tighten piston ram screw.
- f) Place in the loading frame, align and attach piston to clamp, then clamp triaxial cell to the bottom plate.
- g) Place the dual VDT's into their holders, place the extensions in place using potters clay to assure no movement during the test, and

- adjust the LVDT's so that the linear range is maximized. (This is usually achieved by measurement so that each LVDT's core is equidistant from its shaft)
- h) Attach back pressure line to the triaxial cell. Specimen is now ready for testing.
 - i) Microcomputer software package is now activated and cyclic testing is completed through response to computer prompts.

5.3.4. Resilient Modulus Test Results

The average values of the subgrade resilient moduli from lab testing are shown in Table 5-5. The laboratory test specimens were subjected to a range of confining stress as well as deviator stress in order to assess sensitivity to both types of stress. The values shown in Table 5-5 represent the average of all the test values for the various levels of stress.

A more detailed listing of the test results is given in Appendix D. For each combination of confining stress and deviator stress a best estimate value of modulus was determined. The range shown in Appendix D for each of these moduli corresponds to the range of reasonable interpretations that could be applied in computing the moduli from the hysteresis loops obtained.

The data in Table 5-5 show that the lab moduli vary from about 6.4 to 16 ksi. These values are reasonable for moduli of the materials encountered in this study. The comparisons of lab and NDT back-calculated moduli are discussed in Chapter 6. The stress level sensitivity indicated by these lab tests is discussed in Chapter 6 as well. The Atterberg limits of subgrade materials at various sites are shown in Table 5-6. Table 5-7 shows other subgrade material properties as well as R-values reported by ADOT using samples combined from different depths.

TABLE 5-5. SUMMARY OF AVERAGE RESILIENT MODULI OF SOILS SAMPLES

| Site/ Station | Sample Depth (in.) | Dry Density (pct) | Water Content (%) | Confining Stress (kPa) | Deviator Stress (kPa) | Resilient Modulus (ksi) |
|------------------|--------------------------|-------------------------|-------------------------|------------------------------|-----------------------------|-------------------------------|
| 1/1 | 25-32 | 122.1 | 5.28 | 14-31 | 18-93 | 10.43 |
| 2/1 | 19-25 | 118.6 | 7.09 | 12-30 | 18-69 | 13.30 |
| 2/7 | 38-45 | 111.6 | 7.83 | 20-27 | 18-38 | 15.51 |
| 3/7 | 27-34 | 112.3 | 12.4 | 14-31 | 18-86 | 6.44 |
| 4/1 | 25-32 | 111.8 | 10.4 | 17-41 | 20-86 | 9.59 |
| 5/4 | 20-27 | 119.9 | 12.4 | 20-33 | 19-62 | 12.19 |
| 6 | Stiff Layer | | | | | |
| 7/4 | 27-34 | 120.0 | 9.23 | 15-77 | 19-77 | 11.36 |
| 8/1 | 31-38 | 112.88 | 11.1 | 21-29 | 19-47 | 7.99 |
| 9/1 | 50-57 | 104.2 | 22.8 | 26-31 | 19-71 | 16.14 |
| 10/4 | 44-51 | 97.0 | 25.9 | 25-33 | 21-49 | 12.48 |
| 11/1 | 12-19 | 122.8 | 2.21 | 16-48 | 19-80 | 13.33 |
| 12/1 | 32-39 | 120.3 | 8.56 | 15-25 | 18-58 | 7.41 |
| 13/4 | 13-20 | 110.4 | 8.81 | 12-25 | 20-65 | 14.35 |
| 14/4 | 12-19 | 101.7 | 15.4 | 9-22 | 19-58 | 10.42 |
| 15 | Bad Samples | | | | | |
| 16/1 | 17-24 | 117.7 | 7.9 | 12-25 | 20-61 | 9.59 |
| 17/1 | 20-26 | 104.9 | 17.8 | 12-25 | 20-57 | 4.82 |
| 18 | Bad Samples | | | | | |
| 19/1 | 23-30 | 104.2 | 22.7 | 15-27 | 20-55 | 12.01 |
| 19/4 | 31-38 | 96.3 | 28.9 | 15-27 | 19-53 | 15.64 |
| 20 | Bad Samples | | | | | |

TABLE 5-6. ATTERBERG LIMITS OF SUBGRADE MATERIALS

| Site/Station | Depth(in.) | LL | PI | Classification |
|--------------|------------|----|----|----------------|
| 1/1 | 25-32 | 18 | 5 | SC-SM |
| 1/4 | 25-32 | -- | NP | SM |
| 2/1 | 19-25 | 31 | 5 | SM |
| 3/7 | 27-34 | 18 | NP | SM |
| 4/1 | 24.5-31.5 | -- | NP | SM |
| 5/4 | 20-27 | 22 | NP | SM |
| 5/4 | 27-34 | 17 | NP | SM |
| 7/4 | 27-34 | 15 | NP | SM |
| 8/1 | 31-38 | -- | NP | SM |
| 9/1 | 50-57 | 49 | 27 | CL-CH |
| 10/4 | 44-51 | 62 | 38 | CH |
| 11/1 | 11.5-18.5 | 23 | 5 | SC-SM |
| 11/1 | 18.5-25.5 | -- | NP | SM |
| 12/1 | 32-39 | 20 | 5 | SC-SM |
| 13/4 | 13.5-20 | 28 | 13 | SC |
| 14/4 | 11.5-18.5 | 65 | 31 | SC-CH |
| 15/4 | 14-24 | -- | MP | SM |
| 16/1 | 12.5-24 | -- | NP | SM |
| 17/1 | 12-20 | -- | NP | SM |
| 18/1 | 30-36 | -- | NP | SM |
| 18/4 | 30-36 | -- | NP | GM |
| 19/1 | 16-30 | -- | NP | SM |
| 20/1 | 36-42 | -- | NP | GP |

Note: An attempt was made to measure LL, even when the soil was too non-plastic to measure PL. For several soils, neither LL nor PL could be measured because of non-plasticity.

TABLE 5-7. SUBGRADE PROPERTIES AS REPORTED BY ADOT

| Site | Depth (ft) | LL | PI | Sand Equipment | % Passing 200 | Laboratory R-Value | AASHTO Classification |
|------|------------|----|----|----------------|---------------|--------------------|-----------------------|
| 1 | Combined | 26 | 9 | 17 | 26 | 52 | A-2-4(0) |
| 2 | 5-6 | 22 | 1 | - | 45 | - | A-4 (2) |
| 2 | Combined | 24 | 3 | 21 | 21 | 63 | A-1-b (0) |
| 2 | " | 29 | 8 | 16 | 21 | 58 | A-2-4 (0) |
| 3 | " | 21 | 3 | 3 | 49 | 34 | A-4 (3) |
| 4 | 1-3 | 21 | 2 | - | 23 | - | A-2-4 (0) |
| 4 | 3-10 | 34 | 19 | 2 | 68 | 13 | A-6 (6) |
| 5 | Combined | 21 | 2 | 14 | 19 | 74 | A-2-4 (0) |
| 7 | 1-5 | 19 | 2 | 14 | 24 | 75 | A-2-4 (0) |
| 7 | 5-10 | 32 | 16 | 3 | 50 | 23 | A-6 (5) |
| 8 | - | 31 | 4 | 3 | 60 | 34 | A-4 (5) |
| 9 | - | 44 | 26 | 9 | 65 | 18 | A-7-b (7) |
| 11 | 3-9 | 28 | 4 | 15 | 40 | 53 | A-4 (1) |
| 12 | Combined | 19 | 4 | 20 | 24 | 57 | A-1-b (11) |
| 14 | " | 53 | 31 | 10 | 49 | 15 | A-7-b (11) |
| 15/1 | " | 21 | 3 | 20 | 25 | 67 | A-1-b (0) |
| 16 | " | 28 | 6 | 20 | 31 | 60 | A-2-4 (0) |
| 18 | " | 22 | 3 | 15 | 21 | 72 | A-1-b (0) |
| 19 | - | 30 | 1 | - | 44 | - | A-4 (2) |
| 20 | - | 23 | 1 | 16 | 14 | 82 | A-1-a (0) |

CHAPTER 6. THEORETICAL ANALYSES

6.1. STATISTICAL ANALYSES OF NDT DATA

6.1.1. FWD Data

Descriptive statistics for the 9000 lb drop FWD data are given in Table 6-1. Variability in FWD data at a given site, and for a given load (stress level) has been investigated by plotting the results of the 9000 lb FWD data at each station. One plot is available at each site in Appendix A. The variability in FWD data across a 90 ft span can be studied from these plots. Typical variations were within ± 10 to 20%, but variations were as great as $\pm 100\%$. A typical plot is given in Figure 6-1 for site 2. In addition, the coefficients of variation (standard deviation $\times 100$ / mean) of the FWD data are summarized in Table 6-2. The average coefficient of variation is about 13% for all sites and sensors. The coefficient of variation was approximately the same for each sensor, i.e. sensor 1 showed no more variability than say, sensor 7.

The coefficients of variation presented in Table 6-2 are an indication of the site variability. The variation in FWD data at a particular station and a particular site was significantly less than the site variability. The reproducibility of the FWD data for a given site and station was investigated by computing the coefficients of variation at each station and for the first set of test data. Coefficients of variation are given in Table 6-3 for Station 1 at each site. The FWD data was incredibly reproducible at a given spot, as indicated by the low average coefficient of variation of 1.68 percent for Station 1.

6.1.2. Dynaflect Data

Descriptive statistics for the Dynaflect data are given in Table 6-4. The Dynaflect results, as measured in the field, have been plotted at all stations, sites 1 to 13, and site 15, and the results are presented in Appendix A.

Variability across the site for Dynaflect results was also investigated at each site where the dynaflect data were available. Dynaflect data for stations 1 to 10 were plotted together for these sites to obtain a picture of the site variability. Variability was typically $\pm 20\%$, with considerable scatter (as with the FWD). Refer to Figure 6-2 for a typical plot of Dynaflect data for site 1. The coefficients of variation of the Dynaflect data are summarized in Table 6-5. A comparison of Table 6-3 with Table 6-5 shows that the Dynaflect data are more variable than the FWD data, but only slightly so.

6.2. NONLINEARITY AND STRESS SENSITIVITY

As indicated earlier, the subgrade materials have a nonlinear response to load. However, if the load is repeated several times the effect of nonlinearity is reduced as illustrated in Figure 2-2. The nonlinearity is very large when the load is applied for the first time since the strain is

TABLE 6-1. DESCRIPTIVE STATISTICS OF FWD DATA

| SITE/ SENSOR | MEAN DEFLECTION (MILS) | STANDARD DEVIATION (MILS) | COEFF. OF VARIATION (%) |
|-----------------|------------------------------|---------------------------------|-------------------------------|
| 1/ 1 | 18.4 | 1.8 | 9.5 |
| 2 | 11.5 | 0.8 | 6.6 |
| 3 | 5.8 | 0.5 | 7.8 |
| 4 | 2.9 | 0.5 | 15.9 |
| 5 | 1.7 | 0.4 | 23.1 |
| 6 | 1.1 | 0.3 | 26.3 |
| 7 | 0.8 | 0.2 | 23.5 |
| 2/ 1 | 19.5 | 5.3 | 27.0 |
| 2 | 14.6 | 2.5 | 17.0 |
| 3 | 9.3 | 1.1 | 11.6 |
| 4 | 5.6 | 0.5 | 8.6 |
| 5 | 3.3 | 0.3 | 9.4 |
| 6 | 2.0 | 0.2 | 10.9 |
| 7 | 1.4 | 0.2 | 12.2 |
| 3/ 1 | 8.7 | 1.2 | 13.7 |
| 2 | 6.6 | 0.7 | 11.1 |
| 3 | 4.7 | 0.4 | 8.6 |
| 4 | 3.4 | 0.3 | 7.4 |
| 5 | 2.6 | 0.2 | 7.3 |
| 6 | 2.0 | 0.2 | 8.0 |
| 7 | 1.7 | 0.2 | 9.0 |
| 4/ 1 | 8.7 | 0.8 | 8.7 |
| 2 | 6.4 | 0.7 | 11.2 |
| 3 | 4.5 | 0.5 | 10.4 |
| 4 | 3.4 | 0.3 | 9.9 |
| 5 | 2.6 | 0.2 | 9.0 |
| 6 | 2.1 | 0.2 | 8.0 |
| 7 | 1.7 | 0.1 | 8.3 |
| 5/ 1 | 8.4 | 0.4 | 4.9 |
| 2 | 6.8 | 0.4 | 5.6 |
| 3 | 5.1 | 0.3 | 6.3 |
| 4 | 3.8 | 0.3 | 6.7 |
| 5 | 2.8 | 0.2 | 6.4 |
| 6 | 2.0 | 0.2 | 8.6 |
| 7 | 1.4 | 0.2 | 12.7 |
| 6/ 1 | 7.0 | 0.2 | 3.3 |
| 2 | 6.0 | 0.1 | 2.2 |
| 3 | 4.7 | 0.2 | 3.6 |
| 4 | 2.6 | 0.2 | 8.9 |
| 5 | 2.4 | 0.3 | 10.5 |
| 6 | 1.7 | 0.2 | 14.6 |
| 7 | 1.2 | 0.2 | 18.8 |

TABLE 6-1. DESCRIPTIVE STATISTICS OF FWD DATA (CONT.)

| SITE/ SENSOR | MEAN DEFLECTION (MILS) | STANDARD DEVIATION (MILS) | COEFF. OF VARIATION (%) |
|-----------------|------------------------------|---------------------------------|-------------------------------|
| 7/ 1 | 16.0 | 2.1 | 13.4 |
| 2 | 11.8 | 1.6 | 13.5 |
| 3 | 7.8 | 0.9 | 11.4 |
| 4 | 5.3 | 0.5 | 10.3 |
| 5 | 3.8 | 0.3 | 7.1 |
| 6 | 2.9 | 0.2 | 6.6 |
| 7 | 2.4 | 0.2 | 7.0 |
| 8/ 1 | 7.4 | 1.1 | 15.1 |
| 2 | 6.2 | 0.9 | 14.2 |
| 3 | 4.9 | 0.6 | 11.4 |
| 4 | 3.7 | 0.3 | 9.0 |
| 5 | 2.7 | 0.2 | 6.9 |
| 6 | 2.0 | 0.1 | 6.3 |
| 7 | 1.5 | 0.1 | 8.1 |
| 9/ 1 | 11.7 | 0.4 | 3.4 |
| 2 | 8.8 | 0.3 | 3.4 |
| 3 | 5.8 | 0.1 | 2.3 |
| 4 | 3.5 | 0.1 | 3.9 |
| 5 | 2.2 | 0.1 | 6.1 |
| 6 | 1.4 | 0.1 | 10.1 |
| 7 | 0.9 | 0.1 | 15.0 |
| 10/ 1 | 18.1 | 5.6 | 30.9 |
| 2 | 13.3 | 3.0 | 23.0 |
| 3 | 8.0 | 1.3 | 16.5 |
| 4 | 4.9 | 0.7 | 14.6 |
| 5 | 3.2 | 0.4 | 11.4 |
| 6 | 2.3 | 0.4 | 15.9 |
| 7 | 1.8 | 0.3 | 18.1 |
| 11/ 1 | 6.2 | 0.7 | 11.7 |
| 2 | 3.8 | 0.6 | 15.0 |
| 3 | 2.0 | 0.3 | 16.0 |
| 4 | 1.1 | 0.1 | 13.1 |
| 5 | 0.8 | 0.1 | 15.9 |
| 6 | 0.6 | 0.1 | 16.0 |
| 7 | 0.5 | 0.1 | 17.2 |
| 12/ 1 | 16.6 | 1.0 | 6.1 |
| 2 | 11.1 | 0.5 | 4.3 |
| 3 | 6.1 | 0.2 | 2.8 |
| 4 | 3.3 | 0.1 | 1.8 |
| 5 | 1.9 | 0.1 | 4.8 |
| 6 | 1.3 | 0.1 | 7.4 |
| 7 | 1.0 | 0.1 | 9.8 |

TABLE 6-1. DESCRIPTIVE STATISTICS OF FWD DATA (CONT.)

| SITE/ SENSOR | MEAN DEFLECTION (MILS) | STANDARD DEVIATION (MILS) | COEFF. OF VARIATION (%) |
|-----------------|------------------------------|---------------------------------|-------------------------------|
| 13/ 1 | 9.9 | 2.8 | 28.2 |
| 2 | 6.9 | 2.1 | 30.4 |
| 3 | 3.7 | 1.2 | 31.1 |
| 4 | 1.9 | 0.5 | 29.1 |
| 5 | 1.0 | 0.3 | 26.4 |
| 6 | 0.6 | 0.2 | 27.2 |
| 7 | 0.5 | 0.1 | 32.2 |
| 14/ 1 | 28.7 | 4.7 | 16.2 |
| 2 | 6.4 | 1.0 | 15.3 |
| 3 | 2.0 | 0.2 | 12.4 |
| 4 | 1.2 | 0.1 | 8.6 |
| 5 | 0.9 | 0.0 | 5.1 |
| 6 | 0.7 | 0.0 | 6.3 |
| 7 | 0.6 | 0.0 | 7.5 |
| 15/ 1 | 6.0 | 0.7 | 11.5 |
| 2 | 4.6 | 0.5 | 11.5 |
| 3 | 3.1 | 0.4 | 12.0 |
| 4 | 2.1 | 0.3 | 13.1 |
| 5 | 1.4 | 0.2 | 13.6 |
| 6 | 1.0 | 0.2 | 14.6 |
| 7 | 0.8 | 0.1 | 15.0 |
| 16/ 1 | 22.7 | 4.1 | 17.9 |
| 2 | 13.9 | 2.5 | 18.3 |
| 3 | 7.3 | 1.3 | 17.4 |
| 4 | 4.1 | 0.7 | 16.6 |
| 5 | 2.7 | 0.4 | 13.6 |
| 6 | 2.0 | 0.2 | 12.6 |
| 7 | 1.6 | 0.2 | 12.1 |
| 17/ 1 | 24.6 | 6.5 | 26.5 |
| 2 | 14.6 | 3.9 | 26.3 |
| 3 | 8.1 | 2.1 | 26.1 |
| 4 | 4.8 | 1.3 | 27.8 |
| 5 | 3.2 | 0.9 | 29.5 |
| 6 | 2.3 | 0.7 | 29.1 |
| 7 | 1.9 | 0.5 | 27.0 |
| 18/ 1 | 14.0 | 1.5 | 10.6 |
| 2 | 6.4 | 0.7 | 10.1 |
| 3 | 2.3 | 0.4 | 15.3 |
| 4 | 1.2 | 0.1 | 12.0 |
| 5 | 0.9 | 0.1 | 7.4 |
| 6 | 0.8 | 0.1 | 7.3 |
| 7 | 0.6 | 0.1 | 10.2 |

TABLE 6-1. DESCRIPTIVE STATISTICS OF FWD DATA (CONT.)

| SITE/ SENSOR | MEAN DEFLECTION (MILS) | STANDARD DEVIATION (MILS) | COEFF. OF VARIATION (%) |
|-----------------|------------------------------|---------------------------------|-------------------------------|
| 19/ 1 | 18.2 | 1.5 | 8.2 |
| 2 | 13.3 | 1.1 | 8.4 |
| 3 | 8.5 | 0.8 | 9.2 |
| 4 | 5.4 | 0.5 | 9.4 |
| 5 | 3.5 | 0.4 | 10.6 |
| 6 | 2.5 | 0.3 | 10.5 |
| 7 | 2.0 | 0.2 | 12.0 |
| 20/ 1 | 12.5 | 1.9 | 15.0 |
| 2 | 7.0 | 1.1 | 15.4 |
| 3 | 3.1 | 0.5 | 15.7 |
| 4 | 1.5 | 0.2 | 15.1 |
| 5 | 0.9 | 0.1 | 10.7 |
| 6 | 0.7 | 0.1 | 9.4 |
| 7 | 0.5 | 0.1 | 12.1 |

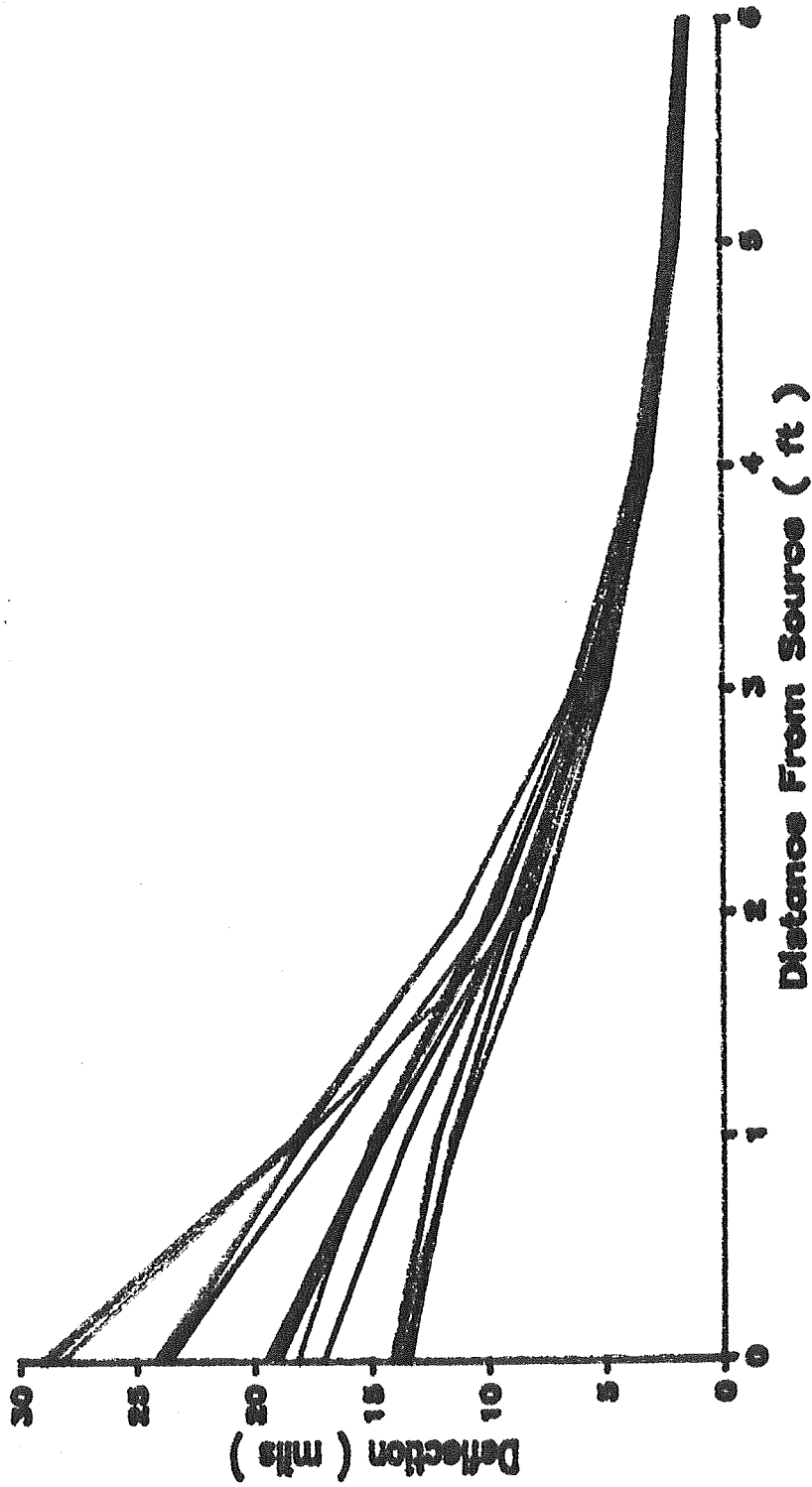


FIGURE 6-1. FWD DATA AT 9000 LB DROP FOR SITE 2

TABLE 6.2 COEFFICIENT OF VARIATION OF FWD DATA WITHIN EACH SITE (%)

| Site | Sensor No. | | | | | | | Average for all |
|----------------------------|------------|----|----|----|----|----|----|--------------------|
| | 1 | 2 | 3 | 4 | 5 | 6 | 7 | |
| 1 | 10 | 7 | 8 | 16 | 23 | 26 | 24 | 16 |
| 2 | 27 | 17 | 12 | 9 | 9 | 11 | 12 | 14 |
| 3 | 14 | 11 | 9 | 7 | 7 | 8 | 9 | 9 |
| 4 | 9 | 11 | 10 | 10 | 9 | 8 | 8 | 10 |
| 5 | 5 | 6 | 6 | 7 | 7 | 9 | 13 | 8 |
| 6 | 3 | 2 | 4 | 7 | 10 | 15 | 19 | 9 |
| 7 | 13 | 14 | 11 | 10 | 7 | 7 | 7 | 10 |
| 8 | 15 | 14 | 11 | 9 | 7 | 6 | 8 | 10 |
| 9 | 3 | 3 | 3 | 4 | 6 | 10 | 15 | 7 |
| 10 | 31 | 23 | 17 | 15 | 11 | 16 | 18 | 19 |
| 11 | 12 | 15 | 16 | 13 | 16 | 16 | 17 | 15 |
| 12 | 6 | 4 | 3 | 2 | 5 | 8 | 10 | 5 |
| 13 | 28 | 30 | 31 | 29 | 27 | 27 | 33 | 29 |
| 14 | 16 | 15 | 12 | 9 | 5 | 7 | 8 | 10 |
| 15 | 12 | 12 | 12 | 13 | 14 | 15 | 15 | 13 |
| 16 | 18 | 18 | 17 | 16 | 13 | 12 | 13 | 15 |
| 17 | 26 | 26 | 26 | 28 | 30 | 29 | 27 | 27 |
| 18 | 11 | 10 | 15 | 12 | 7 | 8 | 11 | 11 |
| 19 | 8 | 8 | 9 | 9 | 11 | 10 | 12 | 10 |
| 20 | 15 | 15 | 16 | 15 | 11 | 10 | 12 | 13 |
| Average of all sites | 14 | 13 | 12 | 12 | 12 | 13 | 15 | 13 |

TABLE 6-3. COEFFICIENT OF VARIATION OF FWD DATA FOR STATION 1
(%) - 9000 lb Drop

| Site | C.V. for Sensor No. | | | | | | | Average for all sensors |
|---------------------------|---------------------|------|------|------|------|------|------|-------------------------------|
| | 1 | 2 | 3 | 4 | 5 | 6 | 7 | |
| 1 | 0.98 | 0.53 | 0.41 | 0.94 | 2.75 | 4.26 | 9.03 | 2.69 |
| 2 | 1.15 | 0.91 | 0.46 | 0.77 | 0.58 | 1.25 | 1.88 | 1.00 |
| 3 | 0.94 | 0.79 | 1.09 | 1.22 | 1.30 | 2.78 | 4.34 | 1.78 |
| 4 | 0.85 | 1.17 | 1.85 | 1.86 | 2.84 | 4.20 | 5.52 | 2.61 |
| 5 | 0.68 | 0.61 | 1.40 | 0.91 | 1.78 | 1.69 | 3.87 | 1.56 |
| 6 | 0.41 | 0.49 | 0.55 | 0.78 | 1.15 | 2.64 | 3.76 | 1.40 |
| 7 | 0.35 | 0.16 | 0.37 | 0.88 | 0.98 | 2.43 | 1.79 | 0.99 |
| 8 | 0.80 | 0.76 | 0.37 | 1.05 | 0.65 | 1.11 | 1.53 | 0.90 |
| 9 | 0.60 | 0.44 | 0.00 | 0.86 | 0.67 | 1.50 | 5.32 | 1.34 |
| 10 | 0.66 | 0.62 | 0.54 | 0.70 | 1.46 | 2.38 | 3.26 | 1.37 |
| 11 | 0.00 | 0.86 | 1.26 | 1.64 | 3.25 | 5.96 | 6.36 | 2.76 |
| 12 | 0.80 | 0.60 | 0.85 | 0.66 | 1.47 | 2.76 | 4.63 | 1.68 |
| 13 | 0.61 | 0.43 | 0.61 | 0.84 | 1.68 | 2.38 | 2.29 | 1.26 |
| 15 | 1.11 | 0.88 | 1.44 | 1.05 | 2.49 | 3.58 | 4.96 | 2.21 |
| Average for all sites* | 0.71 | 0.66 | 0.80 | 1.01 | 1.65 | 2.78 | 4.18 | 1.68 |

* Data from sites 14 and 16 to 20 was not included, but would be expected to exhibit similar low coefficients of variation.

TABLE 6-4. DESCRIPTIVE STATISTICS OF DYNAFLECT DATA

| SITE/ GEOPHONE | MEAN DEFLECTION (MILS) | STANDARD DEVIATION (MILS) | COEFF. OF VARIATION (%) |
|-------------------|------------------------------|---------------------------------|-------------------------------|
| 1/ 1 | 3.7 | 0.9 | 25.6 |
| 2 | 2.4 | 0.7 | 27.5 |
| 3 | 1.3 | 0.5 | 37.1 |
| 4 | 0.8 | 0.3 | 37.1 |
| 5 | 0.5 | 0.2 | 37.0 |
| 2/ 1 | 1.8 | 0.3 | 15.8 |
| 2 | 1.4 | 0.2 | 15.4 |
| 3 | 1.0 | 0.1 | 14.2 |
| 4 | 0.7 | 0.1 | 14.4 |
| 5 | 0.5 | 0.1 | 17.9 |
| 3/ 1 | 3.1 | 0.2 | 7.7 |
| 2 | 2.6 | 0.2 | 9.1 |
| 3 | 2.3 | 0.2 | 6.7 |
| 4 | 2.0 | 0.1 | 6.3 |
| 5 | 1.5 | 0.1 | 5.1 |
| 4/ 1 | 2.9 | 0.3 | 11.1 |
| 2 | 2.6 | 0.2 | 8.6 |
| 3 | 2.2 | 0.2 | 10.9 |
| 4 | 1.9 | 0.2 | 10.7 |
| 5 | 1.5 | 0.1 | 9.8 |
| 5/ 1 | 2.8 | 0.2 | 7.3 |
| 2 | 2.4 | 0.1 | 5.9 |
| 3 | 2.0 | 0.2 | 7.8 |
| 4 | 1.5 | 0.1 | 9.7 |
| 5 | 1.1 | 0.1 | 9.7 |
| 6/ 1 | 2.5 | 0.1 | 3.6 |
| 2 | 2.1 | 0.1 | 3.9 |
| 3 | 1.6 | 0.1 | 5.0 |
| 4 | 1.1 | 0.1 | 9.1 |
| 5 | 0.7 | 0.1 | 11.4 |
| 7/ 1 | 4.8 | 0.7 | 13.7 |
| 2 | 3.9 | 0.5 | 12.1 |
| 3 | 3.1 | 0.3 | 10.9 |
| 4 | 2.4 | 0.3 | 11.7 |
| 5 | 1.8 | 0.2 | 10.3 |
| 8/ 1 | 2.7 | 0.2 | 8.9 |
| 2 | 2.3 | 0.2 | 9.4 |
| 3 | 2.0 | 0.2 | 8.6 |
| 4 | 1.4 | 0.1 | 6.0 |
| 5 | 1.1 | 0.1 | 6.8 |

TABLE 6-4. DESCRIPTIVE STATISTICS OF DYNAFLECT DATA (CONT.)

| SITE/ GEOPHONE | MEAN DEFLECTION (MILS) | STANDARD DEVIATION (MILS) | COEFF. OF VARIATION (%) |
|-------------------|------------------------------|---------------------------------|-------------------------------|
| 9/ 1 | 2.7 | 0.1 | 5.2 |
| 2 | 2.2 | 0.1 | 5.4 |
| 3 | 1.5 | 0.1 | 4.8 |
| 4 | 0.9 | 0.1 | 7.2 |
| 5 | 0.6 | 0.1 | 9.4 |
| 10/ 1 | 5.2 | 1.5 | 29.7 |
| 2 | 3.7 | 0.6 | 16.7 |
| 3 | 2.4 | 0.4 | 14.8 |
| 4 | 1.4 | 0.3 | 19.3 |
| 5 | 0.8 | 0.1 | 11.2 |
| 11/ 1 | 1.4 | 0.2 | 13.6 |
| 2 | 1.0 | 0.2 | 15.3 |
| 3 | 0.7 | 0.1 | 16.2 |
| 4 | 0.4 | 0.1 | 13.0 |
| 5 | 0.3 | 0.0 | 13.4 |
| 12/ 1 | 3.8 | 0.4 | 9.3 |
| 2 | 2.7 | 0.2 | 9.1 |
| 3 | 1.7 | 0.2 | 9.2 |
| 4 | 1.0 | 0.1 | 7.8 |
| 5 | 0.6 | 0.1 | 11.1 |
| 13/ 1 | 2.4 | 0.6 | 24.8 |
| 2 | 1.7 | 0.5 | 28.6 |
| 3 | 1.0 | 0.3 | 27.5 |
| 4 | 0.4 | 0.1 | 25.0 |
| 5 | 0.2 | 0.1 | 26.0 |
| 15/ 1 | 4.5 | 0.9 | 20.3 |
| 2 | 3.4 | 0.4 | 11.4 |
| 3 | 2.2 | 0.1 | 6.6 |
| 4 | 1.2 | 0.2 | 13.3 |
| 5 | 0.7 | 0.1 | 9.6 |

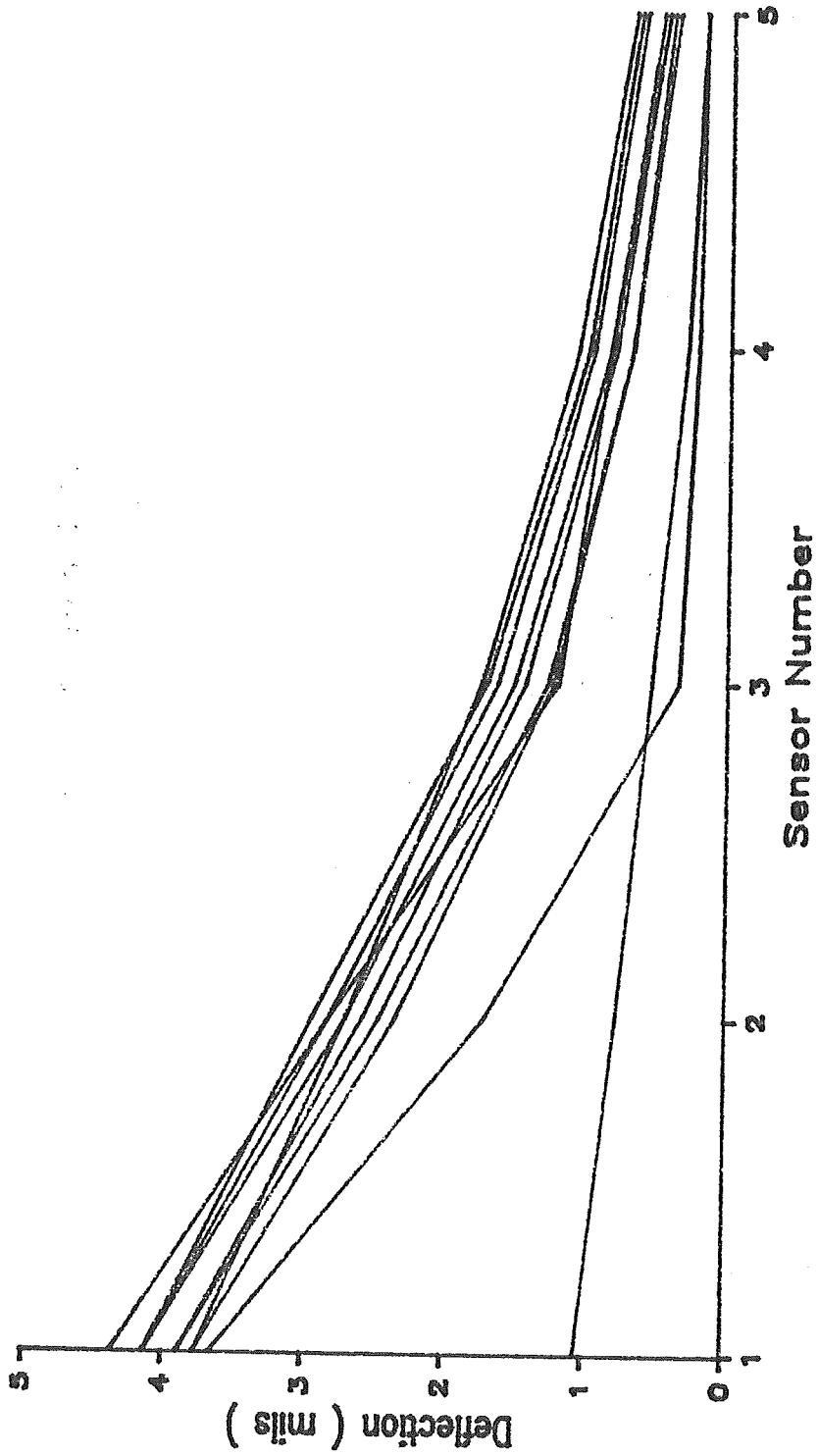


FIGURE 6-2. TYPICAL PLOT OF DYNAFLECT DATA, SITE 1, STATIONS 1-10

TABLE 6-5. COEFFICIENT OF VARIATION OF DYNAFLECT DATA WITHIN EACH SITE (%)

| Site | Geophone | | | | | Average of all sensors |
|----------------------------|----------------|----|----|----|----|------------------------------|
| | 1 | 2 | 3 | 4 | 5 | |
| 1 | 26 | 28 | 37 | 38 | 38 | 33 |
| 2 | 16 | 16 | 14 | 15 | 18 | 16 |
| 3 | 8 | 9 | 7 | 6 | 5 | 7 |
| 4 | 11 | 9 | 11 | 11 | 10 | 10 |
| 5 | 7 | 6 | 8 | 10 | 10 | 8 |
| 6 | 4 | 4 | 5 | 9 | 12 | 7 |
| 7 | 14 | 12 | 11 | 12 | 10 | 12 |
| 8 | 9 | 9 | 9 | 6 | 7 | 8 |
| 9 | 5 | 6 | 5 | 8 | 10 | 7 |
| 10 | 30 | 17 | 15 | 19 | 11 | 18 |
| 11 | 14 | 16 | 16 | 13 | 14 | 15 |
| 12 | 9 | 9 | 9 | 8 | 11 | 9 |
| 13 | 25 | 29 | 28 | 26 | 27 | 27 |
| 14 | was not tested | | | | | |
| 15 | 20 | 11 | 7 | 14 | 10 | 12 |
| Average of all sites | 14 | 13 | 13 | 14 | 14 | 14 |

largely plastic. After many applications the response is still somewhat nonlinear, but much less so.

The modulus is affected by the state of stress of the material. For example, the material properties predicted by the light load of the Dynaflect may not be the same as those predicted by a heavy axle load, even if the difference in the mode of loading is considered. As discussed above, the effect of stress sensitivity is reduced when the load is applied several times.

For example, Figure 2-5 shows the peak stress divided by the corresponding recoverable deflection is almost constant regardless of the applied stress level. However, some variation in the tangent moduli still persists after several load applications.

Although the strains imposed by loading for measurement purposes would be expected to be elastic, they are likely to be non-linear. The significance of this material nonlinearity has been evaluated through a study of the NDT data and the laboratory resilient modulus tests on the subgrade materials.

6.2.1. A Study of Nonlinearity Using NDT Data

A study of nonlinearity was conducted using the NDT data. For stations 1, 5, and 10 at each site where both FWD and Dynaflect data were available, the deflections for the 6000 and 12000 lb tests, as well as the 1000 lb Dynaflect test were "normalized" to equivalent 9000 lb deflections, linearity was assumed for the normalization process. These normalized data were then plotted against the measured 9000 lb deflections, as shown in the typical plot, Figure 6-3. Similar plots for all sites are presented in Appendix A. In general, these normalized deflections indicate that within the range of stress level imposed by the FWD the material nonlinearity is small. This statement is valid for all sensor (geophone) locations, even sensor 7 which is most indicative of subgrade response.

There does appear to be some difficulty in normalizing the data, however, when the stress range considered includes the low stress level applied in the Dynaflect tests. This could be a result of one or more of the following factors: Nonlinearity, data scatter, difference between impulse and harmonic loadings, or difference in material volume tested by FWD and Dynaflect since the FWD uses heavier load than the Dynaflect.

Further quantification of stress sensitivity was achieved by performing a linear regression on the FWD data, including the 6000, 9000, and 12000 lb drops. In the regression analyses deflection was taken as the dependent variable, and stress as the independent variable. The results of the regression analyses are presented in Table 6-6. The coefficients of determination, R^2 , range from 0.26 to 0.98, with a preponderance of R^2 -values around 0.80, indicating that the assumption of linearity is reasonable within the stress range considered in the FWD test series.

- 5700 lbs
- x— 9000 lbs
- ▽— 12100 lbs
- #— 1000 lbs

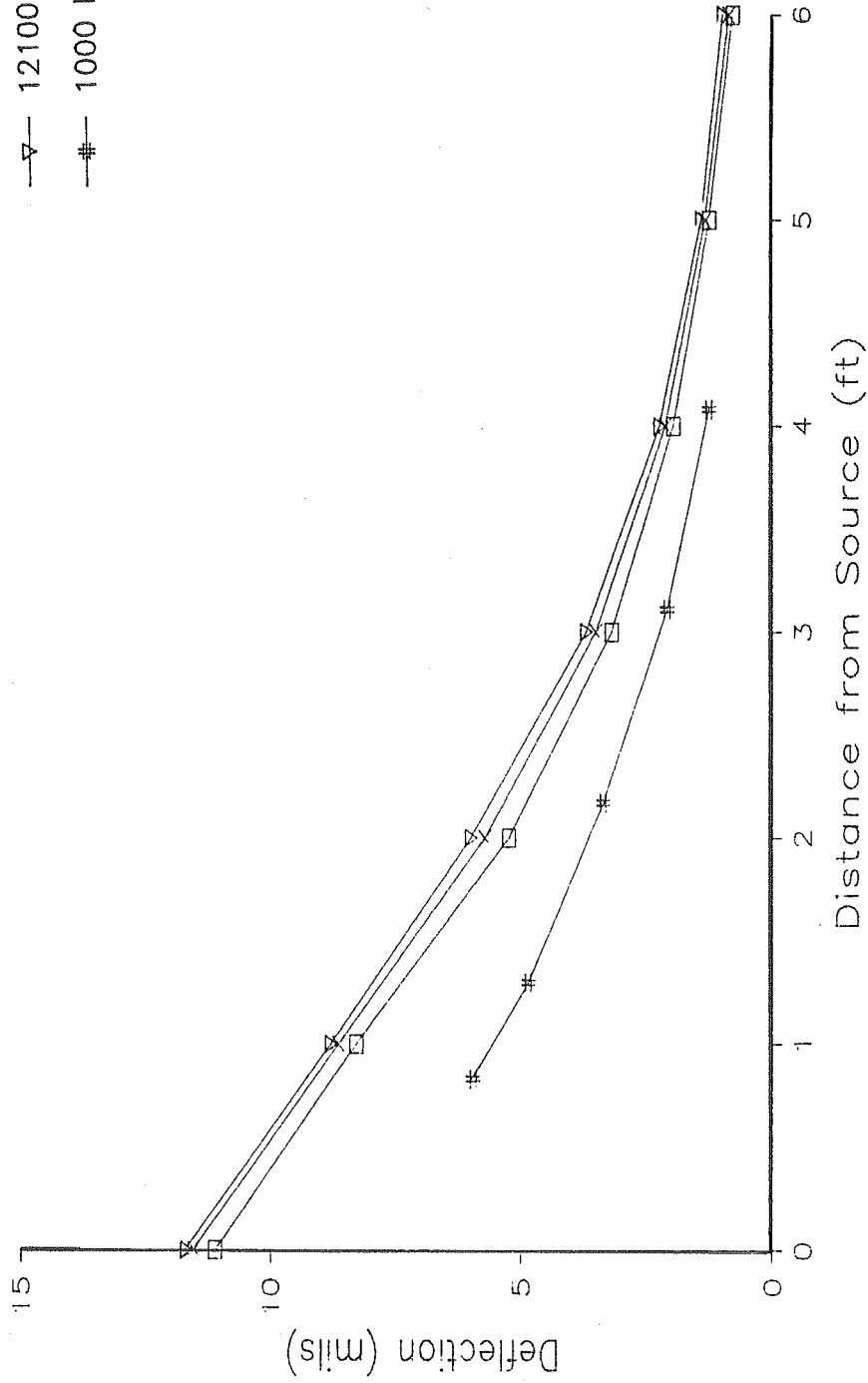


FIGURE 6-3. EQUIVALENT 9000-LB DEFLECTIONS, SITE 9, STATION 10

TABLE 6-6. SUMMARY OF COEFFICIENTS OF DETERMINATION, R^2 FOR FWD DATA
STRESS-DEFLECTION*

| Site | Sensor No. | | | | | | |
|------|------------|------|------|------|------|------|------|
| | 1 | 2 | 3 | 4 | 5 | 6 | 7 |
| 1 | 0.77 | 0.92 | 0.88 | 0.70 | 0.56 | 0.53 | 0.58 |
| 2 | 0.31 | 0.61 | 0.79 | 0.90 | 0.88 | 0.86 | 0.83 |
| 3 | 0.76 | 0.81 | 0.86 | 0.88 | 0.90 | 0.88 | 0.85 |
| 4 | 0.86 | 0.81 | 0.85 | 0.85 | 0.86 | 0.90 | 0.90 |
| 5 | 0.96 | 0.96 | 0.96 | 0.94 | 0.92 | 0.86 | 0.74 |
| 6 | 0.96 | 0.98 | 0.94 | 0.86 | 0.79 | 0.71 | 0.61 |
| 7 | 0.77 | 0.81 | 0.84 | 0.88 | 0.92 | 0.92 | 0.90 |
| 8 | 0.79 | 0.81 | 0.86 | 0.90 | 0.92 | 0.92 | 0.90 |
| 9 | 0.98 | 0.98 | 0.98 | 0.98 | 0.94 | 0.86 | 0.76 |
| 10 | 0.26 | 0.40 | 0.55 | 0.67 | 0.83 | 0.67 | 0.64 |
| 11 | 0.71 | 0.64 | 0.67 | 0.83 | 0.77 | 0.74 | 0.64 |
| 12 | 0.88 | 0.94 | 0.96 | 0.98 | 0.96 | 0.92 | 0.88 |
| 13 | 0.44 | 0.38 | 0.37 | 0.41 | 0.45 | 0.44 | 0.37 |
| 14 | 0.48 | 0.58 | 0.83 | 0.88 | 0.90 | 0.92 | 0.92 |
| 15 | 0.77 | 0.77 | 0.72 | 0.69 | 0.69 | 0.67 | 0.66 |
| 16 | 0.64 | 0.66 | 0.71 | 0.74 | 0.79 | 0.81 | 0.83 |
| 17 | 0.41 | 0.46 | 0.52 | 0.50 | 0.48 | 0.49 | 0.52 |
| 18 | 0.79 | 0.79 | 0.72 | 0.81 | 0.92 | 0.90 | 0.86 |
| 19 | 0.86 | 0.86 | 0.85 | 0.83 | 0.83 | 0.83 | 0.77 |
| 20 | 0.61 | 0.69 | 0.71 | 0.77 | 0.83 | 0.88 | 0.86 |

* Deflection is the dependent variable, stress the independent variable. All FWD stress levels were considered (6000 to 12000 lb drops)

Although the average coefficient of variation at a given site was only slightly higher for the Dynaflect than for the FWD, the range in the data for the Dynaflect was much greater than for the FWD. This indicates that the preponderance of data for the Dynaflect were generally closer to the mean deflection, but that the scatter of data was greater than for the FWD.

6.2.2. Comparison of Site Variability to Nonlinear Effects

The range in deflection data from the 6000 and 12,000 lb FWD tests, as well as the Dynaflect data were normalized to 9000 lb and compared with the 9000 FWD data, as discussed previously. The deviation, expressed as a percent, was calculated by subtracting the equivalent 9000 lb deflection from the measured average 9000 lb deflection. Thus the percent deviation for the 9000 lb FWD test indicates the variability in measurements across the site. In general, the percent deviations calculated for the 6000 lb and 12,000 lb FWD tests were less than the percent deviation obtained from site variability. However, the percent deviations obtained for the Dynaflect equivalent deflections were generally much greater than for the site variability. Thus the "error" expected from assuming that the pavement system behaves as a linear rather than nonlinear material is less than the "error" resulting in spacial variability in properties for stress ranges within the 6000 to 12,000 lb FWD tests. However, assuming linearity over stress ranges extending as low as that for the Dynaflect test would result in greater error than that expected from site variability. This is likely due in part to stress sensitivity, and in part due to data scatter. Bar charts generated from the NDT data which investigated the range in the "9000 lb" normalized deflections for the various field tests were transmitted to ADOT during the March 24, 1987 meeting.

6.2.3. Stress Sensitivity - Laboratory Subgrade Tests

The resilient modulus values obtained from the laboratory testing program on the subgrade materials are presented in Chapter 5. An inspection of Tables in Appendix D shows that for the most clayey soils, sites 9 and 10, the resilient modulus did not vary significantly with confining pressure changes, or with deviator stress changes. However, for the more granular subgrade materials the resilient modulus is sensitive to confining pressure. These trends were anticipated because in general, cohesionless (granular) materials are more sensitive to confining pressure changes than clayey materials.

The confining stress sensitivity of the subgrade material alone, for the case of granular subgrade, is slightly higher than for the pavement system as a whole, as obtained from the studies of NDT data.

Sensitivity of subgrade samples to deviator stress changes would in general be expected, and the expected trend would be decreasing modulus with increasing deviator stress. However, for the laboratory resilient modulus test conducted as a part of this study, the deviator stresses were too low to establish this trend. Further discussion of the effects of confining stress level and deviator stress level is given in Appendix E.

6.3. BACK-CALCULATION OF LAYER MODULI

6.3.1. Background

As indicated earlier, no direct theoretical solution is available in the literature to determine material properties of multi-layered systems if the surface deflections and the layer thicknesses are known. Therefore, it is necessary to employ iterative schemes by varying the material properties until the measured deflection is satisfied. Since Poisson's ratios do not significantly affect the computed deflections, only the layer moduli need to be adjusted.

The back-calculation techniques used vary from one computer program to another. In all cases initial moduli values are assumed and the corresponding surface deflections are computed. The layer moduli are then adjusted using an iterative process until the computed deflections match the measured deflections within a specified tolerance.

The larger the allowable tolerance, the more likely the final values are to depend on the initially assumed values of modulus. However, it is frequently desirable to allow significant tolerance on the difference between the computed and measured deflection because convergence is often times impossible with very tight tolerances. Fortunately, in the CART overlay design procedure described in Chapter 8, the final overlay thickness is not particularly sensitive to the backcalculated moduli provided the shape of the deflection basin is fairly well matched.

Several backcalculation computer programs have been reviewed, including CHEVDEF(50), BKCHEV(58), MODCOM2(59) and others. Some deficiencies were found in these back-calculation techniques such as the unreasonable estimates of the layer moduli or the inability to change the depth to bedrock (or stiff layer) automatically. A modification to program BKCHEV was finally selected as the backcalculation procedure for the CART overlay design method. This program, to be described in detail later in this section, is a simplified microcomputer version of BKCHEV, providing many default values, such as for seed values of layer moduli. In the final version of the backcalculation program all iterations are completely automated.

6.3.2. Research-Phase Backcalculation Studies

In the early part of the study it was decided to use a trial-and-error procedure to evaluate the layer moduli. In this procedure, a set of typical layer moduli and a specific depth to bedrock were assumed and the static and dynamic multilayer elastic programs were used to compute the surface deflections. The layer moduli, as well as the depth to bedrock, were then varied based on the fact that deflections remote from the loaded area are primarily governed by the stiffness of deeper layers. This process was repeated until the computed deflections were close to the measured deflections. Although this manual procedure was time consuming, the operator had the ability to guarantee reasonable estimates of layer moduli, the ability to vary the depth to bedrock, and the ability to use several layers. This procedure was used as a research tool only, in an effort to enhance understanding of the problem and to aid in the subsequent simplifications.

During this research phase of backcalculation analysis, it was decided to represent most of the pavement sites with multilayer systems consisting of:

1. asphalt concrete surface layer
2. base: either stabilized or unstabilized
3. subbase: usually select material or aggregate in most cases
4. a 9 in. compacted subgrade layer in most cases
5. uncompacted subgrade
6. a bedrock or very stiff layer (rigid bottom)

Table 6-7 shows the material properties and thicknesses of various layers used in these analyses.

During the early research phase of the project, both static and dynamic backcalculation analyses were performed. The Chevron program was used in the static analysis, while the DYNAMIC1 program (harmonic loading) and the DYNAMIC2 program (impulse loading) were used in the dynamic analysis. Four sets of layer moduli and depth to rigid bottom were developed under the following four conditions.

1. Static analysis of FWD data
2. Dynamic analysis of FWD data
3. Static analysis of Dynaflect data
4. Dynamic analysis of Dynaflect data

The backcalculated moduli and the corresponding estimated depths to the rigid bottom are shown in Tables 6-8 through 6-11. The back-calculated moduli and the corresponding estimated depth to rigid bottom under the different conditions are different in many cases. Note that sites 14 and 16 to 20 were not tested with the Dynaflect. Also, no dynamic backcalculations of FWD data were performed on these sites.

Since the NDT was performed at different temperatures, the back-calculated asphalt moduli had to be adjusted to a standard temperature to allow for a direct comparison between the back-calculated moduli and the laboratory moduli. The standard temperature was selected to be 77°F. The temperature adjustment method reported in the new AASHTO pavement design manual (Appendix L of the manual) (60) was used in the study. The method required the knowledge of the pavement surface temperature during NDT and the average air temperature for the last 5 previous days. The required air temperature data at all sites were obtained from the Laboratory of Climatology at Arizona State University. Phase relationships between load and deflection as well as stresses, strains and deflections at various points in the pavement sections were computed and stored for further analysis.

6.3.3. Backcalculation Procedure for the CART Overlay Method

For the purpose of the routine overlay design the BKCHEVM program was developed to provide an automated backcalculation procedure. BKCHEVM is a microcomputer program, compatible with the Microsoft Fortran compiler. The program is to be used in the CART overlay method for backcalculation of Young's moduli for the layered pavement system, given the in situ measured deflections from a Falling Weight Deflectometer test. BKCHEVM is a modification to program BKCHEV. The modifications have been relatively minor,

Table 6-7 MATERIAL TYPES AND LAYER THICKNESSES AT DIFFERENT SITES

| Site/ Statn | Layer 1 | | Layer 2 | | Layer 3 | | Layer 4 | | Subgrade class. |
|----------------|---------|---------------|---------|---------------|---------|---------------|---------|---------------|--------------------|
| | Matl. | Thick (in) | Matl. | Thick (in) | Matl. | Thick (in) | Matl. | Thick (in) | |
| 1/1 | AC | 7 | BS | 2.5 | AB | 2 | Select | 12 | SC-SM |
| 2/1 | AC | 6 | BS | 2.5 | Select | 9 | CS | 9 | SM |
| 2/7 | AC | 6.25 | BTB | 2.5 | Select | 9 | CS | 9 | SM |
| 3/1 | AC | 12 | BTB | 3 | Select | 5 | CS | 9 | SM |
| 3/7 | AC | 12.5 | BTB | 3 | Select | 5 | CS | 9 | SM |
| 4/1 | AC | 11.5 | BTB | 2 | Select | 3 | CS | 9 | SM |
| 5/1 | AC | 8 | CTB | 4.5 | Select | 7 | CS | 9 | SM |
| 5/4 | AC | 8 | CTB | 5 | Select | 6 | CS | 9 | SM |
| 6/1 | AC | 9 | AB | 4 | Select | 12 | CS | 9 | - |
| 7/1 | AC | 8 | CTB | 6 | Select | 6 | CS | 9 | SM |
| 7/4 | AC | 6.25 | CTB | 6.75 | Select | 6 | CS | 9 | SM |
| 8/1 | AC | 11 | CTB | 7 | Select | 5 | CS | 9 | SM |
| 9/1 | AC | 6 | BS | 4 | Select | 26 | SGS | 6 | CL-CH |
| 10/1 | AC | 6 | AB | 6 | Select | 24 | CS | 9 | CH |
| 10/4 | AC | 6.5 | AB | 6 | Select | 24 | CS | 9 | CH |
| 10/7 | AC | 6.5 | AB | 6 | Select | 24 | CS | ** | CH |
| 11/1 | AC | 3.25 | BS | 3 | | | CS | ** | SC-SM |
| 11/5 | AC | 2.75 | BS | 2.75 | | | CS | ** | SC-SM |
| 12/1 | AC | 6 | AB | 6 | Select | 18 | CS | 9 | SC-SM |
| 13/1 | AC | 4 | BS | 3 | AB | 4 | CS | 9 | SC |
| 13/4 | AC | 4 | BS | 4 | AB | 4 | CS | ** | SC |
| 14/4 | AC | 9 | BS | 4 | AB | 4 | CS | ** | SC-CH |
| 15/1 | AC | 6 | BS | 3 | AB | 5 | CS | 9 | SM |
| 15/4 | AC | 6 | BS | 3 | AB | 5 | CS | 9 | SM |
| 16/1 | AC | 3.75 | BS | 2 | SM | 6.5 | CS | 9 | |
| 17/1 | AC | 3.25 | BS | 2 | SM | 6 | CS | 9 | |
| 18/1 | AC | 4.25 | AB | 4 | SM | 15 | CS | 9 | |
| 18/4 | AC | 4.1 | AB | 4 | SM | 15 | CS | 9 | |
| 19/1 | AC | 4.8 | BS | 2.2 | AB | 3 | SM | 6 | |
| 19/4 | AC | 4.8 | BS | 2.2 | AB | 3 | SM | 6 | |
| 20/1 | AC | 9.5 | AB | 4 | SM | 15 | CS | 9 | |

Notes:

1. AC : Asphalt concrete, BS :Bituminous treated
BTB: Bituminous treated base, AB: Aggregate base
CS: Compacted subgrade, SGS: Subgrade seal
2. Material types of layers 1,2 and 3 were obtained from construction records.
3. Thickness of layers 1, 2 and 3 were obtained from logs.
4. Layer 4 is compacted subgrade except in sites 1/1 and 9/1. The thickness of layer 4 was assumed as 9 inches for use in the backcalculating process except for sites 1/1 and 9/1. The thickness of layer 4 for the sites indicated by an astrix varies with the different backcalculation methods in order to obtain convergence (see Tables 6-8 to 6-11)
5. Subgrade soil classification is based on the unified soil classification.

TABLE 6-8. BACKCALCULATED MODULI AND THICKNESS OF UNCOMPACTED SUBGRADE USING STATIC ANALYSIS OF FWD DATA (ASPHALT MODULI ARE ADJUSTED TO 77 F)

| Site/ Station | Modulus (ksi) | | | | | Thickness of uncomp. SG (in) |
|------------------|---------------|--------|--------|---------|-----------|------------------------------------|
| | Layer1 | Layer2 | Layer3 | Layer4 | Uncomp SG | |
| 1/1 | 88 | 17 | 23 | 20 | 18 | 140 |
| 2/1 | 600 | 197 | 100 | 70 | 18 | 96 |
| 2/7 | 360 | 98 | 350 | 125 | 13.5 | 120 |
| 3/1 | 150 | 26 | 30 | 30 | 21 | >480 |
| 3/7 | 185 | 26 | 30 | 30 | 20 | >480 |
| 4/1 | 172 | 52 | 75 | 50 | 20.5 | >480 |
| 5/1 | 278 | 140 | 60 | 15 | 7 | 85 |
| 5/4 | 186 | 275 | 120 | 25 | 7 | 82 |
| 6/1 | 218 | 60 | 50 | 30 | 6.5 | 60 |
| 7/1 | 93 | 25 | 20 | 15 | 10 | 300 |
| 7/4 | 139 | 20 | 13.5 | 13.5 | 13.5 | >480 |
| 8/1 | 392 | 90 | 50 | 30 | 12 | 120 |
| 9/1 | 466 | 38 | 19 | 15 | 8.5 | 72 |
| 10/1 | 234 | 30 | 10 | 20 | 19 | >480 |
| 10/4 | 54 | 15 | 15 | 12 | 10 | 240 |
| 10/7 | 63 | 20 | 10 | 20/24* | 16 | >480 |
| 11/1 | 583 | 77 | -- | 100/30* | 19 | 80 |
| 11/5 | 518 | 98 | -- | 85/30* | 19.5 | 80 |
| 12/1 | 227 | 30 | 20 | 17 | 10.5 | 100 |
| 13/1 | 532 | 36 | 25 | 25 | 18 | 150 |
| 13/4 | 504 | 51 | 60 | 45/45* | 24 | 60 |
| 14/4 | 87 | 37 | 7 | 40/48* | 25 | 120 |
| 15/1 | 65 | 31 | 20 | 15 | 5 | 100 |
| 15/4 | 162 | 18 | 18 | 15 | 8 | 120 |
| 16/1 | 92 | 59 | 40 | 20 | 11.5 | 240 |
| 17/1 | 46 | 9 | 15 | 20 | 9 | 300 |
| 18/1 | 462 | 30 | 20 | 40 | 50 | >480 |
| 18/4 | 420 | 30 | 25 | 90 | 22 | 120 |
| 19/1 | 154 | 12 | 30 | 30 | 10 | 240 |
| 19/4 | 112 | 12 | 30 | 20 | 11 | 240 |
| 20/1 | 88 | 40 | 40 | 60 | 45 | 150 |

* thickness of layer in inches

TABLE 6-9. BACKCALCULATED MODULI AND THICKNESS OF UNCOMPACTED SUBGRADE USING DYNAMIC ANALYSIS OF FWD DATA (ASPHALT MODULI ARE ADJUSTED TO 77 F)

| Site/ Station | Modulus (ksi) | | | | | Thickness of uncomp SG (in) |
|------------------|---------------|--------|--------|---------|-----------|-----------------------------------|
| | Layer1 | Layer2 | Layer3 | layer4 | Uncomp SG | |
| 1/1 | 56 | 23 | 30 | 25 | 20 | 67 |
| 2/1 | 680 | 295 | 100 | 50 | 19.5 | 60 |
| 2/7 | 680 | 295 | 160 | 60 | 16 | 68 |
| 3/1 | 179 | 16 | 25 | 22 | 18.5 | >480 |
| 3/7 | 179 | 16 | 25 | 20 | 18 | >480 |
| 4/1 | 177 | 52 | 75 | 30 | 17 | >480 |
| 5/1 | 371 | 120 | 28 | 14 | 12.7 | 72 |
| 5/4 | 390 | 250 | 38 | 15 | 13 | 72 |
| 6/1 | 281 | 50 | 30 | 21 | 20 | 72 |
| 7/1 | 134 | 22 | 12 | 11 | 10.5 | 90 |
| 7/4 | 70 | 25 | 25 | 12 | 10.2 | 90 |
| 8/1 | 392 | 80 | 25 | 18 | 17 | 86 |
| 9/1 | 504 | 34 | 18 | 17 | 14 | 60 |
| 10/4 | 36 | 14 | 17 | 12 | 9.8 | 70 |
| 10/7 | 36 | 16 | 17 | 16 | 10.5 | 70 |
| 11/1 | 389 | 256 | -- | 100/32* | 32 | 72 |
| 11/5 | 486 | 77 | -- | 70/40* | 29 | 60 |
| 12/1 | 220 | 22 | 20 | 18 | 16.5 | 55 |
| 13/1 | 644 | 13 | 25 | 23.6 | 23.4 | 84 |
| 13/4 | 224 | 154 | 180 | 120 | 27 | 58 |
| 14/4 | 113 | 55 | 15 | 30/24* | 22 | 100 |
| 15/1 | 94 | 18 | 12 | 9.3 | 8.4 | 60 |
| 15/4 | 259 | 18 | 12 | 11.5 | 10.8 | 60 |

* thickness of layer in inches

TABLE 6-10. BACKCALCULATED MODULI AND THICKNESS OF UNCOMPACTED SUBGRADE USING STATIC ANALYSIS OF DYNAFLECT DATA (ASPHALT MODULI ARE ADJUSTED TO 77 F)

| Site/ Station | Modulus (ksi) | | | | | Uncomp SG | Thickness uncomp. SG (in) |
|------------------|---------------|--------|--------|---------|--|-----------|---------------------------------|
| | Layer1 | Layer2 | Layer3 | Layer4 | | | |
| 1/1 | 40 | 33 | 40 | 30 | | 20 | 90 |
| 2/1 | 600 | 197 | 200 | 70 | | 20 | 75 |
| 2/7 | 600 | 197 | 200 | 70 | | 13 | 75 |
| 3/1 | 185 | 104 | 30 | 22 | | 16.5 | >480 |
| 3/7 | 290 | 156 | 30 | 22 | | 14 | >480 |
| 4/1 | 370 | 52 | 75 | 50 | | 16.8 | >480 |
| 5/1 | 371 | 250 | 25 | 20 | | 18.3 | >480 |
| 5/4 | 464 | 250 | 25 | 25 | | 23 | >480 |
| 6/1 | 94 | 60 | 50 | 35 | | 15.5 | 90 |
| 7/1 | 162 | 25 | 20 | 15 | | 10.5 | >480 |
| 7/4 | 232 | 25 | 20 | 15 | | 13.5 | >480 |
| 8/1 | 322 | 90 | 50 | 29 | | 20 | >480 |
| 9/1 | 815 | 47 | 30 | 15 | | 12.6 | 70 |
| 10/1 | 234 | 70 | 14 | 13.5 | | 13.5 | 87 |
| 10/4 | 36 | 15 | 15 | 15 | | 9.5 | 60 |
| 11/1 | 259 | 77 | -- | 120/32* | | 11 | 80 |
| 11/5 | 194 | 38 | -- | 65/60* | | 22 | 80 |
| 12/1 | 162 | 85 | 24 | 20 | | 19 | 100 |
| 13/1 | 420 | 77 | 40 | 40 | | 20.5 | 64 |
| 13/4 | 448 | 64 | 80 | 70 | | 42.5 | 72 |
| 14/4 | 150 | 75 | 40 | 30/24* | | 22 | 84 |
| 15/1 | 81 | 18 | 25 | 13 | | 11.7 | 100 |
| 15/4 | 98 | 38 | 50 | 20 | | 14 | 100 |

* thickness of layer in inches

TABLE 6-11. BACKCALCULATED MODULI AND THICKNESS OF UNCOMPACTED SUBGRADE USING DYNAMIC ANALYSIS OF DYNAFLECT DATA (ASPHALT MODULI ARE ADJUSTED TO 77 F)

| Site/ Station | Modulus (ksi) | | | | | Thickness | |
|------------------|---------------|--------|--------|---------|-----------|-----------------------|--|
| | Layer1 | Layer2 | Layer3 | Layer4 | Uncomp SG | of uncomp. SG (in) | |
| 1/1 | 40 | 26 | 40 | 30 | 22.5 | 90 | |
| 2/1 | 600 | 197 | 200 | 70 | 22 | 75 | |
| 2/7 | 1040 | 214 | 200 | 100 | 14 | 75 | |
| 3/1 | 264 | 104 | 30 | 22 | 14.5 | >480 | |
| 3/7 | 317 | 42 | 50 | 25 | 20 | 320 | |
| 4/1 | 290 | 52 | 75 | 50 | 16 | >480 | |
| 5/1 | 348 | 250 | 25 | 18 | 18 | >480 | |
| 5/4 | 464 | 350 | 40 | 19 | 13.2 | 100 | |
| 6/1 | 120 | 60 | 50 | 20 | 20 | 90 | |
| 7/1 | 162 | 25 | 20 | 14 | 9.5 | >480 | |
| 7/4 | 255 | 35 | 20 | 15 | 13 | >480 | |
| 8/1 | 308 | 90 | 50 | 29 | 19 | >480 | |
| 9/1 | 815 | 47 | 30 | 15 | 15 | 70 | |
| 10/1 | 230 | 70 | 14.5 | 14.5 | 9.6 | 40 | |
| 10/4 | 36 | 15 | 15 | 17 | 10.7 | 50 | |
| 11/1 | 454 | 77 | -- | 120/32* | 14.5 | 40 | |
| 11/5 | 486 | 102 | -- | 90/24* | 16 | 40 | |
| 12/1 | 162 | 85 | 24 | 20 | 18.5 | 70 | |
| 13/1 | 225 | 66 | 40 | 40 | 22 | 60 | |
| 13/4 | 448 | 64 | 80 | 70 | 47 | 72 | |
| 14/4 | 130 | 50 | 45 | 60/18* | 40 | 72 | |
| 15/1 | 64 | 16 | 18 | 14.5 | 14.5 | 100 | |
| 15/4 | 162 | 18 | 20 | 14 | 13.5 | 100 | |

* thickness of layer in inches

and have been designed primarily to simplify use and to improve ability to converge. In addition, the iterative scheme (described in detail below) has been modified to obtain a closer match between measured and computed deflection for the inner three sensors so that the strain in the AC will be more representative.

Four distinct layers are assumed in the analysis, and a rock layer may be introduced automatically (i.e. within the program) when it is judged appropriate, based on the measured deflection of the outer sensor. As a part of the simplification process, several default values have been provided for in the computer program. Default values are listed for the user, and the option to modify these values is available. BKCHEVM may only be used to analyze the results of the FWD test. All input is interactive. Output consists of a reflection of input parameters, final layer moduli, and the final error between measured and computed values of deflection at "convergence." When convergence is not reached, the "best-fit" set of layer moduli (based on the sum of the errors of the deflections) will be provided to the user.

The iterative scheme used to obtain the layer moduli in program BKCHEVM is as follows:

1. Using Ullidtz's equation (61) obtain the seed value of the subgrade modulus to be used. Ullidtz's equation, given below, provides an estimate of the subgrade modulus, based on the measured FWD deflection of the outer sensor. The default limits on the subgrade modulus are $0.7E_{Ullidtz}$ to $1.3 E_{Ullidtz}$.

$$E = \frac{P (1-\nu^2)}{\pi(r+d_r)} \quad (6-1)$$

where P = total load (lb.) r = radial dist. to 7th sensor(in)
 ν = Poisson's ratio d_r = measured deflection of sensor 7

2. If the seed modulus of the subgrade, from step 1, is greater than 50,000 psi, a rigid (rock) layer will be automatically introduced at a depth of 20 ft below the subgrade surface.
3. Set the individual tolerances for each sensor to
 $((0.1 \text{ mil}) / (\text{measured deflection in mils})) \times 100$
 or 1.0%, whichever is greater. The effect of computing tolerances by this procedure is to place a heavy weighting on the inner three sensors for the purpose of obtaining a close match of the strain at the bottom of the AC. The inner sensor tolerance will typically be about 1%, while the outer sensor tolerance will be about 10%, with a gradual variation between the inner and outer sensor tolerances.
4. The total allowable sum of the errors is set equal to 90 percent of the sum of the allowable individual tolerances, from step 3.

5. If both of the criteria, outlined above as steps 3 and 4, are not met within four iterations, the individual tolerances at each sensor will be increased by 50% of the original values.
6. If still no convergence is obtained (after four more iterations) the limits on the moduli of the layers (generated as defaults, if desired by the user) will be increased as follows:

New lower bound moduli = 0.7 of old lower bound

New upper bound moduli = 1.3 of old upper bound.

The limits on the moduli of the individual layers will only be changed if these have been "bumped up against" during previous iterations.

Four more iterations will be performed.
7. If still no convergence is obtained, the "best fit" results, based on the lowest sum of the errors in deflections ever achieved, will be printed out for the user.

As mentioned previously, modifications to the original program BKCHEV have been relatively minor. The most significant change that has been implemented is the modification to the convergence criteria which requires a closer match of the deflections for the inner three sensors. A parametric study was performed which demonstrated that the tensile strain computed at the bottom base of the AC was relatively insensitive to selection of a wide range in modulus for the base, subbase, and subgrade. However, the computed tensile strain at the bottom of the AC was quite sensitive to the selection of AC modulus. Therefore, the modification which requires a close match of the deflections of the inner three sensors, and a corresponding improvement of the computed strain at the bottom of the AC, represents an improvement, particularly when these backcalculated moduli are to be used in a fatigue analysis which has, as a major consideration, the tensile strains that are developed at the bottom of the AC.

6.4. CORRELATION AMONG VARIABLES

6.4.1. Comparison between Static and Dynamic Results

As indicated in Section 6.3, both static and dynamic analyses were used to back-calculate the layer moduli from the Dynaflect and the FWD results. In the static analysis, the Chevron program was used, while in the dynamic analysis the DYNAMIC1 program was used with the Dynaflect data and the DYNAMIC2 program was used with the FWD data. In all cases, a trial and error procedure was used to get the best estimates of layer moduli and depth to a stiff layer (rigid bottom) that resulted in matching the computed deflection with the measured deflection. This process resulted in four sets of moduli for each site as shown in Tables 6-8 through 6-11.

The dynamic backcalculation technique used on this project represents a more accurate modeling of the actual loading than does static backcalculation.

The results of dynamic backcalculation are believed to be more accurate than those from static backcalculation. However, the differences in resulting moduli have been found to be relatively small, typically of the same order as the probable error in the moduli.

In view of these small differences, it has been particularly difficult to obtain hard facts to prove one set of calculations superior to the other. At the outset of the project it was hoped that the lab test values would cast some light on this question. However, it was subsequently shown that the lab modulus for subgrade, for example, represents only a 7-inch thick layer near the top of the subgrade; whereas, the backcalculated value represents a single-weighted average value influenced by material as deep as 10 or 20 feet.

Furthermore, subsequent cone penetration data showed that considerable layering typically exists within the first 10 or 20 feet of subgrade, and that the actual modulus varies widely within this range (see Figures 4-5 through 4-9). Therefore, when the subgrade is treated as a single layer (without benefit of cone penetration data, e.g.) and a single average value for the entire subgrade is calculated, it would simply be an accident if this single backcalculated value agreed closely with the lab value for the subgrade.

The differences in the static and dynamic backcalculated "depth to bedrock" were somewhat more pronounced than differences in moduli. The drilling (to 25 feet) and cone penetration testing were used to check which set of calculated depths were more reasonable. The depths backcalculated from dynamic analysis were very slightly better than those from the static analysis, but neither set gave excellent agreement.

For backcalculation, it was assumed that there was a single uniform subgrade down to a "hard rock" layer. What was found in the field were a few sites with "hard rock" basalt or limestone, but most sites simply exhibited "medium-hard" layers at various depths, sometimes going back to relatively soft layers again, beneath the medium-hard layers. For a few sites, nothing that could even be called medium-hard was encountered within the 25 ft depth.

In other words, the geometry actually encountered in the field made it difficult to select a "right answer" with which the two sets of backcalculated values could be compared.

The differences in results obtained from static and dynamic backcalculations are moderately small in most cases, particularly when only FWD data is used. There are greater complexities and time requirements for dynamic analyses than for static analyses. Also, the difference in moduli between static and dynamic backcalculations has been shown subsequently to have small effect on the required overlay thickness.

In view of these findings it is recommended that static analyses be used for routine design purposes, even though dynamic analyses are believed to give slightly more accurate results.

6.4.2. Comparison between Laboratory and Backcalculated Moduli

a. Asphalt Concrete

Tables 6-12 through 6-15 and Figures 6-4 through 6-7 show that the NDT back-calculated (BC) moduli averaged about 1/3 the lab moduli, with significant deviations from this average. Three questions about these differences are relevant.

- 1) Why are the values different? What causes the differences?
- 2) Which values are more nearly "correct"?
- 3) What impact, if any, might these differences have on overlay design?

Each of these questions will be addressed in the sections which follow.

Question 1

The lab moduli were observed to be, on average, about 3 times as high as the BC moduli. To date, the following four possible contributing factors have been identified:

- a) The configuration of applied stresses and the general stress state differs considerably from the lab test (indirect tension test loading) to the field (plate load at surface). In the lab the normal stress in the direction deflections are measured is tensile. In the field the asphalt concrete layer is in both tension and compression generally, but the degree of tensile loading may be significantly different.
- b) The specimen of asphalt concrete is loaded horizontally in the lab. In the field, loading occurs in both the horizontal and vertical directions, and both horizontal and vertical moduli influence the resulting deflection pattern. If anisotropy is significant, then differences in lab and NDT BC moduli would be likely.
- c) When the lab values are calculated from the observed test data, a condition of plane stress is assumed. The fact that the test specimen has finite thickness (2 - 2.5 in.) represents deviation from this assumption, particularly in view of the fact that some friction forces are applied under the diametrically opposed line loads and some friction forces between the screws holding the frame and the specimen.
- d) In the lab tests and the NDT tests, two different "volumes" of material are being tested. The lab tests were typically performed on 2 in. thick specimens from a stiff and uncracked layer; whereas, the BC NDT moduli are composite moduli which represent the entire layer.

To date, only qualitative and semi-quantitative analyses of these factors have been made. A detailed quantitative analysis would constitute a substantial study. Our preliminary assessments are as follows.

The first factor relating to stress state would be expected to make the lab moduli smaller than the NDT BC moduli. This is because the tensile

TABLE 6-12. COMPARISON BETWEEN LABORATORY AND BACKCALCULATED ASPHALT CONCRETE MODULI (AT 77F) USING STATIC ANALYSIS OF FWD DATA

| Site/ Station | Lab E (ksi) | Backcalculated E (ksi) | Backcalculated E ----- Lab E |
|------------------|----------------|---------------------------|------------------------------------|
| 1/1 | 1209 | 88 | 0.07 |
| 2/1 | 770 | 600 | 0.78 |
| 3/1 | 744 | 150 | 0.20 |
| 3/7 | 1375 | 185 | 0.13 |
| 4/1 | 1293 | 172 | 0.13 |
| 5/4 | 698 | 278 | 0.40 |
| 6/1 | 642 | 186 | 0.29 |
| 7/4 | 1671 | 139 | 0.08 |
| 8/1 | 563 | 392 | 0.70 |
| 9/1 | 1159 | 466 | 0.40 |
| 10/4 | 1312 | 54 | 0.04 |
| 11/5 | 2190 | 518 | 0.24 |
| 12/1 | 1117 | 227 | 0.20 |
| 13/1 | 954 | 532 | 0.56 |
| 13/4 | 1049 | 564 | 0.54 |
| 14/4 | 517 | 87 | 0.17 |
| 15/4 | 896 | 162 | 0.18 |
| 16/1 | 1569 | 92 | 0.06 |
| 17/1 | 629 | 46 | 0.07 |
| 18/1 | 1219 | 462 | 0.38 |
| 19/4 | 693 | 112 | 0.16 |
| 20/1 | 1667 | 88 | 0.05 |
| Average = | | | 0.27 |

Note: R² value between lab. E and backcalculated E is 0.002

TABLE 6-13. COMPARISON BETWEEN LABORATORY AND BACKCALCULATE ASPHALT CONCRETE MODULI (AT 77F) USING DYNAMIC ANALYSIS OF FWD DATA

| Site/ Station | Lab E (ksi) | Backcalculated E (ksi) | Backcalculated E ----- Lab E |
|------------------|----------------|---------------------------|------------------------------------|
| 1/1 | 1209 | 56 | 0.05 |
| 2/1 | 770 | 680 | 0.88 |
| 3/1 | 744 | 179 | 0.24 |
| 3/7 | 1375 | 179 | 0.13 |
| 4/1 | 1293 | 177 | 0.14 |
| 5/4 | 698 | 390 | 0.56 |
| 6/1 | 642 | 281 | 0.44 |
| 7/4 | 1671 | 70 | 0.04 |
| 8/1 | 563 | 392 | 0.70 |
| 9/1 | 1159 | 504 | 0.43 |
| 10/4 | 1312 | 36 | 0.03 |
| 11/5 | 2190 | 486 | 0.22 |
| 12/1 | 1117 | 220 | 0.20 |
| 13/1 | 954 | 644 | 0.68 |
| 13/4 | 1049 | 224 | 0.21 |
| 14/4 | 517 | 113 | 0.22 |
| 15/4 | 896 | 259 | 0.29 |
| Average = | | | 0.32 |

Note: R² value between lab. E and backcalculated E is 0.01

TABLE 6-14. COMPARISON BETWEEN LABORATORY AND BACKCALCULATE ASPHALT CONCRETE MODULI (AT 77F) USING STATIC ANALYSIS OF DYNAFLECT DATA

| Site/ Station | Lab E (ksi) | Backcalculated E (ksi) | Backcalculated E ----- Lab E |
|------------------|----------------|---------------------------|------------------------------------|
| 1/1 | 1209 | 40 | 0.03 |
| 2/1 | 770 | 600 | 0.78 |
| 3/1 | 744 | 185 | 0.25 |
| 3/7 | 1375 | 290 | 0.21 |
| 4/1 | 1293 | 370 | 0.29 |
| 5/4 | 698 | 464 | 0.66 |
| 6/1 | 642 | 94 | 0.15 |
| 7/4 | 1671 | 232 | 0.14 |
| 8/1 | 563 | 322 | 0.57 |
| 9/1 | 1159 | 815 | 0.70 |
| 10/4 | 1312 | 36 | 0.03 |
| 11/5 | 2190 | 194 | 0.09 |
| 12/1 | 1117 | 162 | 0.15 |
| 13/1 | 954 | 420 | 0.44 |
| 13/4 | 1049 | 448 | 0.43 |
| 14/4 | 517 | 150 | 0.29 |
| 15/4 | 896 | 98 | 0.11 |
| Average = | | | 0.31 |

Note: R² value between lab. E and backcalculated E is 0.01

TABLE 6-15. COMPARISON BETWEEN LABORATORY AND BACKCALCULATE ASPHALT CONCRETE MODULI (AT 77F) USING DYNAMIC ANALYSIS OF DYNAFLECT DATA

| Site/ Station | Lab E (ksi) | Backcalculated E (ksi) | Backcalculated E ----- Lab E |
|------------------|----------------|---------------------------|------------------------------------|
| 1/1 | 1209 | 40 | 0.03 |
| 2/1 | 770 | 600 | 0.78 |
| 3/1 | 744 | 264 | 0.35 |
| 3/7 | 1375 | 317 | 0.23 |
| 4/1 | 1293 | 290 | 0.22 |
| 5/4 | 698 | 464 | 0.66 |
| 6/1 | 642 | 120 | 0.19 |
| 7/4 | 1671 | 255 | 0.15 |
| 8/1 | 563 | 308 | 0.55 |
| 9/1 | 1159 | 815 | 0.70 |
| 10/4 | 1312 | 36 | 0.03 |
| 11/5 | 2190 | 486 | 0.22 |
| 12/1 | 1117 | 162 | 0.15 |
| 13/1 | 954 | 225 | 0.24 |
| 13/4 | 1049 | 448 | 0.43 |
| 14/4 | 517 | 130 | 0.25 |
| 15/4 | 896 | 162 | 0.18 |
| Average = | | | 0.32 |

Note: R² value between lab. E and backcalculated E is 0.02

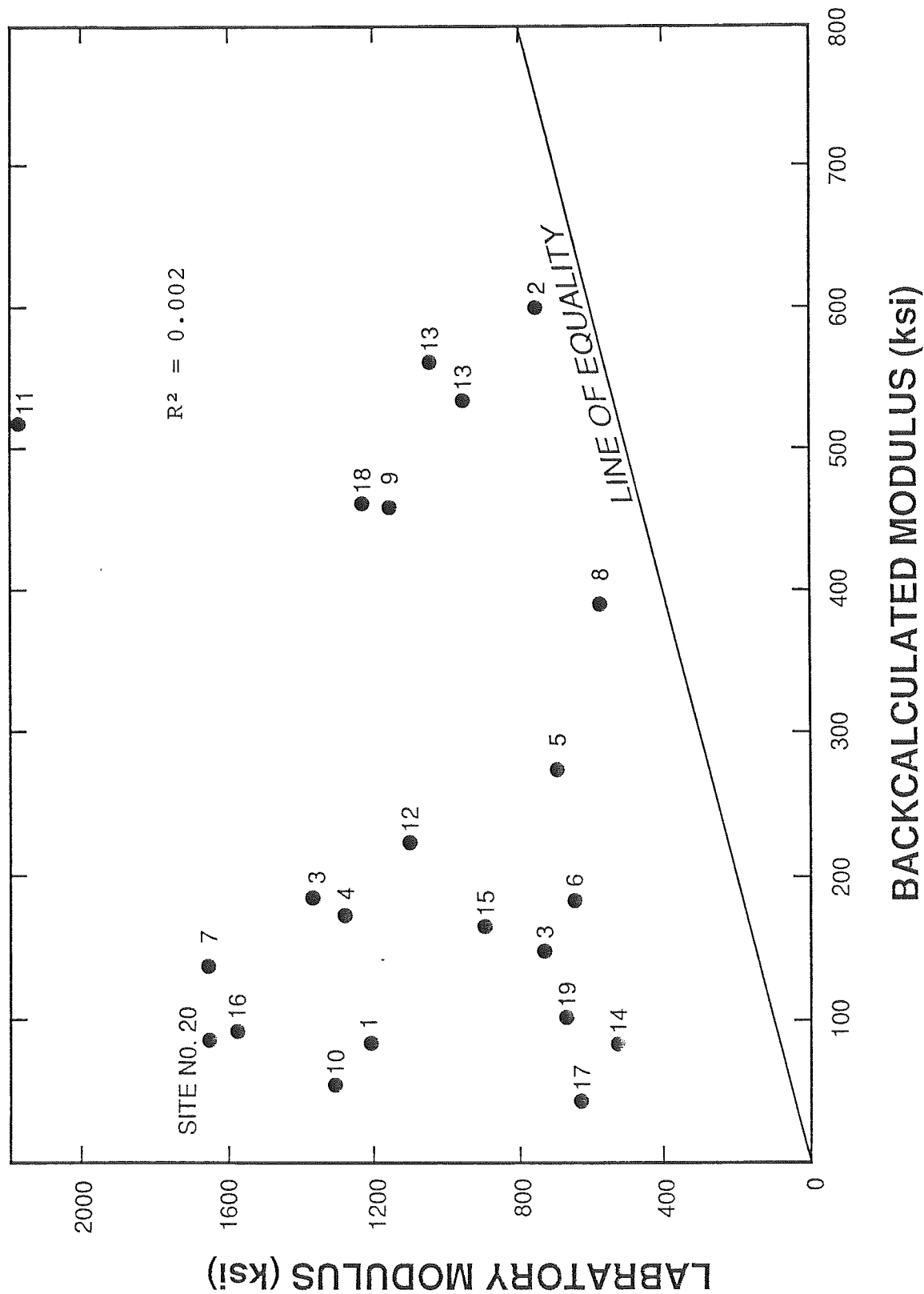


FIGURE 6-4. COMPARISON BETWEEN LABORATORY AND BACKCALCULATED ASPHALT CONCRETE MODULI (AT 77F) USING STATIC ANALYSIS OF FWD DATA

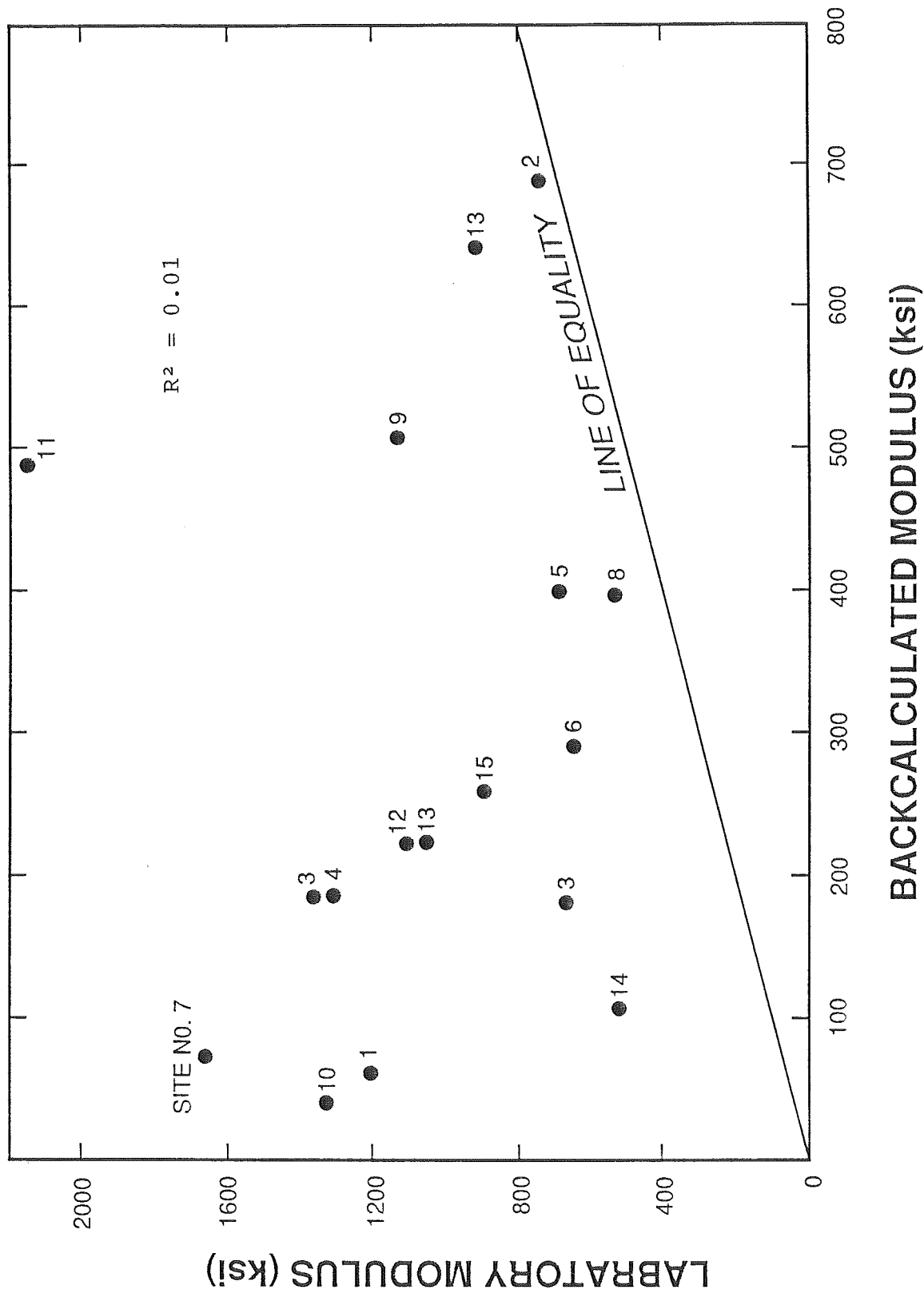
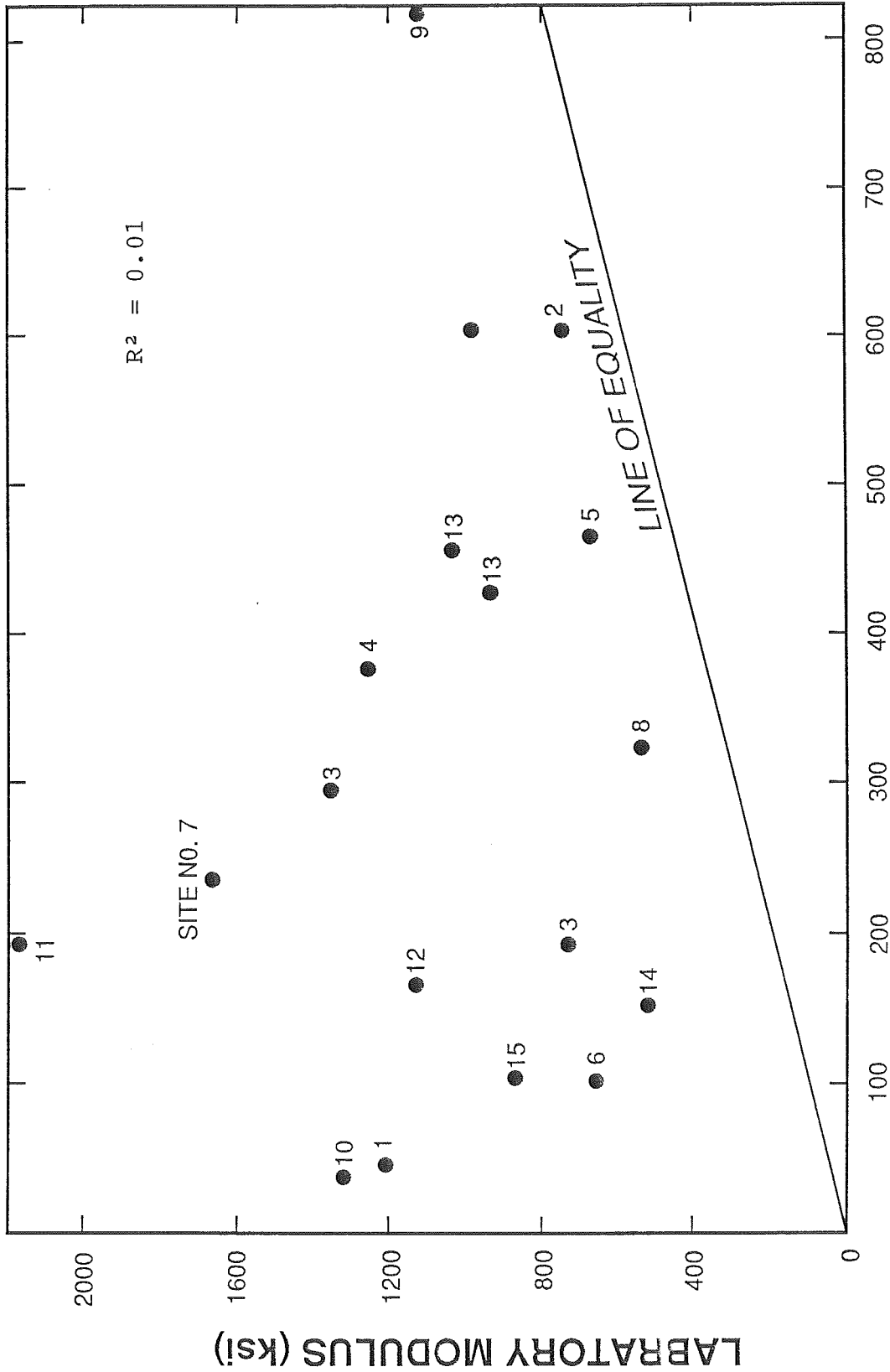


FIGURE 6-5. COMPARISON BETWEEN LABORATORY AND BACKCALCULATED ASPHALT CONCRETE MODULI (AT 77F) USING DYNAMIC ANALYSIS OF FWD DATA



BACKCALCULATED MODULUS (ksi)

FIGURE 6-6. COMPARISON BETWEEN LABORATORY AND BACKCALCULATED ASPHALT CONCRETE MODULI (AT 77F) USING STATIC ANALYSIS OF DYNAFLECT DATA

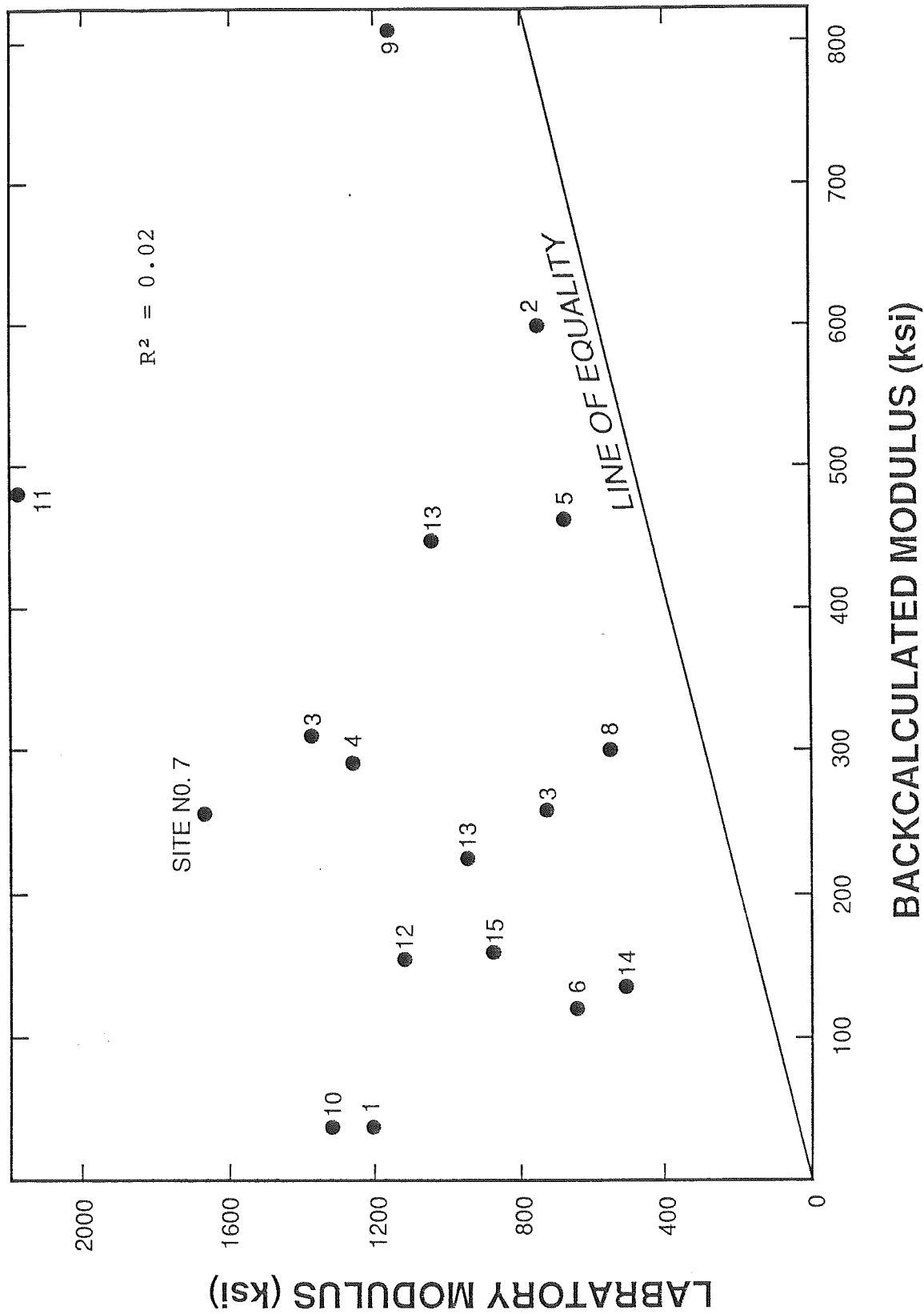


FIGURE 6-7. COMPARISON BETWEEN LABORATORY AND BACKCALCULATED ASPHALT CONCRETE MODULI (AT 77F) USING DYNAMIC ANALYSIS OF DYNAFLECT DATA

modulus is expected to be less than the compressive modulus. When loaded in compression, the asphalt concrete stiffness derives in part from the skeleton of aggregate particles which are mostly in grain-to-grain contact. The stiffness of the asphalt binder also contributes to the compressive stiffness. When loaded in tension, the stiffness derives primarily from the asphalt binder alone. Assuming the degree of tensile loading in the lab exceeds that of NDT testing, which appears likely, the lab moduli should be less than the NDT BC values, though perhaps not by much. Given that the observed results are reversed, this factor is not a good candidate for explaining the difference.

The second factor relates to anisotropy. Although the degree of anisotropy is not well known, there is little doubt that the vertical modulus should exceed the horizontal modulus. Because the degree of "horizontal loading" in the lab is believed to exceed the degree of horizontal loading in the field, this factor should again produce a lab modulus less than the NDT BC modulus, though perhaps not by much. Therefore this factor is also a poor candidate for explaining the observed differences.

The third factor relates to stress state like the first, but it is discarded because it would tend to make the lab moduli higher than the NDT BC moduli, but probably by only a small amount -- much less than the 3:1 factor observed.

At the present time the fourth factor appears to be the prime candidate for explaining the observed differences between lab moduli and NDT BC moduli. In order to simplify the back-calculation process, the entire assemblage of asphaltic sublayers was lumped into one asphalt concrete surface layer. However, in the lab the specimens were taken from an intact and uncracked part of the cone which would be biased to the stiff side.

Question 2

The answer to Question 2, which values are more correct, depends on the relative contributions of the four factors discussed. If the fourth factor, relating to heterogeneity within the surface layer, is the primary factor -- which is currently believed to be the case -- then the answer to Question 2 is:

- a) The lab value of E is probably the best estimate for E for the zone represented by the test specimen, and
- b) The NDT BC value of E is probably the best estimate for the composite, weighted average E for the entire surface layer.

Question 3

The impact of the observed differences in lab and NDT BC asphalt concrete moduli on overlay design is likely to be fairly small for the following reasons. By making a few simplifying assumptions about the deflection shape function, it is possible to use the surface deflection basin data to compute directly the tensile strain at the bottom of the asphalt layer, without utilizing an asphalt concrete modulus (62). A better job of computing this

tensile strain can be done if the asphalt concrete modulus is used together with the surface deflection basin, but only slightly better in most cases.

b. Subgrade Materials

Tables 6-16 through 6-19 and Figures 6-8 through 6-11 show that the NDT BC moduli exceed the lab moduli by roughly 50 to 75 percent, on average. These differences are in the opposite direction to those for the asphalt concrete surface layer.

It should be noted that, compared to differences in lab and field moduli reported historically in the literature, 50 to 75 percent is not a particularly large difference. However, there were significant deviations from this average, and it is relevant to address the same three questions as was done in the preceding section for asphalt concrete.

Question 1.

Three possible contributing factors that might explain the observed differences are as follows:

- a) Differences in water content between the lab specimen and the subgrade at the time of NDT.
- b) Disturbance effects of sampling.
- c) In the lab tests and the NDT tests, two different volumes of material are being tested. The lab values relate only to the 7 in. of soil actually tested, which was typically from the "top" of the subgrade zone. By contrast, the NDT BC values of moduli represent weighted averages for the entire subgrade layer, down to hard material.

Considering these factors one at a time, the first factor, water content variation, could have a significant effect if the variation actually occurred. The samples were taken fairly soon after NDT and moisture migration in the field during this brief period is believed to be negligible. Water was introduced during asphalt concrete coring, but the driller and the boring logs indicated that none of this water reached the subgrade. The samples could have dried somewhat during transportation to the lab and/or storage. However, they were well-sealed at both ends with wax. In addition, any drying would have resulted in high lab modulus, which is opposite to what was observed. Water content variation is considered to be a very unlikely candidate for the observed differences in moduli.

The second factor, disturbance due to sampling, was considered at length. Disturbance could occur during sampling, transportation to the lab, and/or specimen extrusion and preparation. Disturbance during sampling and transportation are difficult to assess, but disturbance due to extrusion and preparation could often be observed visually. A few of the specimens tested showed visible signs of disturbance and these were noted in the test record. If a cyclic loading pre-conditioning was not performed on each specimen, then of course disturbance would be expected to materially reduce the moduli -- perhaps much more than the differences observed. However, pre-conditioning was performed on each specimen, in an effort to erase the effects of disturbance. The test record for each specimen was examined to see if those

TABLE 6-16. COMPARISON BETWEEN LABORATORY AND BACKCALCULATED SOIL MODULI
USING STATIC ANALYSIS OF FWD DATA

| Site/Station | Lab E (ksi) | Backcalculated E (ksi) | <u>Backcalculated E</u> Lab E |
|--------------|----------------|---------------------------|----------------------------------|
| 1/1 | 10.43 | 18 | 1.73 |
| 2/1 | 13.30 | 18 | 1.35 |
| 2/7 | 15.51 | 13.5 | 0.87 |
| 3/7 | 6.44 | 20 | 3.11 |
| 4/1 | 9.59 | 20.4 | 2.14 |
| 5/4 | 12.19 | 7 | 0.57 |
| 6/1 | ----- | 6.5 | ----- |
| 7/4 | 11.36 | 13.4 | 1.19 |
| 8/1 | 7.99 | 12 | 1.50 |
| 9/1 | 16.14 | 8.5 | 0.53 |
| 10/4 | 12.48 | 10 | 0.80 |
| 11/1 | 13.33 | 19 | 1.42 |
| 12/1 | 7.41 | 10.5 | 1.42 |
| 13/4 | 14.35 | 24 | 1.67 |
| 14/4 | 10.42 | 25 | 2.40 |
| 15/4 | ----- | 8 | ----- |
| 16/1 | 9.59 | 11.5 | 1.20 |
| 17/1 | 4.82 | 9 | 1.87 |
| 18/1 | ----- | 50 | ----- |
| 19/4 | 12.01 | 11 | 0.92 |
| 20/1 | 15.64 | 45 | 2.88 |
| | | | Average = 1.52 |

Note: R² value between lab. E and backcalculated E is 0.09

TABLE 6-17. COMPARISON BETWEEN LABORATORY AND BACKCALCULATED SOIL MODULI USING DYNAMIC ANALYSIS OF FWD DATA

| Site/Station | Lab E (ksi) | Backcalculated E (ksi) | <u>Backcalculated E</u> Lab E |
|--------------|----------------|---------------------------|----------------------------------|
| 1/1 | 10.43 | 20 | 1.92 |
| 2/1 | 13.30 | 19.5 | 1.47 |
| 2/7 | 15.51 | 16 | 1.03 |
| 3/7 | 6.44 | 18 | 2.80 |
| 4/1 | 9.59 | 17 | 1.77 |
| 5/4 | 12.19 | 13 | 1.07 |
| 6/1 | ----- | 20 | ----- |
| 7/4 | 11.36 | 10.2 | 0.90 |
| 8/1 | 7.99 | 17 | 2.13 |
| 9/1 | 16.14 | 14 | 0.87 |
| 10/4 | 12.48 | 9.8 | 0.79 |
| 11/1 | 13.33 | 32 | 2.40 |
| 12/1 | 7.41 | 16.5 | 2.23 |
| 13/4 | 14.35 | 27 | 1.88 |
| 14/4 | 10.42 | ----- | ----- |
| 15/4 | ----- | 10.8 | ----- |
| | | | Average = 1.64 |

Note: R² value between lab. E and backcalculated E is 0.24

TABLE 6-18. COMPARISON BETWEEN LABORATORY AND BACKCALCULATED SOIL MODULI USING STATIC ANALYSIS OF DYNAFLECT DATA

| Site/Station | Lab E (ksi) | Backcalculated E (ksi) | <u>Backcalculated E</u> Lab E |
|--------------|----------------|---------------------------|----------------------------------|
| 1/1 | 10.43 | 20 | 1.92 |
| 2/1 | 13.30 | 20 | 1.50 |
| 2/7 | 15.51 | 13 | 0.84 |
| 3/7 | 6.44 | 14 | 2.17 |
| 4/1 | 9.59 | 16.8 | 1.75 |
| 5/4 | 12.19 | 23 | 1.89 |
| 6/1 | ----- | 15.5 | ----- |
| 7/4 | 11.36 | 13.5 | 1.19 |
| 8/1 | 7.99 | 20 | 2.50 |
| 9/1 | 16.14 | 12.6 | 0.78 |
| 10/4 | 12.48 | 9.5 | 0.76 |
| 11/ 1 | 13.33 | 11 | 0.83 |
| 12/1 | 7.41 | 19 | 2.56 |
| 13/4 | 14.35 | 42.5 | 2.96 |
| 14/4 | 10.42 | ----- | ----- |
| 15/4 | ----- | 14 | ----- |
| Average = | | | 1.66 |

Note: R² value between lab. E and backcalculated E is 0.004

TABLE 6-19. COMPARISON BETWEEN LABORATORY AND BACKCALCULATED SOIL MODULI USING DYNAMIC ANALYSIS OF DYNAFLECT DATA

| Site/Station | Lab E (ksi) | Backcalculated E (ksi) | <u>Backcalculated E</u> Lab E |
|--------------|----------------|---------------------------|----------------------------------|
| 1/1 | 10.43 | 22.5 | 2.16 |
| 2/1 | 13.30 | 22 | 1.65 |
| 2/7 | 15.51 | 14 | 0.90 |
| 3/7 | 6.44 | 20 | 3.10 |
| 4/1 | 9.59 | 16 | 1.67 |
| 5/4 | 12.19 | 13.2 | 1.08 |
| 6/1 | ----- | 20 | ----- |
| 7/4 | 11.36 | 13 | 1.14 |
| 8/1 | 7.99 | 19 | 2.37 |
| 9/1 | 16.14 | 15 | 0.93 |
| 10/4 | 12.48 | 10.7 | 0.86 |
| 11/1 | 13.33 | 14.5 | 1.08 |
| 12/1 | 7.41 | 18.5 | 2.49 |
| 13/4 | 14.35 | 47 | 3.27 |
| 14/4 | 10.42 | ----- | ----- |
| 15/4 | ----- | 13.5 | ----- |
| | | | Average = 1.75 |

Note: R² value between lab. E and backcalculated E is 0.11

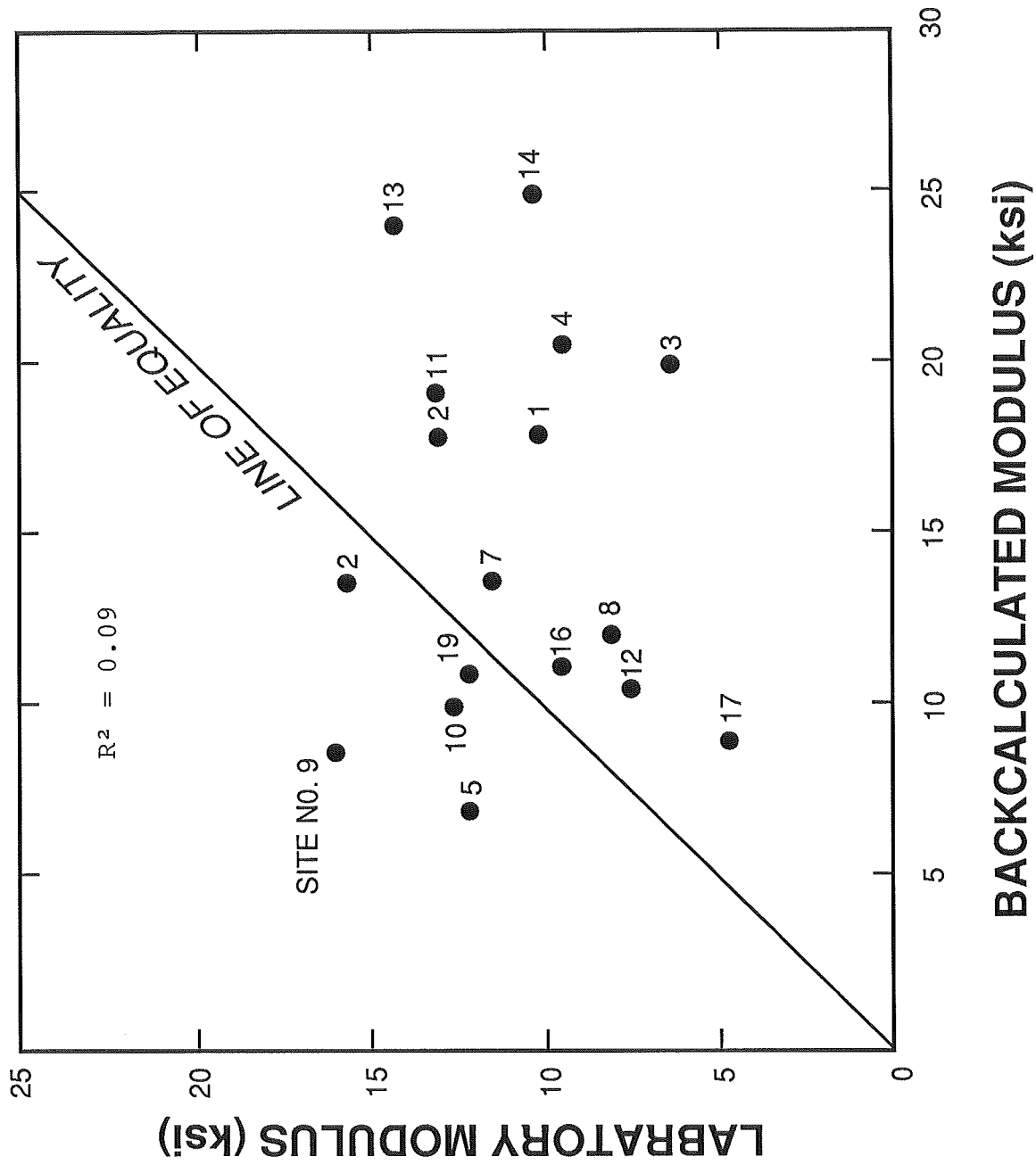


FIGURE 6-8. COMPARISON BETWEEN LABORATORY AND BACKCALCULATED SOIL MODULI USING STATIC ANALYSIS OF FWD DATA

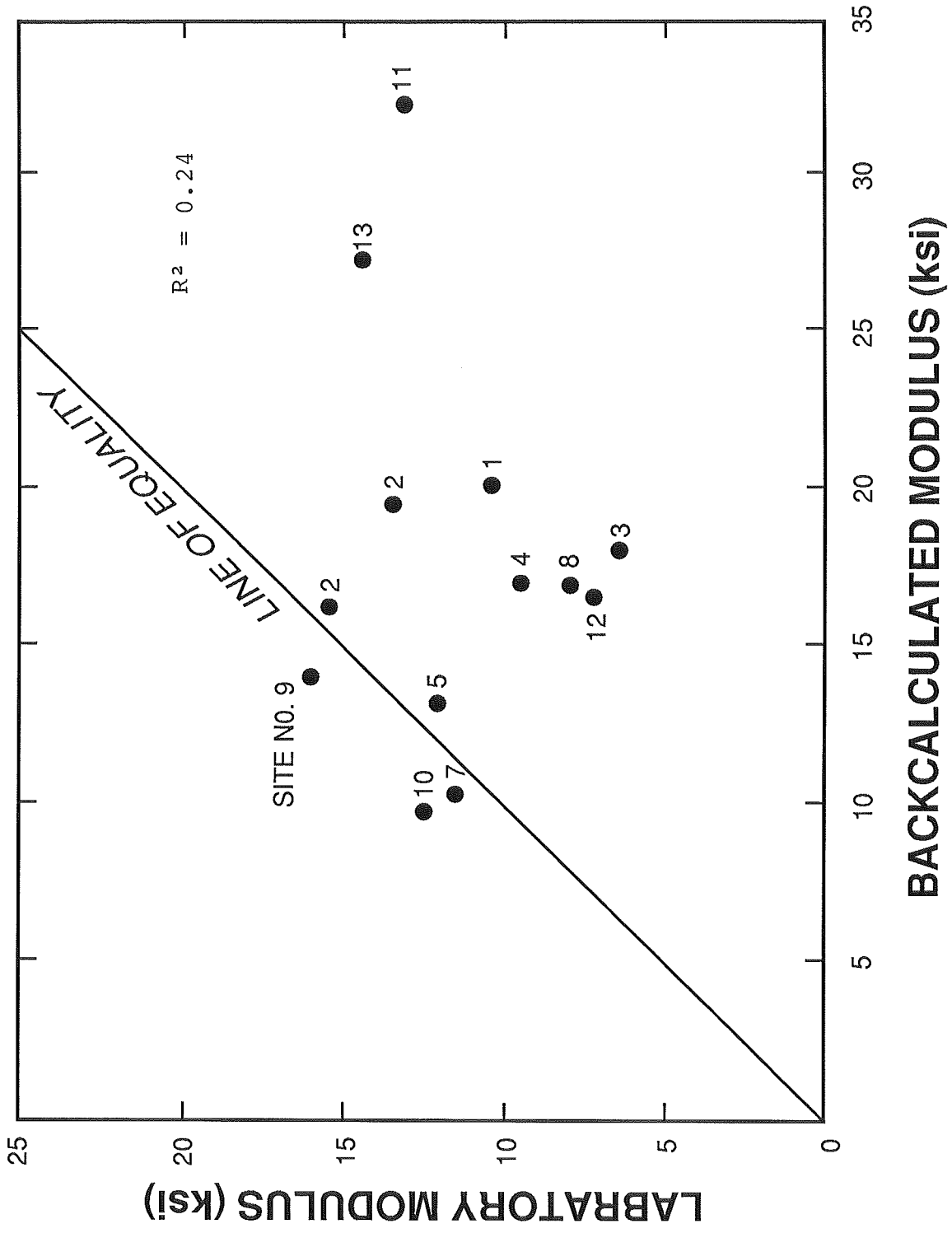
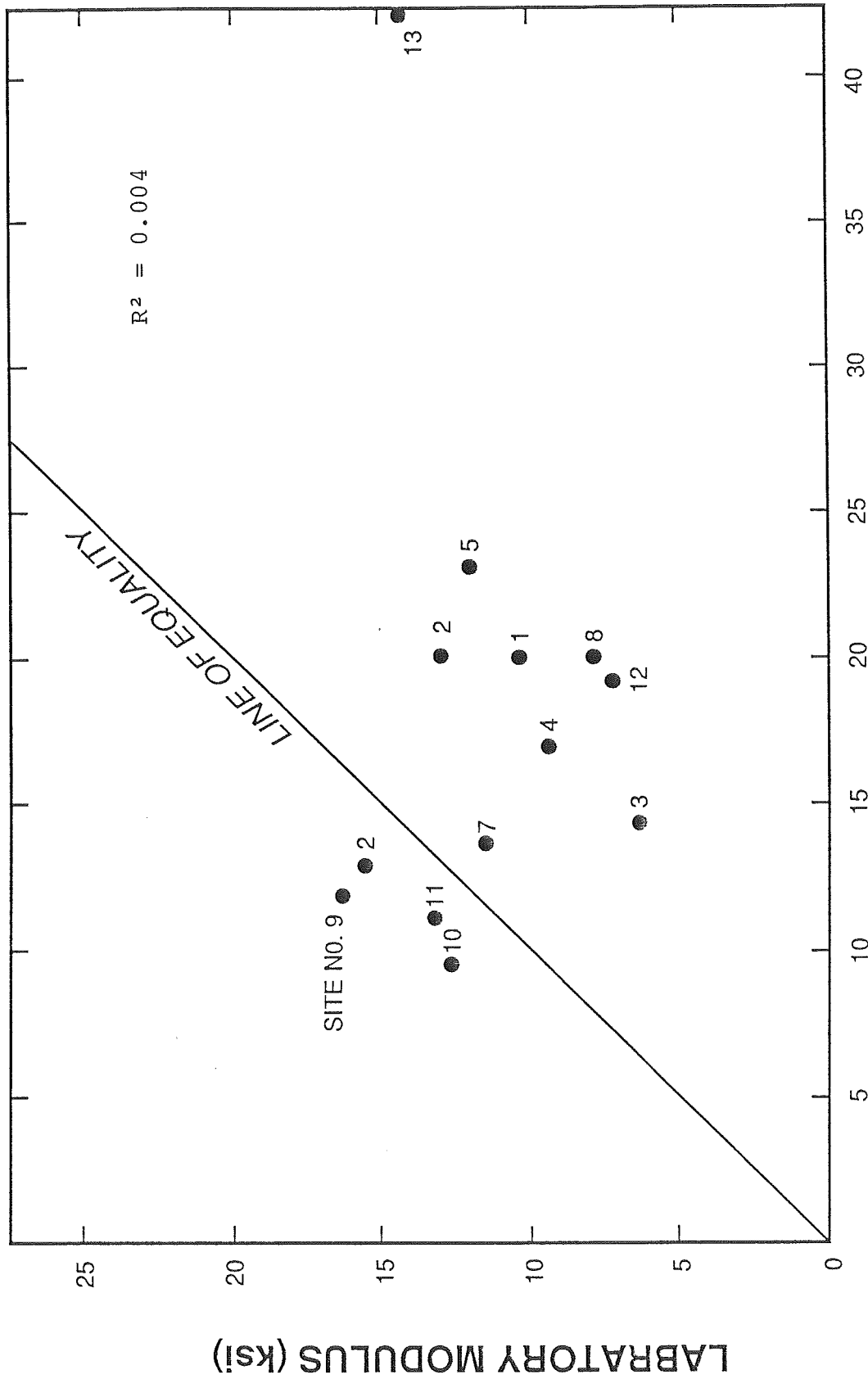


FIGURE 6-9. COMPARISON BETWEEN LABORATORY AND BACKCALCULATED SOIL MODULI USING DYNAMIC ANALYSIS OF FWD DATA



BACKCALCULATED MODULUS (ksi)

FIGURE 6-10. COMPARISON BETWEEN LABORATORY AND BACKCALCULATED SOIL MODULI USING STATIC ANALYSIS OF DYNAFLECT DATA

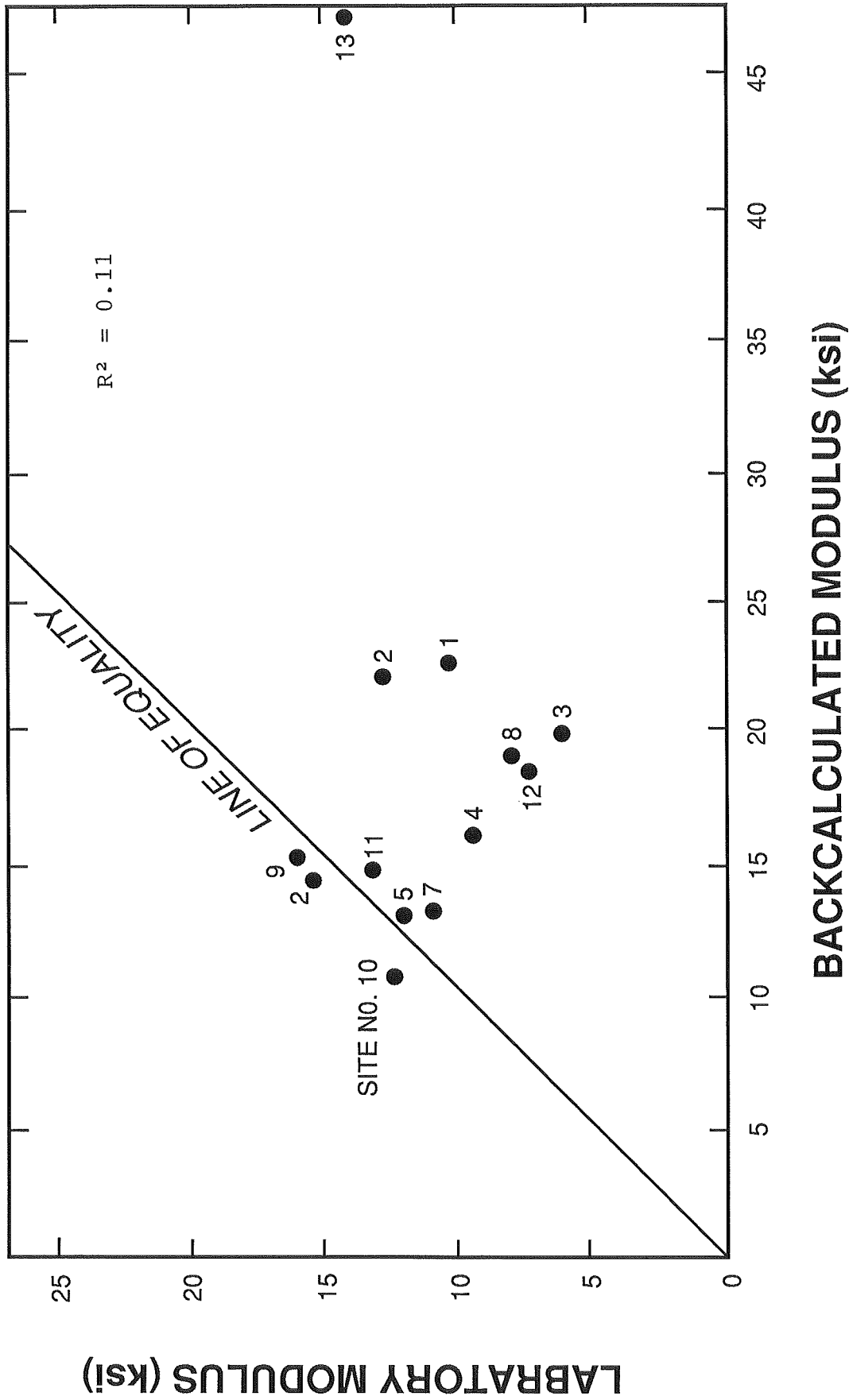


FIGURE 6-11. COMPARISON BETWEEN LABORATORY AND BACKCALCULATED SOIL MODULI USING DYNAMIC ANALYSIS OF DYNAFLECT DATA

specimens showing the most signs of disturbance were also the specimens with abnormally low moduli. No such trend was observed, indicating, perhaps, that the preconditioning was fairly effective in erasing the effects of disturbance. It was observed that the two most plastic clays yielded the highest moduli of all, and in fact, gave lab moduli which significantly exceeded the NDT BC moduli, a result contrary to the average ratio. However, these two data points cannot yet be said to constitute a trend. Based on the preceding observations and studies it was concluded that sample disturbance effects are unlikely to account for the majority of the moduli differences observed.

The third factor, relating to different volumes being tested, was again judged to be the primary factor in producing the observed differences. The back-calculations showed that the modulus of the subgrade was important down to depths 10 feet and sometimes even 20 feet or more. Although the importance of the subgrade modulus in contributing to surface deflections decreases with depth, the modulus of the subgrade between sample depth and say 10 or 12 feet would have a significant effect on the outer sensor deflections.

If the modulus of the subgrade was constant all the way down to "firm" material, then differences between lab and NDT BC moduli would not necessarily be expected. However, if the subgrade is highly layered and heterogeneous, then differences would be expected -- both positive and negative differences. This is because the NDT BC modulus is a weighted average or "lumped" value for the entire subgrade, including all of the sublayers it might have. By contrast, the lab value would be expected to reflect only the thin layer from whence the sample came.

In an attempt to solve this problem, the subgrade was divided into two layers: a "compacted subgrade" and an "uncompacted subgrade." This subdivision may well have been a step in the right general direction, but in all likelihood it was still a grossly oversimplified model of the subgrade in most cases. The cone penetration testing led to data that demonstrate highly variable moduli in the subgrade.

Question 2.

Which values of moduli are more nearly correct depends on whether the observed differences arises primarily from the second or third factor cited. If it is the second factor, sample disturbance, causing the differences, then the NDT BC moduli would be "better" values.

If the differences come primarily from the third factor -- that is, testing different volumes of soil -- then the lab modulus may be the best estimate for its depth interval and the NDT BC modulus may be the best value for the weighted average of the entire subgrade composite layer.

Question 3.

The impact of the observed differences in the lab and NDT BC subgrade moduli on overlay design is expected to be fairly small. The fatigue part of the overlay design criteria deals with tensile strain at the bottom of the asphalt concrete which is not largely affected by the subgrade modulus. Other aspects of overlay design are not very sensitive to the value of modulus of the AC.

It should be noted that observed deviations between lab moduli and backcalculated moduli is not new. Newcomb (63), for example, noted this deviation, but it took a different trend.

6.4.3 Comparison between Laboratory Moduli and R-Values

The laboratory resilient moduli of subgrade materials reported in Table 5-5 were compared with the laboratory R-values reported by ADOT (Table 5-7). The statistical package SPSS was used to evaluate the degree of correlations between the two parameters. For a number of observations of 12 a coefficient of determination (R^2) of 0.007 was obtained. This result indicates that the two parameters are not correlated and it is not recommended to predict the resilient moduli from the R-values, even if the R-value test is simpler and more convenient to perform than the resilient modulus test. Figure 6-12 shows the resilient moduli versus R-values used for the correlation evaluation.

There are several reasons to explain why the resilient modulus and the R-value are not correlated. The most obvious reason is that the modulus is a measure of elasticity of the material, while the R-value is an index value representing the resistance to deformation. Since these two properties are not directly related to each other, there is no guarantee that they are correlated. Another reason of this poor correlation is the fact that the conditions of the samples of the two tests are different. For example, the moisture contents and the densities of the samples of the two tests are different.

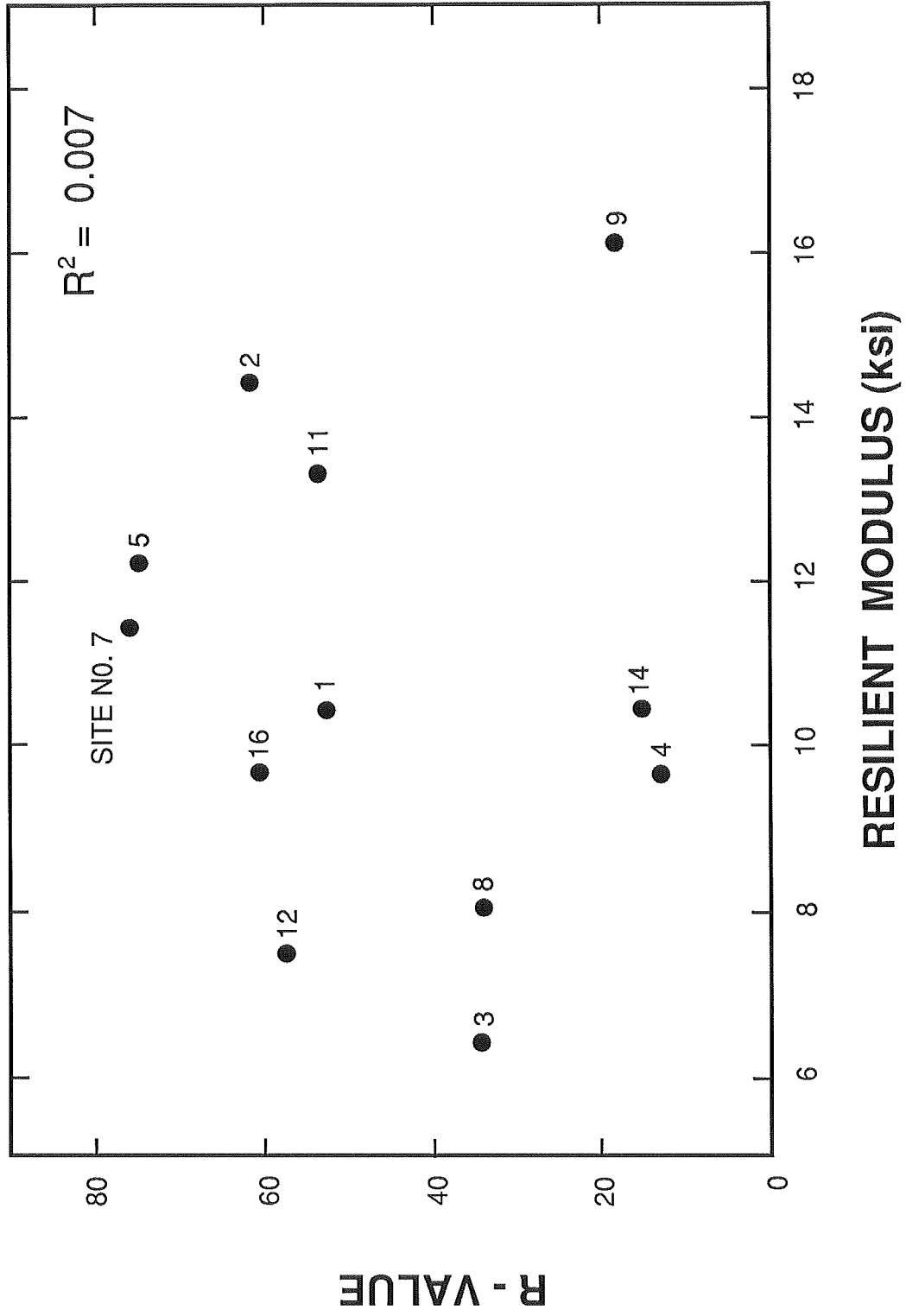


FIGURE 6-12. LABORATORY RESILIENT MODULI VS. R-VALUE USED FOR THE CORRELATION EVALUATION

CHAPTER 7. DEVELOPMENT OF OVERLAY DESIGN METHODOLOGY

7.1. OVERVIEW OF OVERLAY DESIGN

To a large extent, the highway infrastructure in Arizona is in place. With the exception of major construction projects in Phoenix and Tucson, maintenance and restoration of the existing pavement is the major task facing the Department of Transportation. Effective overlay design and construction is an important means of ensuring the quality of the system. This is a common situation throughout the United States and has generated numerous research projects yielding overlay design methods. The research team reviewed these methods, including the SODA method developed by ADOT. It was decided that sufficient new data was available to develop a new procedure tailored to the conditions in Arizona.

Figure 7-1 is a generic representation of the elements of an overlay design method. The process is initiated with the collection and evaluation of the input data. The input data are measured deflections, structural data, traffic, environment, and costs. These data are analyzed to define the material properties required for overlay design. The next step requires evaluating the critical response of the pavement. Based on the response of the pavement, feasible strategies are defined. For overlay design, different overlay thicknesses are the only strategies considered. The performance of the strategies is then evaluated with respect to time and traffic. Once the performances of the strategies are evaluated, economic analyses are performed to ensure the selected strategy will provide the best service at the most economical cost.

Based on this conceptual overlay design procedure, a specific design procedure was developed. The research team met with ADOT engineers to define the parameters for the overlay design process. Three critical performance parameters were defined; roughness, fatigue cracking, and permanent deformation. Based on the original project definition and research performed in the first phase of the project, the Falling Weight Deflectometer was selected as the primary tool for evaluating the structural condition of the existing pavement. Finally, the objective of the research was for the development of rational procedures for selecting the most economical overlay thickness. However, overlaying is just one strategy for reconditioning a pavement. ADOT has successfully used several other strategies for reconditioning pavements including recycling, milling, and asphalt-rubber. Thus, the computer model was structured to perform the analysis of the required overlay thickness and perform economic analysis for any strategy for which the construction and maintenance costs are known.

Figure 7-2 shows the flow of calculations required to meet the problem constraints. A general set of input data are required to define the parameters of the problem. The analyst can then select one or more of four options; overlay design, remaining life of an existing pavement, life of a user specified overlay or economic analysis. If the user selects the overlay design option, the roughness, fatigue and plastic deformation models are used to obtain the required overlay thickness. If the user selects the remaining life option, the program uses both roughness and fatigue models to evaluate the remaining life. If the user selects a specific overlay thickness, the

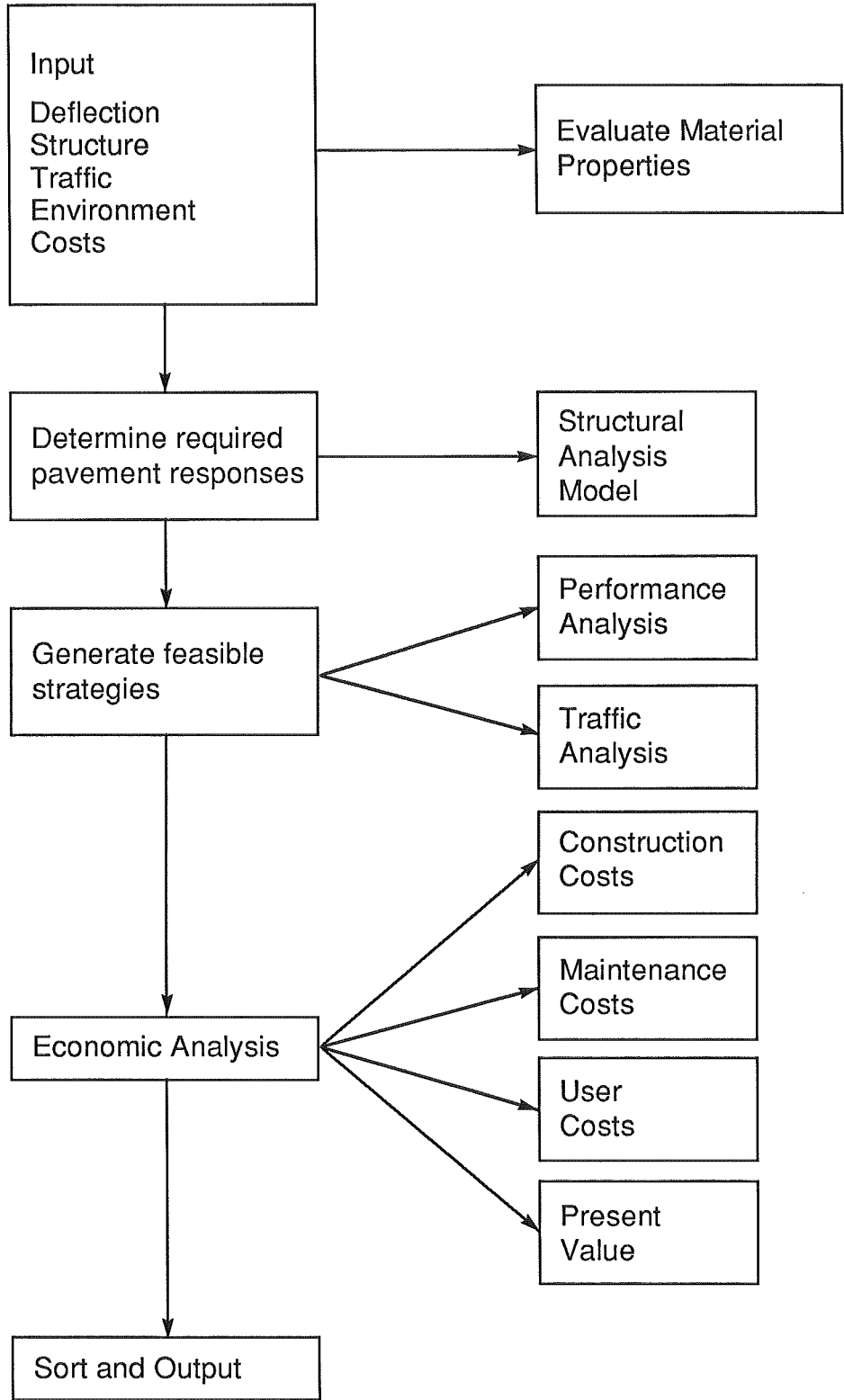


FIGURE 7-1. OVERVIEW OF THE OVERLAY DESIGN PROCESS

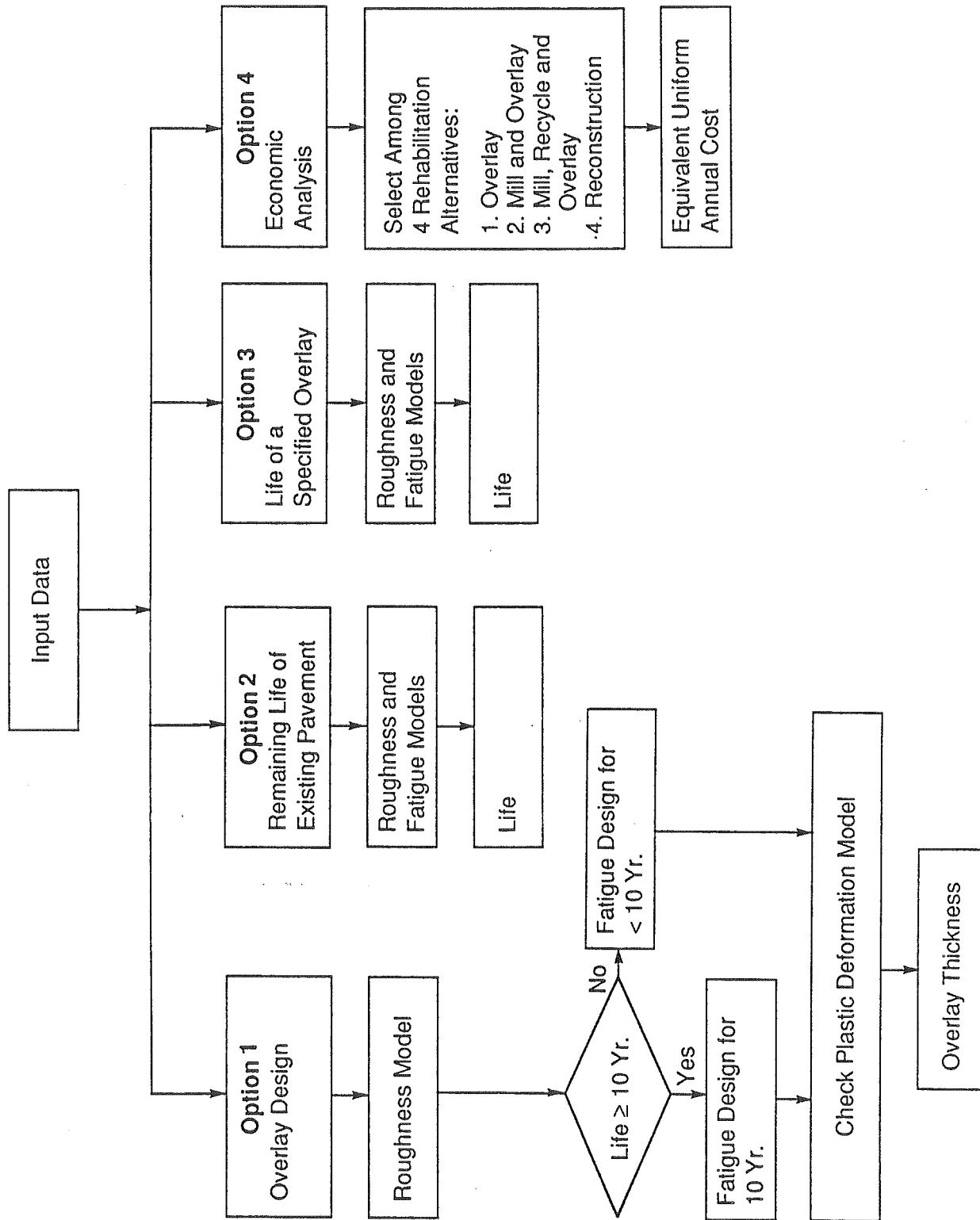


FIGURE 7-2. FLOW CHART OF THE OVERLAY DESIGN PROCEDURE

program determines its life based on both roughness and fatigue models. Finally, the user has the option of performing an economic analysis to determine the equivalent uniform annual cost of four rehabilitation strategies; overlay only, mill plus overlay, mill and recycle plus overlay, and reconstruction. The development of the roughness, fatigue and plastic deformation models are described in the following sections.

7.2. ROUGHNESS MODELS

Roughness is the single measure of pavement performance or condition which correlates with the highway user's opinion of the quality of the pavement. Roughness criteria are a major factor in the project selection process used in ADOT's pavement management system. Thus, a roughness model is an important component in the overlay design process.

Roughness is generally defined as random variations in the longitudinal profile of the pavement surface. The development of random variations in the profile depend on traffic loads, environment, soil support, construction variations, etc. The number of variables, and their interactions, which contribute to the development of roughness are too numerous to permit rigorous mathematical modeling. Hence, empirical methods are used for the development of roughness models. Fortunately, the ADOT pavement management data base provides an extensive source of data for the development of roughness performance models.

In an overlay design method, two forms of roughness models are required; the initial roughness of the pavement after overlay and the rate of roughness development as a function of either time or traffic.

The ADOT pavement management system data base contains records for each mile post in the ADOT highway system. Each record contains data describing the type of route, route or road number, traffic levels, regional factors, maintenance costs, performance measures and the most recent construction projects. The performance measures are roughness, cracking and skid resistance. Roughness has been measured annually since 1972 using calibrated Maysmeters.

For the development of roughness performance models, the ADOT microcomputer pavement management system data base was queried to identify all overlay projects constructed since 1960. The construction history fields were used to identify an overlay project for the development of the roughness model. Overlay projects were defined as having one, two or three layers. A single-layer overlay consists of an asphalt concrete layer. A two-layer overlay can have either a leveling layer followed by asphalt concrete or an asphalt concrete layer followed by an asphalt concrete friction course. A three-layer overlay consists of a leveling course followed by an asphalt concrete layer and an asphalt concrete friction course. A flush coat or seal coat could be used as a final treatment for any of these overlay types. The projects selected for the analyses had "conventional" overlays, i.e. an asphalt concrete layer placed directly on an existing pavement surface. Other rehabilitation options such as milling, recycling, asphalt-rubber membranes, etc. were excluded from the data base analyzed during this project.

The data were separated into homogenous overlay projects. A homogenous overlay project is defined by having a constant project number, route number, direction and overlay thickness. The other data fields were then averaged across each mile post included in each project. Thus, the roughness data used for the statistical analysis consisted of the average roughness on the project for each year. Data for interstate, state and U. S. routes were analyzed separately.

7.2.1. Change in Roughness Due to Overlay

The initial roughness after an overlay is modeled as the roughness prior to the overlay minus the reduction in roughness due to the overlay. This analysis considered all overlay projects performed since 1972. The data were analyzed with the STATPACK programs for statistical analysis on microcomputers. The level of roughness after overlay and the change in roughness due to the overlay were used as dependent variables. The roughness prior to overlay, thickness of overlay and type of surfacing layer were used as independent variables.

The reduction in roughness due to overlays versus the roughness prior to overlay are shown in Figures 7-3 through 7-5 for each of the highway types. These figures show a definite trend between the change in roughness and the roughness prior to overlay. This trend is expected simply because there is a greater opportunity to improve the roughness of rough roads than to improve the roughness of smooth roads. It is interesting to note from these graphs that several routes with relatively low roughness were overlaid.

The changes in roughness versus overlay thicknesses are shown in Figures 7-6 through 7-8 for each highway type. These figures do not show any identifiable correlation between overlay thicknesses and the change in roughness due to the overlay. It is very interesting to note the extent of improvement in roughness that can be achieved with overlays as thin as 1.25 inches. On one U.S. route shown on Figure 7-7, a reduction in roughness of over 300 inches/mile was obtained with a 1.25 inch overlay.

Conceptually, one would expect a correlation between the thickness of the overlay and the change in roughness, especially for thick overlays constructed in multiple lifts. However, the data indicate that contractors can achieve very significant reductions in roughness with a thin overlay; subsequent lifts do not necessarily further improve the roughness.

Table 7-1 shows the frequency distribution of the roughness after overlay for the three highway types. The interstate highways show a fairly uniform distribution and only 5% of the overlays have an initial roughness of more than 100 inches per mile. The distribution of the roughness for the other two highway types are more normally distributed and the median roughness after overlay is much higher than for interstates. The mean values of roughness before and after overlay are:

| | <u>Before Overlay</u> | <u>After Overlay</u> |
|--------------|-----------------------|----------------------|
| Interstate | 166.6 | 68.3 |
| U.S. Routes | 222.3 | 95.2 |
| State Routes | 242.6 | 102.6 |

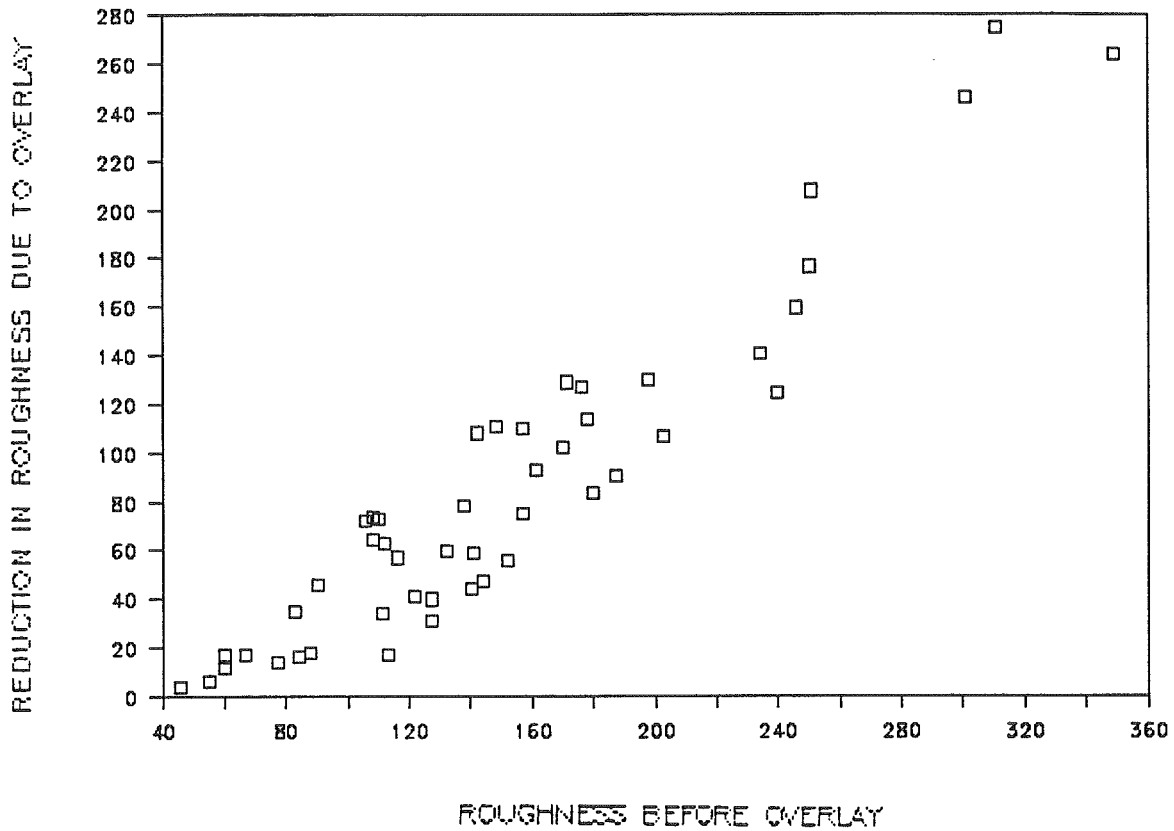


FIGURE 7-3. REDUCTION IN ROUGHNESS DUE TO OVERLAY VS ROUGHNESS BEFORE OVERLAY FOR INTERSTATE HIGHWAYS

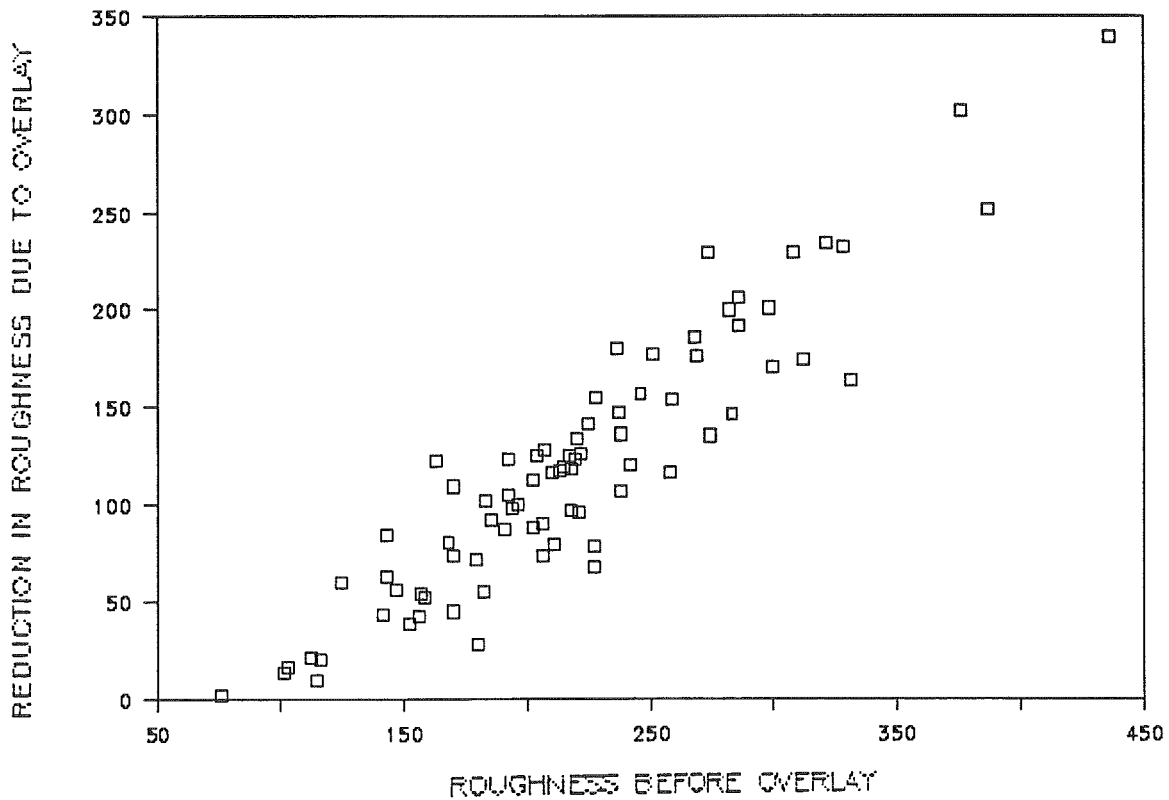


FIGURE 7-4. REDUCTION IN ROUGHNESS DUE TO OVERLAY VS ROUGHNESS BEFORE OVERLAY FOR U.S. ROUTES

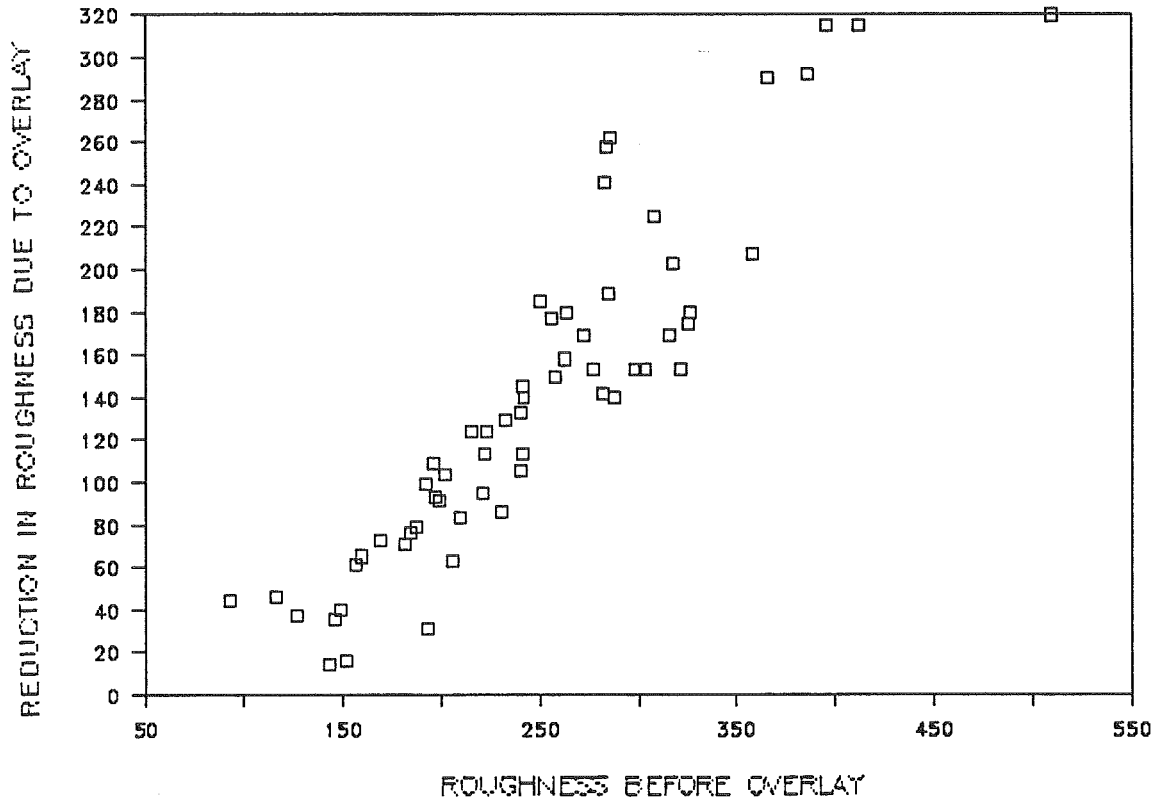


FIGURE 7-5. REDUCTION IN ROUGHNESS DUE TO OVERLAY VS ROUGHNESS BEFORE OVERLAY FOR STATE ROUTES

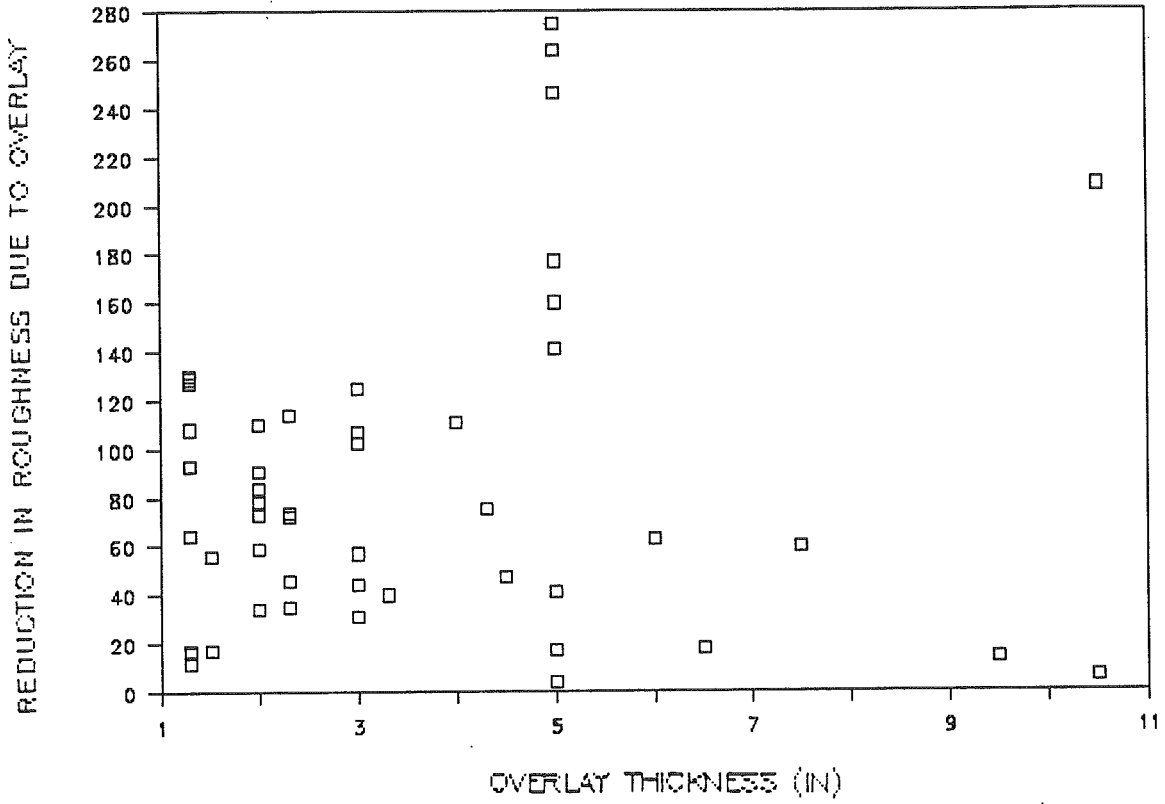


FIGURE 7-6. REDUCTION IN ROUGHNESS DUE TO OVERLAY VS OVERLAY THICKNESS FOR INTERSTATE HIGHWAYS

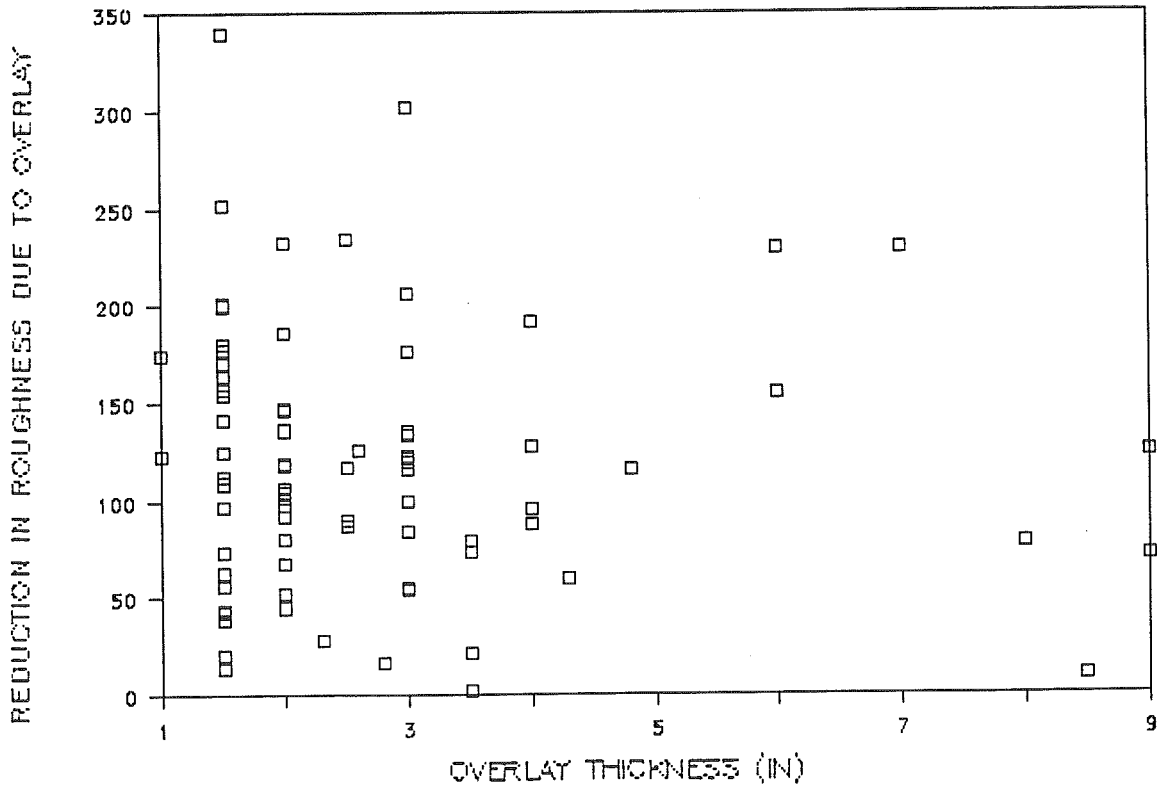


FIGURE 7-7. REDUCTION IN ROUGHNESS DUE TO OVERLAY VS OVERLAY THICKNESS FOR U.S. ROUTES

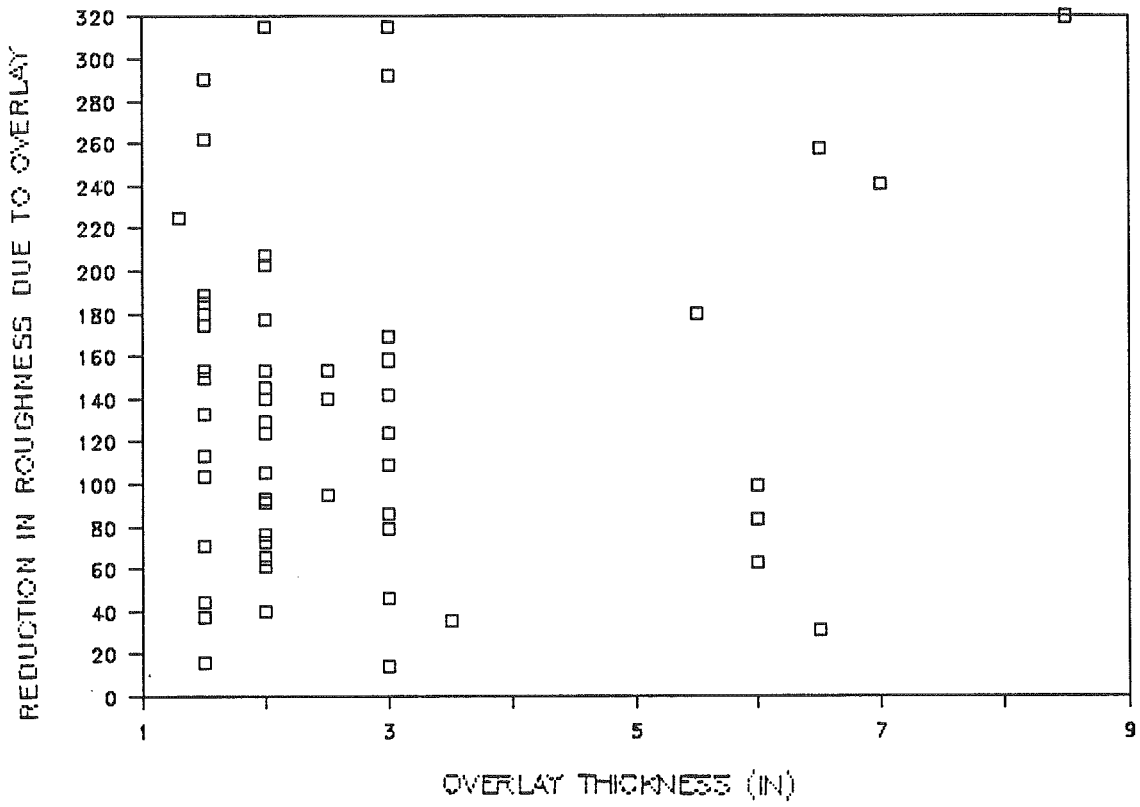


FIGURE 7-8. REDUCTION IN ROUGHNESS DUE TO OVERLAY VS OVERLAY THICKNESS FOR STATE ROUTES

A multiple regression analysis was performed to define equations for the change in roughness. Only routes with roughness of more than 100 inches per mile prior to overlay were included in the regression analysis. The smooth pavements were removed from the analysis to avoid placing an artificial limit on the change in roughness that could be obtained with an overlay. For each highway type, there was a significant relationship between the change in

TABLE 7-1. FREQUENCY DISTRIBUTION OF ROUGHNESS AFTER OVERLAY

| Roughness (in.) After Overlay | Frequency (%) | | |
|----------------------------------|---------------|------|-------|
| | Interstate | U.S. | State |
| 20-39 | 15.3 | 1.5 | 1.9 |
| 40-59 | 28.1 | 7.6 | 3.8 |
| 60-79 | 15.2 | 12.2 | 15.2 |
| 80-99 | 35.8 | 43.0 | 28.9 |
| 100-119 | 5.0 | 16.9 | 27.8 |
| 120-139 | - | 15.3 | 7.6 |
| 140-159 | - | 1.5 | 9.5 |
| 160-179 | - | 1.5 | 3.8 |
| 180-199 | - | - | - |

roughness and the roughness prior to overlay. There was no relationship between overlay thickness and the change in roughness due to overlay. An indicator variable was used to define if the construction project included an asphalt concrete friction course, ACFC. All interstate projects had ACFC layers so this factor could not be evaluated for interstates. ACFC layers were used on about one third of both U.S. and state routes. The regression equations for change in roughness are:

| | Equation | R ² | SEE | N | |
|--------------|--|----------------|-------|----|-------|
| Interstate | $\Delta R = -61.76 + 0.948R_b$ | 0.86 | 24.50 | 33 | (7-1) |
| U.S. Routes | $\Delta R = -73.02 + 0.9R_b + 0.153KR_b$ | 0.85 | 24.42 | 65 | (7-2) |
| State Routes | $\Delta R = -78.92 + 0.896R_b + 0.104KR_b$ | 0.85 | 30.04 | 58 | (7-3) |

where:

ΔR = Roughness before overlay - roughness after overlay

R_b = Roughness before overlay

K = ACFC indicator

K = 1 if ACFC was placed

K = 0 no ACFC

SEE = Standard error of the estimate

It is interesting to note the slope of the relationship between change in roughness and the roughness before overlay is almost identical across the three highway types. It is also interesting that an ACFC significantly increases the change in roughness on both U.S. and state routes.

7.2.2. Rate of Change in Roughness

For each project a regression analysis was performed between roughness and time in order to find the rate of increase of roughness (inches/year) after an overlay. For projects overlaid prior to 1972, the rate was calculated using the data between 1972 and 1987 as no roughness data prior to 1972 were available. A linear model was used for the change of roughness versus time. Nonlinear models were tested but they did not improve the correlation. The slope of the relationship between roughness and time was used to define the rate of change in roughness. Figures 7-9 to 7-11 show typical relationships between roughness and years since overlay for interstate, U.S. routes and state highways. For most projects, there was a strong correlation between roughness and time. Table 7-2 shows the distribution of the rate of change in roughness for each of the highway types. The average change in roughness per year, in inches per mille as measured with the Maysmeter, are 6.7 for interstates, 5.1 for U.S. routes, and 5.8 for state highways.

The independent variables available in the database were the regional factor, ADL, structural number and the overlay thickness. Graphs plotted between the rate of change of roughness (in/year) and the above variables for interstates, U.S. routes and state routes were analyzed but they did not show any specific trends. Multiple regression analysis was performed for each class of highway taking the rate of increase of roughness as the dependent variable and the regional factor, ADL, structural number and overlay thickness as independent variables. Forward stepwise regression analyses were performed using the computer program STATPACK. No correlations were found for this analysis.

As indicated earlier, the rate of increase of roughness for projects overlaid before 1972 were obtained by extrapolating the data available from 1972-1987. To determine whether the inclusion of projects overlaid before 1972 has any effect on the regression, a multiple regression analysis was performed again considering only projects that were overlaid on or after 1972. In addition to the variables considered before, roughness after overlay was also considered as an independent variable.

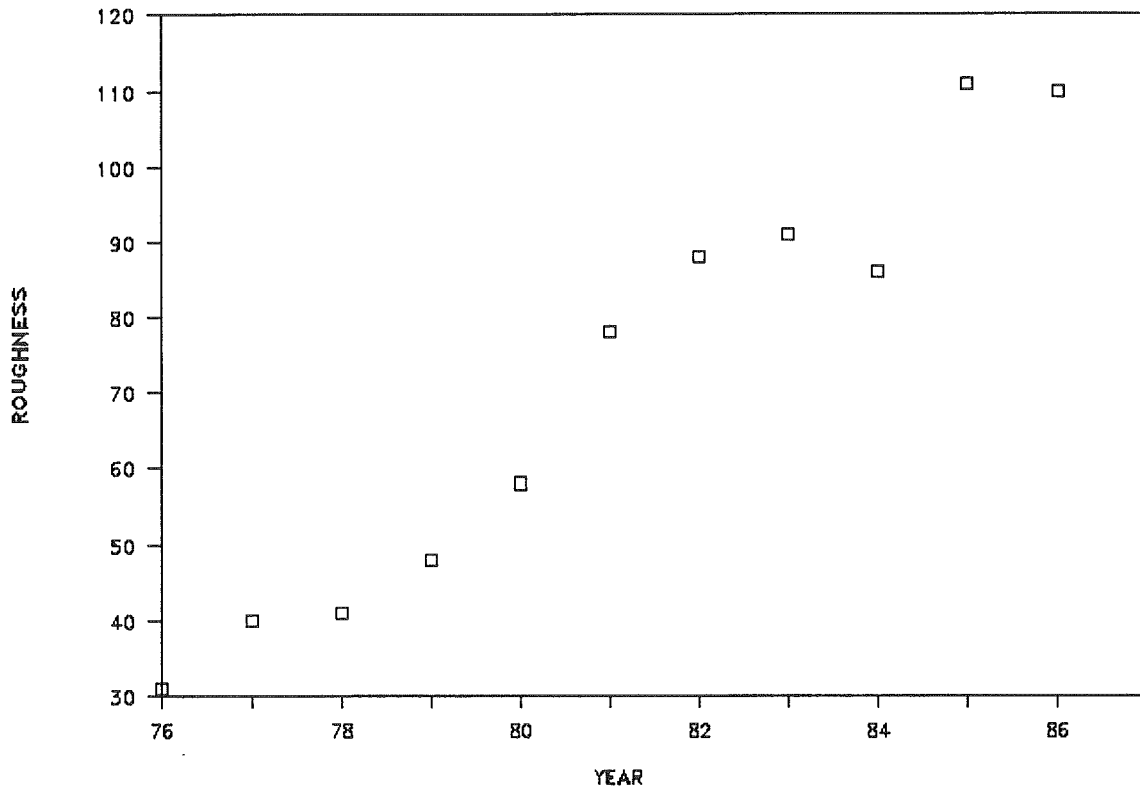


FIGURE 7-9. TYPICAL RATE OF CHANGE OF ROUGHNESS VS. TIME FOR INTERSTATE HIGHWAYS

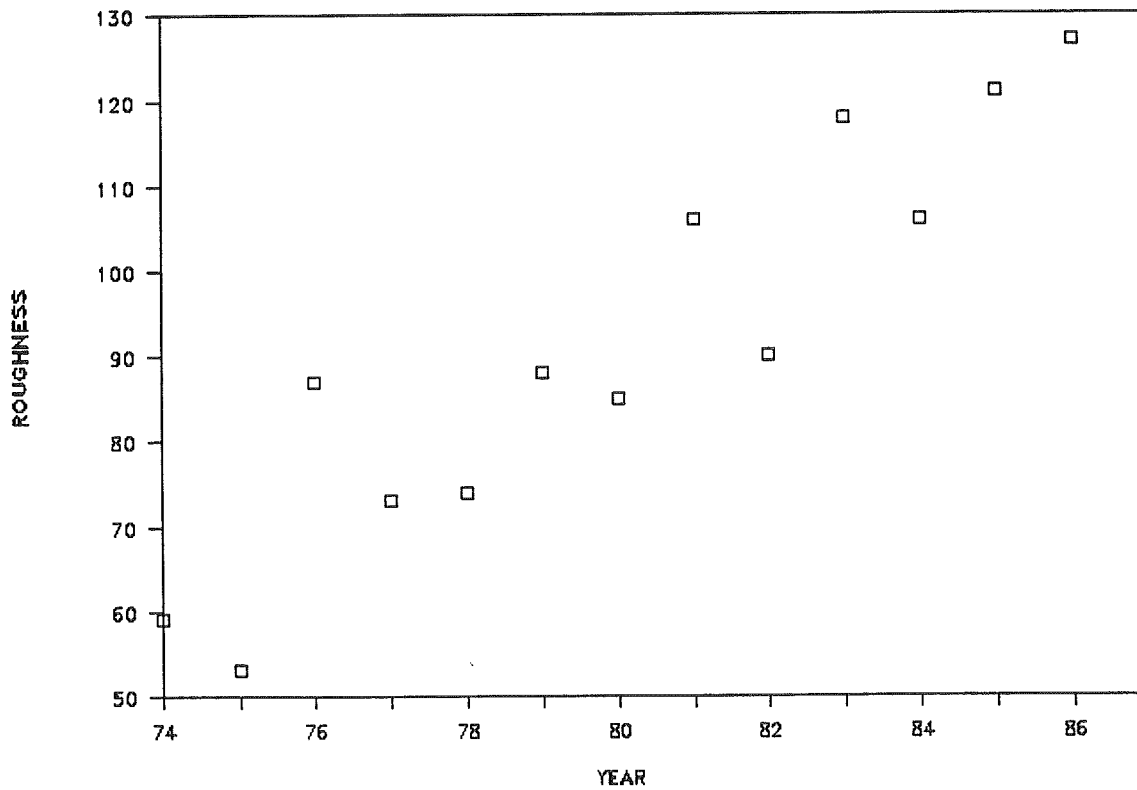


FIGURE 7-10. TYPICAL RATE OF CHANGE OF ROUGHNESS VS. TIME FOR U.S. ROUTES

STATE ROUTES

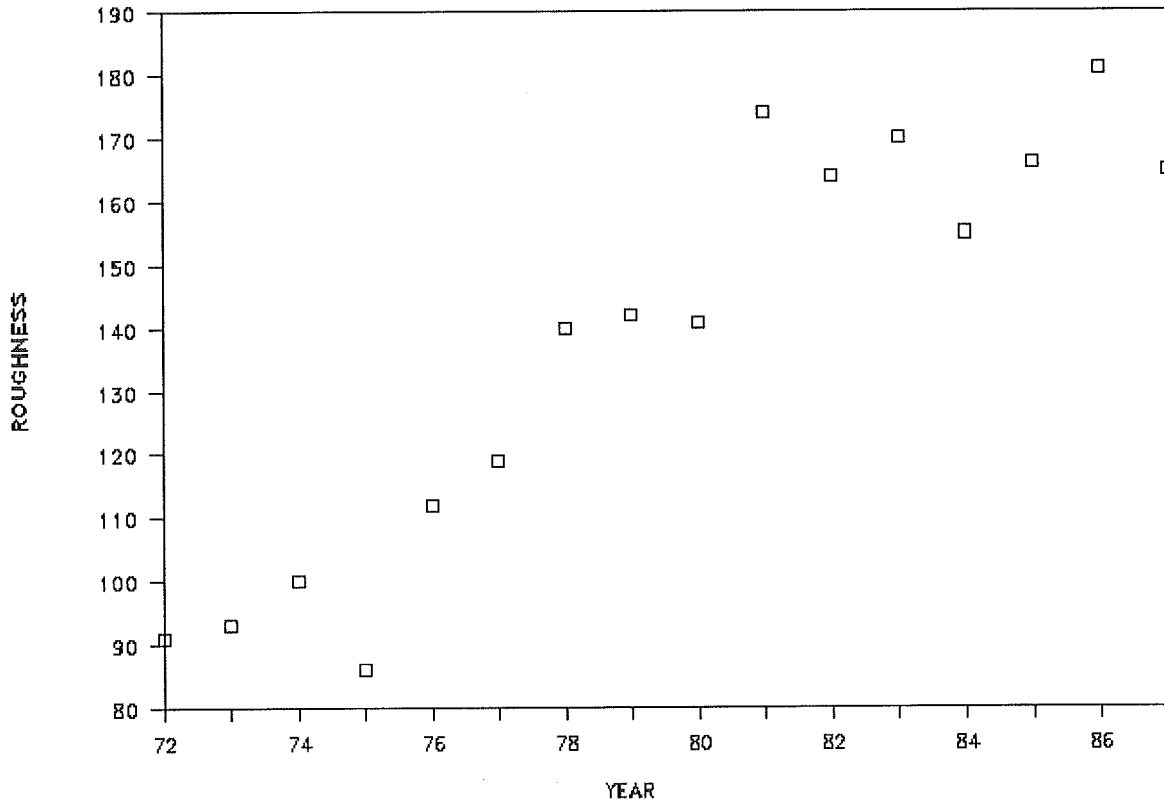


FIGURE 7-11. TYPICAL RATE OF CHANGE OF ROUGHNESS VS. TIME FOR STATE ROUTES

TABLE 7-2. DISTRIBUTION OF THE RATE OF CHANGE OF ROUGHNESS
(PROJECTS OVERLAID BETWEEN 1972 and 1981)

| Change in Roughness Per Year (in./mile) | Interstate | State | U.S. Routes |
|--|------------|-------|-------------|
| 0.00 - 0.99 | 1 | 0 | 0 |
| 1.00 - 1.99 | 0 | 2 | 0 |
| 2.00 - 2.99 | 0 | 1 | 5 |
| 3.00 - 3.99 | 4 | 5 | 2 |
| 4.00 - 4.99 | 5 | 7 | 6 |
| 5.00 - 5.99 | 9 | 5 | 6 |
| 6.00 - 6.99 | 6 | 3 | 6 |
| 7.00 - 7.99 | 11 | 2 | 4 |
| 8.00 - 8.99 | 5 | 3 | 2 |
| 9.00 - 9.99 | 1 | 1 | 2 |
| 10.00 - 10.99 | 3 | 0 | 1 |
| 11.00 - 11.99 | 1 | 0 | 0 |
| 12.00 - 12.99 | 1 | 0 | 0 |
| 13.00 - 13.99 | 0 | 0 | 0 |
| 14.00 - 14.99 | 0 | 0 | 0 |
| 15.00 - 15.99 | 0 | 0 | 0 |
| 16.00 - 16.99 | 0 | 0 | 0 |
| 17.00 - 17.99 | 0 | 0 | 0 |
| Number of Projects | 47 | 29 | 34 |
| Average | 6.7 | 5.1 | 5.8 |
| Std. Deviation | 2.3 | 2.1 | 2.1 |
| Minimum | 0.6 | 1.3 | 2.3 |
| Maximum | 12.9 | 9.9 | 11.0 |
| Total Mileage of All Projects | 189 | 203 | 208 |

The plots of rate of increase of roughness for projects overlaid on or after 1972 versus the independent variable considered (regional factor, ADL, structural number, overlay thickness and roughness after overlay) did not show any identifiable trends. Multiple regression analysis was also performed between the rate of increase of roughness and the independent variables mentioned above. No correlations were found for this analysis.

Since none of the independent variables were correlated with the rate of change in roughness, models could not be developed for predicting the increase in roughness as a function of pavement design variables. Hence, the average rate of change in roughness for each highway type, given in Table 7-2, can be used for estimating the performance of overlays.

It should be noted that the data in the ADOT PMS file are recorded at each whole milepost only. Meanwhile, typical overlay projects do not necessarily start and end at the milepost. Therefore, overlay projects less than one mile long were not considered in the analysis in order to obtain more accurate models. In addition, data recorded at the last milepost of each overlay project were also removed from the analysis.

7.2.3. Use of the Roughness Model

The analysis performed on this project indicates a good correlation between the change in roughness due to an overlay and the roughness before the overlay and the rate of increase in roughness over time. However, there was no correlation between these factors and engineering factors which logic dictates should govern the performance of the pavement. This could be attributed to a commonality between the pavement design and the subsequent performance. Until an improved data base is developed, possibly during the SHRP project, the equations developed during this project should be used for the analysis of overlays. The life of an overlay may be estimated as:

$$N = (R_L - R_b + \Delta R)/C \quad (7-4)$$

where:

- N = life of overlay in years
- R_L = limiting criteria for roughness
- R_b = roughness before overlay
- ΔR = predicted change in roughness due to overlay
- C = rate of change in roughness per year.

The roughness of the section to be overlaid, R_b , is determined by direct measurement with the Maysmeter. Alternatively, R_b may be determined from the ADOT PMS data base. The change in roughness, ΔR , is estimated with equation 7-1, 7-2, or 7-3 for interstate, U.S. routes and state routes, respectively. The average slope of the rate of change in roughness, C, is given in Table 7-2. R_L is the roughness level corresponding to the failure of the overlay. Using relationships previously developed by ADOT, R_L would equal 260 for a present serviceability rating, PSR, of 2.5, and 190 for a PSR of 3.0 (23). The selection of an R_L value is a policy decision by ADOT and is in line with the procedures used in the department's pavement management system. The value of R_L can be selected as a function of highway type.

7.3 FATIGUE MODEL

7.3.1 Background

The evaluation of fatigue life for asphalt concrete pavements is complex and has been the subject of study by a number of researchers for many years. Among the reasons that make the fatigue analysis difficult are:

1. the limited knowledge as to fatigue damage relations for real pavements,
2. the limited knowledge as to the effect of the type of asphalt layer on the fatigue life,

3. the limited information as to how the fatigue life potential of an asphalt concrete pavement varies with temperature and mixture characteristics,
4. typical pavement sections may have been overlaid several times producing different fatigue lives for the different asphalt layers, and
5. the unavailability of accurate traffic history and construction and maintenance records.

The form of the fatigue relations in common use is derived from a logarithmic relation between either stress or strain and the number of load cycles to failure. The relations between the logarithm of strain and the logarithm of load cycles are considered to be linear for asphalt concrete, which results in the following general equation:

$$N_i = K_1 \left(\frac{1}{\epsilon_i} \right)^{K_2} \quad (7-5)$$

where

N_i = number of load cycles at strain level i until fatigue failure,

ϵ_i = calculated tensile strain at the bottom of asphalt layer,

K_2 = slope of logarithmic function, and

$K_1 = N_i \epsilon_i^{K_2}$ for any pair N_i and ϵ_i that satisfies the logarithmic function.

Both K_1 and K_2 are empirical material constants.

A very important problem with this form of fatigue life characterization is the extreme sensitivity of the equation to small variations in K_2 , while test results for lab specimens that fail in tension are quite scattered. Further, the occurrence of fatigue cracking in the field is itself quite variable, even for apparently identical sections (64).

A number of fatigue models have been developed in previous studies as shown in Figure 7-12 (64). Six relations were obtained from standard laboratory beam tests (66, 69-73). Two relations were also obtained from laboratory tests, but the specimens rested on elastic supports (68, 74). Three relations were obtained from laboratory beam test results transformed to represent field conditions (65, 75, 76). Two other relations were produced from multiple regression analyses of the American Association of State Highway Officials (AASHO) Road Test data and are related to present serviceability index (PSI) (26,67). Witczak (67) specifically related tensile strain in the bottom of the AASHO Road Test pavements to number of load

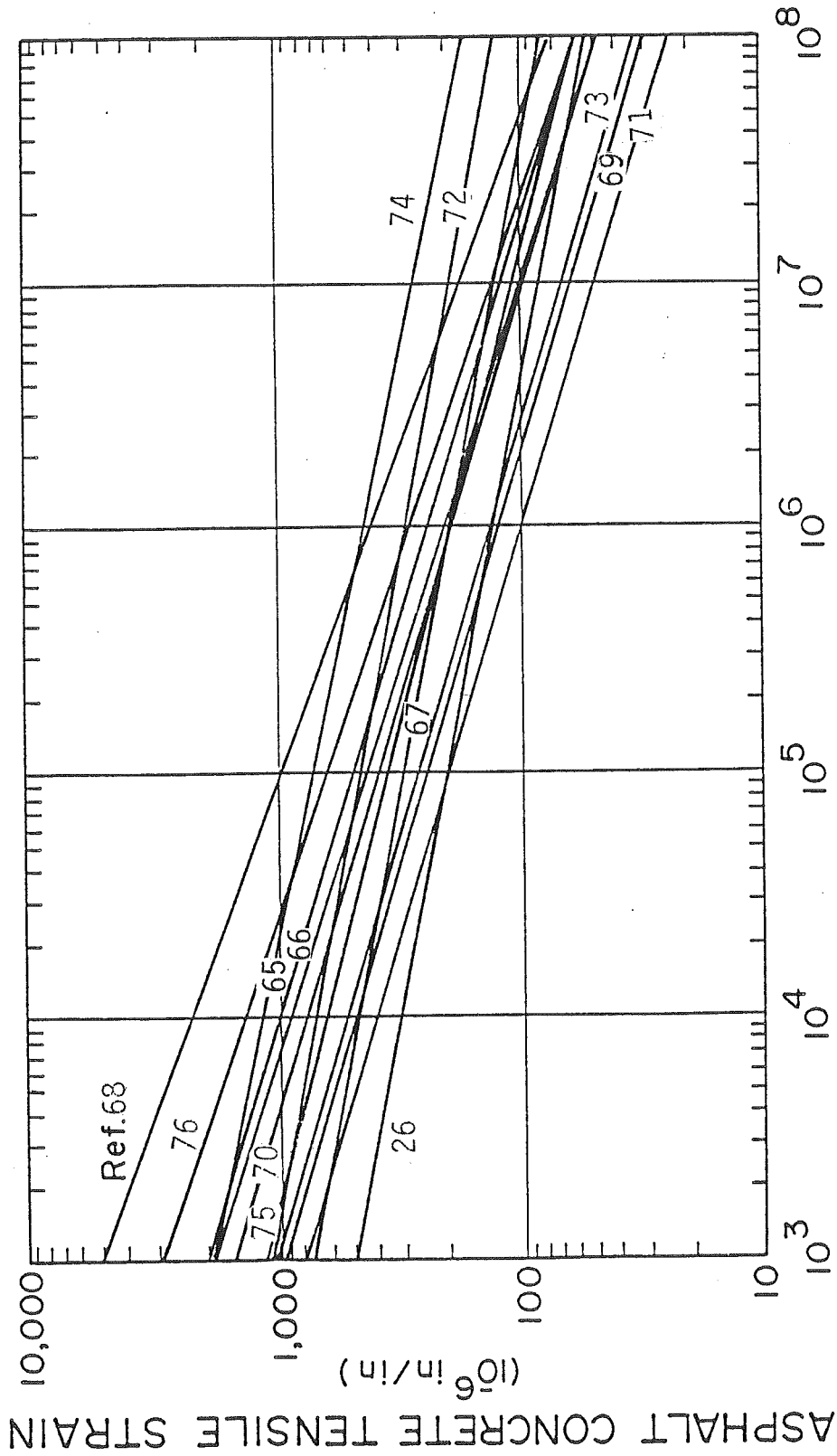


FIGURE 7-12. SOME FATIGUE RELATIONS INCLUDING RESULTS OF LABORATORY TESTING, WHEEL-TRACKING TESTS, AND EFFORTS TO REPRESENT FIELD CONDITIONS (64)

repetitions to reduce the PSI to 2.5. ARE Inc. (26) related tensile strain to measured cracking, but in terms of 18-kip equivalent single-axle load (ESAL) based on PSI. Three relations were obtained from laboratory beam-test results transformed to represent field conditions (65,75,76).

The slopes of these logarithmic functions shown in Figure 7-12 range between 2.70 and 5.51 with an average value of 3.84.

Jimenez (77) recommended another fatigue criterion for the design of asphalt pavements which relates the number of load applications to the radial tensile stress at the bottom of the asphalt layer. Jimenez's equation, however, was not considered in this study since it does not use the strain which is commonly used by other researchers.

7.3.2. Model Development

The fatigue model developed in this study is based on data obtained from the 20 selected sites and the fatigue models previously developed by other researchers (64). Table 7-3 shows the data used to develop the model. The average daily load (ADL) in 1987 and the traffic growth factor (GF) were obtained from the data base file. In order to compute the equivalent single axle load (ESAL) in the design lane, the lane distribution factor was selected as 1, 0.9 or 0.8 for one, two or three lanes in each direction.

The next step was to compute the cumulative ESALs that were applied on the first AC layer, the first overlay (if any), the second overlay (if any), etc. For this purpose the traffic growth factor was assumed constant for each site throughout the life of the pavement. This assumption was based on historical data that show almost linear population growth, vehicle registration growth and vehicle miles of travel growth (VMT) in Arizona in the last three decades (78).

Since each site has different environmental conditions from other sites, the ESAL data had to be normalized. The regional factor which is currently used by ADOT was selected as an adjustment factor in order to account for the difference in environmental conditions among various sites. It was further assumed that the regional factor changes the effect of traffic loads in a linear manner.

Another adjustment that had to be considered was due to the fact that the tensile strain at the bottom of the AC layer due to a standard wheel load varies when the pavement is overlaid. In other words, changing the pavement cross section changes the strain level the pavement is exposed to due to the same load applied at the pavement surface. Therefore, the ESAL applications had to be adjusted to a single stress level for each site.

For the original AC layer, Equation 7-5 becomes

$$N_1 = K_1 \left(\frac{1}{\epsilon_1} \right)^{K_2} \quad (7-6)$$

TABLE 7-3. CUMULATIVE ESAL AND TENSILE STRAIN AT BOTTOM OF AC

| Site / Sta. | ADL 1987 (1) | GF (%) (2) | Lane Dist. FAC. (3) | Start Yr (4) | Unadj. Cum. ESAL (5) | End Yr (6) | Reg. Fac. (7) | Max% Cracking (8) | Dvly Adj. Fac. (9) | Strain E-06 (10) | Adj. Cum. ESAL (11) | Refer. E-06 (12) | Total Adj. Cum. ESAL (13) | Crack. ked? (14) | Crack. (15) |
|-------------|--------------|------------|---------------------|--------------|----------------------|------------|---------------|-------------------|--------------------|------------------|---------------------|------------------|---------------------------|------------------|-------------|
| 1/1 | 2830 | 2.2 | .9 | 65 | 6.70e6 | 75 | 1.9 | 12 | 1 | 628.36 | 1 | 1.27e7 | 628.36 | 1.27e7 | Yes |
| | | | | 75 | 1.07e7 | 88 | 1.9 | 3 | 1 | 312.3 | 1 | 2.04e7 | 312.3 | 2.04e7 | No |
| 2/1 | 1220 | .7 | .9 | 55 | 5.11e6 | 70 | .7 | -- | 1 | 86.19 | 1 | 3.58e6 | | | |
| | | | | 70 | 6.81e6 | 88 | .7 | 5 | .515 | 72.49 | .515 | 2.45e6 | 86.19 | 6.03e6 | No |
| 3/7 | 2783 | 4.6 | .9 | 58 | 5.83e6 | 71 | 1.7 | -- | 1 | 440.52 | 1 | 9.91e6 | | | |
| | | | | 71 | 4.64e6 | 79 | 1.7 | 0 | .349 | 334.82 | .349 | 2.75e6 | | | |
| | | | | 79 | 7.02e6 | 88 | 1.7 | 0 | .007 | 119.61 | .007 | 80364. | 440.52 | 1.27e7 | No |
| 4/1 | 2783 | 4.6 | .9 | 58 | 5.83e6 | 71 | 1.7 | -- | 1 | 241.3 | 1 | 9.91e6 | | | |
| | | | | 71 | 4.64e6 | 79 | 1.7 | 0 | .948 | 237.98 | .948 | 7.48e6 | | | |
| | | | | 79 | 7.02e6 | 88 | 1.7 | 0 | .038 | 102.72 | .038 | 451042 | 241.3 | 1.78e7 | No |
| 5/4 | 1846 | 3.6 | .9 | 60 | 4.52e6 | 73 | 1.8 | 33 | 1 | 42.92 | 1 | 8.14e6 | 42.92 | 8.14e6 | Yes |
| | | | | 73 | 5.08e6 | 84 | 1.8 | 0 | 1 | 300.88 | 1 | 9.15e6 | | | |
| | | | | 84 | 2.27e6 | 88 | 1.8 | 0 | 1.38 | 326.98 | 1.38 | 5.63e6 | 300.88 | 1.48e7 | No |
| 6/1 | 1846 | 5.4 | .9 | 66 | 1.17e6 | 70 | 3.5 | -- | 1 | 267.33 | 1 | 4.09e6 | | | |
| | | | | 70 | 4.11e6 | 81 | 3.5 | 15 | .133 | 158.02 | .133 | 1.92e6 | 267.33 | 6.01e6 | Yes |
| | | | | 81 | 3.66e6 | 88 | 3.5 | 1 | 1 | 137.41 | 1 | 1.28e7 | 137.41 | 1.28e7 | No |
| 7/4 | 2535 | 3.6 | .9 | 61 | 6.93e6 | 75 | 1.8 | 39 | 1 | 588.61 | 1 | 1.25e7 | 588.61 | 1.25e7 | Yes |
| | | | | 75 | 9.10e6 | 88 | 1.8 | 0 | 1 | 311.78 | 1 | 1.64e7 | 311.78 | 1.64e7 | No |

TABLE 7-3. CUMULATIVE ESAL AND TENSILE STRAIN AT BOTTOM OF AC (CONT.)

| Site / Sta. | ADL 1987 (1) | GF (%) (2) | Lane Dist Fac. (3) | Start Yr (4) | Unadj. Cum. ESAL (5) | End Yr (6) | Reg. Fac. (7) | Max% Crac king (8) | Strain E-06 (9) | Ovly Adj. Fac. (10) | Adj. Cum. ESAL (11) | Refer. Strain E-06 (12) | Total Adj. Cum. ESAL (13) | Crac ked? (14) |
|-------------|--------------|------------|--------------------|--------------|----------------------|------------|---------------|--------------------|-----------------|---------------------|---------------------|-------------------------|---------------------------|----------------|
| 8/1 | 2535 | 3.6 | .9 | 61 | 6.93e6 | 75 | 1.8 | 30 | 155.84 | 1 | 1.25e7 | 155.84 | 1.25e7 | Yes |
| | | | | 75 | 9.10e6 | 88 | 1.8 | 0 | 167.61 | 1 | 1.64e7 | 167.61 | 1.64e7 | No |
| 9/1 | 1616 | 4.3 | .9 | 67 | 3.97e6 | 79 | 2.5 | 5 | 304.39 | 1 | 9.93e6 | | | Yes |
| | | | | 79 | 4.11e6 | 88 | 2.5 | 30 | 318.79 | 1.19 | 1.23e7 | 304.39 | 2.22e7 | Yes |
| 10/1 | 1382 | 3.7 | .9 | 69 | 3.76e6 | 81 | 2.7 | 50 | 408.33 | 1 | 1.02e7 | 408.33 | 1.02e7 | Yes |
| | | | | 81 | 2.85e6 | 88 | 2.7 | 1 | 292.06 | 1 | 7.70e6 | 292.06 | 7.70e6 | No |
| 11/5 | 354 | 4.3 | .9 | 76 | 1.16e6 | 88 | 3.4 | 5 | 139.01 | 1 | 3.94e6 | 139.01 | 3.94e6 | No |
| 12/1 | 2544 | 1.1 | .9 | 67 | 8.64e6 | 79 | 1.9 | 0 | 455.08 | 1 | 1.64e7 | | | No |
| | | | | 79 | 7.18e6 | 88 | 1.9 | 5 | 303.72 | .212 | 2.89e6 | 455.08 | 1.93e7 | No |
| 13/4 | 14 | 2.3 | 1 | 79 | 42046. | 88 | 2.3 | 0 | 180.32 | 1 | 96707. | 180.32 | 96707. | No |
| 14/4 | 61 | 3 | 1 | 78 | 91219. | 83 | 3.3 | 15 | 308.53 | 1 | 301024 | 308.53 | 301024 | Yes |
| | | | | 83 | 104065 | 88 | 3.3 | 0 | 373.61 | 1 | 343413 | 373.61 | 343413 | No |
| 15/4 | 348 | 2.9 | 1 | 61 | 1.34e6 | 77 | 1.2 | -- | 654.83 | 1 | 1.61e6 | | | Yes |
| | | | | 77 | 1.23e6 | 88 | 1.2 | 35 | 421.4 | .184 | 271726 | 654.83 | 1.88e6 | Yes |
| 16/1 | 265 | .3 | .8 | 77 | 837584 | 88 | 1 | 7 | 271.2 | 1 | 837584 | 271.2 | 837584 | No |
| 17/1 | 176 | 2.6 | 1 | 79 | 523343 | 88 | 3.2 | 0 | 842.02 | 1 | 1.67e6 | 842.02 | 1.67e6 | No |

TABLE 7-3. CUMULATIVE ESAL AND TENSILE STRAIN AT BOTTOM OF AC (CONT.)

| Site / Sta. | ADL (1) | GF (%) (2) | Lane Dist Fac. (3) | Start Yr (4) | Unadj. Cum. ESAL (5) | End Yr (6) | Reg. Fac. (7) | Max% Cracking (8) | Strain E-06 (9) | Ovly Adj. Fac. (10) | Refer. Cum. ESAL (11) | Total Adj. Strain E-06 (12) | Cracked? (13) | Crack (14) |
|-------------|---------|------------|--------------------|--------------|----------------------|------------|---------------|-------------------|-----------------|---------------------|-----------------------|-----------------------------|---------------|------------|
| 18/1 | 290 | 1.9 | .9 | 65 | 1.86e6 | 88 | 1.5 | 30 | 286.81 | 1 | 2.79e6 | 286.81 | 2.79e6 | Yes |
| 19/4 | 65 | 0 | 1 | 78 | 237250 | 88 | 4.5 | 0 | 639.56 | 1 | 1.07e6 | 639.56 | 1.07e6 | No |
| 20/1 | 2225 | 6.2 | .9 | 67 | 5.79e6 | 81 | 1.8 | 35 | 457.01 | 1 | 1.04e7 | 457.01 | 1.04e7 | Yes |
| | | | | 81 | 4.34e6 | 88 | 1.8 | 1 | 373.41 | 1 | 7.82e6 | 373.41 | 7.82e6 | No |

Notes:

Column 3: Traffic growth factor (%)

Column 11: The overlay adjustment factor is equal 1 for original AC layers or overlays over a cracked AC layer. It is equal $(\epsilon_1/\epsilon_2)^k$ for overlays over uncracked AC layers, where ϵ_1 and ϵ_2 are the strains of the lowest uncracked AC layer before and after overlay.

Column 12: The adjusted cumulative ESAL = Unadjusted cumulative ESAL X Regional factor X Overlay adjustment factor

Column 13: The referance strain is the strain of the lowest uncracked AC layer

Column 14: Summation of the adjusted cumulative ESAL's since the original AC layer or since the first overlay over a cracked AC layer

and for the uncracked original AC and the overlay, Equation 7-5 becomes

$$N_2 = K_1 \left(\frac{1}{\epsilon_2} \right)^{K_2} \quad (7-7)$$

From Equations 7-6 and 7-7,

$$\frac{N_1}{N_2} = \left(\frac{\epsilon_2}{\epsilon_1} \right)^{K_2} = \text{Overlay adjustment factor} \quad (7-8)$$

where ϵ_1 and ϵ_2 are the strains under the original AC before and after overlay, respectively. Thus, the ESAL after overlay has to be adjusted according to Equation 7-8 then added to the ESAL before overlay in order to calculate the total ESAL that is matching the tensile strain before overlay (reference strain). The K_2 value was taken as 3.84 which is the average of K_2 values of existing fatigue functions (64). The overlay adjustment factor is shown in Table 7-3 (Column 11). In the case when the old AC layer is cracked, the ESAL before overlay cannot be added to the ESAL after overlay and the periods before and after overlay have to be treated separately. In this study the AC layer was considered to be cracked if cracking was 10% or more.

The tensile strain was calculated using Chevron computer program (79) for a standard wheel load of 9000 lb and a tire pressure of 100 psi. No adjustment was used for tire pressure since the tire pressure has not largely changed for the last two decades with an average value in the high 90's and an 80th percentile of a slightly more than 100 psi (80-83). In addition, the FHWA study (84) showed that the strain at the bottom of the AC layer is affected more by load than by tire pressure. For example the study showed that doubling the load (from 9,400 to 19,000 lb) increased predicted damage by 1,000 percent while doubling tire pressure (from 76 to 140 psi) increased predicted damage only 20 percent. Thus, even if there was a minor change in tire pressure in Arizona in the last two decades, the effect of this change on the tensile strain is not expected to be large.

The total adjusted cumulative ESAL shown in Table 7-3 is the summation of adjusted cumulative ESAL's since the original AC layer or since the first overlay over a cracked AC layer.

The total adjusted cumulative ESAL was plotted versus the reference tensile strain using a log-log scale as shown in Figure 7-13. A straight line (fatigue function) was selected close to the upper boundary of the band of previous fatigue functions (64) with a slope of 3.84 which is the average of other slopes. This selected fatigue line lies above most of the uncracked pavement sections which indicates that they have some remaining life. A few uncracked sections lie above the fatigue line and several cracked sections lie below the line which indicate some discrepancies. These discrepancies are,

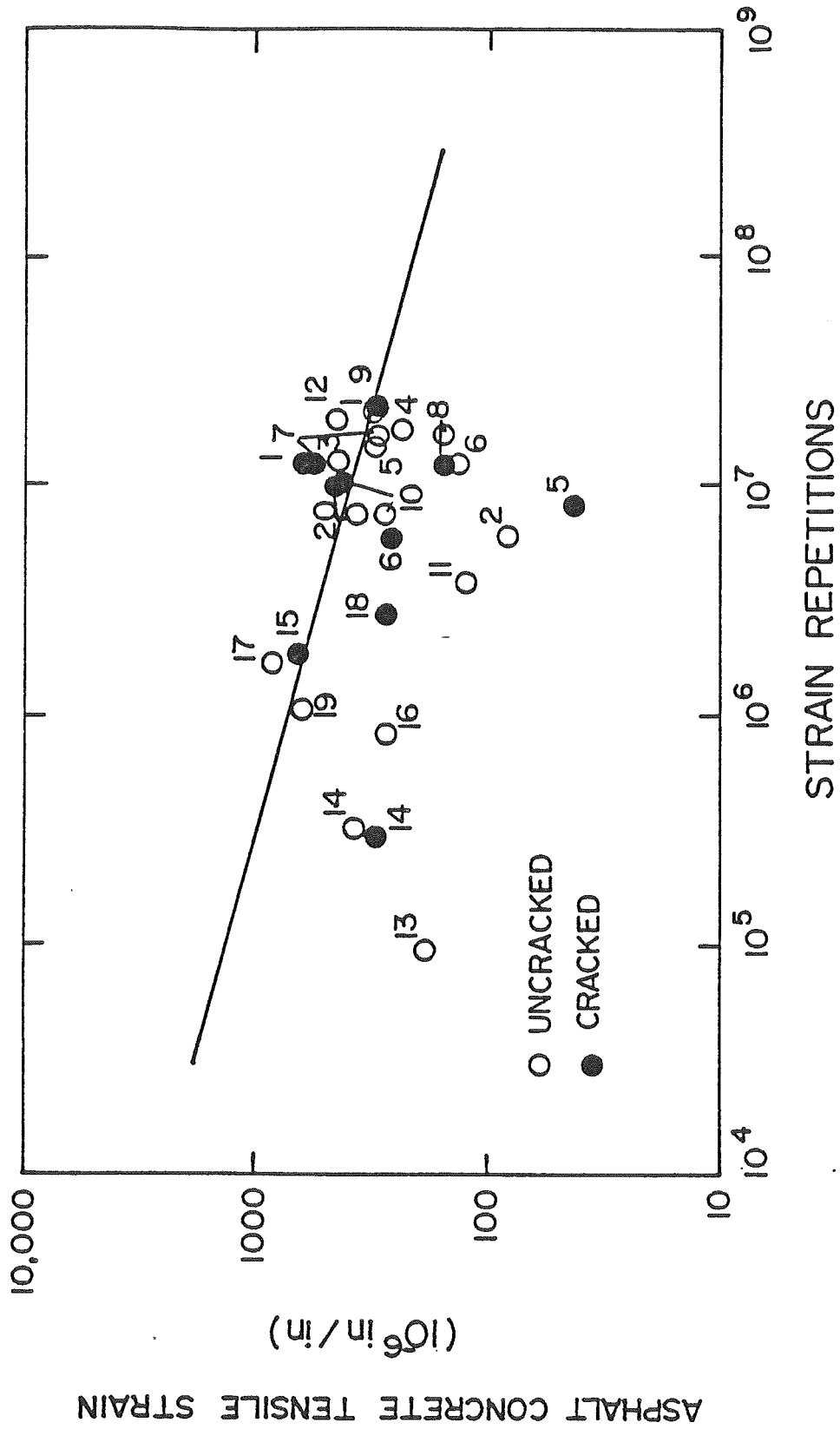


FIGURE 7-13. ASPHALT CONCRETE TENSILE STRAIN VS STRAIN REPETITIONS FOR ALL 20 SITES

however, considered acceptable. The equation of the selected fatigue function is

$$N = \frac{1}{10^{6.03}} \left(\frac{1}{\epsilon_{AC}} \right)^{3.84} \quad (7-9)$$

where

N = theoretical number of ESAL repetitions until fatigue failure, and

ϵ_{AC} = tensile strain at the bottom of the AC layer.

It should be noted that Equation 7-9 is valid for various conditions such as different regions, temperatures, etc., since these conditions were normalized to standard conditions. For example, different regions were normalized using the ADOT regional factors and AC moduli were normalized to the modulus at 70°F, etc. Therefore, if the tensile strain at the bottom of the AC layer is known under these standard conditions, the number of ESAL repetitions until fatigue failure can be computed.

7.4. PLASTIC DEFORMATION MODEL

7.4.1. Introduction

Damage to a pavement structure can arise through a variety of mechanisms, including plastic deformations in the layers of the structure. The ultimate result of these deformations may be cracking, rutting or simply the development of excessive roughness. However, the initial cause being considered in this part of the design process is plastic or permanent deformations.

This design model deals only with plastic deformations in layers below the AC surface layer. It is assumed that plastic deformations in the overlay layer, which may lead to rutting, will be corrected by improvements in mix design and construction techniques.

In the plastic deformation model, attention is devoted to the plastic strains which are permanent; i.e., not recoverable. However, permanent deformations are much more troublesome to measure in the field than total deformations (elastic & plastic). It has therefore been assumed that the onset of significant plastic deformation corresponds to the onset of non-linear load-deflection response. In other words, as long as the load-deflection curve is linear, it is assumed that the plastic deformations are negligible.

Two types of non-linearity may arise, as indicated in Figure 7-14 as Type A and Type B. Non-linearity of Type B is interpreted as strain-hardening, as might occur when a seating load is applied, and is believed not to represent a problem with respect to plastic deformations. Therefore, non-linearity of Type B is ignored and only Type A is considered in this design model.

The design procedure is based on the assumption that the onset of significant non-linear response can be measured directly with the FWD test.

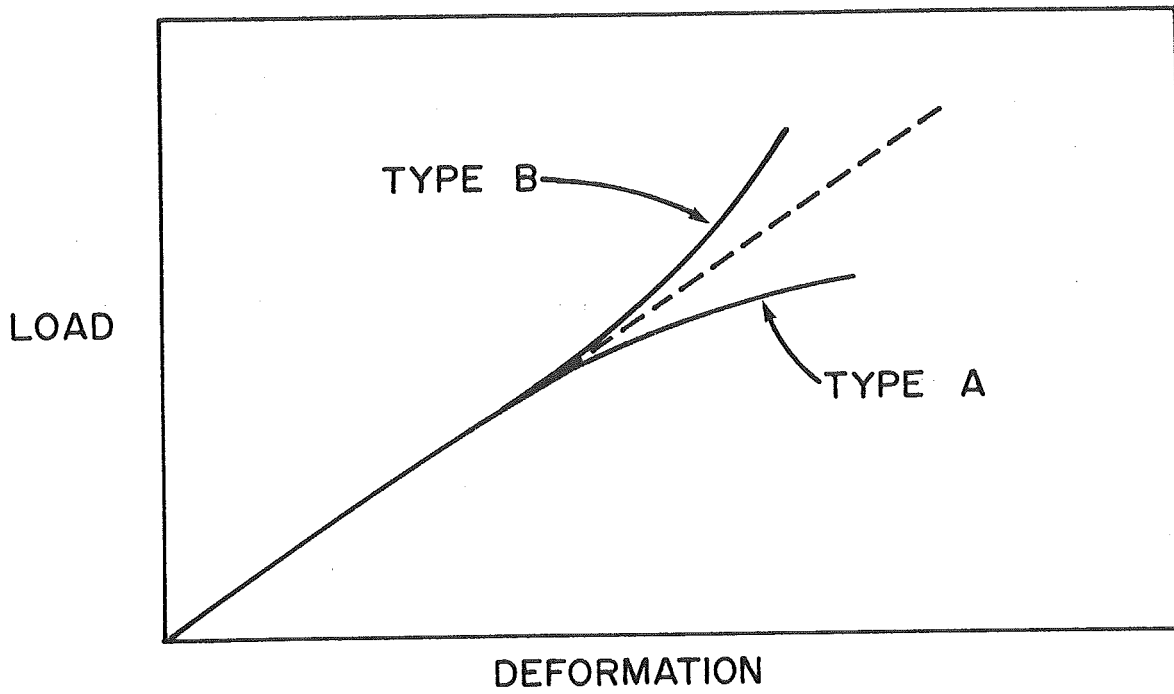


FIGURE 7-14. NONLINEARITY OF SUBGRADE MATERIALS

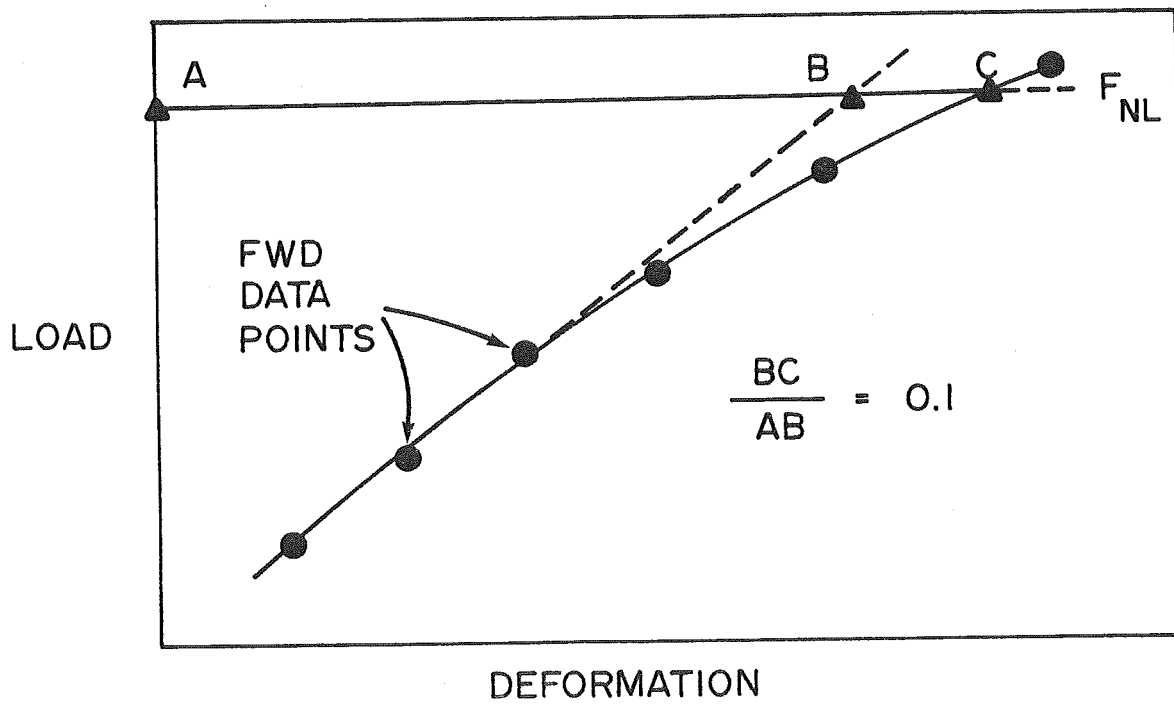


FIGURE 7-15. DEFINITION OF F_{NL}

The load corresponding to the onset of significant non-linear response is designated F_{NL} .

Based on data examined to date, it is believed that most pavement sections being considered for an overlay have sufficient factor of safety in the structural design that plastic deformations are unlikely to be a source of problem. This part of the design procedure is intended to detect and correct those few cases where vulnerability to excessive plastic deformations is indicated by the FWD test results. Thus the objective of design procedure may be stated as follows.

7.4.2. Objective

When the pavement gets older the ability of the pavement surface to spread the load to the underlying layers may be decreased due to cracking or other surface failures. In addition, the pavement might be subjected to heavier traffic load in the future which have not been applied before. Therefore, the objective of plastic deformation design is to provide sufficient overlay thickness that expected traffic loads will not induce significant plastic deformations in the underlying layers. In application, this objective corresponds to providing a pavement section for which the expected traffic loads will not produce stresses in the underlying layers greater than those induced by F_{NL} from the FWD test. If this objective is met then the plastic deformations can be expected to be tolerably small.

7.4.3. General Description of Design Procedure

With reference to Figure 7-14, the exact point at which deviation from linear behavior occurs is difficult to select. Therefore, F_{NL} has been defined as the load at which the Type A curve deviates 10%, measured horizontally, from the straight-line extension of the early portion of the curve.

Figure 7-15 illustrates the definition of F_{NL} and shows how it can be obtained by interpolation. The equation of the straight-line portion is obtained by fitting a least-squares line to the first three data points, corresponding to loads of 6, 9 and 12 kips. The FWD loads of 15, 18 and 21 kips are the loads where non-linear response is expected, if it occurs at all. If non-linearity of 10% or more is not exhibited at 21 kips, then it is assumed that plastic deformation is not a problem for this section and this part of the design is by-passed.

Ideally the FWD measurements should be made during that part of the year when plastic deformations are most likely. These times would correspond to either the hottest period, when the load-spreading capability of the surfacing is minimized, or the wettest period, when the subgrade is expected to be weakest. At the present time it is unknown which time during the year is more critical and it is recommended that measurements be made at both times until it is learned which is more critical.

The traffic loading to be used for design has been chosen so that the number of load repetitions expected to exceed the design value, F_{des} , is relatively small, regardless of the highway classification. The weigh-in-motion data shown in Table 7-4 served as the basis for the selection. The means and standard deviations are shown on the left and the loads corresponding to various probabilities of exceedence are given in the rest of the table.

The first decision which was needed was the selection of the most critical loading configuration. For a given probability of exceedence, such as 0.0001, the WIM loads for the steering axle, single axle dual wheel and tandem axle dual wheel were compared. The stress state in an underlying typical pavement section was calculated and it was found that the single axle dual wheel loading was the most critical, by a small margin. It was also found that the stresses in the subgrade were the most critical for design. Therefore, only stresses in subgrade were considered thereafter.

In comparing the stress states, several different stresses were considered for comparison, including the principal stress difference, or deviator stress, the maximum shear stress, the maximum octahedral shear stress, and the maximum vertical normal stress. Because shear stress is more indicative of plastic deformations in a pavement structure than normal stress, a shear stress was preferred. Maximum shear stress, τ_{max} , is quite a reasonable choice if only laboratory test results were to be used. In consideration of the complex stress states in the field under an FWD plate or a dual wheel of a truck, the maximum octahedral shear stress, $(\tau_{oct})_{max}$, was chosen because it reflects all the components of the stress tensor. This stress is therefore the best for translating behavior from the lab to the field or from one field location to another. The definition and equations for τ_{oct} are given in Appendix E.

Thus the choice of F_{des} is made by entering Table 7-4 at the row corresponding to WIM single axle loads and selecting a probability of exceedence and axle load such that the expected number of load repetitions larger than F_{des} in the period of a year is no more than a few repetitions. The ADL in the design lane (ADL x lane distribution factor) is used as an estimate of the total number of load repetitions in a day. Therefore, the total number of load repetitions for a year would be 365 x ADL in the design lane.

The mean and standard deviation axle loads in Table 7-4 are assumed to be the same for interstate, U.S. and state highways, but the ADL values differ significantly. Therefore, differing levels of probability of exceedence are needed to provide comparable levels of protection against plastic deformation. Table 7-5 shows the mean and standard deviation axle load, recommended probability of exceedence, corresponding design axle load, F_{des} , typical ADL in the design lane and expected number of load repetitions per year greater than F_{des} .

TABLE 7-4. AXLE LOADS FOR DIFFERENT PROBABILITIES

| Axle Type | Mean (kips) | Std Dev (kips) | Load (kips) | | | |
|-----------------------|----------------|-------------------|-------------|-------|--------|--------|
| | | | Probability | | | |
| | | | .001 | .0001 | .00008 | .00001 |
| WIM Steering Axles | 8.66 | 2.78 | 17.25 | 19.00 | 19.168 | 20.364 |
| Static Steering Axles | 9.71 | 1.49 | 14.31 | 15.25 | 15.342 | 15.983 |
| WIM Single Axles | 16.33 | 6.95 | 37.81 | 42.18 | 42.601 | 45.590 |
| Static Single Axles | 11.06 | 5.4 | 27.75 | 31.15 | 31.472 | 33.794 |
| WIM Tandem Axles | 32.25 | 10.87 | 65.84 | 72.69 | 73.339 | 78.013 |
| Static Tandem Axles | 22.76 | 9.6 | 52.42 | 58.47 | 59.048 | 63.176 |

Notes:

1. Means and standard deviations were obtained by ADOT. Static data are from truck weight studies in 1982, 1984 and 1986. WIM data are from 3 interstate locations in 1985, 48 hours each.
2. Data were assumed to follow normal distributions.
3. A probability of 0.0001, for example, means 1 out of 10,000 axles exceeds the value shown.

TABLE 7-5. TYPICAL DATA USED IN MODEL DEVELOPMENT

| Highway Type | Mean Axle Load (kips) | Std. Dev. of Axle Load (kips) | Probability of Exceedence (kips) | Design Axle Load (kips) | F_{des}^* | Typical ADL in design lane | Expected No. of Load Repetitions per yr $>F_{des}$ |
|--------------|-----------------------|-------------------------------|----------------------------------|-------------------------|-------------|----------------------------|--|
| Interstate | 16.33 | 6.95 | 0.00001 | 45.6 | 22.8 | 2000 | 7 |
| U.S. State | 16.33 | 6.95 | 0.00008 | 42.6 | 21.3 | 225 | 7 |

* F_{des} = load on a dual wheel = $\frac{1}{2}$ x (Design Axle Load)

The following is an example computation of the expected annual number of load repetitions which would exceed F_{des} .

Assume: Project is on U.S. highway. Therefore Probability of exceedence = 0.00008, F_{des} = 21.3 and ADL in the design lane = 225

Total expected number of load repetitions per year = 365 ADL
 = (365)(225) = 82,125

Expected no. of load repetitions greater than F_{des} =
 probability of exceedence x total expected no. of load repetitions per year

= 0.00008x365(ADL)

= 0.00008x82,125 =7

A user of the design procedure is not required to compute the expected number of load repetitions per year greater than F_{des} , because typical values of ADL have already been assigned to each highway type and the probability of exceedence values have been chosen so as to make the last column in Table 7-4 about 7. The reason for showing the example computation above was to enhance the reader's understanding of what was done and to illustrate a mechanism by which the user could modify the design procedure in the future to make it less or more conservative, as desired. The design could be made less conservative by increasing the probability of exceedence which could in turn reduce F_{des} and increase the expected number of load repetitions greater than F_{des} .

CHAPTER 8.

CART OVERLAY DESIGN METHOD FOR ARIZONA

In this chapter a discussion of how the overlay design method was developed by the Center for Advanced Research in Transportation (CART) at Arizona State University is presented. The CART Overlay Design for Arizona (CODA) considers the three common types of pavement failure; roughness, fatigue, and plastic deformation. The method is limited to flexible overlays over flexible pavements. The method was incorporated in the microcomputer program CODA which accompanies this report together with the user's guide.

The traffic load requirements in this method are the current ADL and the traffic growth factor. The ESAL in the design lane is assumed to be 100, 90, 80 and 70% of the ADL/direction for 1, 2, 3 and 4 lanes in each direction, respectively. In order to compute the cumulative ESAL during the design period, the CODA program assumes that the growth factor remains constant throughout the design period.

Since both fatigue and plastic deformation models require the knowledge of pavement and subgrade layer moduli, the first step in the procedure is to run the FWD test on the pavement section under consideration. The fatigue model requires performing the FWD test at a load level of 9000 lb only, while the plastic deformation model (if used) requires running the FWD test at several load levels as discussed below.

The FWD deflection data at 9000 lb load level are further used to calculate the pavement and subgrade layer moduli using the BKCHEVM program as discussed in Section 6.3. Since the modulus of the AC layer is significantly affected by temperature, a subroutine TEMP was developed in the CODA program to adjust the AC modulus to a standard temperature of 70°F. The adjustment of the AC modulus is based on the method recommended in the 1986 AASHTO guide (60). This method requires the knowledge of the pavement surface temperature at the time of FWD testing and the 5-day mean air temperature prior to FWD testing.

The procedure for the CART overlay design method for Arizona can be divided into four areas as shown in Figure 7-2:

1. Overlay design,
2. Remaining life analysis,
3. Life of a user specified overlay, and
4. Economic analysis.

These four areas are presented in the following sections.

8.1. OVERLAY DESIGN

This part of the CODA procedure can be used to design an overlay for an existing failed pavement. The overlay design is based on the use of three criteria; roughness, fatigue and plastic deformation, as discussed below.

8.1.1. Roughness Criterion

As indicated in Section 7.2, the life of an overlay can be estimated as follows using the Maysmeter roughness data.

$$N = (R_L - R_b + \Delta R)/C \quad (8-1)$$

where:

N = life of overlay in years

R_L = limiting criteria for roughness

R_b = roughness before overlay

ΔR = predicted change in roughness due to overlay

C = slope of roughness versus time relationship

Since Equation 8-1 is not a function of overlay thickness, it cannot be used to determine the thickness requirements directly. In other words, previous experience with Arizona highways indicates that any practical overlay thickness will support approximately the same number of load applications before reaching the roughness failure condition. Since the normal overlay design life in Arizona is 10 years, Equation 8-1 can be used to check if a 10-year life is feasible. If the roughness equation results in an overlay life of 10 years or more, the roughness model is satisfied and the overlay is later designed for a 10-year life using the fatigue model. On the other hand, if the roughness equation results in a predicted overlay life of less than 10 years, this shorter life is used as the fatigue life for the fatigue deformation model unless milling or another special treatment is used.

8.1.2. Fatigue Criterion

The fatigue part of the overlay design is based on the fatigue model developed in Section 7.3.

$$N = \frac{1}{10^{6.03}} \left(\frac{1}{\epsilon_{AC}} \right)^{3.84} \quad (8-2)$$

where

N = number of ESAL applications until fatigue failure, and

ϵ_{AC} = tensile strain at the bottom of the AC layer due to a standard wheel load (in./in.).

The Chevron program (79) is used to compute the tensile strain at the bottom of the AC layer. The program requires the knowledge of the layer moduli as obtained from backcalculation as discussed earlier. Also, the method is configured to recognize that in many cases the pavement is overlaid before it is significantly cracked. Therefore, the method considers the remaining fatigue life of the existing pavement and adds it to the overlay life.

The fatigue criterion can be used for two different cases:

1. Pavement has not been overlaid before, and
2. Pavement has been overlaid once, twice or thrice.

Case 1. Pavement has not been overlaid before:

The design procedure varies depending on the cracking condition of the existing pavement before overlay.

a. If cracking is less than 10% - In this case both cumulative ESAL before and after overlay are used in the design. For the period before overlay, the tensile strain at the bottom of the existing AC layer without overlay is computed. The theoretical allowable number of ESAL repetitions until failure is then calculated using the fatigue model (Equation 8-2). For the period after overlay, the tensile strain at the bottom of the existing AC layer is computed assuming an overlay layer of 1.5 inches. The corresponding theoretical allowable number of ESAL repetitions is then computed from Equation 8-2. Using the concept of cumulative damage [Minor's law (85)] and assuming that the 1.5 inch overlay will fail due to fatigue at the end of the design period, therefore,

$$\frac{n_1}{N_1} + \frac{n_2}{N_2} = 1$$

or
$$n_2 = N_2 \left(1 - \frac{n_1}{N_1}\right) \quad (8-3)$$

where

- n_1 = actual cumulative ESAL in the design lane before overlay
- N_1 = allowable cumulative ESAL in the design lane before overlay
- n_2 = actual cumulative ESAL in the design lane after overlay
- N_2 = allowable cumulative ESAL in the design lane after overlay

This process is repeated for 3.5 and 5.5 inch overlays and the corresponding cumulative ESAL's for each overlay are computed. Using the three overlay thicknesses of 1.5, 3.5 and 5.5 inches and the corresponding cumulative ESAL's predicted from Equation 8-3, a polynomial equation is fitted in the form:

$$t = a + bn_2 + cn_2^2 \quad (8-4)$$

where

- t = overlay thickness

n_2 = cumulative ESAL after overlay, and

a, b and c = constants

By knowing the expected cumulative ESAL computed from the current ESAL and traffic growth, the overlay thickness can be computed for Equation 8-4.

b. If cracking is 10% or more - In this case it is assumed that the old AC layer will not contribute to the cumulative fatigue life after overlay. Therefore, the tensile strain is computed at the bottom of the overlay. In addition, the cracked AC layer is assumed to have a modulus of 40 ksi.

The minimum overlay thickness considered in this analysis is 3 inches. As shown in Figure 8-1(86) the tensile strain at the bottom of the overlay increases as the thickness of the overlay increases from 1.5 to approximately 3 inches. Due to the increase in strain, overlays on cracked pavements in this thickness range are not cost effective with respect to fatigue life.

Similar to the case of less than 10% cracking, three overlay thicknesses are assumed and the corresponding cumulative ESALs are computed. A polynomial curve is then fitted to the data and the specific overlay that corresponds to the predicted cumulative ESAL is computed.

Case 2. Pavement has been overlaid once, twice or thrice

If the existing pavement has been previously overlaid either once or more and cracking has not reached 10%, the cumulative fatigue is added for each period corresponding to a specific AC thickness. In all cases, the tensile strain is computed at the bottom of the original AC layer.

On the other hand if cracking has reached 10% or more at any time during the life of the old pavement, the tensile strain is computed at the bottom of the AC layer above the cracked layer and the cracked layer together with any AC layer underneath are not considered in the cumulative fatigue equation. Also, the cracked AC layer is assumed have a modulus of 40 ksi.

8.1.3. Plastic Deformation Criterion

Detailed Step-by-Step Procedure for Plastic Deformation Overlay Design

1. Input existing pavement structure geometry, moduli from backcalculation analyses, and highway type (interstate, U.S. or state).
2. Input FWD data for loads from 6 kips to 15 kips or more. Use 6-12 kip data to establish the straight line (least square fit) and check the higher loads for deviation from the straight line at each sensor.
3. If none of the loads show 10% or more deviation, report that F_{NL} > the maximum FWD applied load and bypass plastic deformation design. If one or more loads show deviation \geq 10%, proceed to step 4.

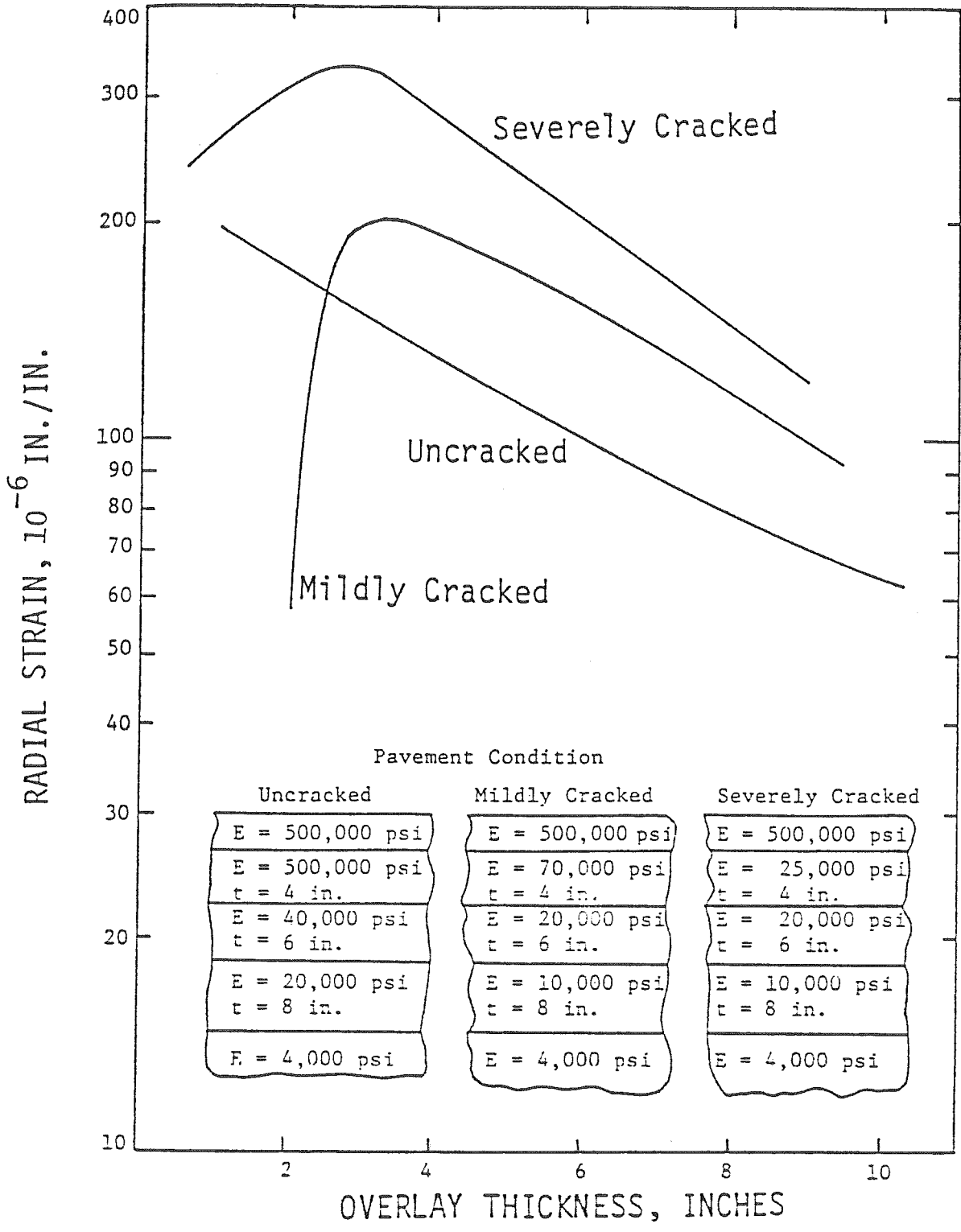


FIGURE 8-1. RELATION BETWEEN CRITICAL STRAIN AND OVERLAY THICKNESS WITH A REDUCTION IN THE EXISTING SURFACE MODULUS FOR VARIOUS CONDITIONS

4. Use linear interpolation to find the load corresponding to 10% deviation, F_{NL} .
5. Use Chevron program with F_{NL} applied to the FWD plate to calculate the maximum τ_{oct} which occurs in the subgrade TOCTMFNL.
6. Using the input highway type select F_{des} , the load on a dual wheel, from Table 7-5.
7. Use Chevron program with F_{des} applied to a dual wheel and calculate τ_{oct} in the subgrade, TOCTFDES.
8. If $TOCTFDES \leq TOCTMFNL$, report this fact and bypass plastic deformation design. If not, proceed to step 9.
9. With the overlay obtained from fatigue analysis in place, use Chevron program with F_{des} applied to a dual wheel and calculate τ_{oct} in the subgrade, TOCTOLAY.
10. Compare TOCTOLAY and TOCTMFNL. If $TOCTOLAY < TOCTMFNL$, the pavement is safe against plastic deformation with the overlay. If $TOCTOLAY > TOCTMFNL$, proceed to step 11.
11. Increment the thickness of the overlay in steps until $TOCTOLAY < TOCTMFNL$ and use interpolation to obtain the overlay thickness at which $TOCTOLAY = TOCTMFNL$.

The preceding step-by-step procedure has been programmed under the subroutine name PLASDEF and incorporated in the CODA program. The needed parameters from Table 7-5 have been placed in PLASDEF as fixed values and the entire plastic deformation design procedure has been automated. The user is required only to input the data indicated in steps 1 and 2. Of course, modifications to the "fixed values" from Table 7-5 can be made readily to program PLASDEF if desired. If the user desires to use the plastic deformation model independent of the fatigue analysis, after step 8 he should proceed to step 11.

Discussion of Plastic Deformation Design Procedure

Referring back to Table 7-5, the last column was used to judge the reasonableness of the F_{des} column, which is used directly in the design procedure. The last column was based on the probability of exceedence values, which were in turn based on normal distribution functions. Comparisons of the actual data histograms with the normal distribution curves shows that the fit is not excellent and that the normal distribution may overestimate somewhat the number of very heavily loaded tracks. On the other hand, illegally loaded heavy trucks typically escape the database, which has a compensating effect.

In view of the above factors it would appear that the last column of Table 7-5 is not a very accurate estimate of the number of load repetitions

expected to exceed F_{des} annually, but it may be a more or less unbiased estimate.

Another relevant factor relates to F_{NL} , however. If F_{NL} is measured during the hottest and wettest time of the year and the minimum is taken as F_{NL} , as recommended, the design value of F_{NL} will be less than the average value for the year. Although this last factor relates to the conservatism in F_{NL} rather than F_{des} , it is the comparison of F_{NL} and F_{des} which controls design. Therefore, it is probably reasonable to conclude that the last column in Table 7-5 is somewhat conservative; that is, the actual expected number of annual load applications producing significant plastic deformations may be somewhat less than those of the last column of Table 7-5.

As a final point of discussion of the plastic deformation design procedure, it deserves to be called a mechanistic procedure because it addresses permanent deformations, a particular mechanism of damage. Even though some plastic deformation occurs with every load application, the intent of this procedure is to keep the plastic deformations small. This intention corresponds to an attempt to maintain the deformations almost entirely within the elastic range.

The strongest feature of this design procedure is that it is based firmly on the results of a field test, the FWD. When the F_{NL} from the FWD test shows that a section is particularly vulnerable to plastic deformations, this section will get more overlay for protection.

Likewise, the overlay design is related - even if only approximately - to the traffic loads applied. The higher ADL on interstate highways compared to U.S. routes would cause plastic deformations to accumulate more rapidly on interstates. To prevent this development, higher F_{des} values are used for interstates, as explained earlier and shown in Table 7-5.

An extension of this method to include an estimate of the "expected life" of a pavement structure with respect to plastic deformations is theoretically possible. However, the art and science of predicting plastic deformations is not sufficiently well-developed to justify this extension at the present time. For now, this part of the design is simply to be used as a check on overlay thicknesses derived from fatigue and roughness analyses, and is to be treated as a minimum overlay thickness.

8.1.4. Comparison with SODA Method

In this study, the CART Overlay Design for Arizona (CODA) was compared with the Structural Overlay Design for Arizona (SODA) (22). For this purpose, sites 1 to 20 were used. The required overlay thicknesses using the two methods are presented in Table 8-1 to last for 10 years.

For the purpose of comparison, three columns of overlay thickness are included in the table. The first column represents values of overlay thickness as calculated directly from the SODA equation. The second column represents default thicknesses by limiting the thicknesses between 0 and 6 in. The third column represents the practical thicknesses by selecting a minimum value of 1.5 in. assuming that the decision to overlay has already been made.

In the CODA method, both the remaining life of the existing pavement and the required overlay thickness are shown. Again, a minimum overlay thickness of 1.5 in. was selected so that the basis for comparison between SODA and CODA methods would be the same. Note that when the remaining life, as computed from the CODA method, is large, the need for an overlay with respect to fatigue and roughness is not pressing. In addition, the fatigue analysis performed in CODA requires input with regard to the percent cracking of the existing AC layers. If the cracking exceeds 10% then a reduced value for the modulus is assumed for the cracked layer. This leads to a value of overlay thickness which may be apparently inconsistent with the remaining life computations. Further, when the surface layer is cracked at the time of overlay, a minimum thickness of 3.0 inches is assigned for the purpose of minimizing reflection cracking.

This comparison shows that both SODA and CODA methods provide close results. The CODA method, however, seems to provide more rational results. For example, the CODA method is capable of computing the remaining life of the existing pavement based on mechanistic approaches. Also, the CODA required thicknesses are directly related to the remaining life and to the cracking condition of the existing surface layer.

8.2. REMAINING LIFE ANALYSIS

An existing pavement could have a remaining life if the roughness has not reached the failure roughness, the cumulative fatigue has not reached the failure fatigue and plastic deformation has not reached the failure plastic deformation. If any of these failure conditions has been reached, the existing pavement needs to be overlaid.

According to the roughness model developed in this study (Equation 8-1), roughness changes with time. If roughness has not reached the failure roughness, the remaining roughness life can be easily computed from this equation.

If the current cracking is 10% or more, it is assumed that the pavement does not have any remaining fatigue life. However, if cracking is less than 10%, the remaining fatigue life can be computed using the fatigue model developed in this study (Equation 8-2). In this case, the tensile strain at the bottom of the uncracked AC layer is computed and the total allowable

TABLE 8-1. COMPARISON OF SODA AND CODA OVERLAY DESIGN FOR STUDY SITES

| Site/ Station | SODA Thickness (in.) | | | CODA | | | |
|------------------|----------------------|----------------------|------------------------|---------------------------|------------------|---------------------------------|--|
| | Equation | Default ² | Practical ¹ | Remaining Life (yr) | Critical Failure | Thickness ¹ (in.) | 10% Cracking before overlay ? ³ |
| 1/1 | 13.6 | 6 | 6 | 7 | Roughness | 6 | No |
| 2/1 | -1.2 | 0 | 1.5 | 10 | Roughness | 1.5 | No |
| 3/7 | 0 | 0 | 1.5 | 3 | Roughness | 1.5 | No |
| 4/1 | 0.8 | 1.5 | 1.5 | 4 | Roughness | 1.5 | No |
| 5/4 | -1.2 | 0 | 1.5 | 7 | Roughness | 2 | No |
| 6/1 | -0.2 | 0 | 1.5 | 9 | Roughness | 1.5 | No |
| 7/4 | 3.8 | 4 | 4 | 0 | Roughness | 6 | No |
| 8/1 | -3.2 | 0 | 1.5 | 3 | Roughness | 1.5 | No |
| 9/1 | 3.4 | 3.5 | 3.5 | 0 | Roughness | 3 | Yes |
| 10/1 | 2.5 | 2.5 | 2.5 | 0 | Roughness | 3.5 | No |
| 11/5 | 4.6 | 5 | 5 | 26 | Roughness | 1.5 | No |
| 12/1 | 8.1 | 6 | 6 | 0 | Roughness | 3 | No |
| 13/4 | -11.8 | 0 | 1.5 | 7 | Roughness | 1.5 | No |
| 15/4 | -2.1 | 0 | 1.5 | 0 | Fatigue | 3.5 | Yes |
| 16/1 | -1.4 | 0 | 1.5 | 28 | Roughness | 1.5 | No |
| 17/1 | 0.5 | 1.5 | 1.5 | 1 | Fatigue | 6 | No |
| 18/1 | 5.3 | 5.5 | 5.5 | 22 | Roughness | 1.5 | No |
| 19/1 | -5.9 | 0 | 1.5 | 23 | Roughness | 1.5 | No |
| 20/1 | 13.1 | 6 | 6 | 3 | Fatigue | 4 | No |

Notes

1. The minimum practical overlay thickness was selected as 1.5 in. for both SODA and CODA - assuming that a decision to overlay has already been made.
2. SODA method forces the overlay thickness to range from 0 to 6 in. regardless of the equation value.
3. If the original surface is cracked, a minimum overlay thickness of 3.0 in. is required in CODA to decrease reflection cracking.

cumulative ESAL is computed from the fatigue model. The remaining ESAL is obtained by subtracting the consumed ESAL repetitions from the total ESAL repetitions. The remaining life in years can easily be computed by knowing the current ADL and the traffic growth. The method can be used either with pavements which have not been overlaid before or with pavements with one, two or three previous overlays. In all cases the tensile strain is computed at the bottom of the uncracked AC layer since the cracked layer together with all underneath layers are assumed to have no effect on the remaining fatigue life.

The plastic deformation model was not incorporated in the remaining life analysis since the model does not allow for accumulating the damage. Thus, the remaining pavement life computed in the CODA method is governed only by either the roughness condition or the fatigue condition.

8.3. LIFE OF A USER SPECIFIED OVERLAY

For a number of reasons including economic factors it would be of interest not to design the overlay to last for 10 years but to specify a certain overlay thickness and solve for its life. The CODA program computes the useful life using both roughness and fatigue models. The procedure followed in this analysis is similar to that used to determine the remaining life in Section 8.2.

8.4. ECONOMIC ANALYSIS

The CART overlay design for Arizona (CODA) is capable of determining the equivalent uniform annual cost of the designed overlay. This method also allows for the economic comparison among rehabilitation alternatives as follows:

1. overlay only,
2. milling plus overlay,
3. milling plus recycling plus overlay, and
4. reconstruction.

This method considers the costs of the following items for the case of overlay only:

1. tack coat
2. apply bituminous tack coat
3. asphalt concrete (end product)
4. asphalt cement
5. AC admixture
6. emulsified asphalt for seal coat
7. cover material for seal coat
8. fog coat
9. blotter material
10. mobilization
11. traffic control
12. asphalt concrete friction course (ACFC)
13. asphalt cement for ACFC
14. maintenance

15. salvage value
16. other

The cost of the following items are considered in the case of milling plus overlay:

1. removal of asphaltic concrete pavement
2. asphaltic concrete (end product)
3. asphalt cement
4. bituminous tack coat
5. apply bituminous tack coat
6. fog coat
7. ACFC
8. asphalt cement for ACFC
9. blotter material
10. asphalt concrete (recycled)
11. asphalt cement (AC recycled)
12. mobilization
13. traffic control
14. maintenance
15. salvage value
16. other

The cost of the following items are considered in the case of milling, recycling and overlay:

1. asphalt cement
2. asphalt cement (AC recycled)
3. bituminous tack coat
4. apply fog coat
5. blotter material
6. asphaltic concrete
7. asphaltic concrete (recycled)
8. removal of asphaltic concrete
9. ACFC
10. mobilization
11. traffic control
12. asphalt cement for ACFC
13. AC admixture
14. maintenance
15. salvage value
16. other

For reconstruction the costs of the following items are considered:

1. removal of asphaltic concrete pavement
2. blotter material
3. asphalt concrete (end product)
4. asphalt cement
5. asphalt cement for ACFC
6. bituminous tack coat
7. apply bituminous tack coat
8. ACFC
9. fog coat

10. aggregate subbase
11. aggregate base
12. maintenance
13. salvage value
14. other

For each item, the user is required to input the measurement unit, quantity and unit price. The maintenance cost can be specified for each year individually. The discount rate needs to be specified. The program computes the equivalent uniform annual cost for each alternative so the user can determine which rehabilitation alternative is more economical. In this analysis, the equivalent uniform annual cost method was selected since different rehabilitation alternatives may have different design lives.

CHAPTER 9. SUMMARY, CONCLUSIONS, AND RECOMMENDATIONS

9.1. SUMMARY AND CONCLUSIONS

The work performed in this study resulted in the generation and assemblage of a large amount of data which relates to overlay design. Some of the key findings are summarized in the following paragraphs, together with conclusions drawn from these findings.

9.1.1. Site Variability/Stress Sensitivity from NDT Data

Variability in NDT data across a 90 ft span (in the direction of traffic) can be attributed primarily to spacial variability in material properties. Typical variations in NDT deflection measurements, for a given sensor, were ± 10 to 20%. Variations were approximately the same for FWD and Dynaflect test results. Coefficients of variation were typically 10 to 15%.

Stress sensitivity was studied from the NDT data by assuming material linearity and computing equivalent 9000 lb FWD deflections for the 6000 and 12,000 lb FWD data and for the Dynaflect data. Within the stress range of the FWD tests, the effect of material nonlinearity was less significant than the effect of spacial variability in material properties. In other words, the "error" in an FWD deflection measurement resulting from assuming linearity would be insignificant in comparison to random variability. However, at stress levels associated with the Dynaflect, there may be a more significant effect of material nonlinearity due to scatter in the Dynaflect data, making it difficult to distinguish between nonlinearity effects and data scatter.

9.1.2. Layer Thicknesses and Material Types

The logging of the 20 test sites resulted in estimating the layer thicknesses of the material types. This accurate estimation of layer thicknesses and the material types allowed for direct comparison between construction records and actual conditions. Generally, there were no large discrepancies between construction records and actual conditions. In cases where there were some discrepancies in layer thicknesses, the thicknesses obtained from logging were considered more accurate and they were used in the backcalculation analysis.

The second phase of the project included revisitation of the sites for drilling and sampling to depths up to 25 ft and cone penetration testing. From these data it was possible to construct profiles extending much deeper than is normal for overlay design projects. The CPT data was a major contribution to the analysis in that it allowed the delineation of layering in the subgrade down to considerable depth. The large number of distinct layers and the wide variation in stiffness typically exhibited in the first 20 ft or so of subgrade was surprising.

9.1.3. Dynamic Analysis vs Static Analysis

A dynamic analysis technique was developed in this study to analyze various NDT data. The advantage of this approach over the static approach is

that it allows consideration of the inertial forces developed in the pavement system due to the application of different modes of loading. For example, the harmonic load of the Dynaflect is treated in a manner different than the impulsive load of the FWD, while in the static approach no difference between different modes of loading can be made.

Three computer programs based on the dynamic analysis approach were refined and/or developed in this study and made available to ADOT for future use. These programs are DYNAMIC1, DYNAMIC2 and DYNAMIC3 whose user's guides and flow charts have been transmitted to ADOT. The first two programs can compute the harmonic and the impulsive response of pavements respectively, while the latter program can be used to backcalculate the layer moduli due to harmonic loadings. DYNAMIC1 and DYNAMIC2 programs can also be used to backcalculate the layer moduli under harmonic and impulsive loading conditions using manual adjustments of moduli so that the user would have more control on the relative values of the moduli of individual layers.

The differences between the results of static and dynamic analyses are moderately small. Although the dynamic analysis results are considered to be more accurate, the differences are too small to justify the greater complexities and time requirements of dynamic analyses for routine design computations.

9.1.4. Estimation of Layer Moduli

The manual method of estimating the layer moduli discussed earlier was used in this study to analyze the deflection data obtained by the FWD and the Dynaflect. The Chevron program was used in the static analysis while the DYNAMIC1 and DYNAMIC2 programs were used in the dynamic analysis. Four sets of backcalculated layer moduli were obtained from the static and dynamic analyses of FWD and Dynaflect data. In addition, four sets of depth to bedrock (or a stiff layer) associated with the four sets of layer moduli were also developed. Using the method proposed in the 1986 AASHTO guide, the backcalculated moduli of asphaltic layers were adjusted to a reference temperature of 77°F for the purpose of comparison with the lab moduli and to 70°F for the purpose of developing the overlay design method.

Additional backcalculations were performed manually on the CPT data. Although the CPT data delineated many layers (often more than 10), a solution could be obtained as long as the ratio of moduli from layer to layer was held fixed. However, when ratios were allowed to vary, manual back-calculation become essentially impossible.

Although manual backcalculation is suitable, and perhaps even preferable, for research purposes, it is too tedious and time-consuming for routine design. Automated computerized backcalculation using a simplified profile has been developed for use in design, as described in chapters 6 and 7.

9.1.5. Laboratory Testing

Asphalt concrete cores were collected from the 20 selected sites and tested in the laboratory for bulk density and resilient modulus. The

resilient modulus test was performed according to ASTM D4123-82 procedure at 41, 77 and 104^oF.

Unstabilized base and subbase materials were tested for gradation. Asphalt stabilized base materials were unable to be tested for resilient modulus due to the irregularity of the core surface. One sample of cement stabilize base was tested for resilient modulus and proved the feasibility of testing CTB material using the diametral method.

Undisturbed subgrade soil samples were collected from the sites and tested for Aterberg limits, gradation, classification and resilient modulus. The AASHTO T274-82 method was used for resilient modulus test with some modifications.

9.1.6. Comparisons between Backcalculated and Lab Moduli

Values of asphalt concrete resilient moduli were backcalculated from NDT data and compared with lab-measured values from cores. The comparison showed that, on the average, the lab-measured values were about three times as high as the backcalculated values, with significant deviations from the average.

A number of factors which might contribute to these differences were presented and discussed. It was concluded that the factor most likely to be the major contributor to the observed differences was heterogeneity within the asphalt concrete layer. Because sampling and specimen preparation tend to break up and destroy the weaker zones of the surface layer, the segments actually tested in the lab are biased toward the stronger, stiff portions of the layer. The backcalculated values from NDT data represent weighted average values of the entire surface layer, including its weaker zones. For most overlay design procedures, the NDT values would be more useful.

In a similar manner lab-measured resilient moduli for the subgrade materials were compared with values backcalculated from the NDT data. It was found that, on the average, the backcalculated values were about 50 percent higher than the lab values, with significant deviations from the average.

Values of moduli measured by laboratory testing represent only the small specimens on which the tests were performed. By contrast, backcalculated values of moduli from NDT are weighted-average values representing relatively large volumes of material. Although the moduli of materials close to the load have a higher weighting factor, moduli of materials 10 to 20 ft in depth and 5 to 10 ft radially from the load have a significant influence on the average, backcalculated values from NDT.

The cone penetration tests have shown that the moduli in the first 10 to 20 ft of subgrade vary quite pronouncedly, and over very short distances. The greater the variation in modulus within a zone, the less likely it is that a point value within the zone (like a lab test specimen) will match the overall average modulus for the zone.

It has therefore been concluded that it is essentially an accident if a lab test value of modulus on a single specimen agrees well with an NDT backcalculated value of modulus. The moduli are different because greatly

different volumes of material are being tested in the lab and the field. Consideration was given to the question of which modulus is better for use in overlay design. It was concluded that for computing tensile strain at the bottom of the asphalt concrete, the NDT backcalculated values of subgrade moduli would be better.

9.1.7. Comparison between Lab Moduli and R-Values

The results of this study indicated that the laboratory resilient moduli of subgrade materials and the laboratory R-values are not correlated. The main reason for this poor correlation is that the two tests measure two different material properties which are not related to each other. Another reason is the fact that the sample conditions of the two tests are different. Therefore, it is not recommended to predict the resilient modulus value from the R-value.

9.1.8. Modes of Pavement Failure

For purposes of this study, pavement failure has been broadly defined as all conditions under which an overlay is needed. It has been concluded that this condition can arise due to development of excessive roughness, fatigue failure with excessive cracking, excessive plastic deformation, and rutting.

Some of these mechanisms are believed to be inter-related, but quantification of the relationships has proven difficult. The design approach adopted corresponds to selection of an overlay design which is simultaneously satisfactory with respect to all of the above factors. Some key points and conclusions relative to each of the design models follow.

a) Roughness Model

A key parameter of this model is the rate at which roughness develops after an overlay is constructed. The average value of this rate was found to be a remarkably stable parameter, even from one class of highway to another. The rate correlated poorly with overlay thickness, moduli of pavement layers, level of traffic loading and regional factors.

Although the rate is believed to be influenced by the foregoing factors, these effects are evidently masked by other sources of variation in the rate. Other sources which have been considered are variations in the AC mix parameters and variations in construction techniques such as lift thickness and compaction.

The relative stability of the rate of roughness development suggests a time-dependent breakdown of the AC, as might be caused by an aging of the asphalt binder. Also, it was found that there is a relation between roughness after overlay and roughness before overlay. Thus, if roughness before overlay is known, the time after which the roughness failure is reached can be computed.

b) Fatigue Model

The actual thickness of overlay is obtained by exercising the fatigue model. Use of the thickness of overlay needed for fatigue resistance insures that the pavement will not fail prematurely due to fatigue.

The fatigue model was developed through consideration of fatigue curves from the literature for other asphalt pavements and from data from Arizona highways. The data from Arizona included both projects considered to have failed by fatigue and projects which had not failed by fatigue. The fatigue curve selected for Arizona pavements shown in Chapter 7 indicates that they are somewhat more resistant to fatigue failure than other pavements.

In developing the fatigue curve it was assumed that all types of cracks were fatigue-related. Thus when the percentage of cracks was high the pavement failure was classed as fatigue failure, regardless of the crack pattern.

c) Plastic Deformation Model

The plastic deformation model was developed to insure that the thickness required for fatigue resistance is also adequate for protection against excessive plastic deformation. Due to common levels of factor of safety in the pavement structural design, the plastic deformation requirement is expected to govern design very rarely. However, if a pavement section shows weakness during FWD testing, this design feature will become operative.

This design is expected to provide protection against rutting due to excessive deformation in the deeper pavement layers. However rutting due to plastic deformation in the overlay layer itself is to be prevented by improved mix design and construction techniques.

9.1.9. Economic Analysis

An economic analysis procedure was developed to compare among different rehabilitation strategies as follows:

1. overlay only,
2. milling plus overlay,
3. milling, recycling plus overlay, and
4. reconstruction.

If various costs are known such as initial construction costs, maintenance costs and salvage value, the equivalent uniform annual cost of each rehabilitation alternative can be computed. These equivalent uniform annual costs help the highway engineer decide which alternative to use. In this analysis, the equivalent uniform annual cost method was selected since different rehabilitation alternatives may have different design lives.

9.1.10. CART Overlay Design for Arizona (CODA)

The three pavement failure criteria (roughness, fatigue and plastic deformation) together with the economic analysis were incorporated in an

integrated CART Overlay Design for Arizona (CODA). The method is capable of performing four functions as follow:

1. Determining the required overlay thickness.
2. Determining the remaining life of an existing pavement.
3. Determining the design life of a user specified overlay.
4. Determining the equivalent uniform annual cost of four rehabilitation alternatives.

The method is based on the use of the roughness Maysmeter and FWD data. The method is considered mechanistic-empirical which combines rigorous mechanistic analysis and previous observations of actual pavements in Arizona. The method is computerized in an IBM or IBM compatible microcomputer program (CODA). The computer program is interactive and user friendly while it can also read from a data file. A copy of the CODA program and the user's guide were transmitted to ADOT with this report.

The CODA method provides results close to the SODA method, although the CODA results seem to be more rational. The CODA required overlay thickness is directly related to the remaining life and to the cracking condition of the existing pavement.

9.2. RECOMMENDATIONS

1. The CART Overlay Design for Arizona (CODA) is a rational method and is tailored to conditions in Arizona. Highway engineers are encouraged to use it and study the concepts used in its development for proper utilization. Although the method is expected to provide good design parameters, verification and experience in its use are needed in the next several years.

2. The resilient modulus obtained from a laboratory test on a sample from one of the pavement layers represents the modulus at only the spot where the sample was taken, a very small volume. By contrast, the modulus backcalculated from NDT data represents a "weighted-average" value of all the moduli within the zone of influence of the load, which is a relatively large zone. Because there is typically a very significant variation in modulus both horizontally and vertically in each layer (especially within the subgrade) no correlation between the lab values and NDT backcalculated values of moduli could reasonably be expected. The NDT backcalculated moduli are most closely related to pavement response parameters of interest such as tensile strain at the bottom of the AC layer, and are therefore far preferable for use in overlay design.

3. Because of the same reason stated in recommendation number 2 and due to the poor correlation between the modulus and the R-value, the use of the backcalculated subgrade modulus in overlay design is preferred over the subgrade modulus predicted from R-value correlations.

4. The use of FWD deflections to predict pavement properties for design is preferred over the Dynaflect or lab testing.

5. Although the latest mechanistic technology has been used to develop the CODA method, its results can not be guaranteed without proper construction techniques and rational asphalt concrete mix design. In fact, the results of

this research program suggest that the expected life of a pavement and variations in expected life may be very closely tied to construction control. It is therefore recommended that research into these factors be continued or initiated.

6. The CODA program gives the designer the tools needed for life-cycle-cost analysis of overlays and rehabilitation options. This analysis should be performed to ensure selection of the most cost-effective strategy.

7. The concepts used for the development of the CODA procedure are generally applicable to the analysis of other rehabilitation strategies. Further research to extend the CODA method to include the analysis of nonoverlay rehabilitation strategies would provide ADOT with a unified and coherent methodology for pavement rehabilitation.

REFERENCES

- 1 . J. W. Hall, "Comparative Study of Nondestructive Pavement Testing - MacDill Air Force Base," U. S. Army Engineer Waterways Experiment Station, Vicksburg, Miss., 1984.
- 2 . O. Tholen, J. Sharma, and R. L. Terrel, "Comparison of FWD with other Deflection Testing Devices," TRB, Record No. 1007, 1985.
3. R. E. Smith, M. I. Darter, and R. L. Lytton, "Mechanistic Overlay Design Procedures Available to the Design Engineer," Presented at the Annual TRB meeting, 1986.
4. M. S. Mamlouk and T. G. Davies, "Elasto-Dynamic Analysis of Pavement Deflections," ASCE Transportation Engineering Journal, Vol. 110, No. 6, Nov. 1984.
5. M. S. Mamlouk, "Use of Dynamic Analysis in Predicting Field Multilayer Pavement Moduli," TRB, Record 1043, 1985.
6. T. G. Davies and M. S. Mamlouk, "Theoretical Response of Multilayer Pavement Systems to Dynamic Nondestructive Testing," TRB, Record 1022, 1985.
7. B. E. Sebaaly and M. S. Mamlouk, "Typical Curves for Evaluation of Pavement Stiffness from Dynaflect Measurements," TRB, Record 1070, 1986.
8. B. E. Sebaaly, M. S. Mamlouk and T. G. Davies, "Dynamic Analysis of FWD Data," TRB, Record 1070, 1986.
9. B. E. Sebaaly, T. G. Davies, and M. S. Mamlouk, "Dynamics of the Falling Weight Deflectometer," ASCE Transportation Engineering Journal, Vol. 111, No. 6, Nov. 1985.
10. M. S. Mamlouk, "Dynamic Analysis of Pavement -- theory, Significance and Verification," Proceedings, Sixth International Conference - Structural Design of Asphalt Pavements, Ann Arbor, Michigan, July 1987.
11. B. E. Sebaaly, "Dynamic Models for Pavement Analysis," Ph.D. dissertation, Department of Civil Engineering, Arizona State University, 1987.
12. J. M. Roesset and K. Shaeo, "Dynamic Interpretation of Dynaflect and FWD Tests", TRB, Record 1022, 1985.
13. B.E. Sebaaly and M.S. Mamlouk, "Development of Dynamic Fatigue Failure Criterion," Vol. 114, No. 4, ASCE Journal of Transportation Engineering, July 1988.
14. P. Sweatman, "Dynamic Road Loading: Instrumented Vehicles," presented at the FHWA Load Equivalency Workshop, Washington, D.C., September 1988.

15. G.T. Hu, "Use of a Road Simulator for Measuring Dynamic Wheel Loads," presented at the FHWA Load Equivalency Workshop, Washington, D.C., September 1988.
16. T. G. Gillespie, "Modeling Truck Dynamic Loads," presented at the FHWA Load Equivalency Workshop, Washington, D.C., September 1988.
17. G. L. Dehlen, and C. L. Monismith, "Effect of Nonlinear Material Response on the Behavior of Pavements Under Traffic," Highway Research Record 310, Washington, D.C., 1970.
18. R. G. Hicks, "Factors Influencing the Resilient properties of Granular Materials," Ph.D. Dissertation, University of California, 1970.
19. C. L. Monismith and F. N. Finn, "Overlay Design - A Synthesis of Methods," Prepared for Symposium, "Asphalt Concrete Overlays: Theory and Practice," Association of Asphalt Paving Technologist, Scottsdale, AZ, April 9-11, 1984.
20. P. S. Pell, "Characterization of Fatigue Behavior," Symposium on Structural Design of Asphalt Concrete Pavements to Prevent Fatigue Cracking, Highway Research Board Special Report 40, Washington, D.C., 1973.
21. H. B. Seed, C. K. Chan, and C. E. Lee, "Resilience Characteristics of Subgrade Soils and Their Relation to Fatigue Failures in Asphalt Pavements," Proceedings, International Conference on the Structural Design of Asphalt Pavements, Ann Arbor, Michigan, 1962.
22. J. F. Eisenberg, G. B. Way, J. P. Delton, and J. E. Lawson, "Overlay Deflection Design Method for Arizona," ADOT, Report No. FHWA/AZ83/182, March 1984.
23. G. B. Way, J. F. Eisenberg, J. P. Delton, and J. E. Lawson, "Structural Overlay Design for Arizona," AAPT, Vol. 53, 1984.
24. R. L. Lytton and R. E. Smith, "Use of NDT in the Design of Overlays for Flexible Pavements," TRB, Record No. 1007, 1985.
25. R. E. Smith, R. P. Palmieri, M. I. Darter, and R. L. Lytton, "Pavement Overlay Design Procedures and Assumptions, Vol. I, II and III," FHWA/RD-85/006-008, Federal Highway Administration, October, 1984.
26. Austin Research Engineers, Inc., "Asphalt Concrete Overlays of Flexible Pavements, Volume 1, Development of New Design Criteria," FHWA Report No. FHWA-RD-75-75, August, 1975.
27. K. Majidzadeh, G. Ilves, "Flexible Pavement Overlay Design Procedures," Volume 1. Evaluation and Modification of the Design Methods, Final Report, FHWA.RD-81/032, Resource International, Worthington, Ohio, 1981.
28. K. Majidzadeh, G. Ilves, "Flexible Pavement Overlay Design Procedures Volume 2. User Manual," Final Report, FHWA/RD-81/033, Resource International, Worthington, Ohio, 1981.

29. "Asphalt Overlays for Highway and Street Rehabilitation," The Asphalt Institute, Manual Series ;No. 17, 1983.
30. A. I. M. Claessen and R. Ditmarsch, "Pavement Evaluation and Overlay Design," Proceedings, Fourth International Conference on Structural Design of Asphalt Pavements, Ann Arbor, Michigan, 1977.
31. R. W. Bushey, et al., "Structural Overlays for Pavement Rehabilitation," CA-DOT-TL-3128-3-74-12, California Department of Transportation, Sacramento, California, 1974.
32. "Asphalt Concrete Overlay Design Manual," California Department of Transportation, Sacramento, California, 1979.
33. H. F. Southgate, G. W. Sharpe, and R. C. Deen, "A Rational Thickness Design System for Asphaltic Concrete Overlays," Research Report 507, Division of Research, Bureau of Highways, Department of Transportation, Commonwealth of Kentucky, October, 1978.
34. R. W. Kincehn, and W. H. Temple, "Asphaltic Concrete Overlays of Rigid and Flexible Pavements," Report No. FHWA/LA-80/147, Louisiana Department of Transportation and Development, Baton Rouge, Louisiana, October, 1980.
35. A. C. Bhajandas, G. Cumberledge, and G. L. Hoffman, "Flexible Pavement Evaluation and Rehabilitation," ASCE Symposium on Pavement Design, Atlanta, Georgia, June, 1975.
36. J. L. Brown, H. E. Orellana, "An Asphaltic Concrete Overlay Design Subsystem," Research Project 1-8-66-101, Highway Design Division, Research Section Texas Highway Department, 1970.
37. D. E. Peterson, et al., "Asphalt Overlays and Pavement Rehabilitation-Evaluating Structural Adequacy for Flexible Pavement Overlays," Report No. 8-996, Utah Department of Transportation, January, 1976.
38. N. K. Vaswani, "Method for Separately Evaluating Structural Performance of Subgrades and Overlaying Flexible Pavements," Highway Research Record 362, Highway Research Board, Washington, D.C., 1971.
39. M. S. Hoffman and M. R. Thompson, "Mechanistic Interpretation of Nondestructive Pavement Testing Deflections," Department of Civil Engineering, University of Illinois, 1981.
40. M. R. Thompson, "Concepts for Developing a Nondestructive Based Asphalt Concrete Overlay Thickness Design Procedure," Illinois Department of Transportation, Dept. of civil Engineering, University of Illinois, Urbana-Champaign, 1982.
41. R. L. Lytton, "Comments on FAA Overlay Design Procedure," Consulting Report of the U.S. Army Corps of Engineers Waterways Experiment Station, February 8, 1982.
42. M. S. Mamlouk and B. E. Sebaaly, "Overlay Thickness Design for Flexible Pavement," TRB, Record No. 993, 1984.

43. P. E. Paris and Erdogan, "A Critical Analysis of Crack Propagation," Transactions, ASME Journal of Basic Engineering, Series D-85, No. 3, 1963.
44. R. A. Weiss, "Pavement Evaluation and Overlay Design: Method that Combines Layered-Elastic Theory and Vibratory Nondestructive Testing," TRB, Record No. 700, 1979.
45. A. C. Eringen and E. S. Suhubi, "Elastodynamics, Vol. 2, Linear Theory," Academic Press, New York, 1975.
46. E. Kausel and R. Peek, "Dynamic Loads in the Interior of a Layered Stratum: An Explicit Solution," Bulletin of the Seismological Society of America, vol. 72, No. 5, October 1982.
47. M. S. Hoffman and M. R. Thompson, "Nondestructive Study of Selected Nondestructive Testing Devices," TRB, Record No. 852, 1982.
48. J. L. Green and J. W. Hall, "Nondestructive Vibratory Testing of Airport Pavements," Vol. 1, Technical Report S-75-14, U.S. Army Engineer Waterways Experiment Station, Vicksburg, Miss., Sept. 1975.
49. M. S. Hoffman, "Loading Mode Effects on Pavement Deflections," ASCE Journal of Transportation Engineering, Vol. 109, No. 5, Sept. 1983.
50. A. J. Bush, "Nondestructive Testing for Light Aircraft Pavements," Phase II, U.S. Army Engineer Waterways Experiment Station, Geotechnical laboratory, Vicksburg, Miss., Nov. 1980.
51. F. E. Richart, Jr., J. R. Hall, Jr., and R. D. Woods, "Vibrations of Soils and Foundations," Prentice-Hall, New Jersey, 1970.
52. D. L. Allen and R. C. Dren, "Modulus of Damping of Asphaltic Concrete Using the Resonant column," ASTM Geotechnical Testing Journal, Vol. 3, No. 4, Dec. 1980.
53. R. W. Clough and J. Panzien, "Dynamics of Structures," McGraw-Hill, 1975.
54. D. A. Kasianchuk and G. H. Argue, "A Comparison of Plate Load Testing with the Wave Propagation Technique," Proc., 3rd International conference on the Structural Design of Asphalt Pavements, Vol. 1, London, 1972.
55. G. B. Way, "Environmental Factor Determination from In-Place Temperature and Moisture Measurements under Arizona Pavements, ADOT, Report No. FHA/AZ-80/157, Aug. 1980.
56. "Selected Soil Features and Interpretations for Major Soils of Arizona, Supplement to Arizona General Soil Map," U.S. Department of Agriculture, Dec. 1975.
57. R. J. Schmidt, "A Practical Method for Measuring the Resilient Modulus of Asphalt Treated Mixes," HRB, Record 404, 1972.

58. M. S. Mamlouk, "Development of Microcomputer Program for Moduli Prediction of Pavement Layers," CART, Arizona State University, Aug. 1986.
59. L. H. Irwin, "User's Guide to MODCOMP2," Cornell Local Roads Report No. 83-8, Cornell University, Nov. 1983.
60. "AASHTO Guide for Design of Pavement Structures," AASHTO, 1986.
61. P. Ullidtz, "Pavement Analysis", Elsevier Science Publishers, 1987
62. F. W. Jung, "Top Layer Horizontal Strain in Pavements from Impulse Load Deflection Measurements", Presented at the 67th Annual TRB Meeting, Washington, D. C., Jan . 1988.
63. D. E. Newcomb, "Comparison of Field and Laboratory Estimated Resilient Moduli of Pavement Materials," Presented at the Annual AAPT Meeting, Reno, Nevada, Feb. 1987.
64. J.B. Rauhut and T.W. Kennedy, "Characterizing Fatigue Life for Asphalt Concrete Pavements," TRB, Record No. 888, 1982.
65. F.N. Finn, C. Saraf, and R. Kulkarni, "Development of Structural Subsystems," Final Report, NCHRP, NCHRP Project 1-10B, July 1976.
66. F.R.P. Meyer, A. Cheetham and R.C.G. Haas, "A Coordinated Method for Structural Distress Predictions in Asphalt Pavements," Proc., Association of Asphalt Paving Technologists, Vol. 47, February 1978.
67. M.W. Witczak, "Design of Full-Depth Asphalt Airfield Pavements," Proc., Third International Conference on Structural Design of Asphalt Pavements, Univ. of Michigan, Ann Arbor, 1972.
68. W. Van Dijk, "Practical Fatigue Characterization of Bituminous Mixes," Proc., Association of Asphalt Paving Technologists, Vol. 44, February 1975.
69. J.A. Epps and C.L. Monismith, "Influence of Mixture Variables on the Flexural Fatigue properties of Asphalt Concrete," Proc., Association of Asphalt paving Technologists, Vol. 38, 1969.
70. C.L. Monismith, D.A. Kasianchuk and J.A. Epps, "Asphalt Mixture Behavior in Repeated Flexure--A Study of an In-Service Pavement Near Morro Bay, California," Univ. of California, Berkeley, IER Rept. TE 67-4, 1967.
71. W. Van Dijk and W. Visser, "The Energy Approach to Fatigue for Pavement Design, : Paper presented at Annual Meeting of Association of Asphalt Paving Technologists, February 1977.
72. W.S. Smith and K. Nair, "Development f Procedures for Characterization of Untreated Granular Basecourse and Asphalt-treated Base Course Materials," FHWA, Rept. FHWA-RD-74-61, October 1973.

73. R.D. Barksdale, "Development of Equipment and Techniques for Evaluating Fatigue and rutting Characteristics of Asphalt Concrete Mixes," School of Civil Engineering, Georgia Institute of Technology, Atlanta, June 1977.
74. "Bitumens Mix Manual," Chevron Asphalt Research Company, richmond, CA, 1975.
75. J.B. Rauhut, J.C. O'Quin and W. R. Hudson, "Sensitivity Analysis of FHWA Structural Model VESYS IIM, Vol. 1: Preparatory and Related Studies," FHWA, Rept. FHWA-RD-76-23, March 1976.
76. P.S. Pell, "Fatigue Characteristics of Bitumen and Bituminous Mixes," Proc., International Conference on Structural Design of Asphalt Pavements, Univ. of Michigan, Ann Arbor, 1962.
77. R. A. Jimenez, "Structural Design of Asphalt Pavements," Report ADOT-RS-10-142, Arizona Department of Transportation, May 1973.
78. "Arizona State Highway System Plan," Growth and development Chapter, 1988.
79. J. Michelow, "Analysis of Stress and Displacements in N-Layered Elastic System Under a Load Uniformly Distributed on a Circular Area," California Research Corp., September 1963.
80. F.L. Roberts, "Overview: Tire Types, Pressures and Models to Evaluate Pressure Effects," presented at the FHWA Load Equivalency Workshop, Washington, D.C., September 1988.
81. J. Zekoski, "Impact of Truck Tire Selection on Contact Pressures," presented at the FHWA Load Equivalency Workshop, Washington, D.C., September 1988.
82. "Pavement Newsletter," FHWA, Issue 11, January 1988.
83. R. A. Jimenez, "Structural Design of Asphalt Pavements," Arizona Transportation and Traffic Institute, University of Arizona, Nov. 1975.
84. R. Bonaquist, C. Churilla and D. Freund, "Effect of Load, Tire Pressure and Type on Flexible Pavement Response," Presented at the 67th Annual TRB Meeting, Jan. 1988.
85. M. A. Minor, "Cumulative Damage in Fatigue", Trans., AMSE, Vol. 67, 1945.
86. J. P. Zaniewski, "Design Procedure for Asphalt Concrete Overlays of Flexible Pavements," Ph.D. Dissertation, University of Texas, Austin, Texas, 1978.

APPENDIX A

SUMMARY OF NDT DATA

PLOTS OF FWD DTA - 9000 LB DROP

VARIABILITY IN FWD MEASUREMENTS ACROSS THE SITE

The following 20 plots are of field measurements of deflections resulting from the 9000 lb FWD tests. For each site, the deflections at each station are plotted together so that the variability in the measurements at each sensor location may be studied. At a given site, the 10 stations are 10 ft apart, and cover a 90 ft span.

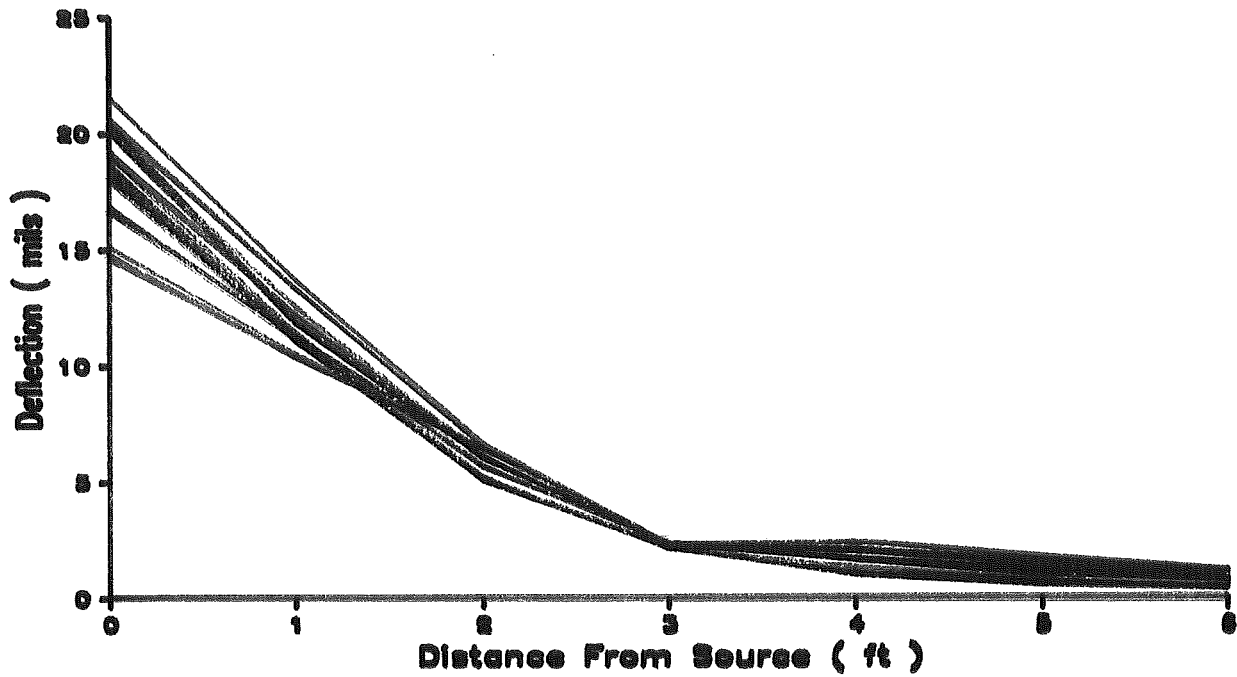


FIGURE A- 1 . FWD DATA AT 9000 LB DROP FOR SITE 1

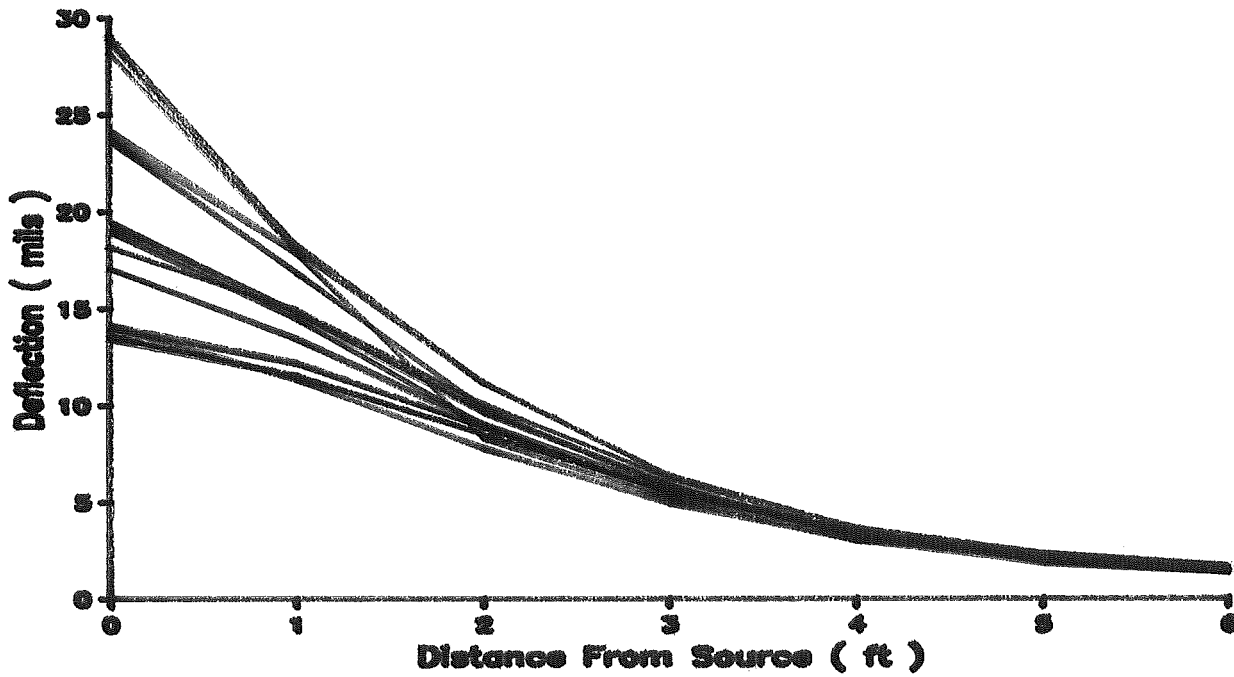


FIGURE A- 2 . FWD DATA AT 9000 LB DROP FOR SITE 2

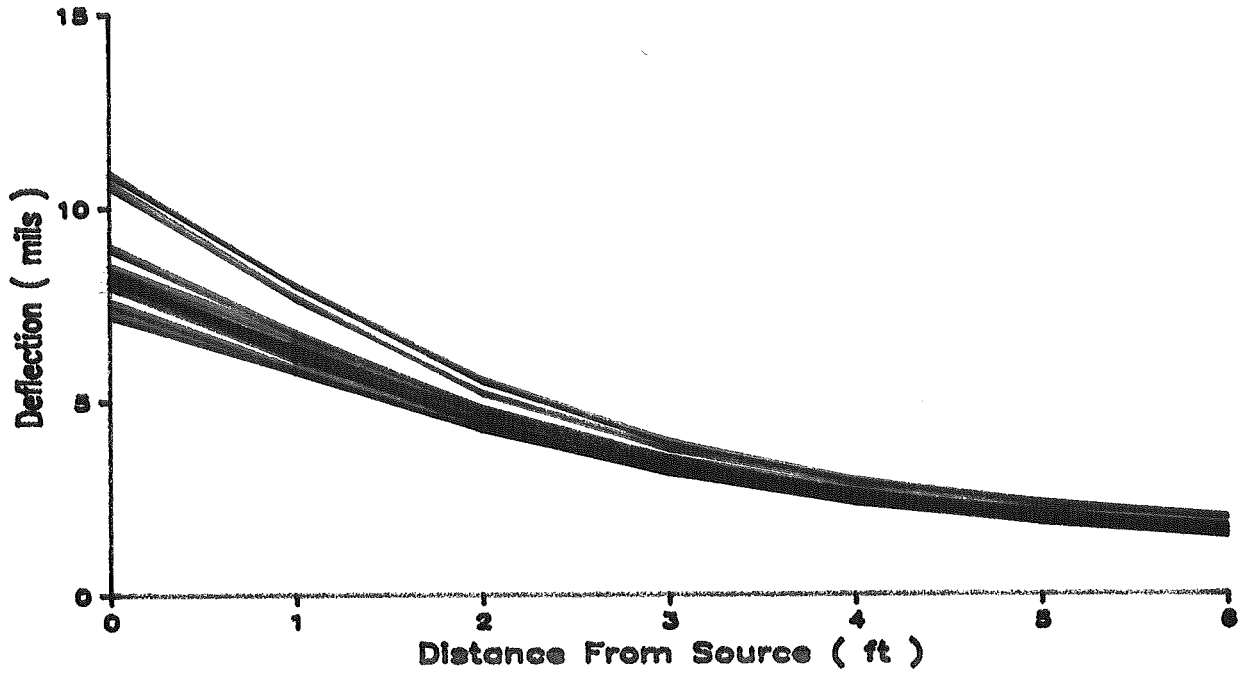


FIGURE A- 3 . FWD DATA AT 9000 LB DROP FOR SITE 3

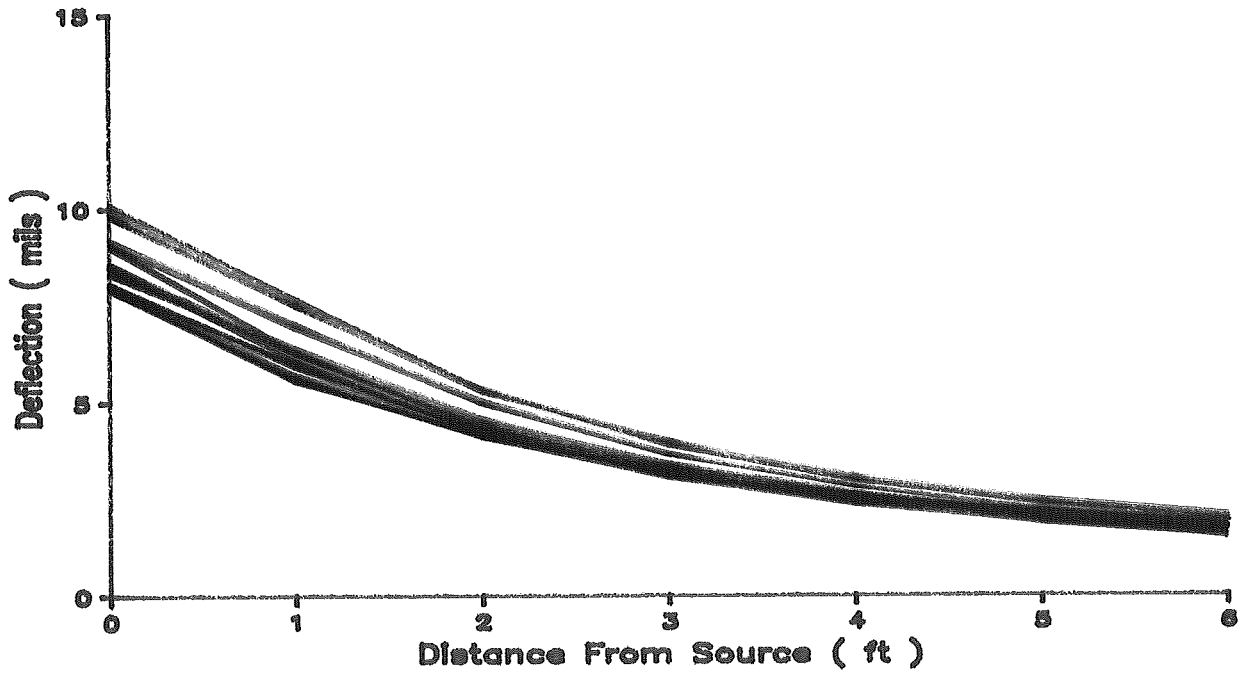


FIGURE A- 4 . FWD DATA AT 9000 LB DROP FOR SITE 4

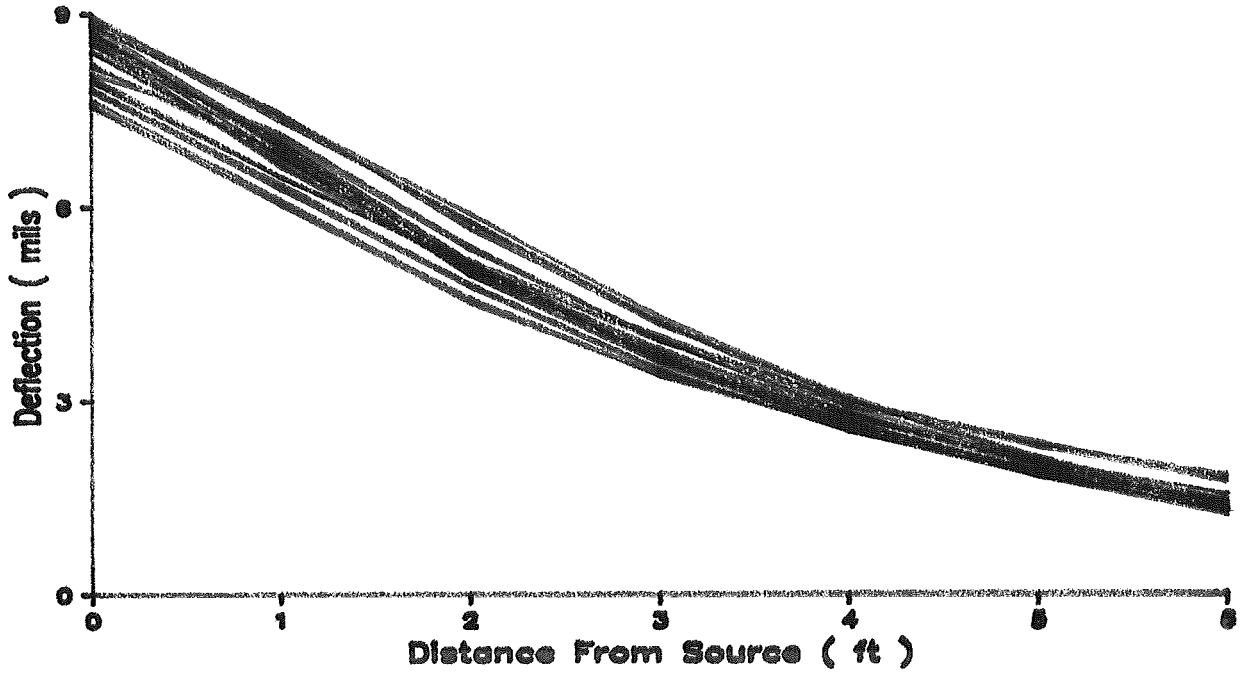


FIGURE A- 5 . FWD DATA AT 9000 LB DROP FOR SITE 5

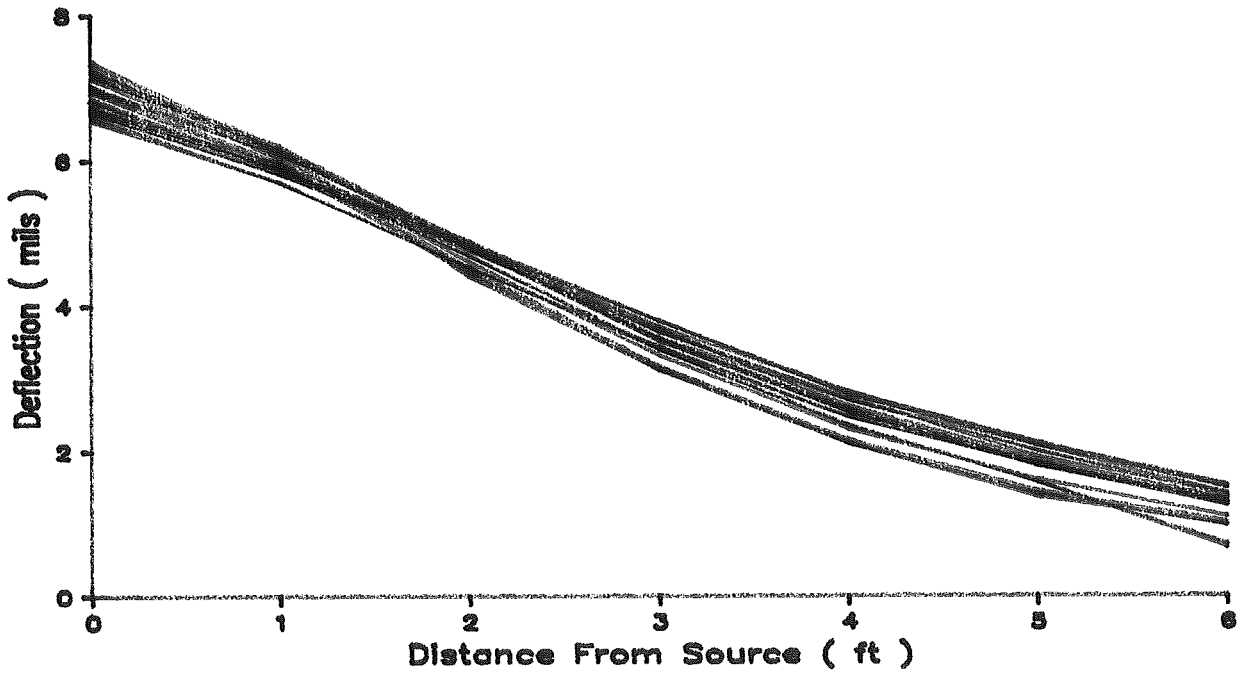


FIGURE A- 6 . FWD DATA AT 9000 LB DROP FOR SITE 6

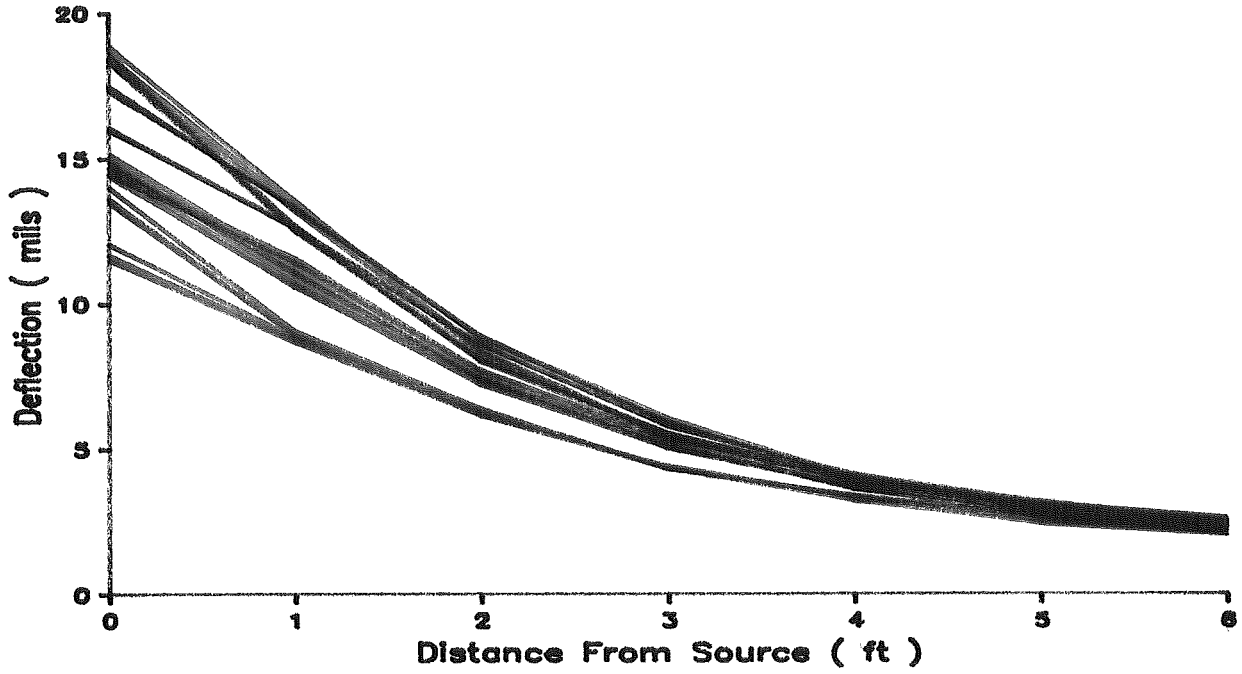


FIGURE A- 7 . FWD DATA AT 9000 LB DROP FOR SITE 7

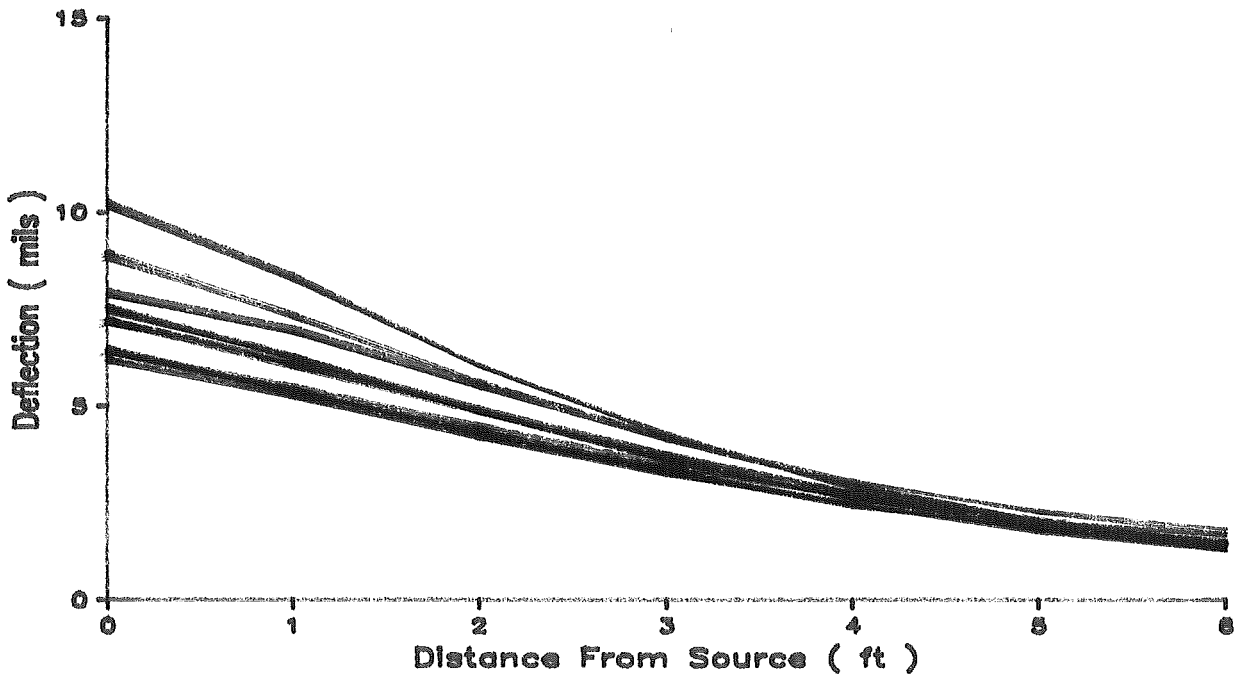


FIGURE A- 8 . FWD DATA AT 9000 LB DROP FOR SITE 8

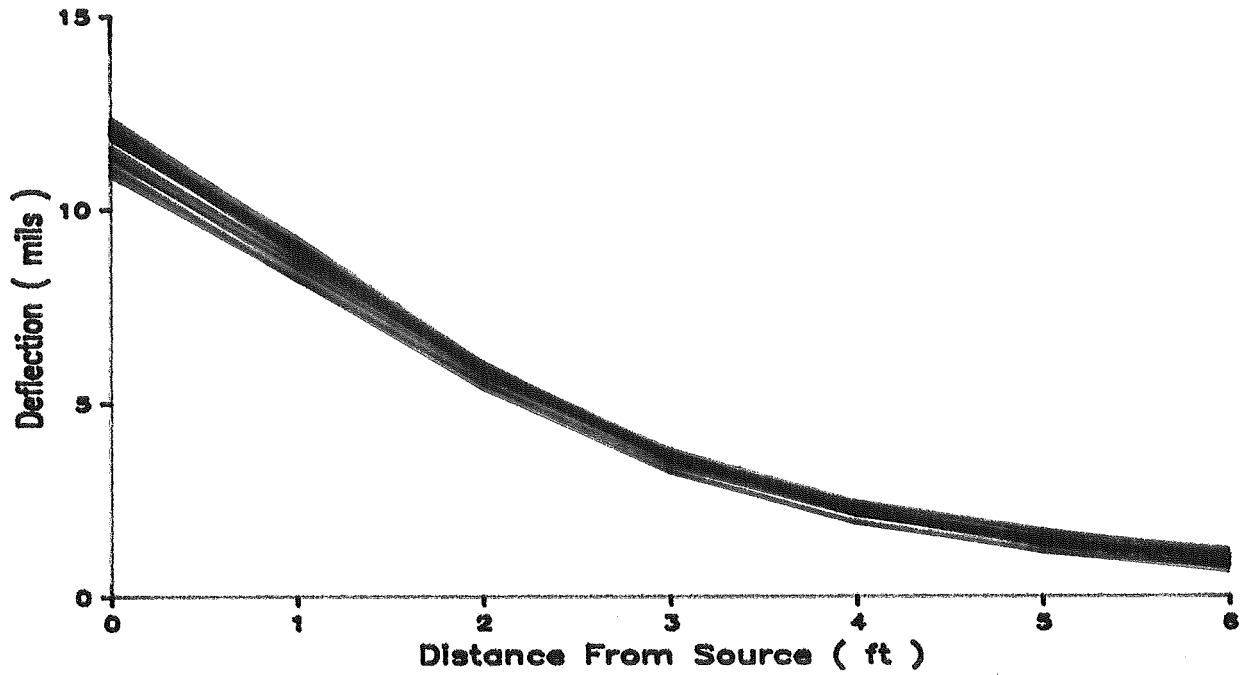


FIGURE A- 9 . FWD DATA AT 9000 LB DROP FOR SITE 9

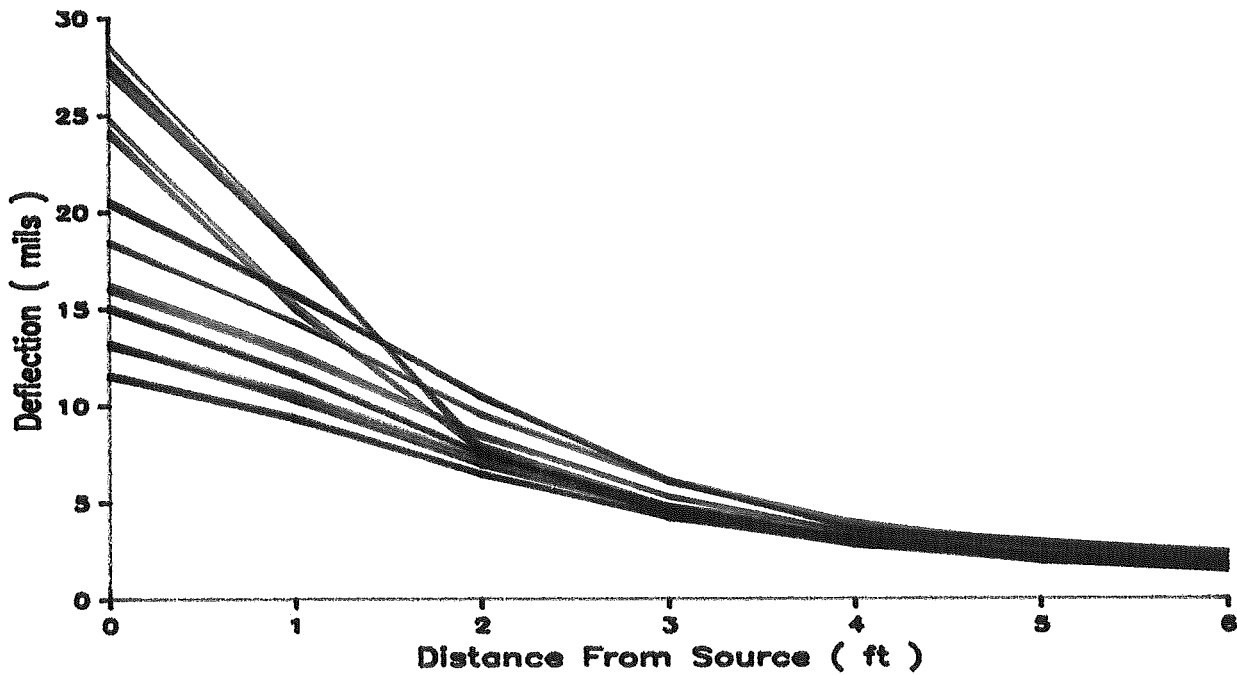


FIGURE A- 10. FWD DATA AT 9000 LB DROP FOR SITE 10

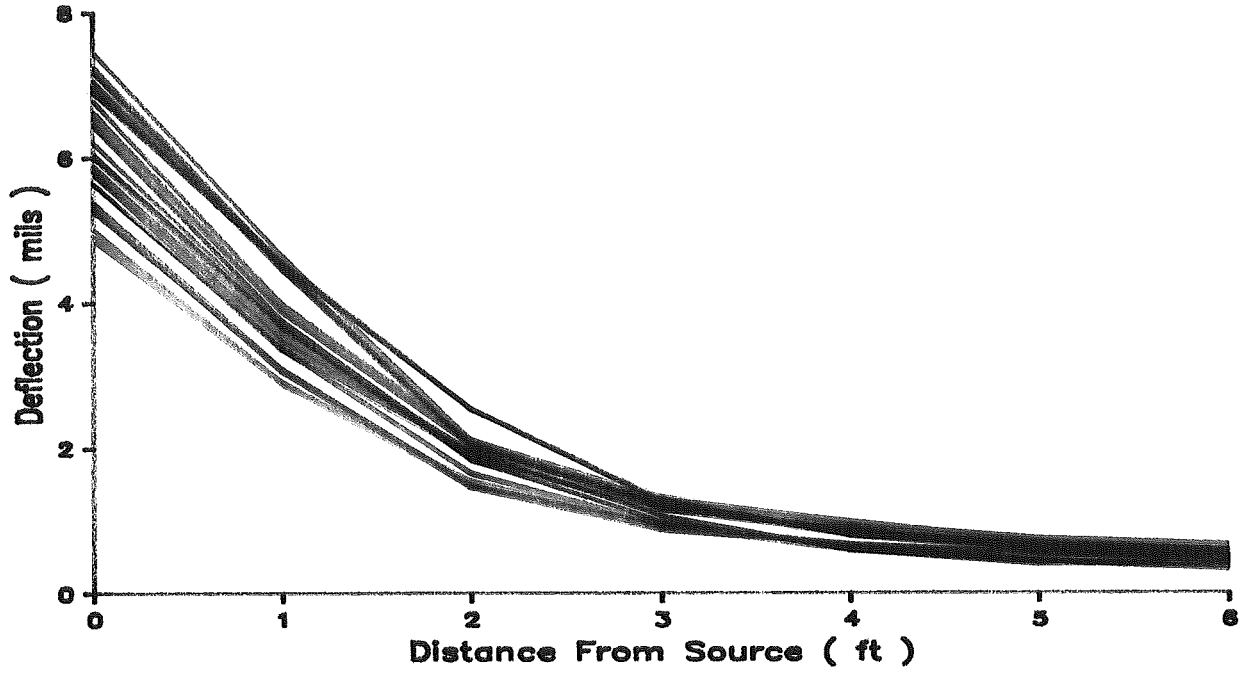


FIGURE A- 11. FWD DATA AT 9000 LB DROP FOR SITE 11

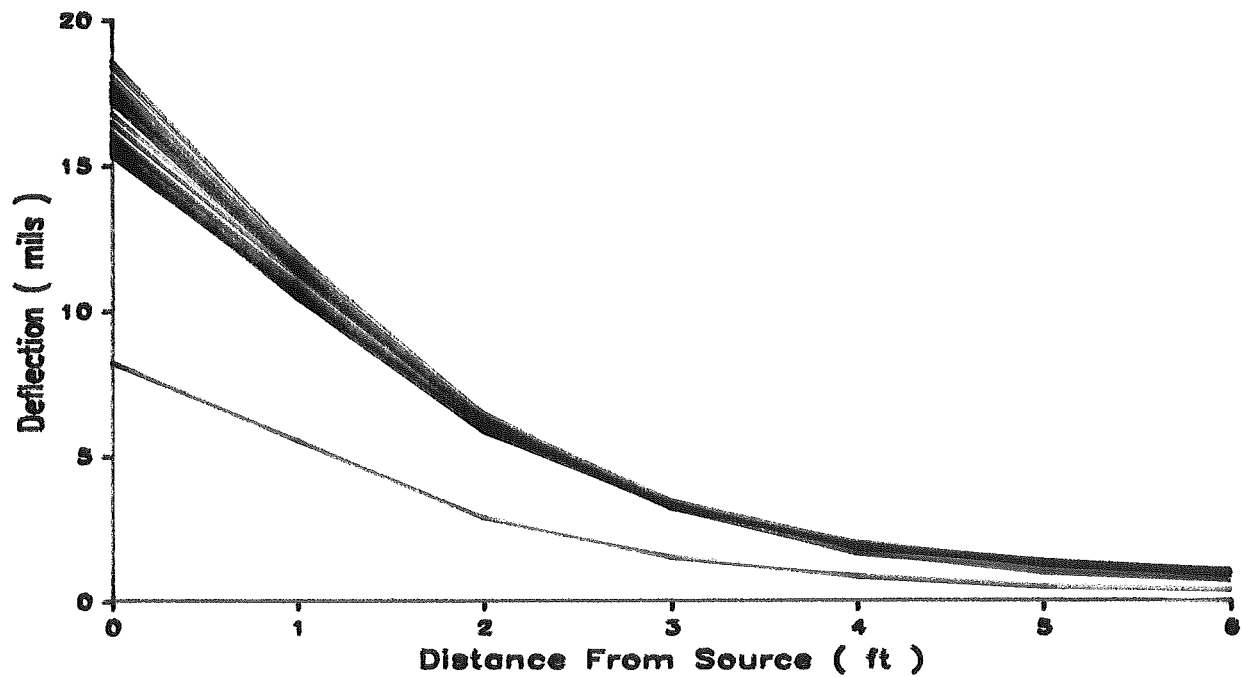


FIGURE A- 12. FWD DATA AT 9000 LB DROP FOR SITE 12

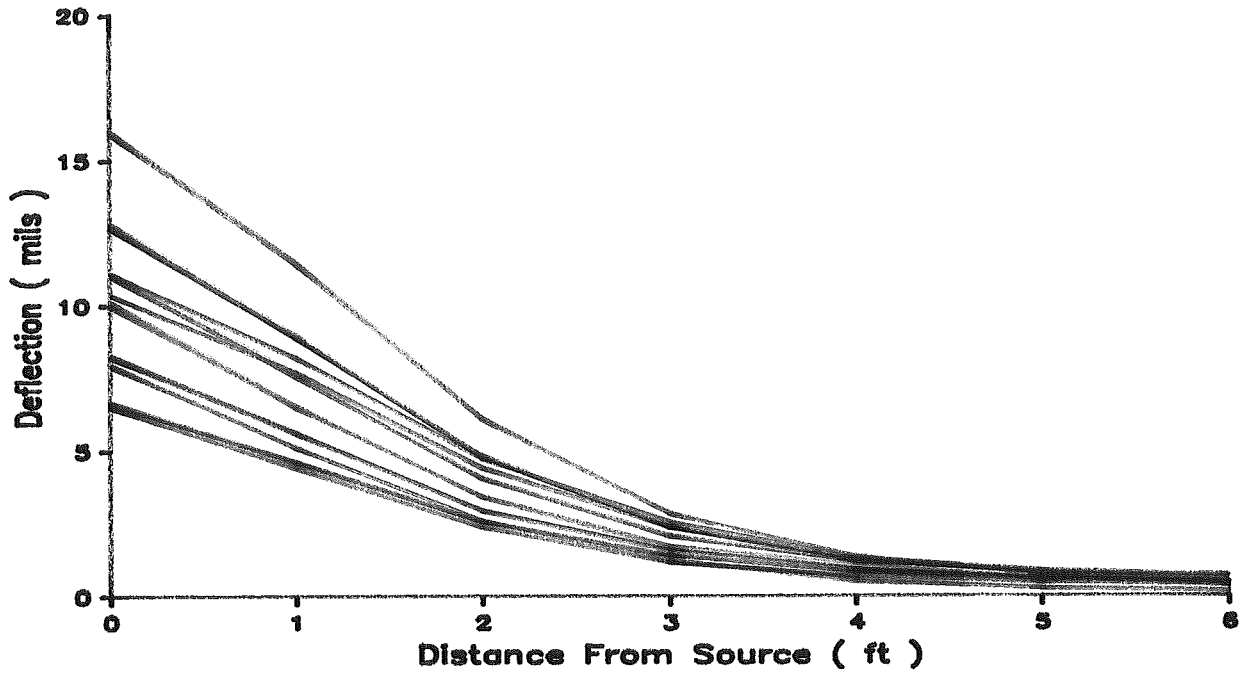


FIGURE A- 13. FWD DATA AT 9000 LB DROP FOR SITE 13

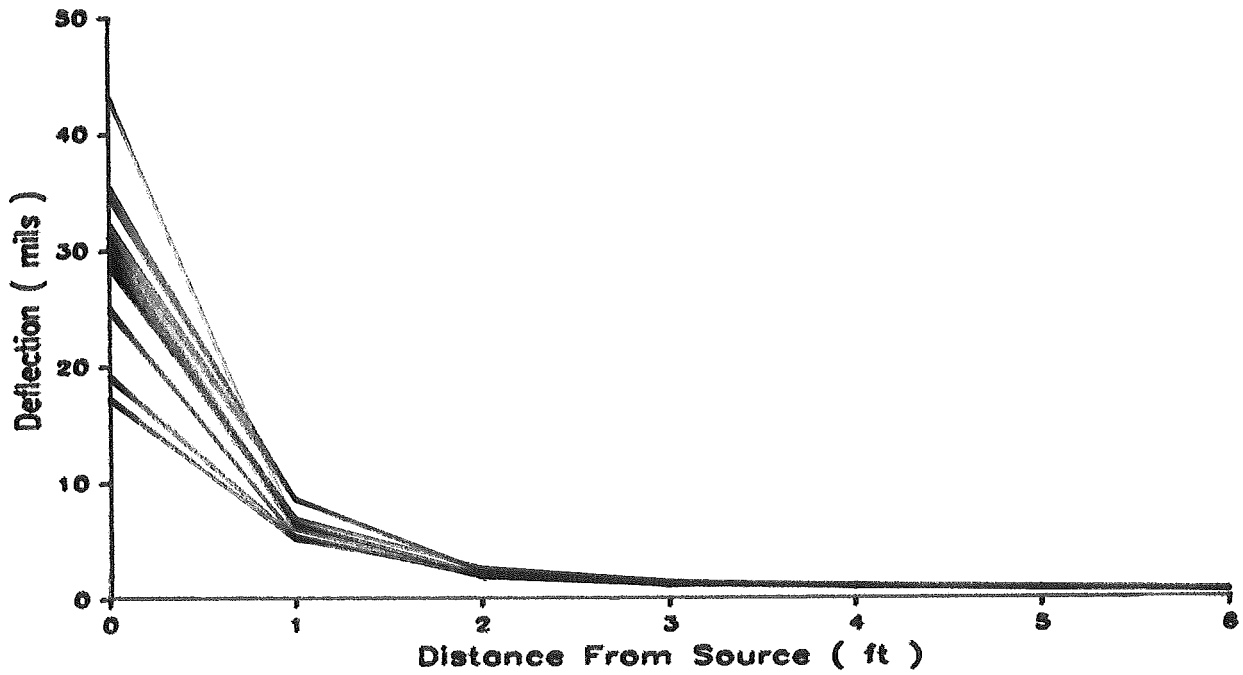


FIGURE A- 14. FWD DATA AT 9000 LB DROP FOR SITE 14

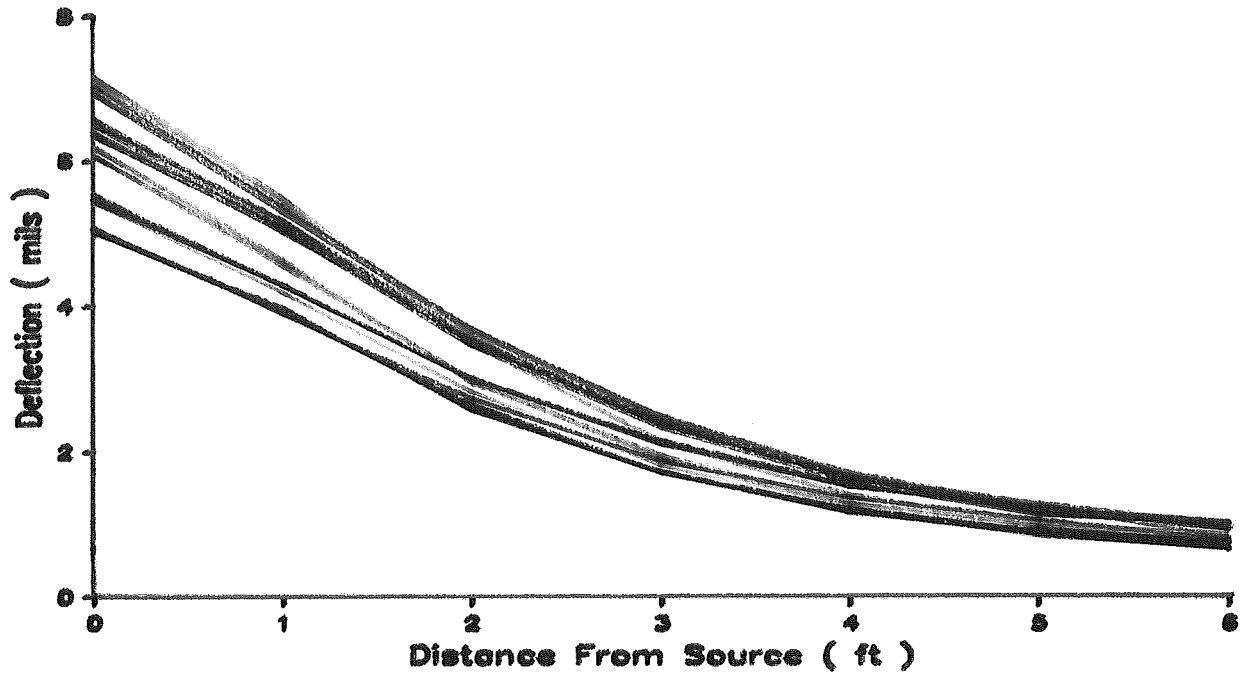


FIGURE A- 15. FWD DATA AT 9000 LB DROP FOR SITE 15

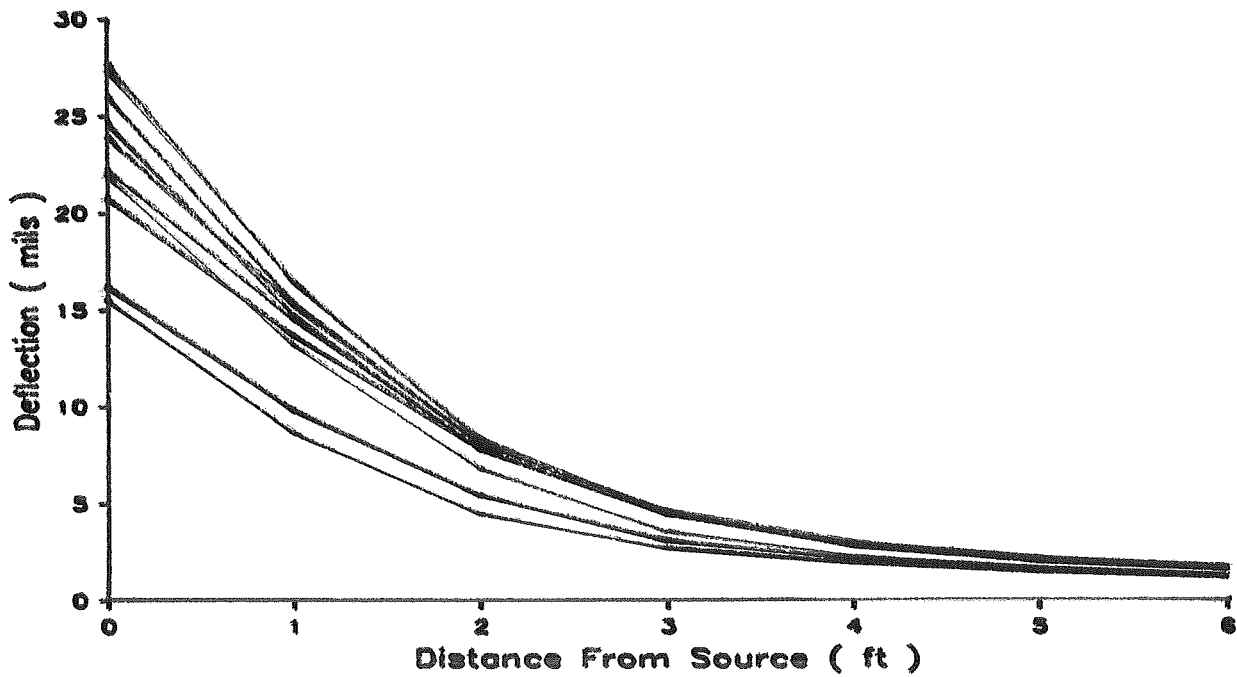


FIGURE A- 16. FWD DATA AT 9000 LB DROP FOR SITE 16

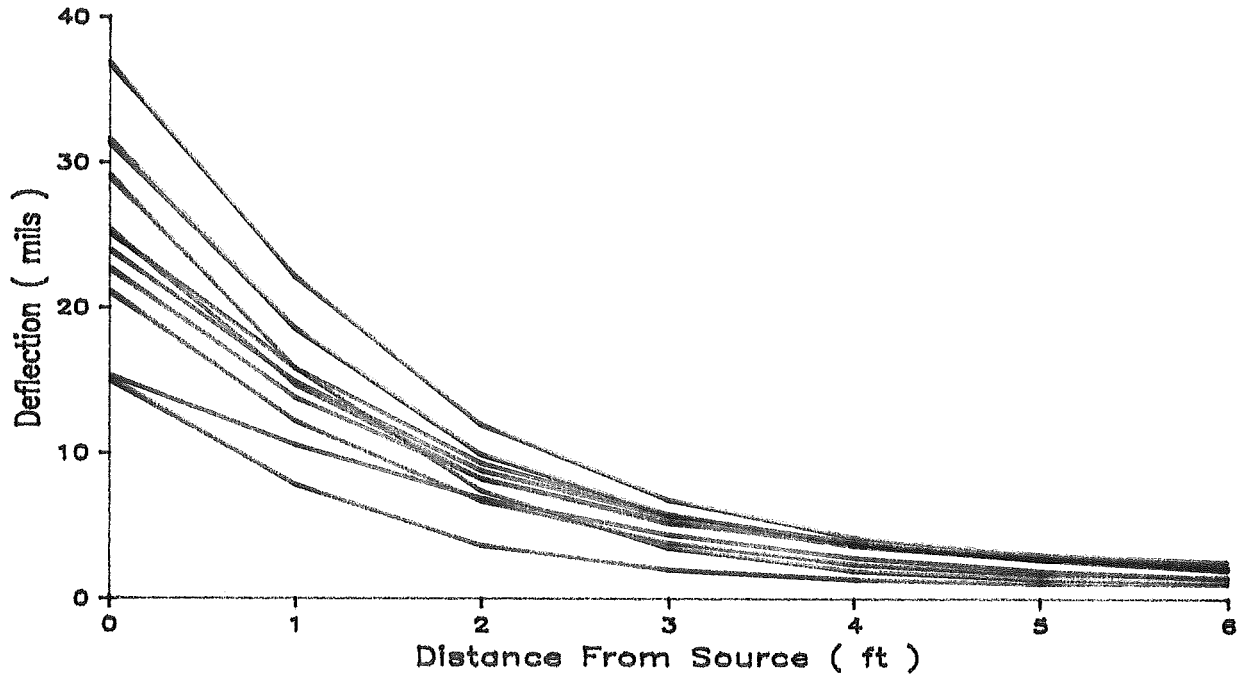


FIGURE A- 17. FWD DATA AT 9000 LB DROP FOR SITE 17

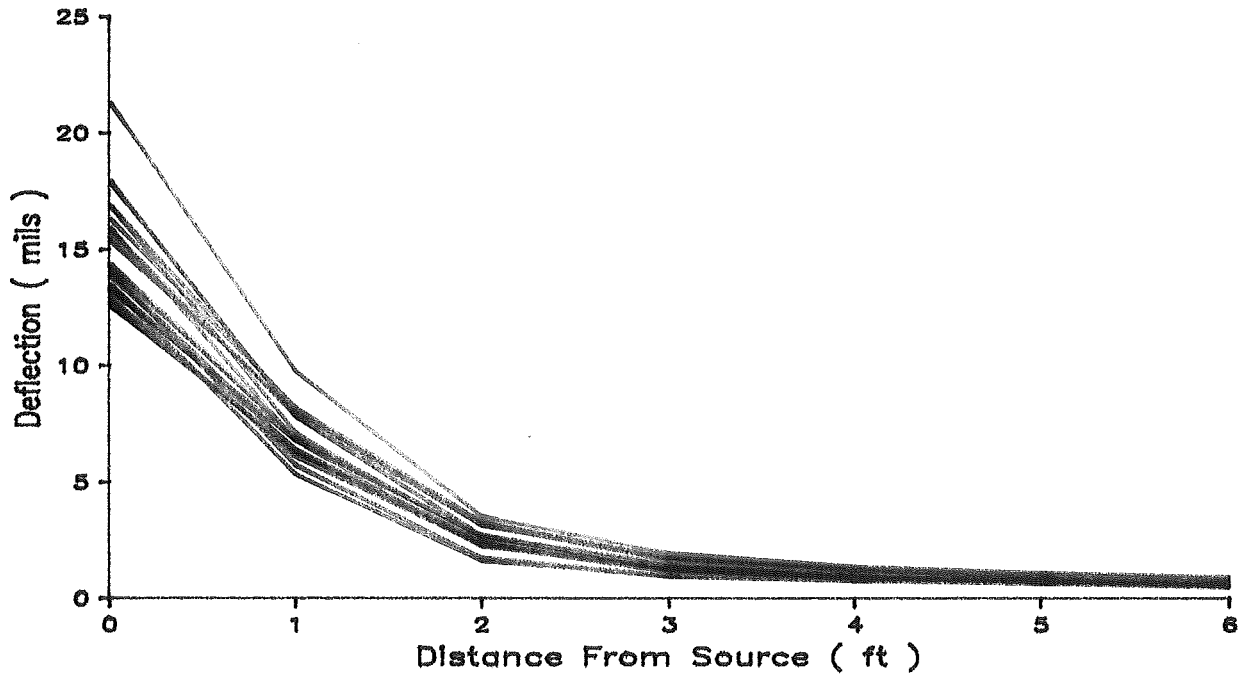


FIGURE A- 18. FWD DATA AT 9000 LB DROP FOR SITE 18

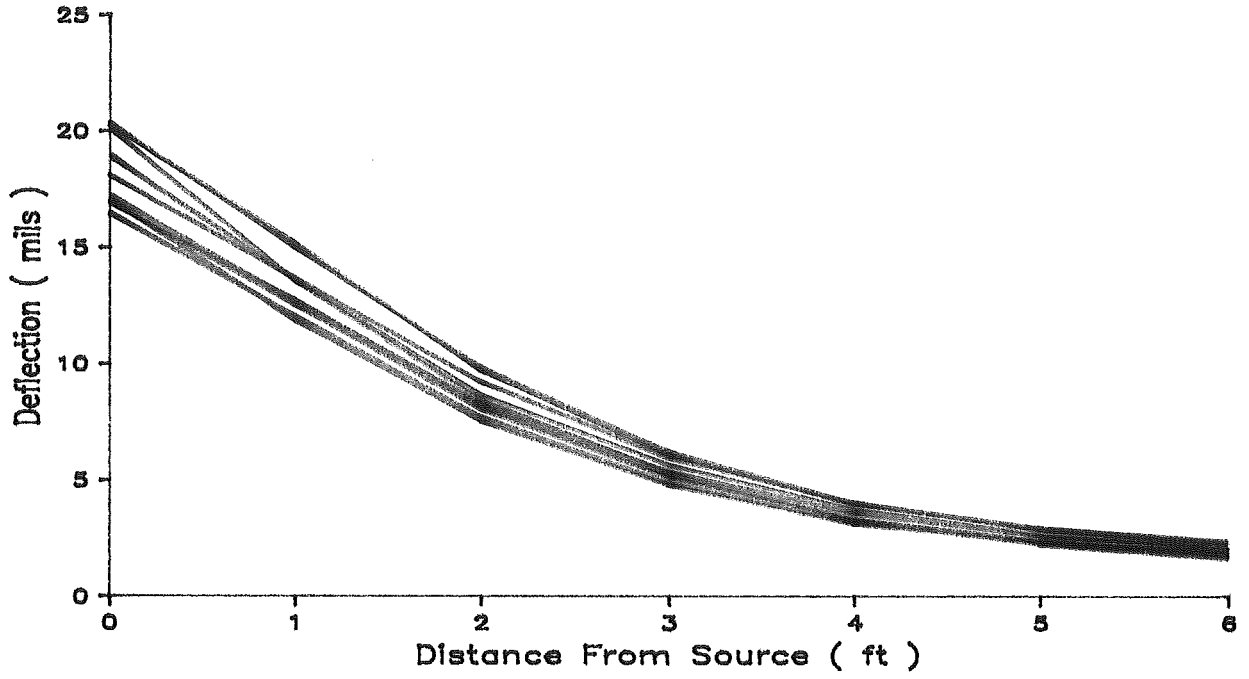


FIGURE A- 19. FWD DATA AT 9000 LB DROP FOR SITE 19

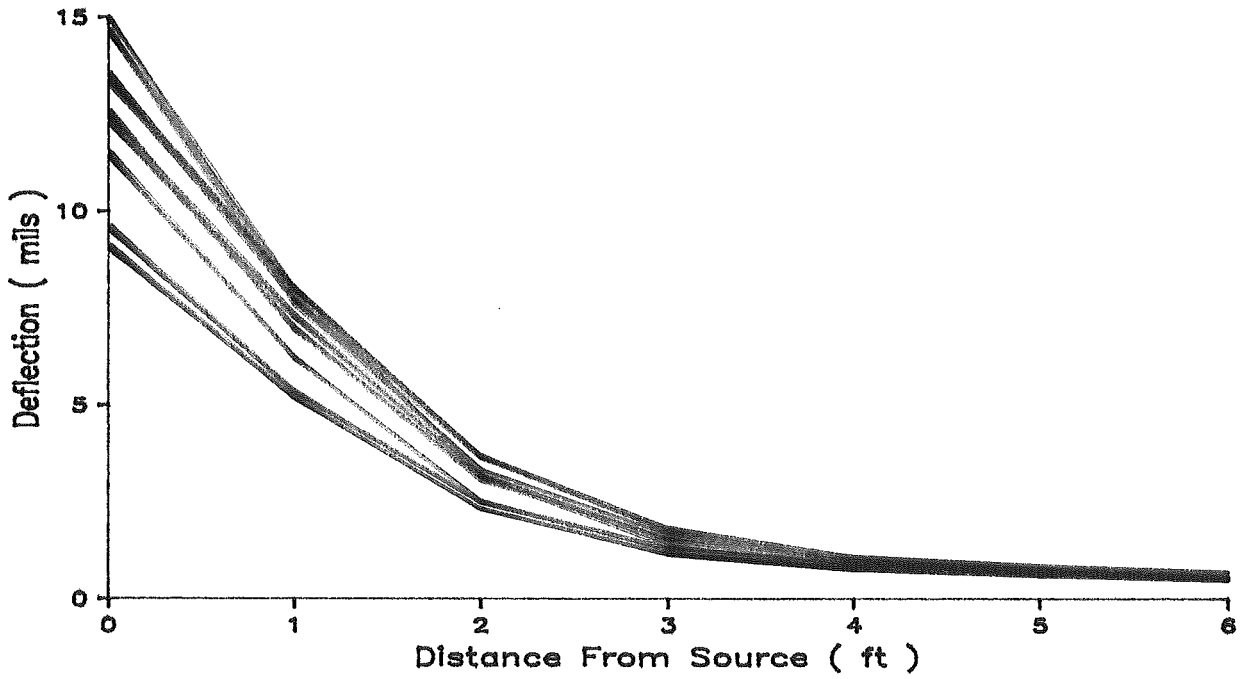


FIGURE A- 20. FWD DATA AT 9000 LB DROP FOR SITE 20

PLOTS OF THE DYNAFLECT DATA

VARIABILITY IN FIELD MEASUREMENTS ACROSS THE SITE

The following 14 plots are of the field measurements of deflections resulting from the Dynaflect test. At each site, the measurements taken at each site. Each station is 10 ft away from the previous station, covering a span of 90 ft in the direction of traffic.

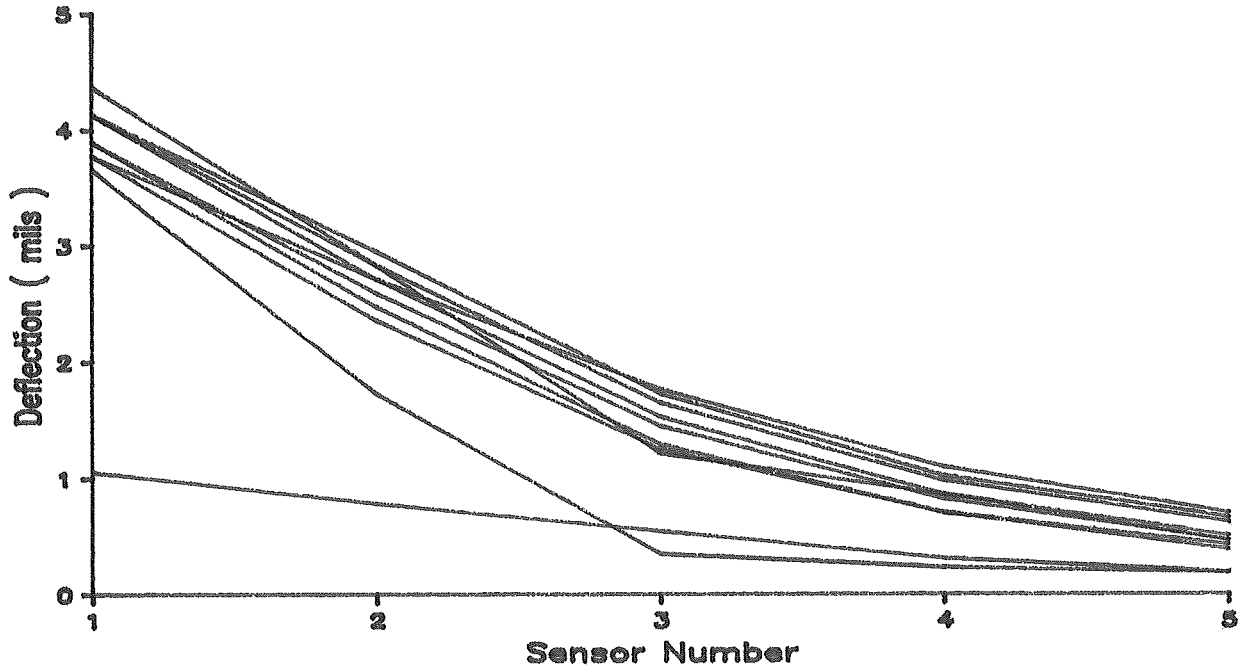


FIGURE A- 21. DYNAFLECT DATA FOR SITE 1

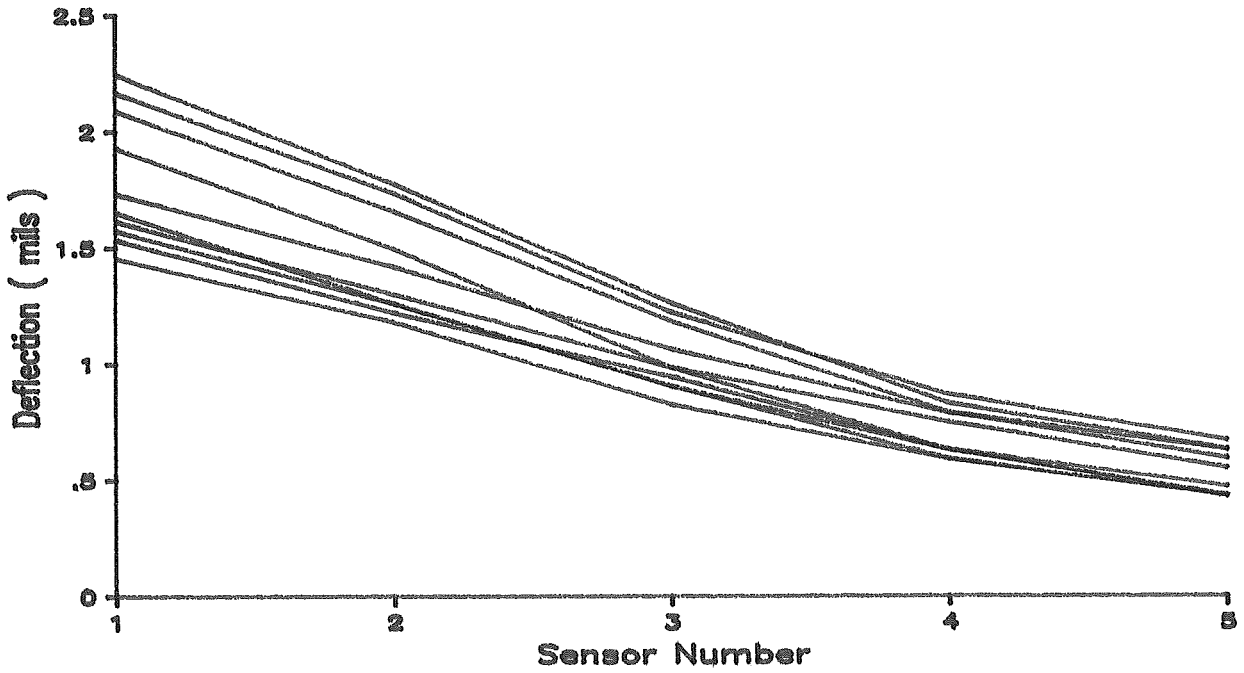


FIGURE A- 22. DYNAFLECT DATA FOR SITE 2

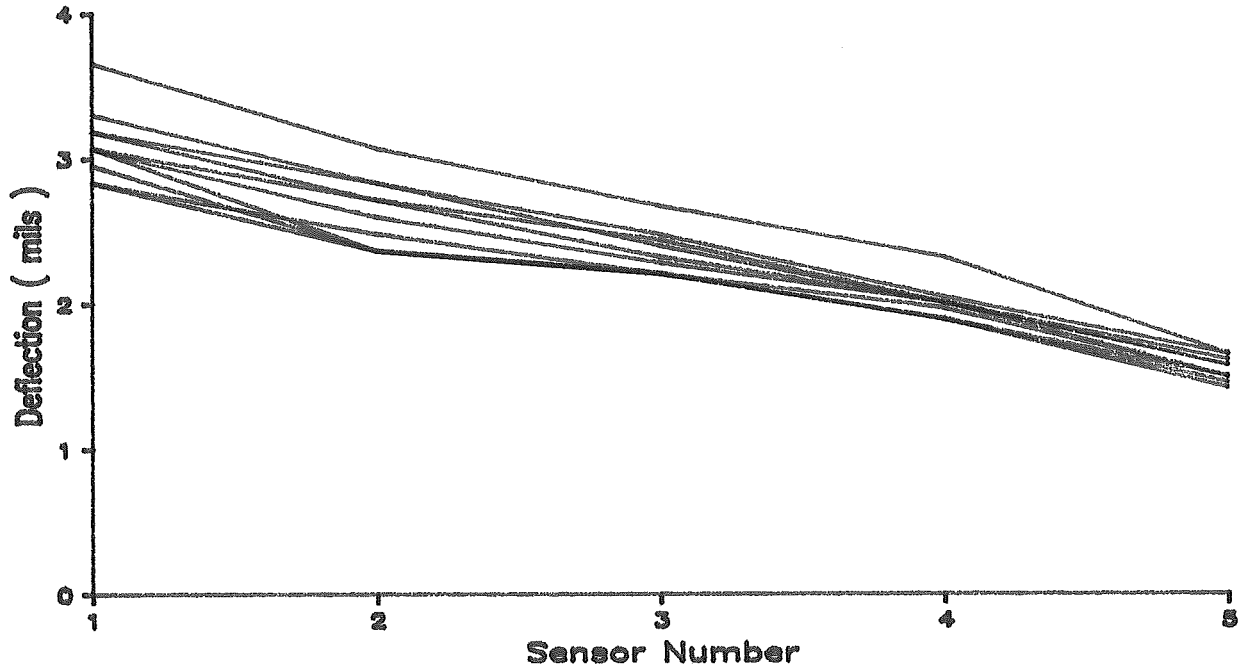


FIGURE A- 23. DYNAFLECT DATA FOR SITE 3

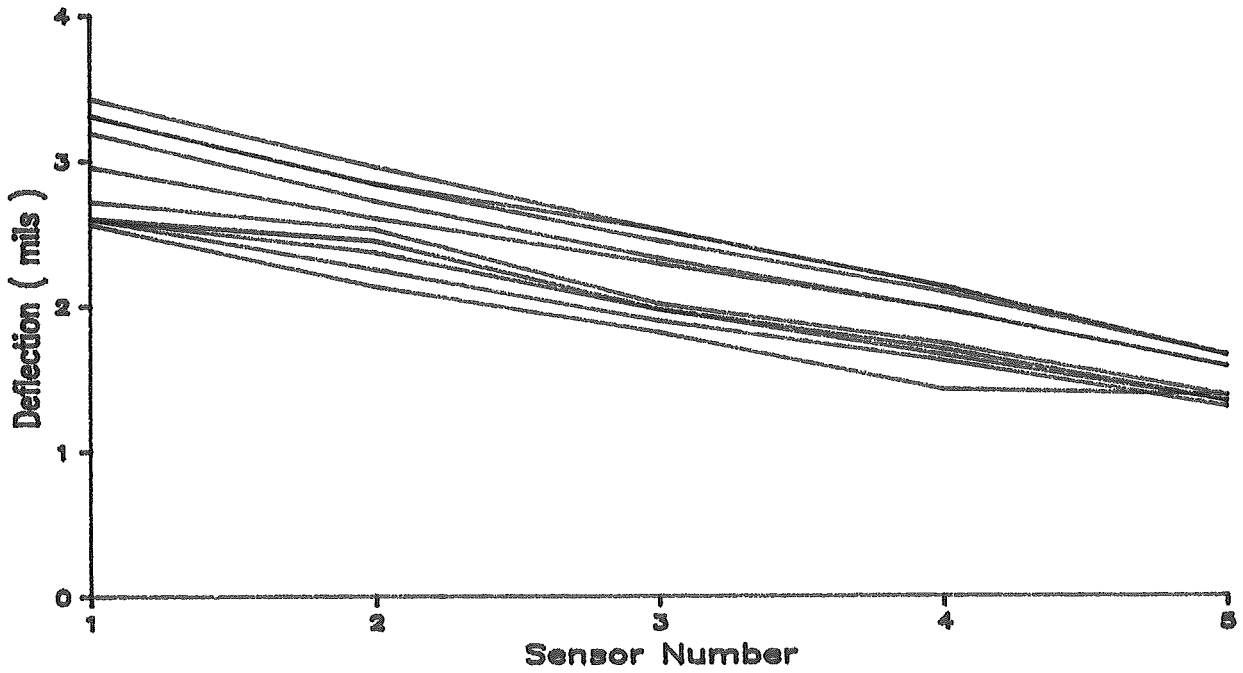


FIGURE A- 24. DYNAFLECT DATA FOR SITE 4

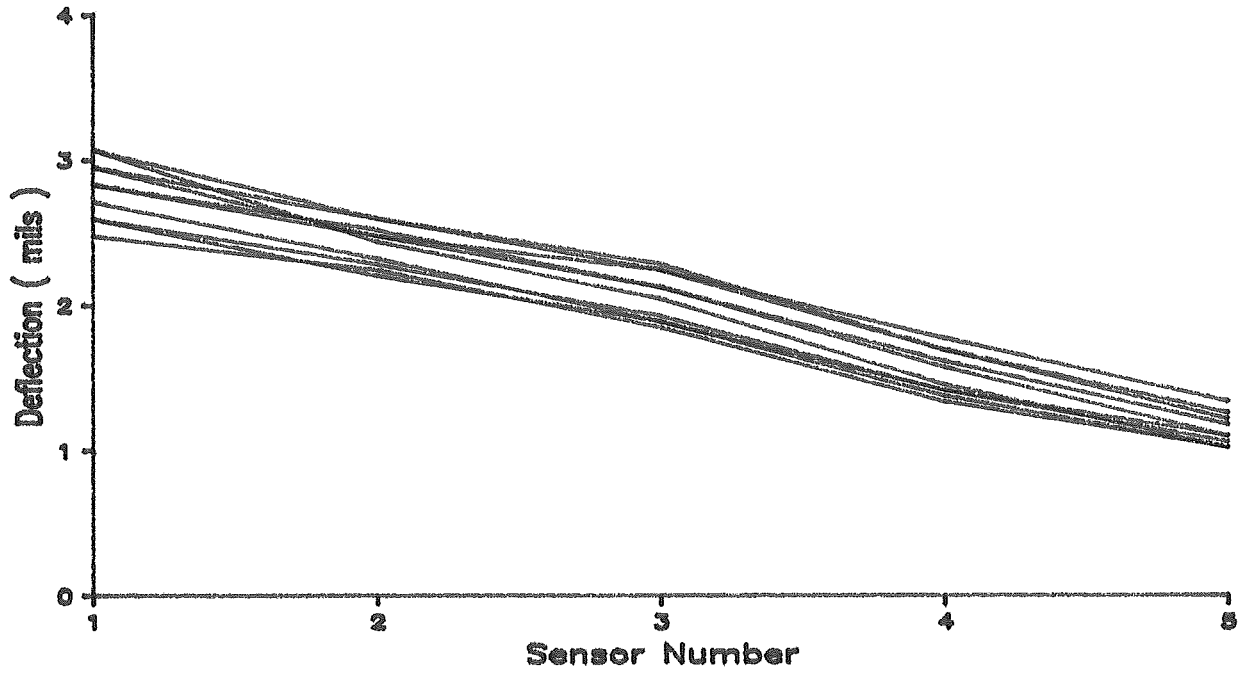


FIGURE A- 25. DYNAFLECT DATA FOR SITE 5

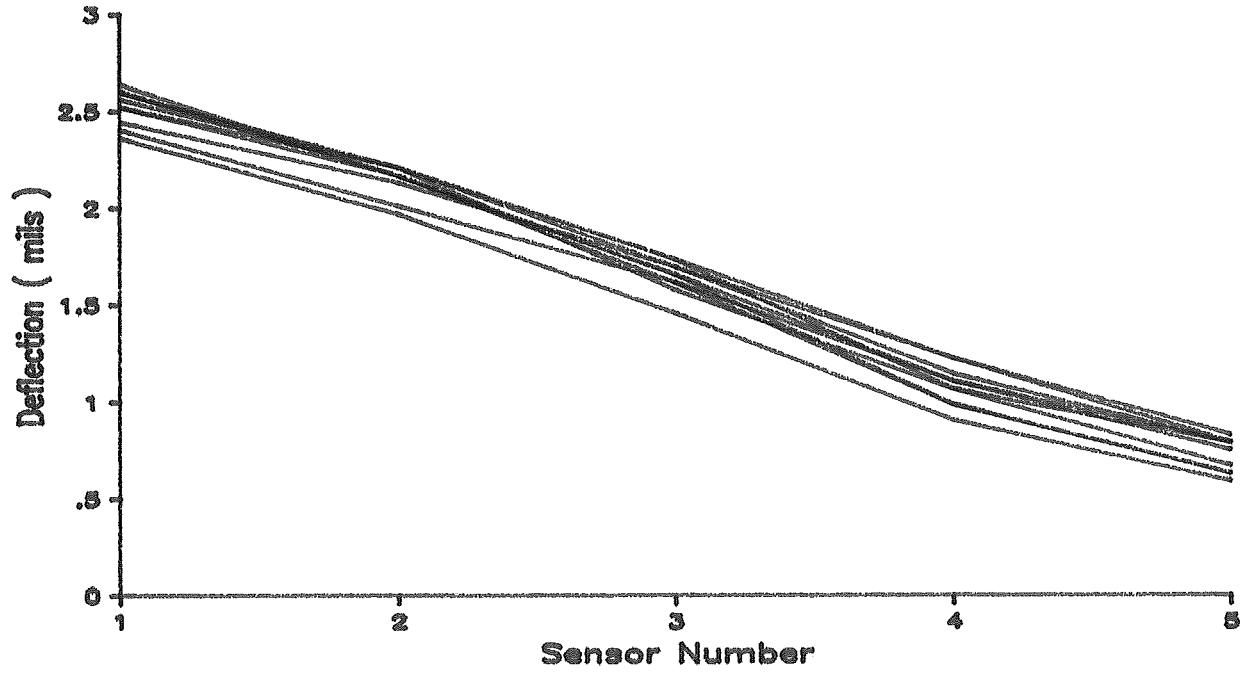


FIGURE A- 26. DYNAFLECT DATA FOR SITE 6

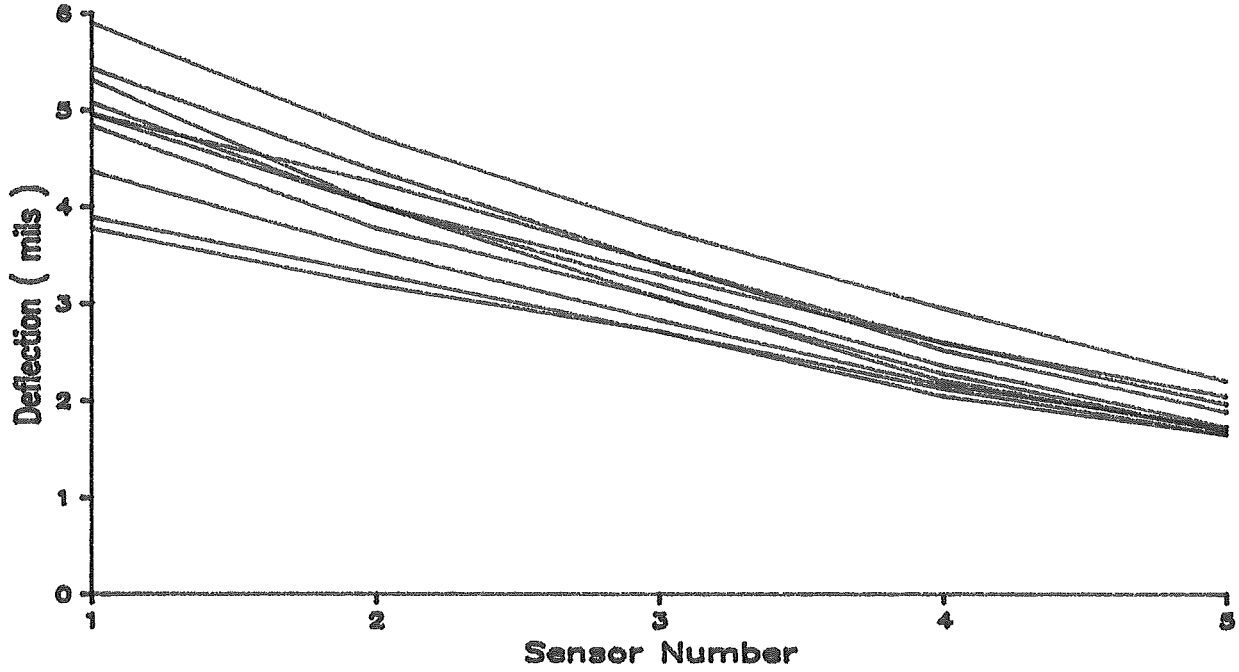


FIGURE A- 27. DYNAFLECT DATA FOR SITE 7

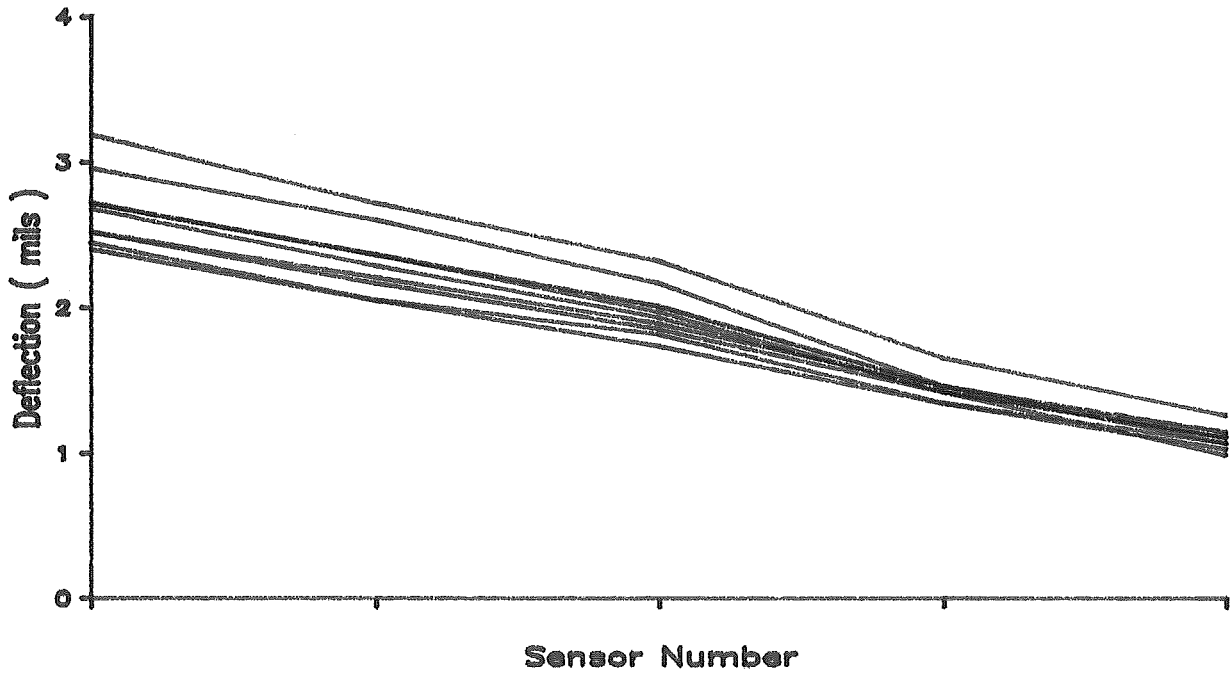


FIGURE A- 28. DYNAFLECT DATA FOR SITE 8

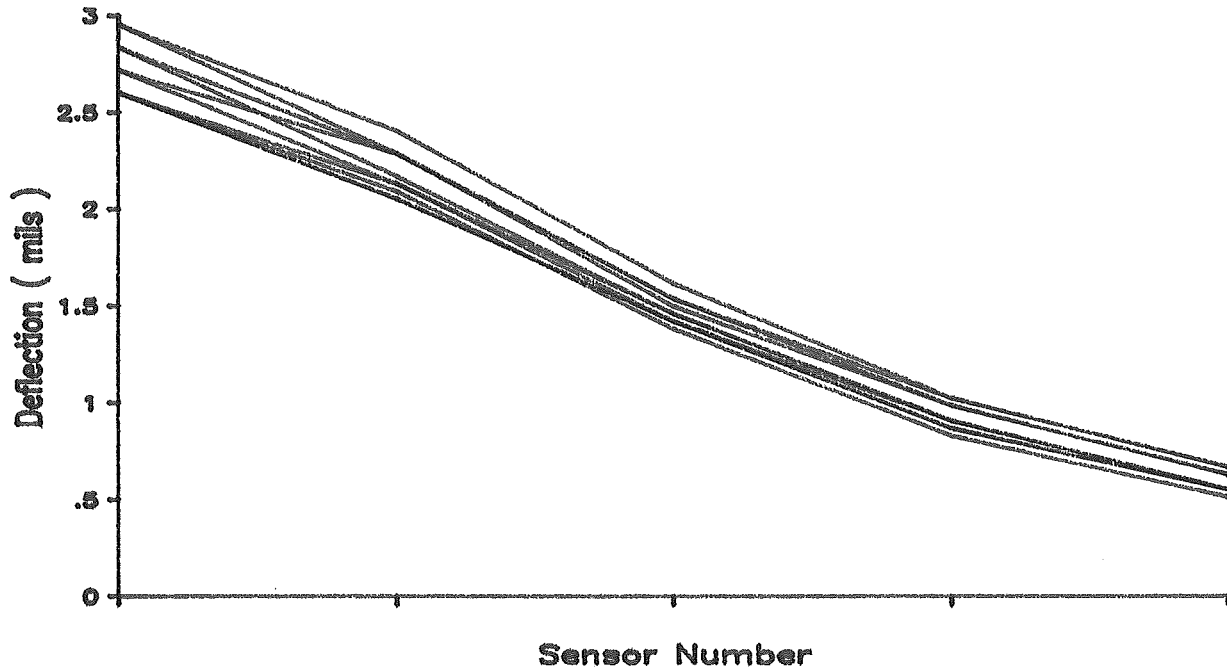


FIGURE A- 29. DYNAFLECT DATA FOR SITE 9

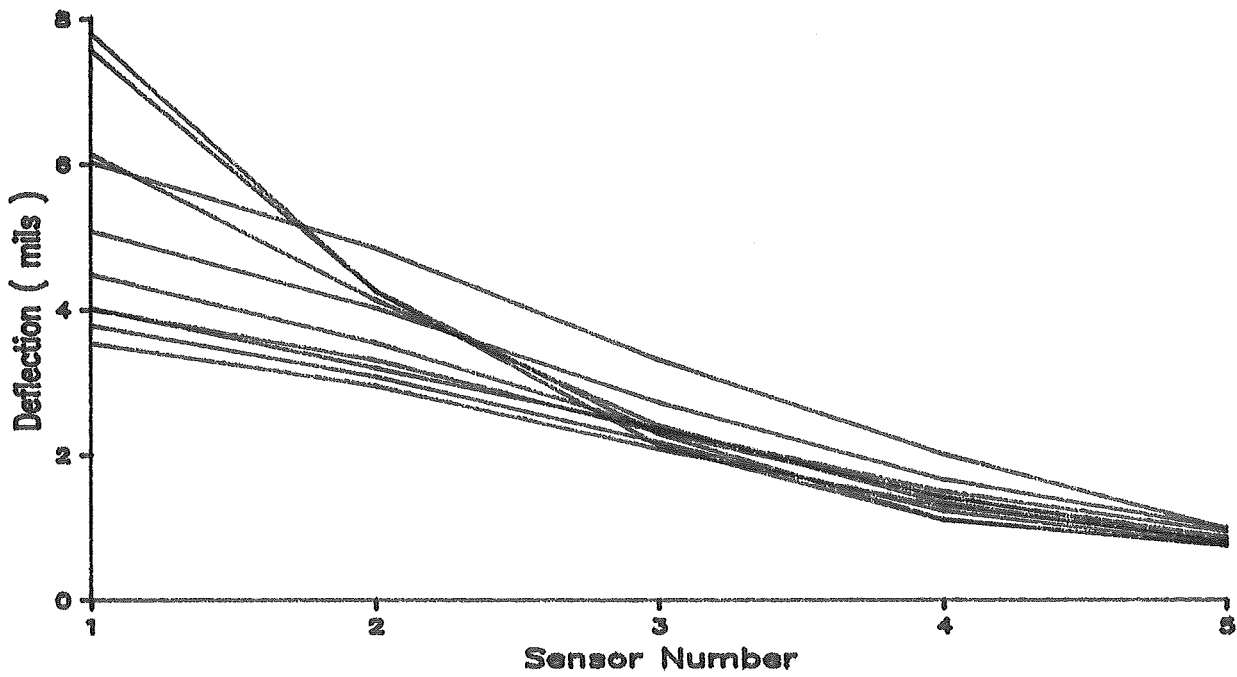


FIGURE A- 30. DYNAFLECT DATA FOR SITE 10

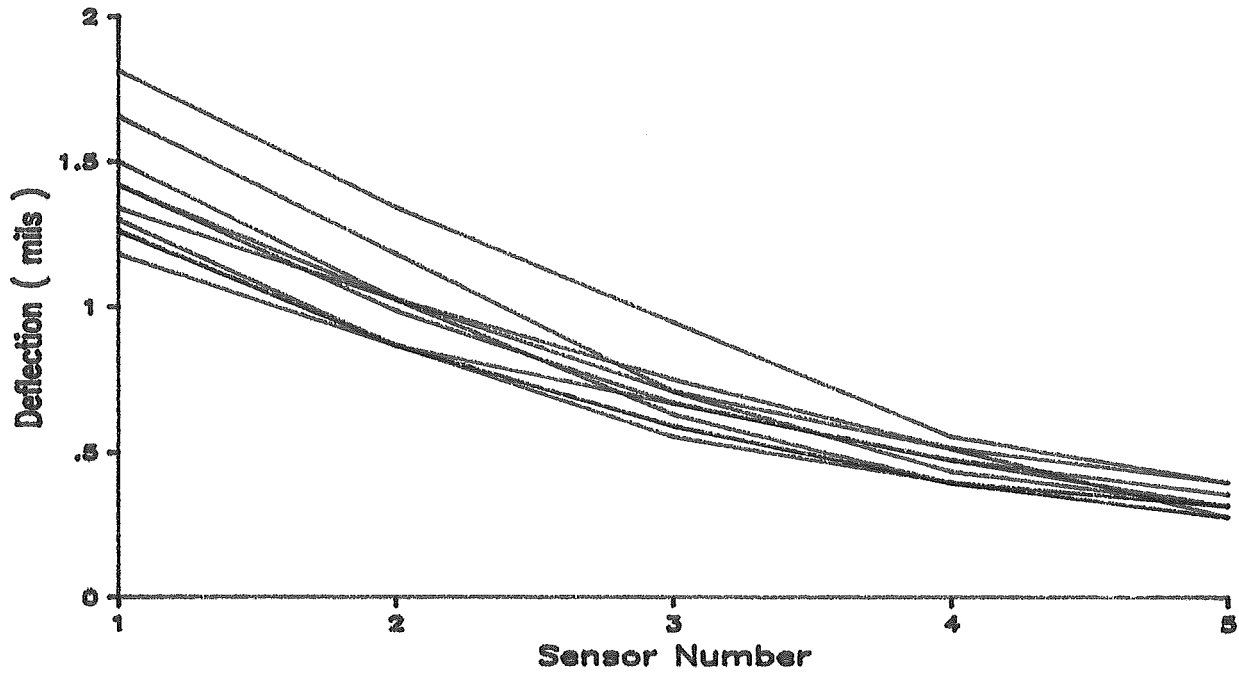


FIGURE A- 31. DYNAFLECT DATA FOR SITE 11

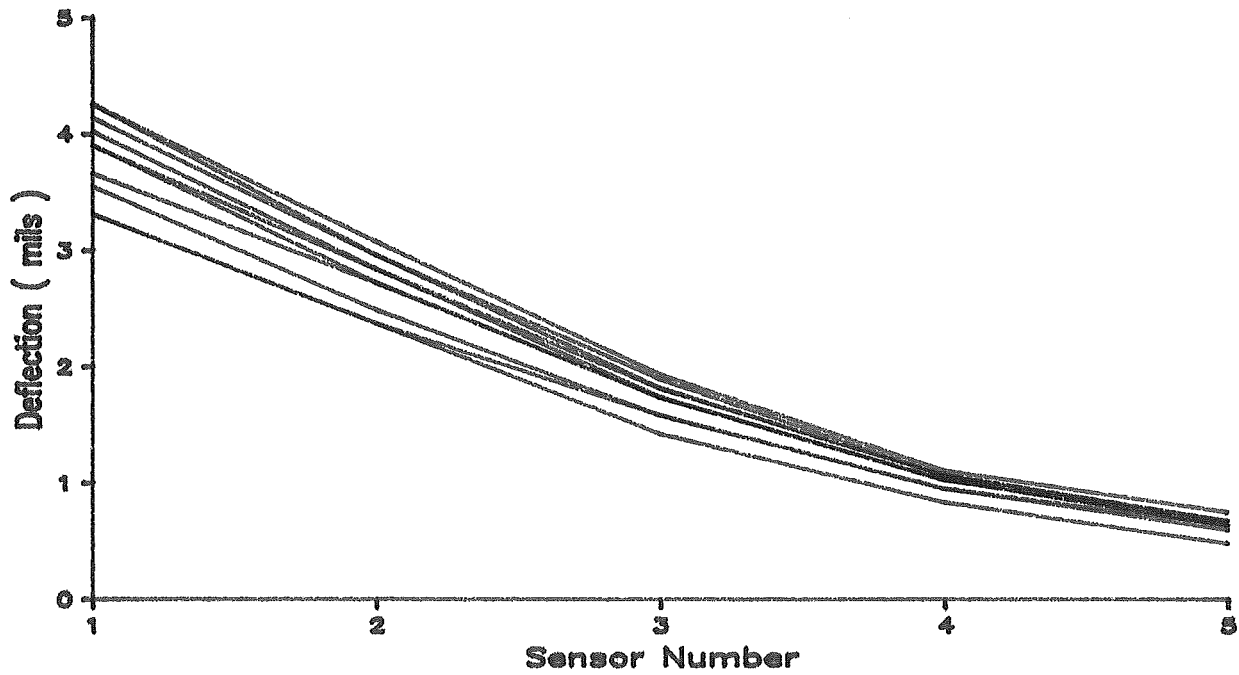


FIGURE A- 32. DYNAFLECT DATA FOR SITE 12

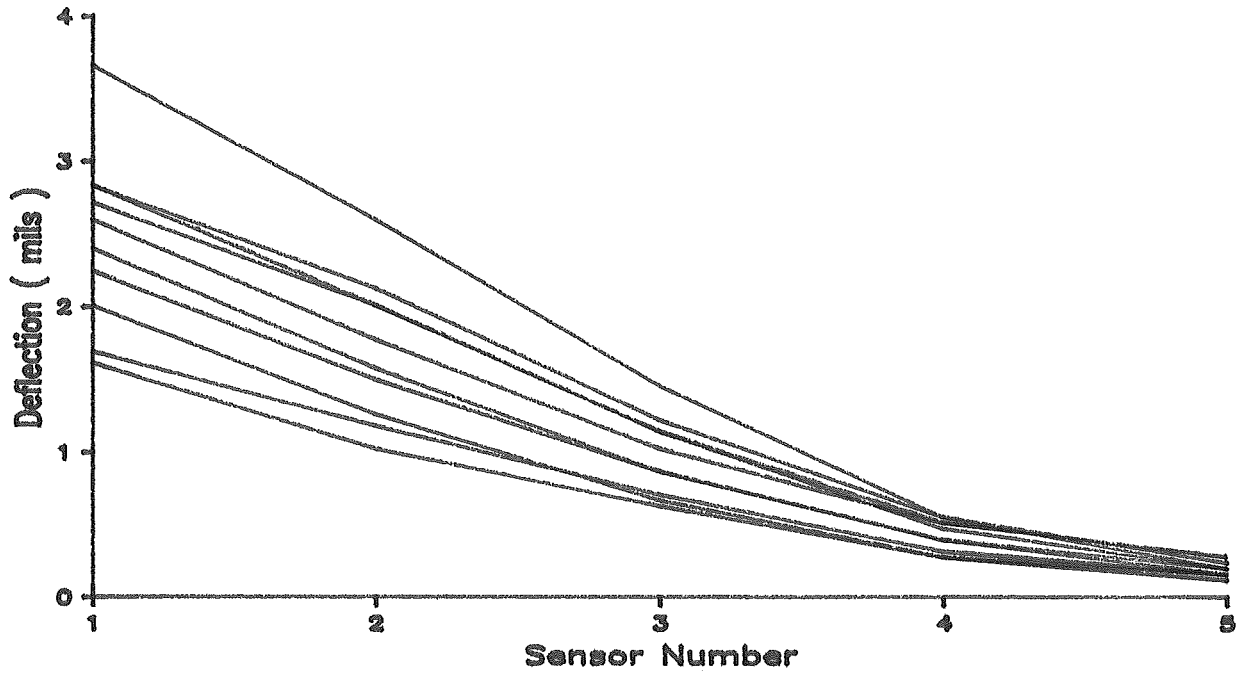


FIGURE A- 33. DYNAFLECT DATA FOR SITE 13

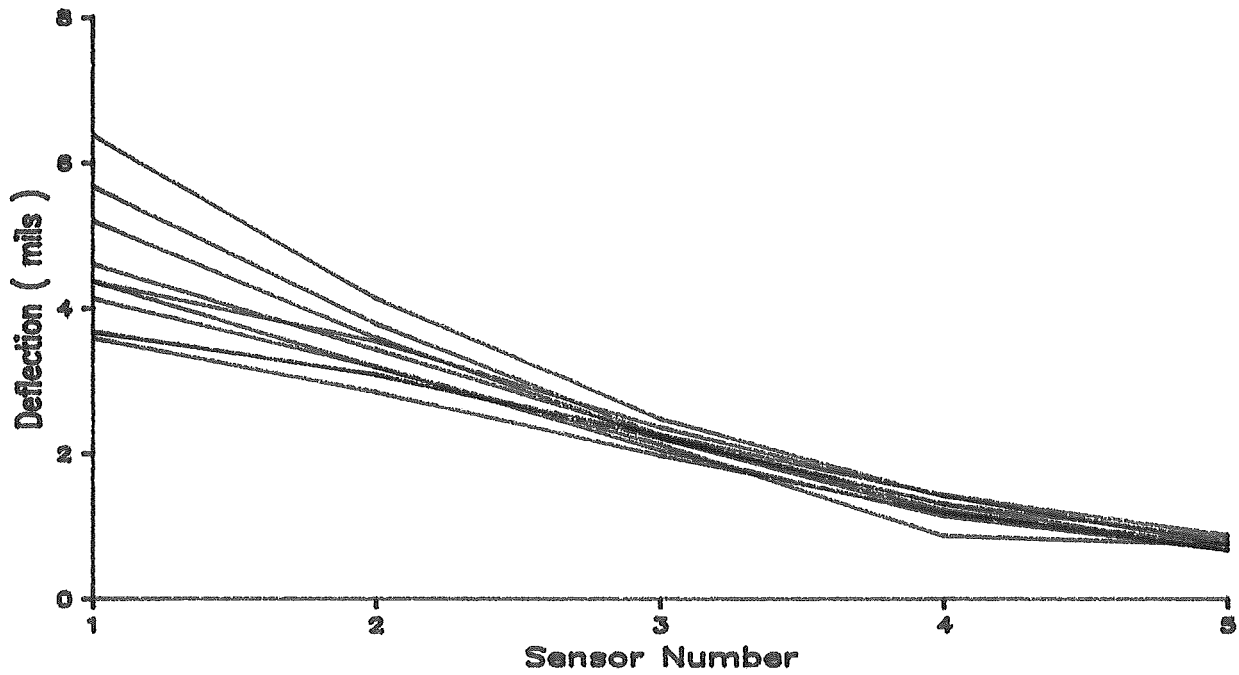


FIGURE A- 34. DYNAFLECT DATA FOR SITE 15

EQUIVALENT 9000 LB DEFLECTIONS

The following series of plots were developed to study the nonlinearity of the pavement system from the field NDT measurements. The deflections resulting from the 6000 and 1200 lb FWD tests, and the deflections resulting from the Dynaflect tests have been "normalized" to 9000 lb deflections by assuming that the pavement system behaves perfectly linearly. These equivalent 9000 lb deflections have been plotted together with the deflections measured directly in the field upon conducting the 9000 lb FWD tests. Thus, if the material behaved perfectly linearly, all of the equivalent deflections would be expected to fall on top of the deflections obtained from the actual 9000 lb FWD test. Plots included in this section are for sites 1 to 13 and site 15.

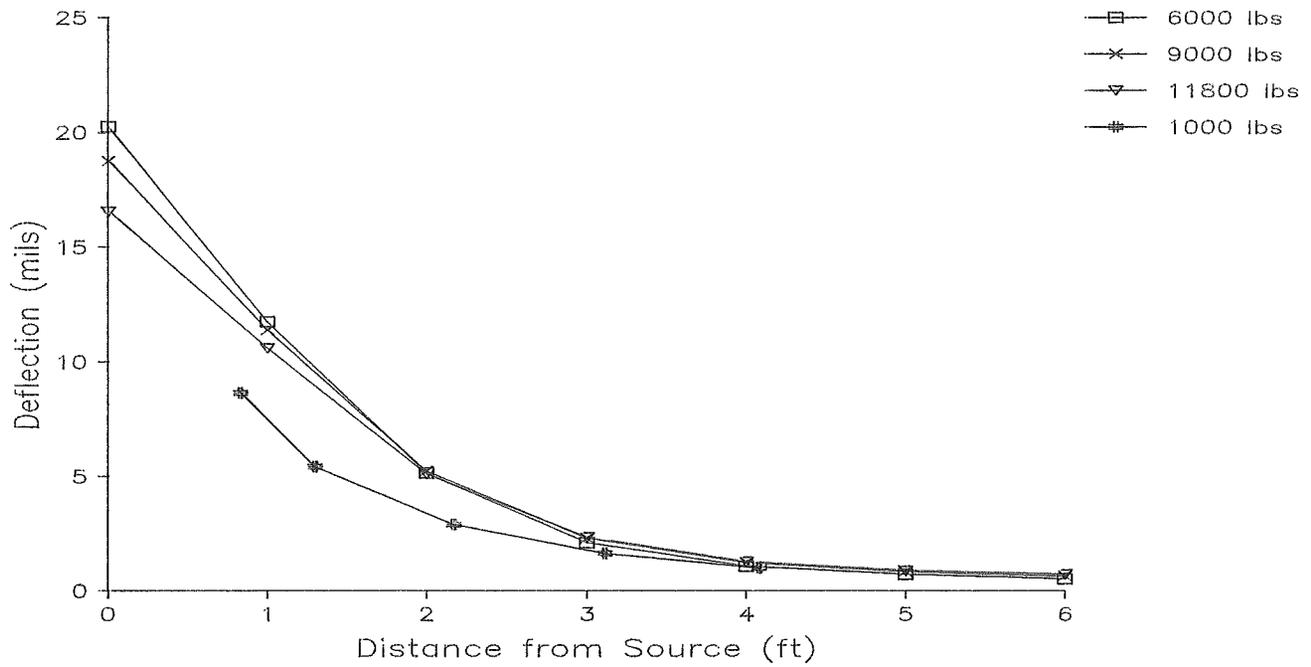


FIGURE A- 35. EQUIVALENT 9000 LB FWD DEFLECTIONS FOR SITE 1 STATION 1

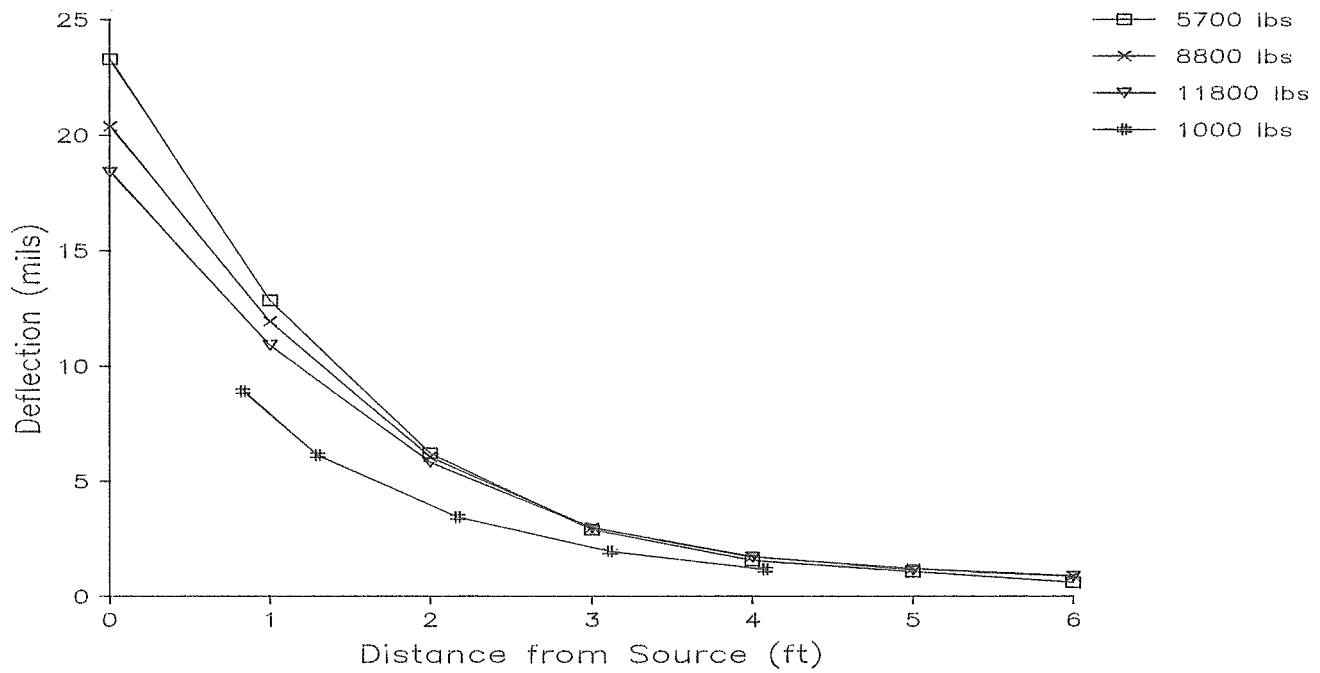


FIGURE A- 36. EQUIVALENT 9000 LB FWD DEFLECTIONS FOR SITE 1 STATION 5

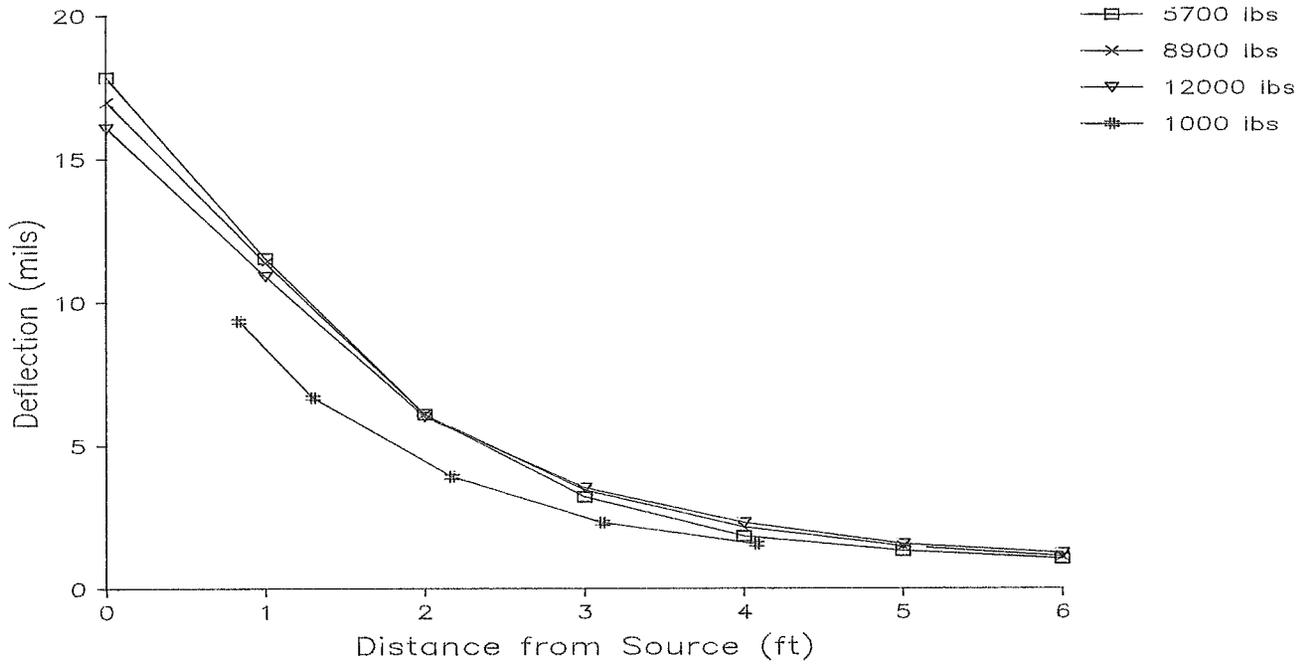


FIGURE A- 37. EQUIVALENT 9000 LB FWD DEFLECTIONS FOR SITE 1 STATION 10

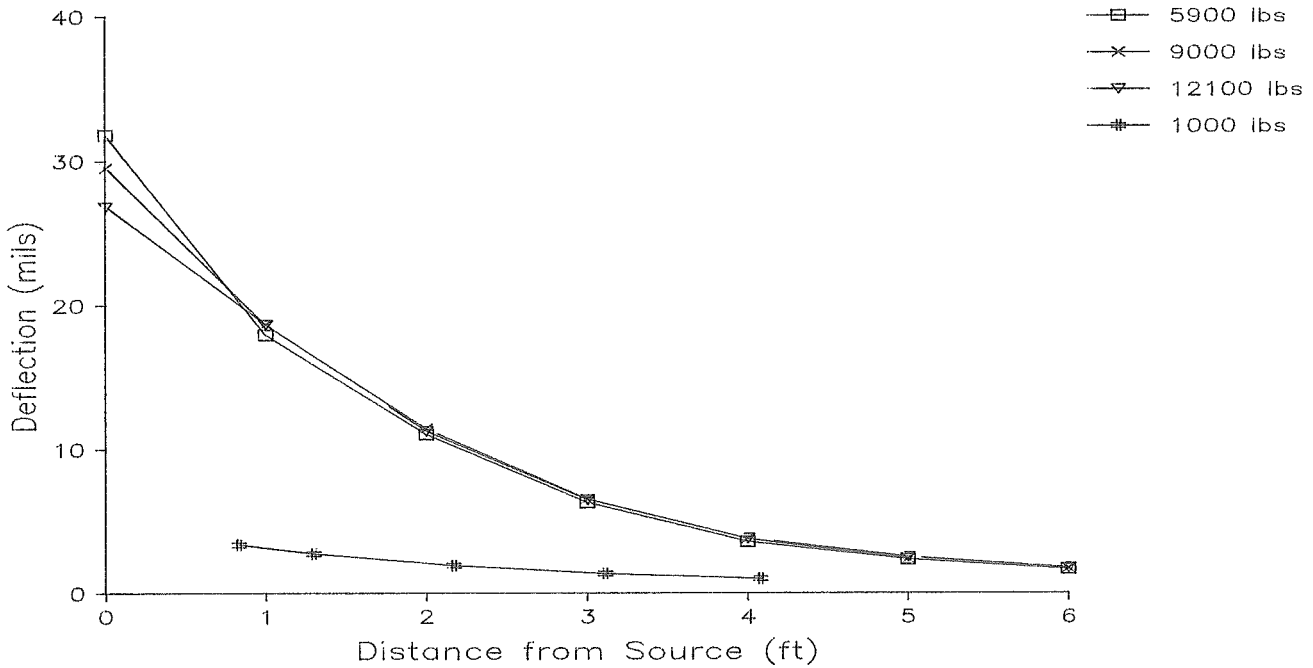


FIGURE A- 38. EQUIVALENT 9000 LB FWD DEFLECTIONS FOR SITE 2 STATION 1

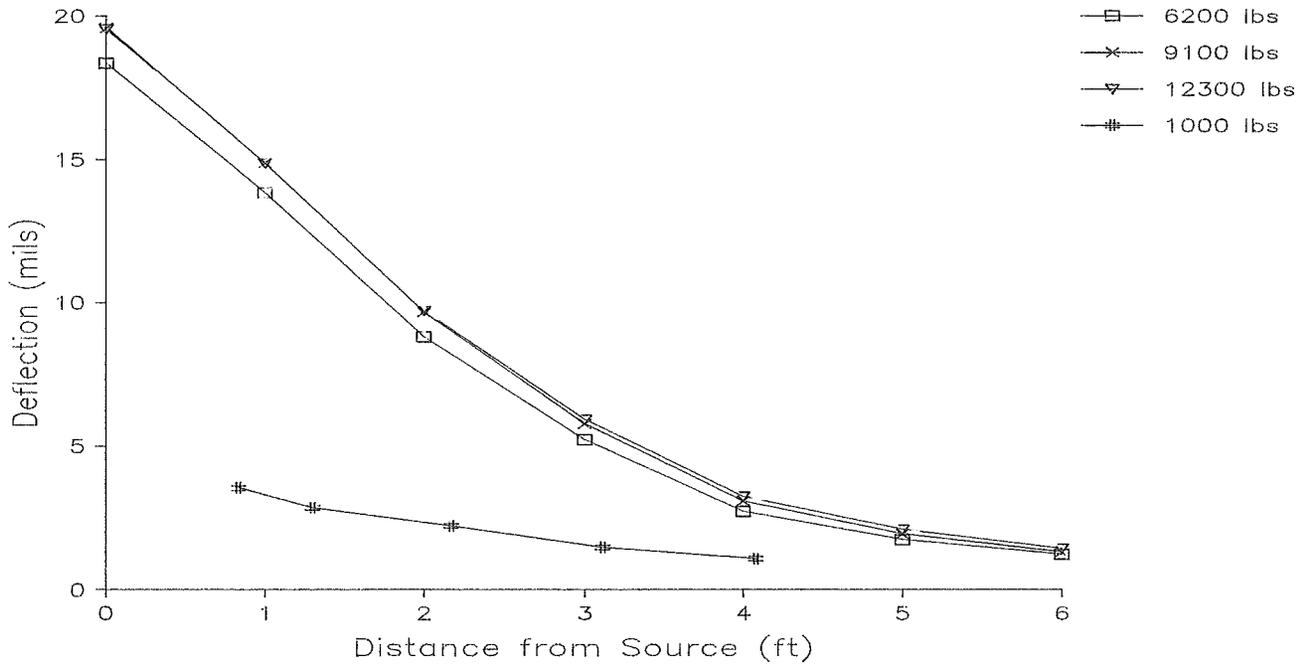


FIGURE A- 39. EQUIVALENT 9000 LB FWD DEFLECTIONS FOR SITE 2 STATION 5

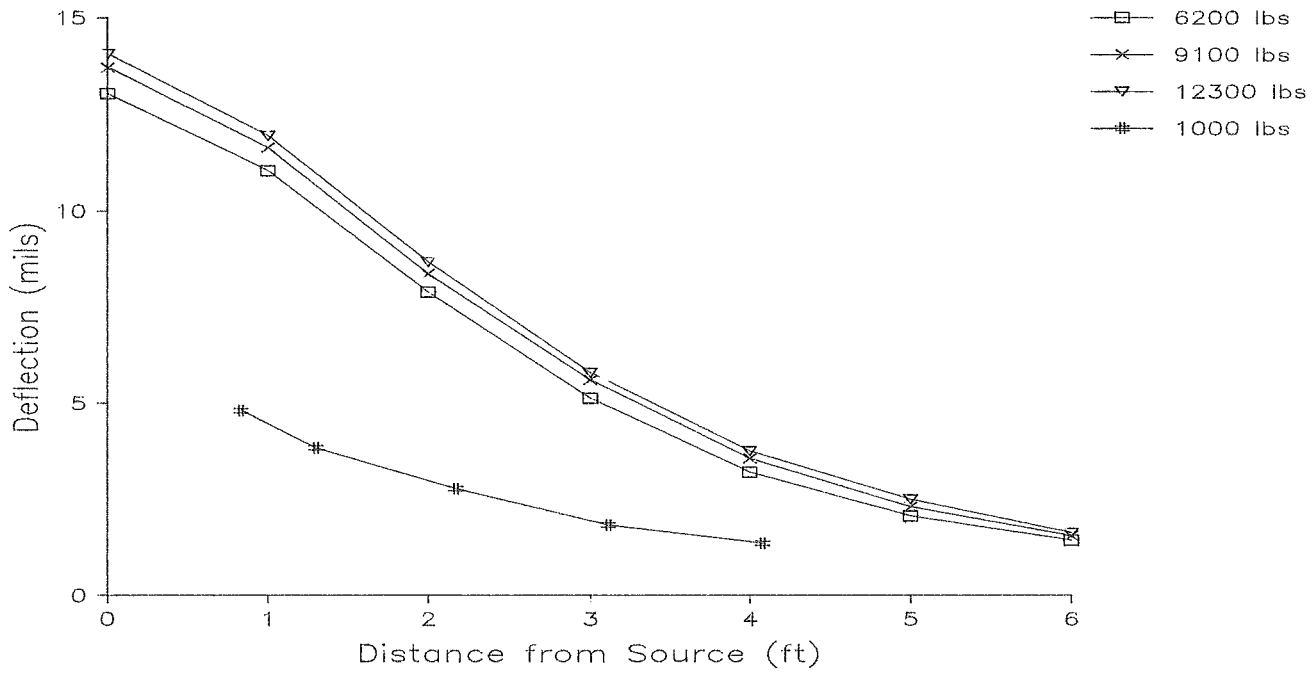


FIGURE A- 40. EQUIVALENT 9000 LB FWD DEFLECTIONS FOR SITE 2 STATION 10

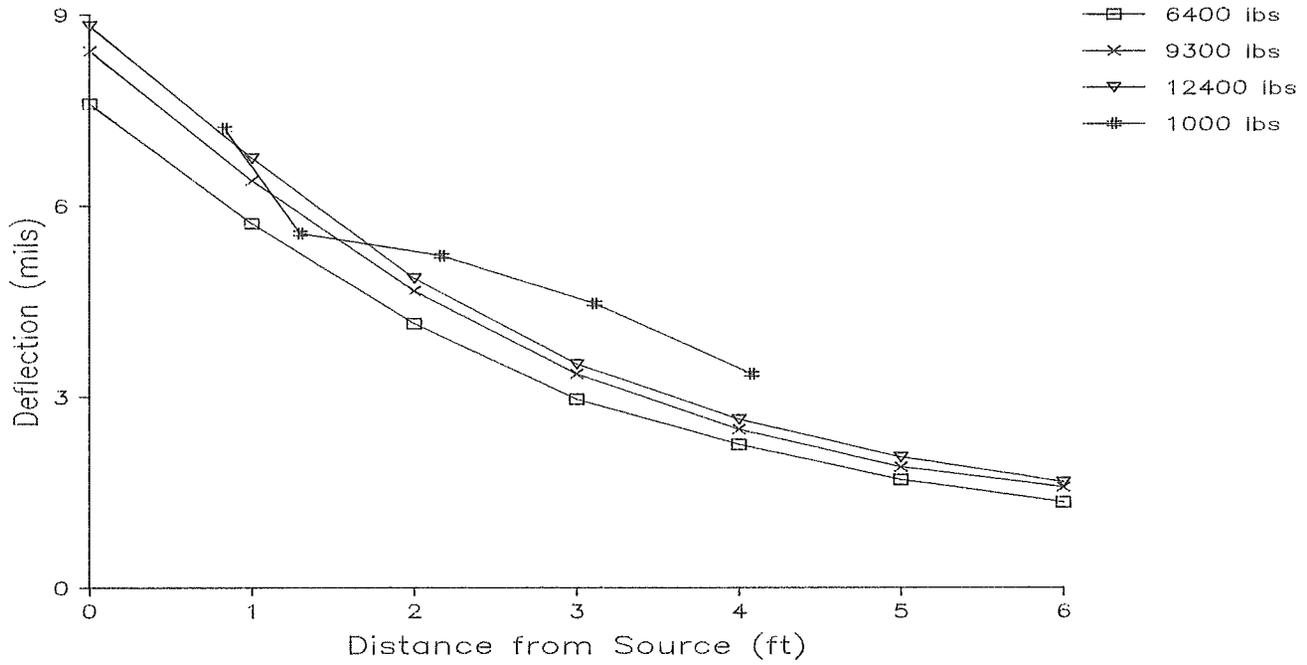


FIGURE A- 41. EQUIVALENT 9000 LB FWD DEFLECTIONS FOR SITE 3 STATION 1

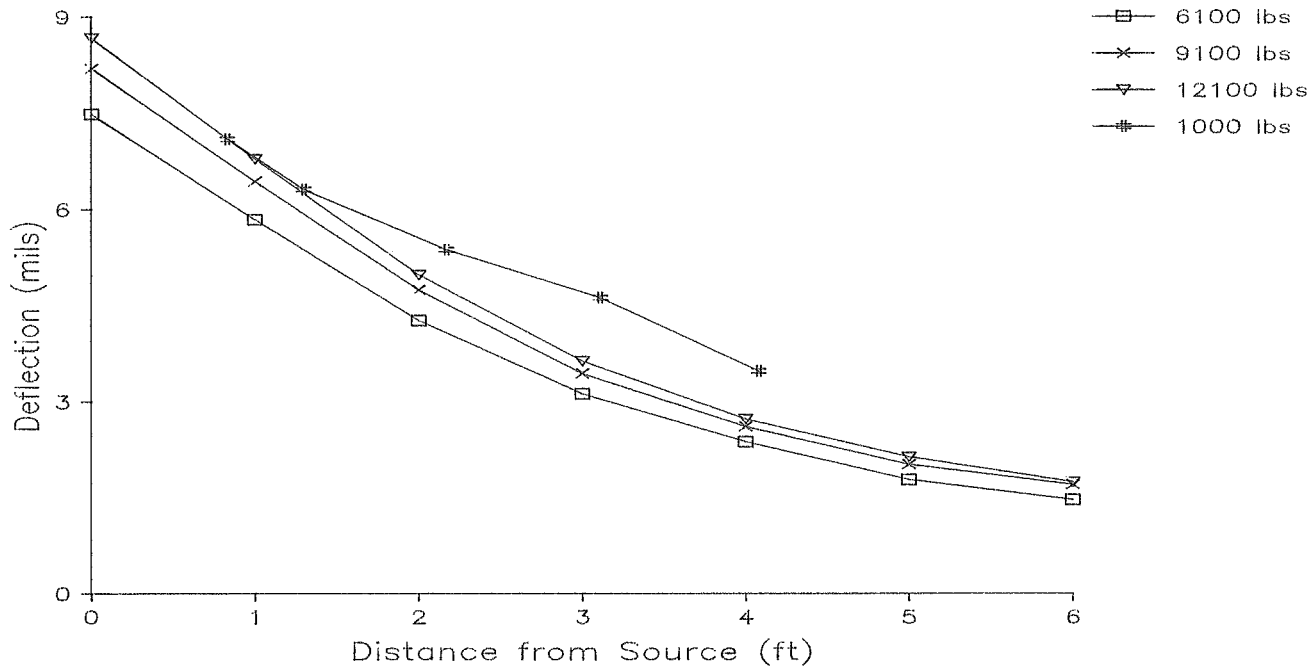


FIGURE A- 42. EQUIVALENT 9000 LB FWD DEFLECTIONS FOR SITE 3 STATION 5

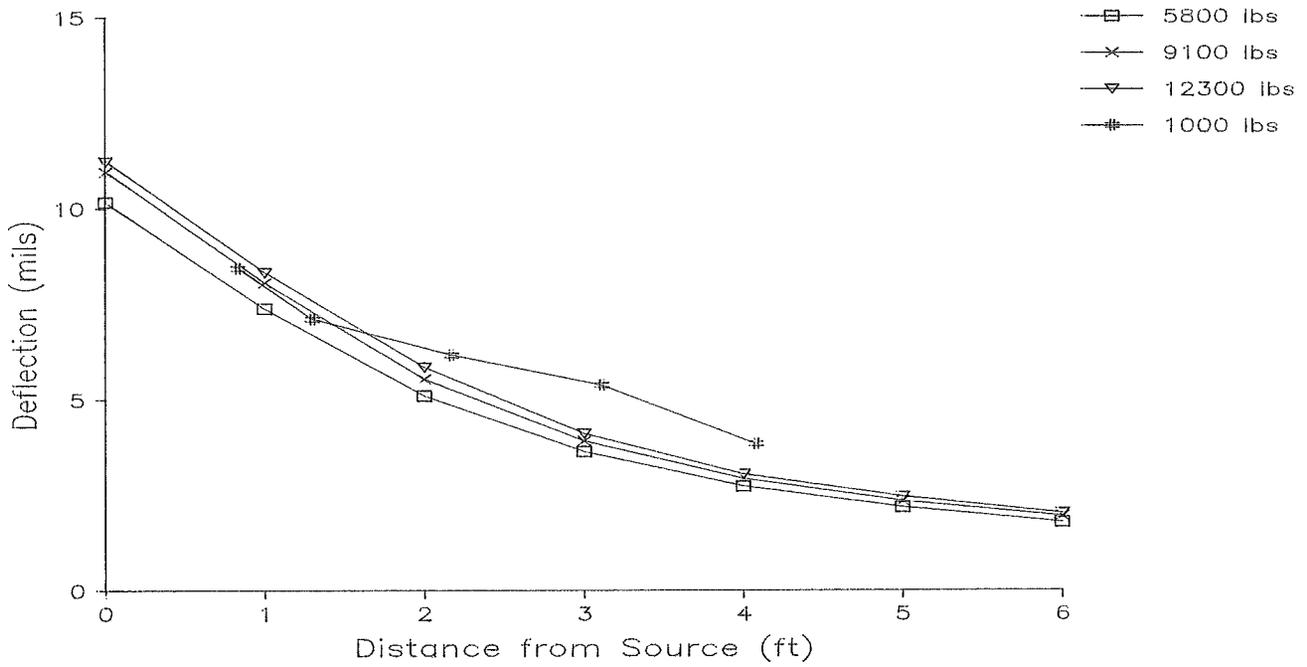


FIGURE A- 43. EQUIVALENT 9000 LB FWD DEFLECTIONS FOR SITE 3 STATION 10

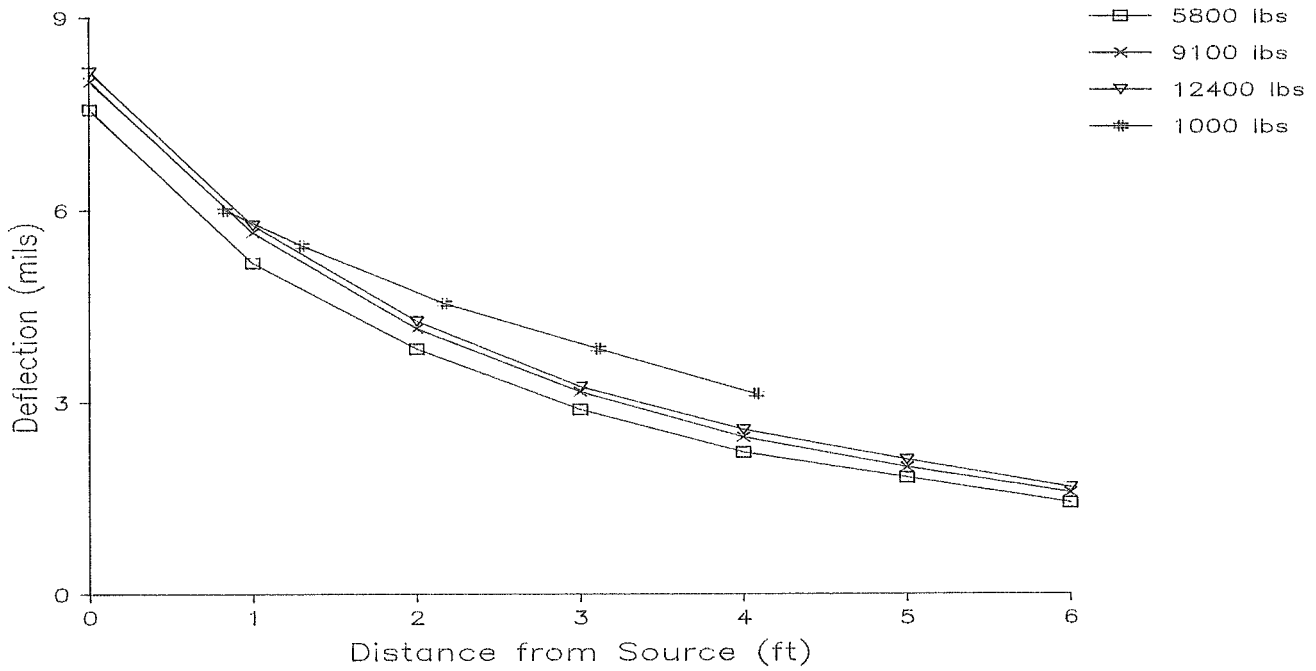


FIGURE A- 44. EQUIVALENT 9000 LB FWD DEFLECTIONS FOR SITE 4 STATION 1

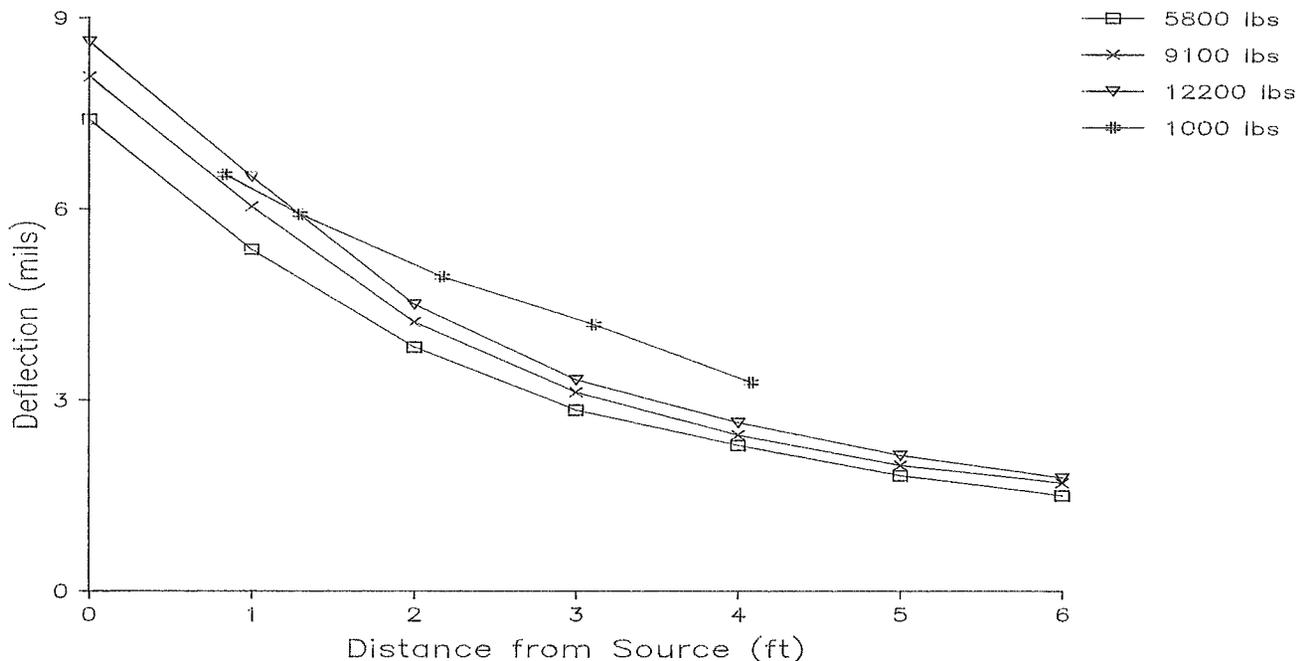


FIGURE A- 45. EQUIVALENT 9000 LB FWD DEFLECTIONS FOR SITE 4 STATION 5

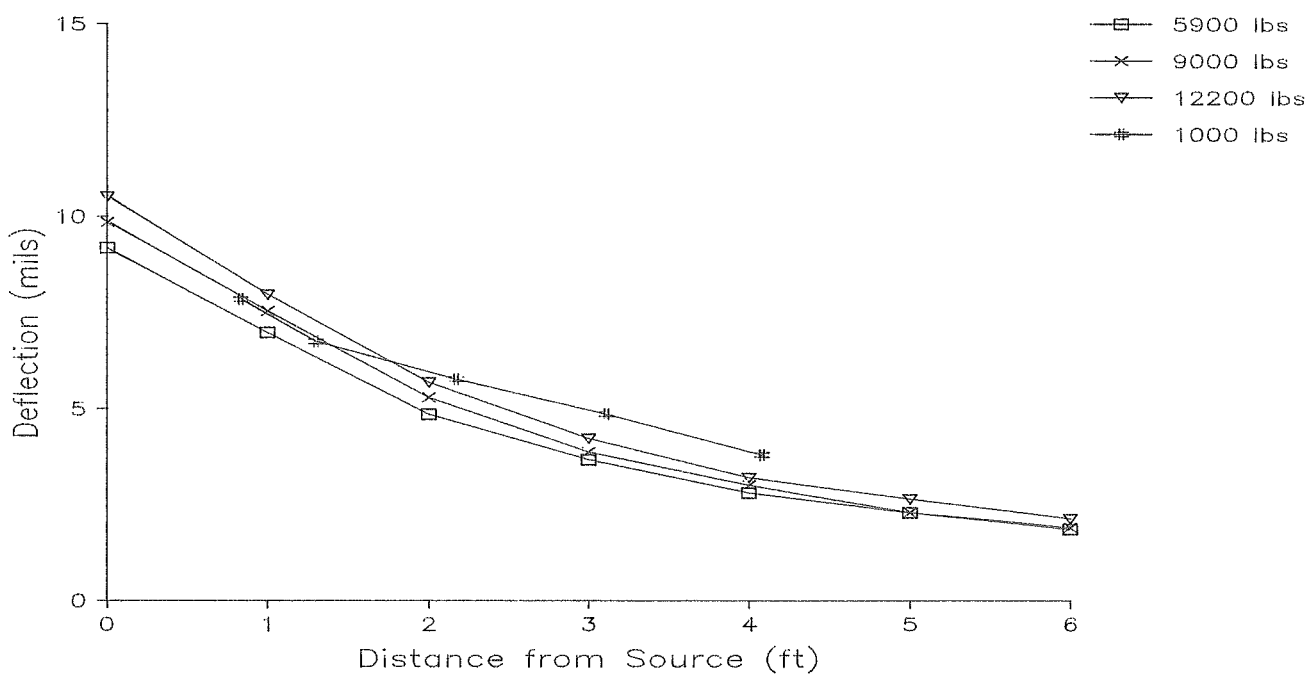


FIGURE A- 46. EQUIVALENT 9000 LB FWD DEFLECTIONS FOR SITE 4 STATION 10

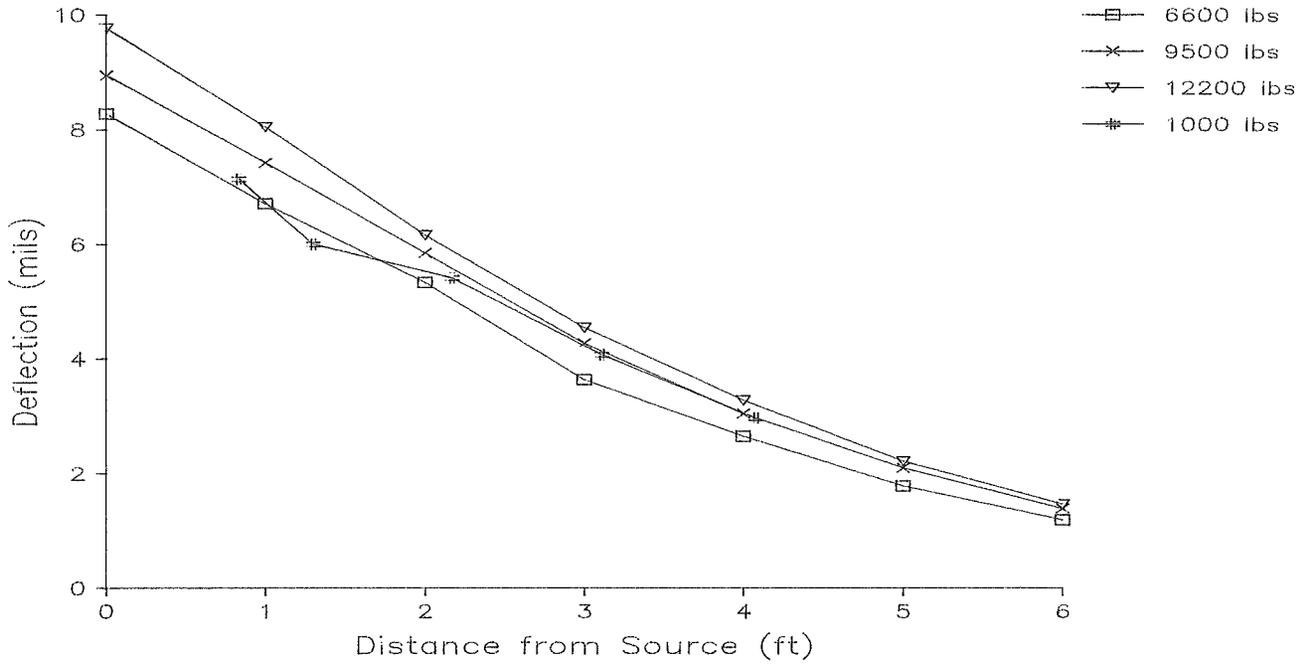


FIGURE A- 47. EQUIVALENT 9000 LB FWD DEFLECTIONS FOR SITE 5 STATION 1

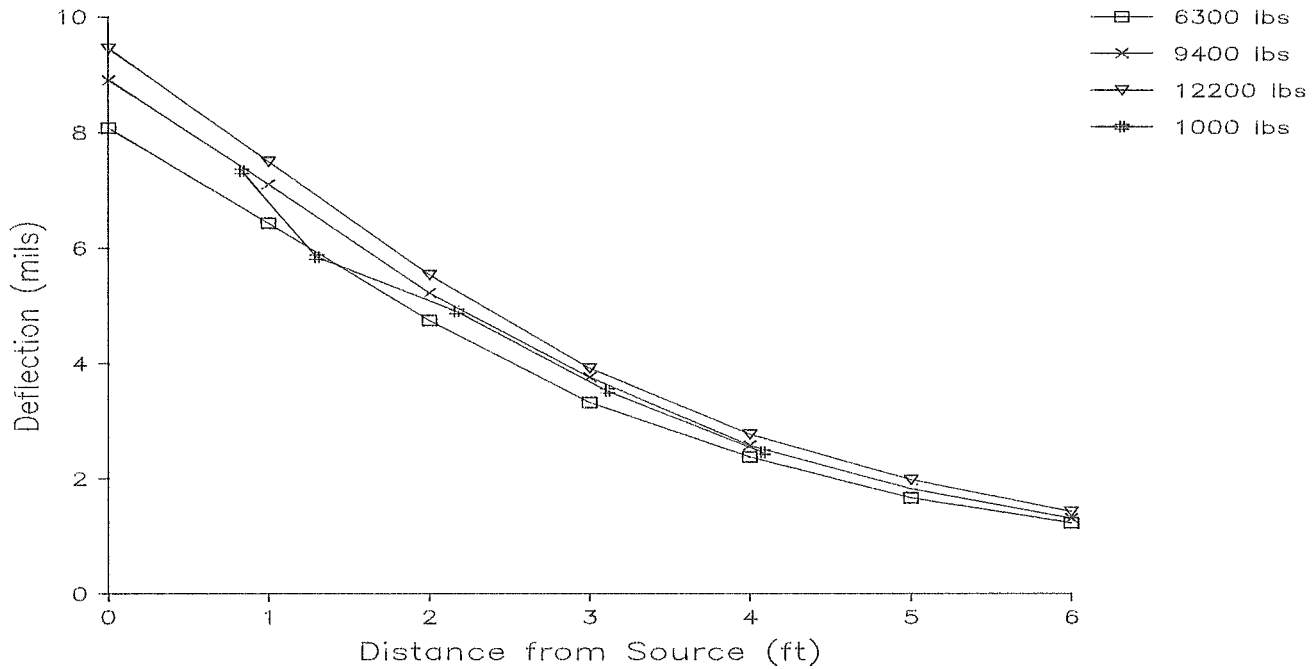


FIGURE A- 48. EQUIVALENT 9000 LB FWD DEFLECTIONS FOR SITE 5 STATION 5

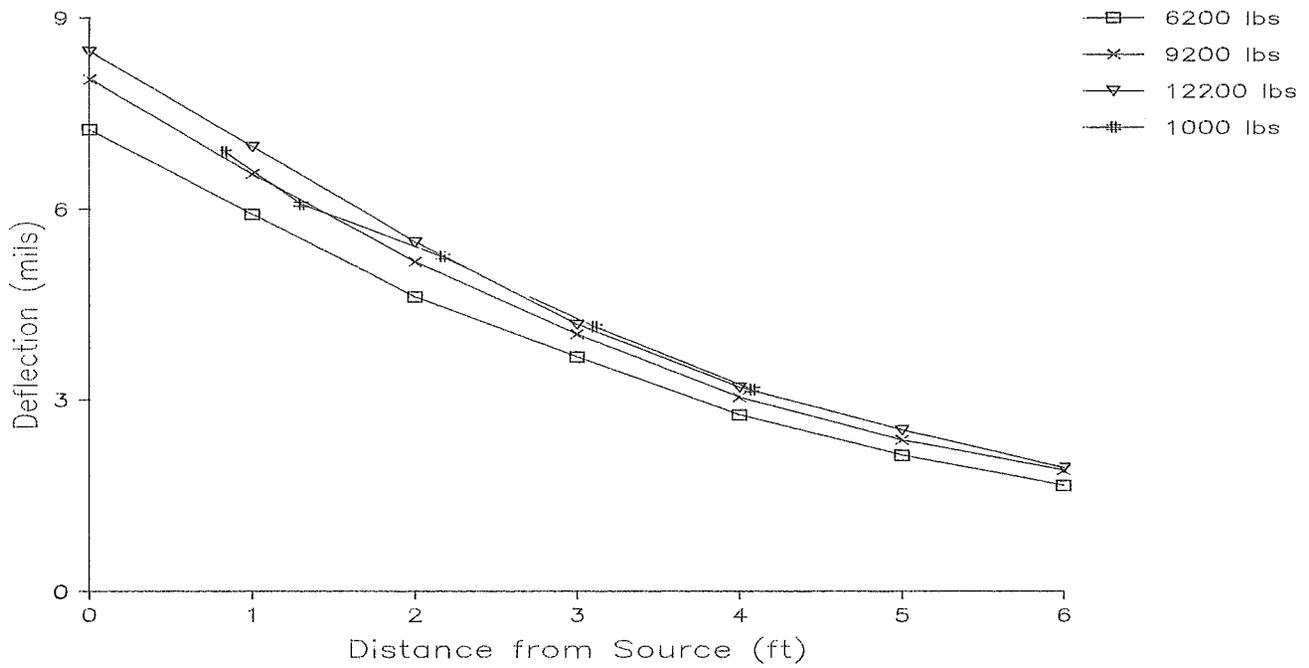


FIGURE A- 49. EQUIVALENT 9000 LB FWD DEFLECTIONS FOR SITE 5 STATION 10

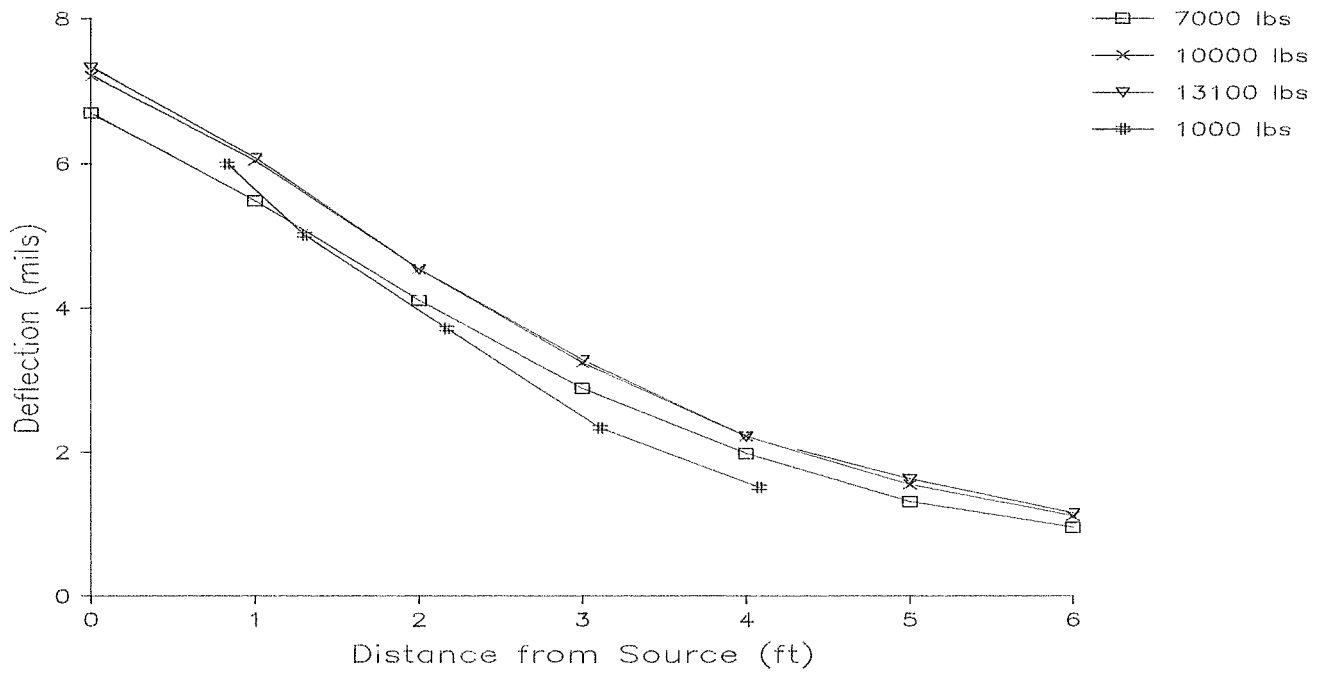


FIGURE A- 50. EQUIVALENT 9000 LB FWD DEFLECTIONS FOR SITE 6 STATION 1

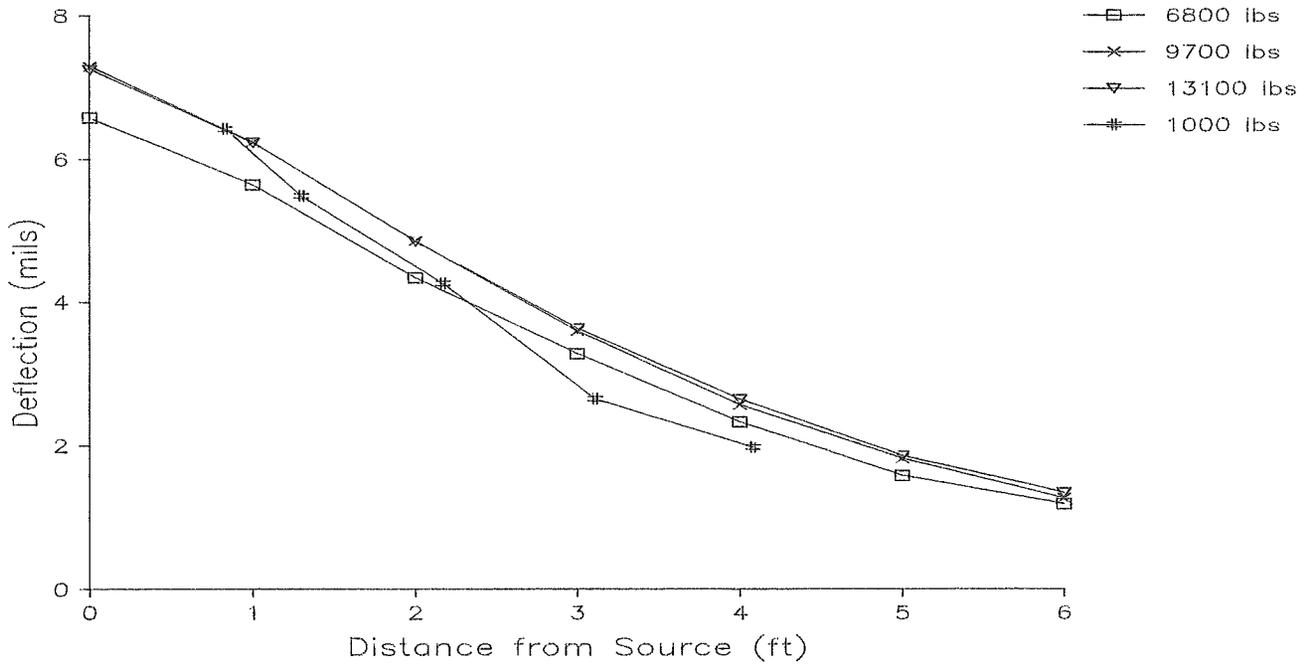


FIGURE A- 51. EQUIVALENT 9000 LB FWD DEFLECTIONS FOR SITE 6 STATION 5

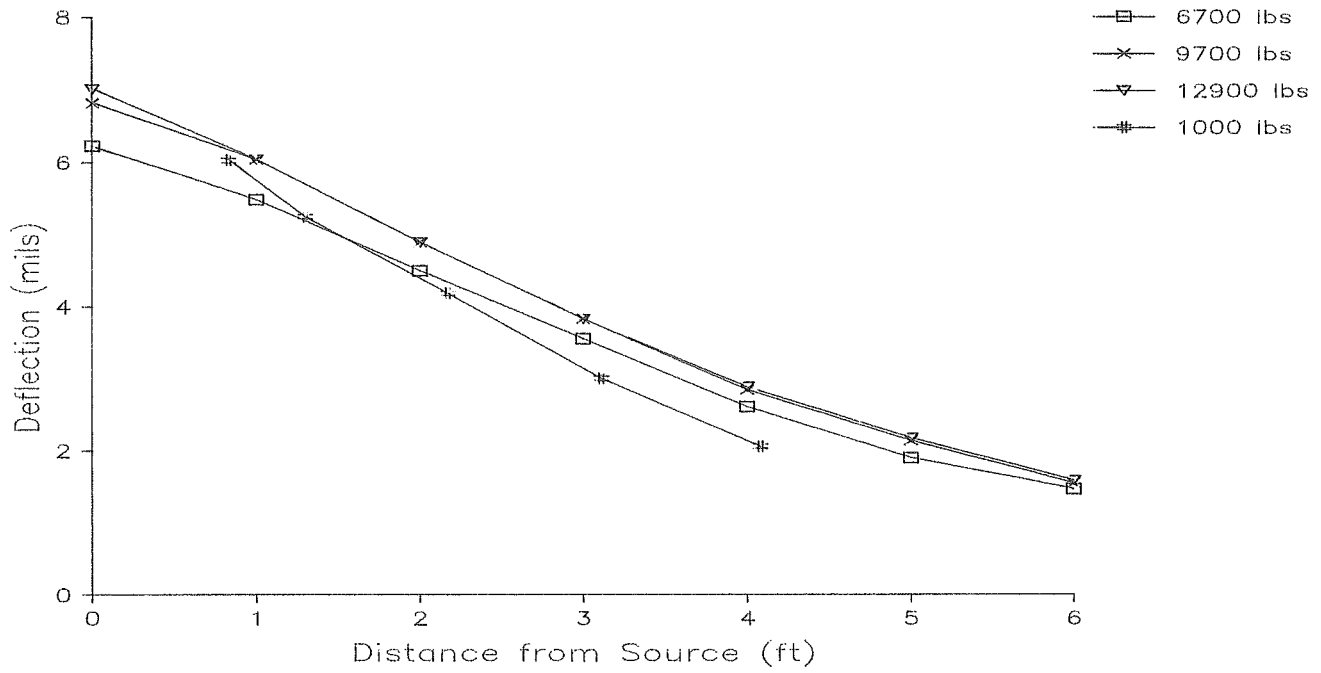


FIGURE A- 52. EQUIVALENT 9000 LB FWD DEFLECTIONS FOR SITE 6 STATION 10

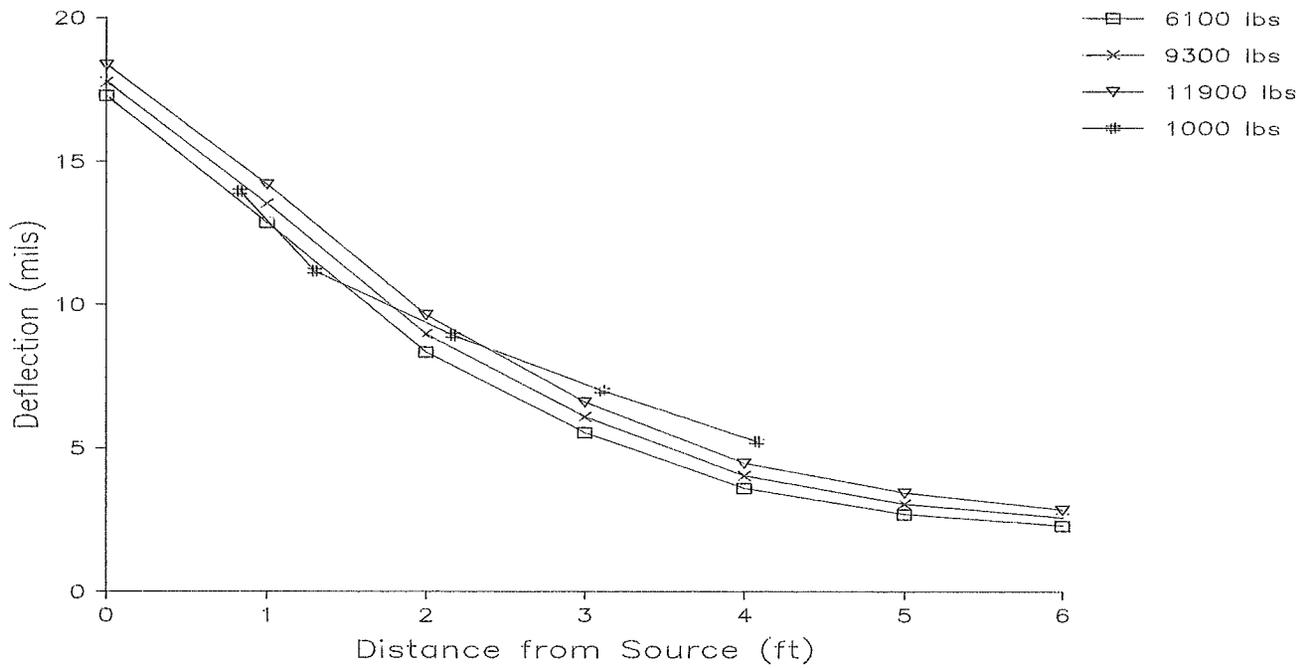


FIGURE A- 53. EQUIVALENT 9000 LB FWD DEFLECTIONS FOR SITE 7 STATION 1

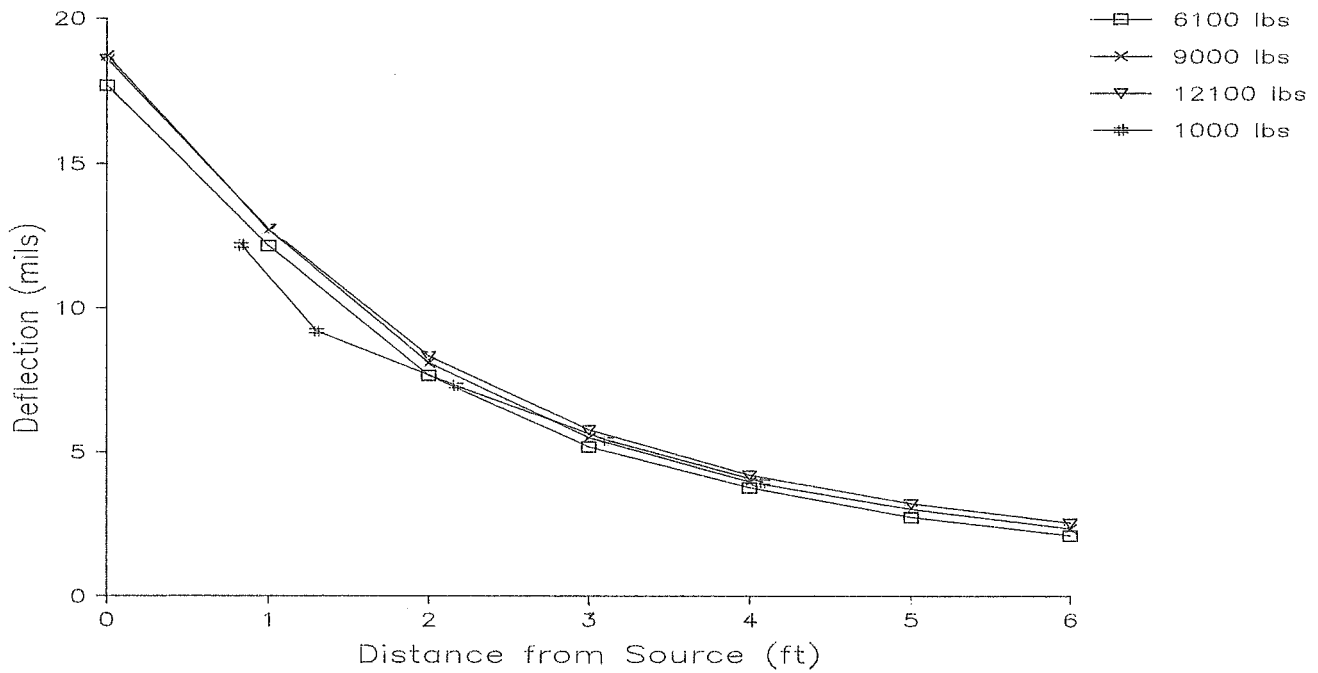


FIGURE A- 54. EQUIVALENT 9000 LB FWD DEFLECTIONS FOR SITE 7 STATION 5

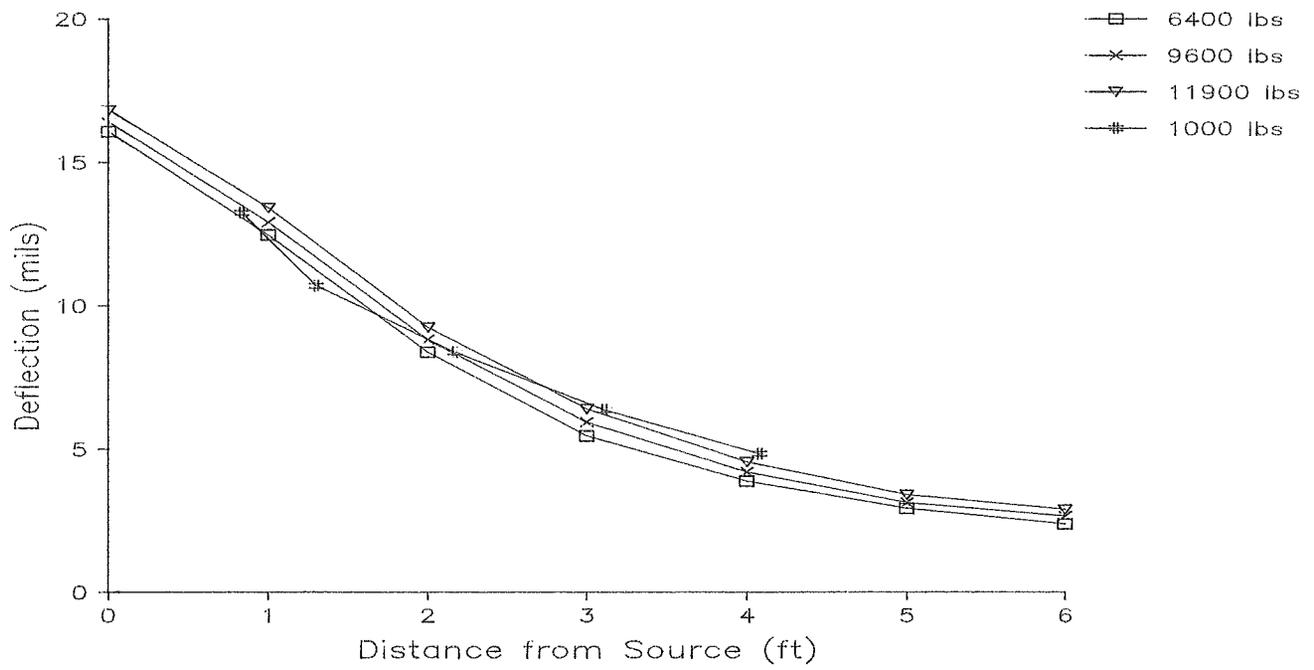


FIGURE A- 55. EQUIVALENT 9000 LB FWD DEFLECTIONS FOR SITE 7 STATION 10

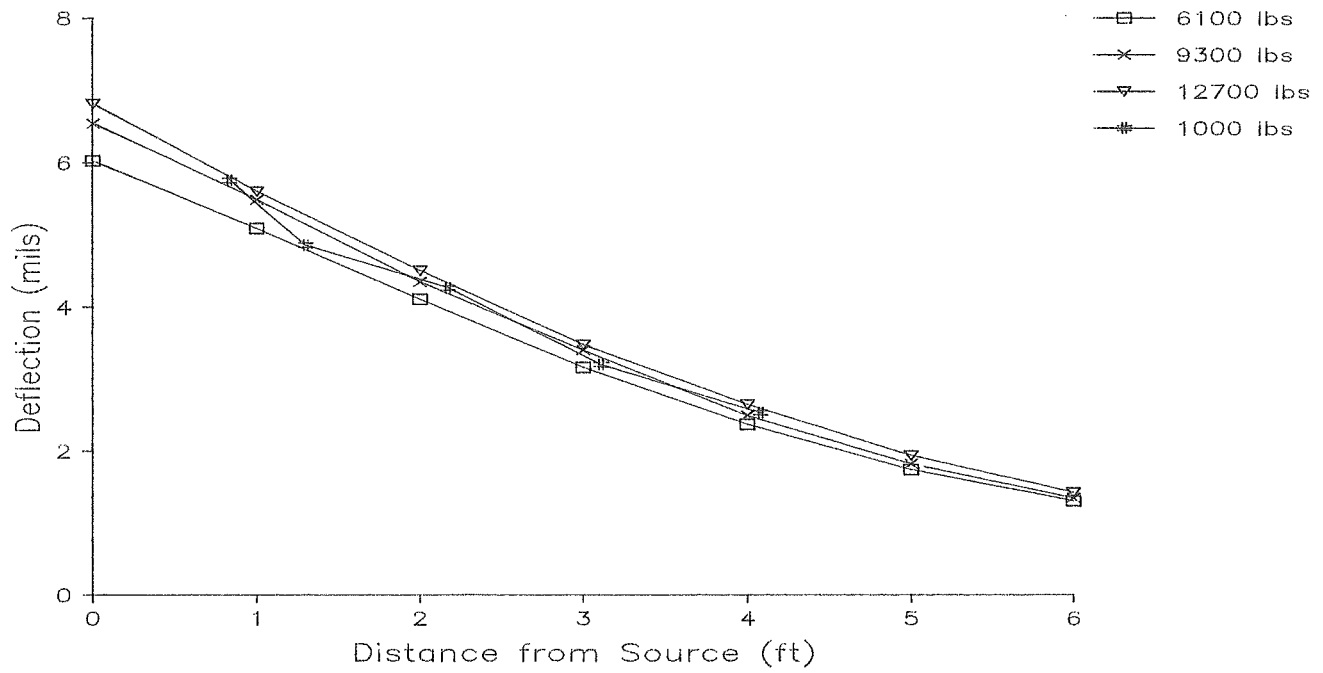


FIGURE A- 56. EQUIVALENT 9000 LB FWD DEFLECTIONS FOR SITE 8 STATION 1

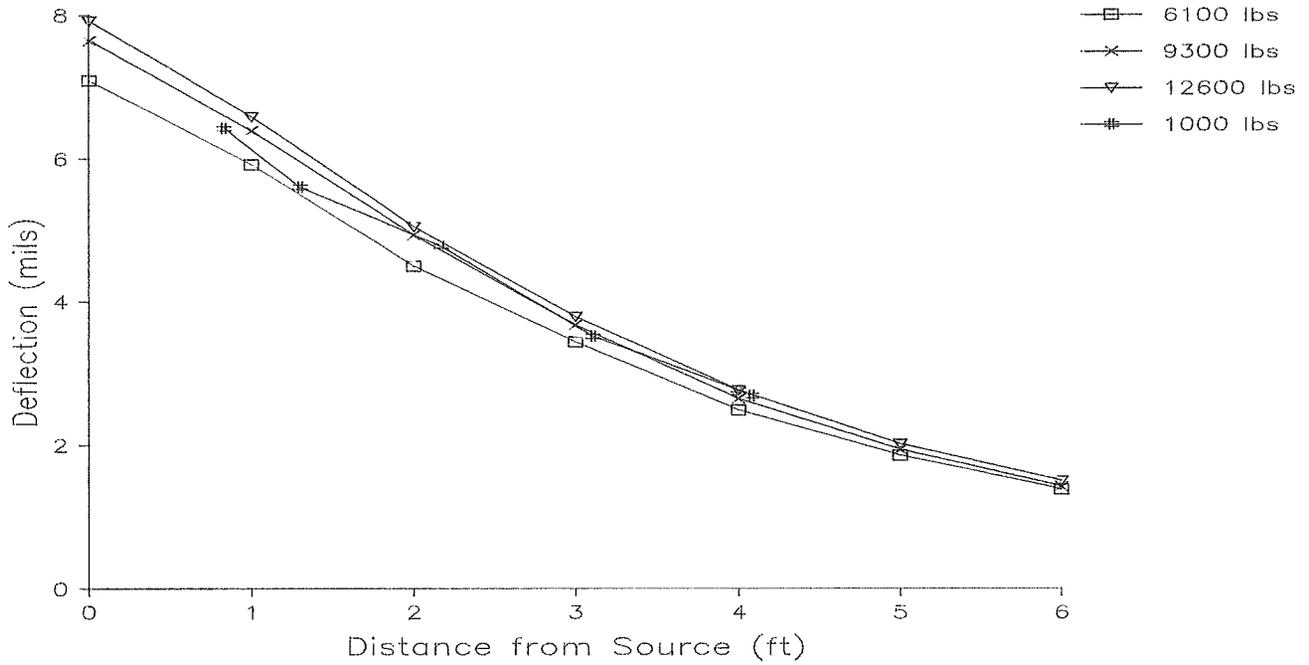


FIGURE A- 57. EQUIVALENT 9000 LB FWD DEFLECTIONS FOR SITE 8 STATION 5

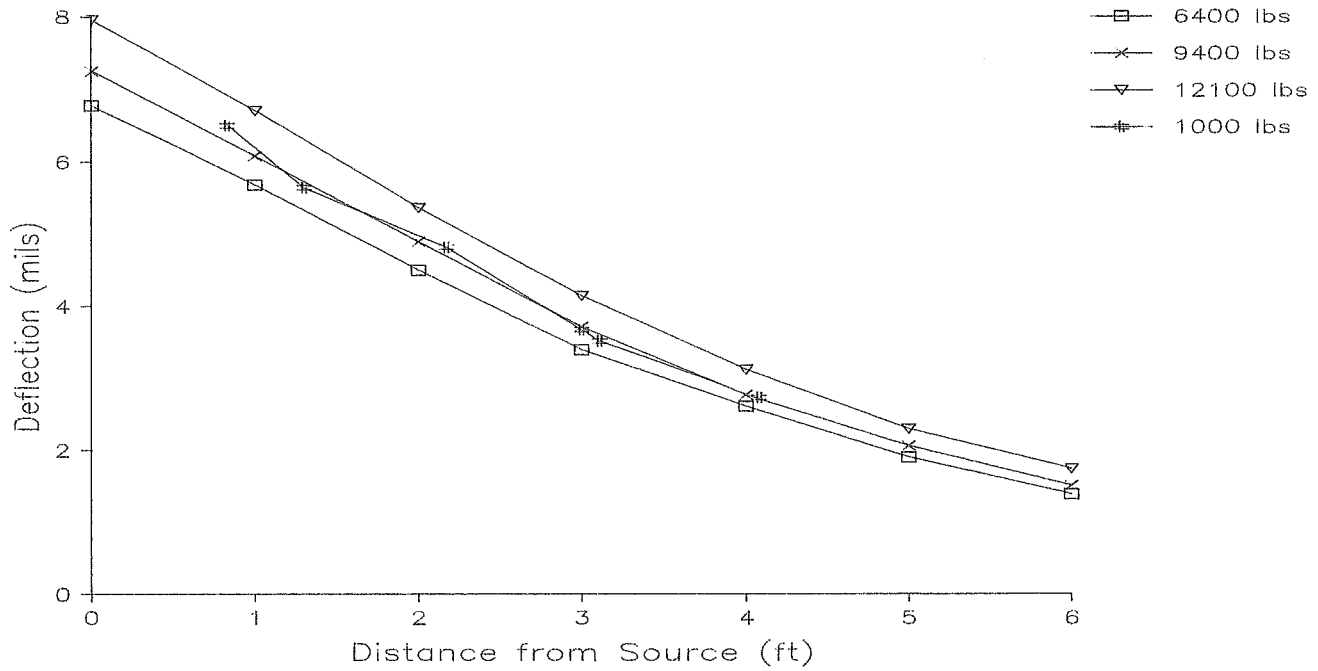


FIGURE A- 58. EQUIVALENT 9000 LB FWD DEFLECTIONS FOR SITE 8 STATION 10

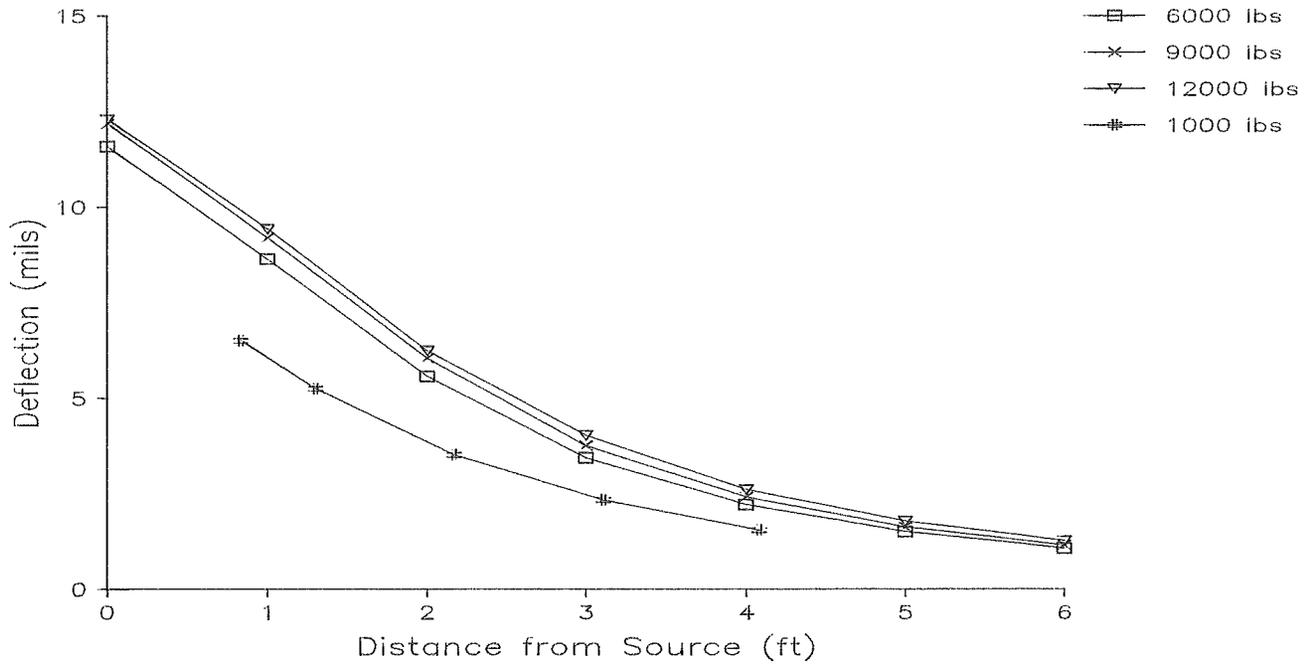


FIGURE A- 59. EQUIVALENT 9000 LB FWD DEFLECTIONS FOR SITE 9 STATION 1

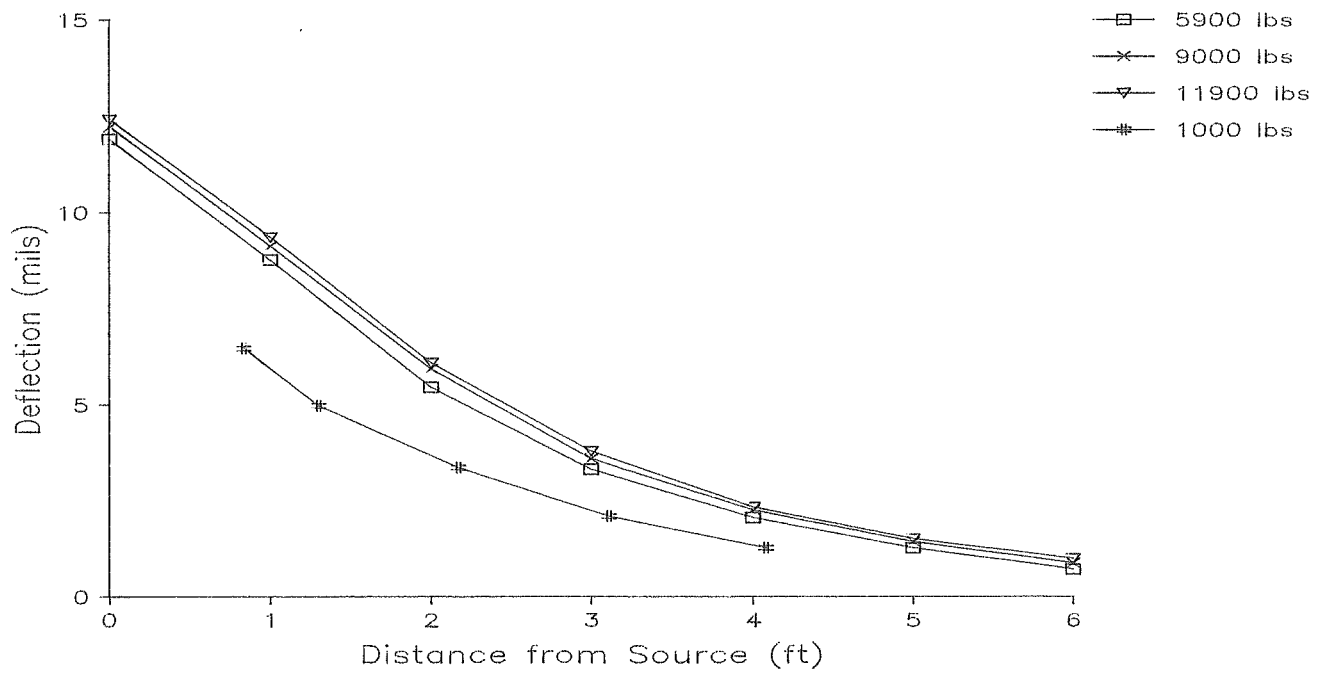


FIGURE A- 60. EQUIVALENT 9000 LB FWD DEFLECTIONS FOR SITE 9 STATION 5

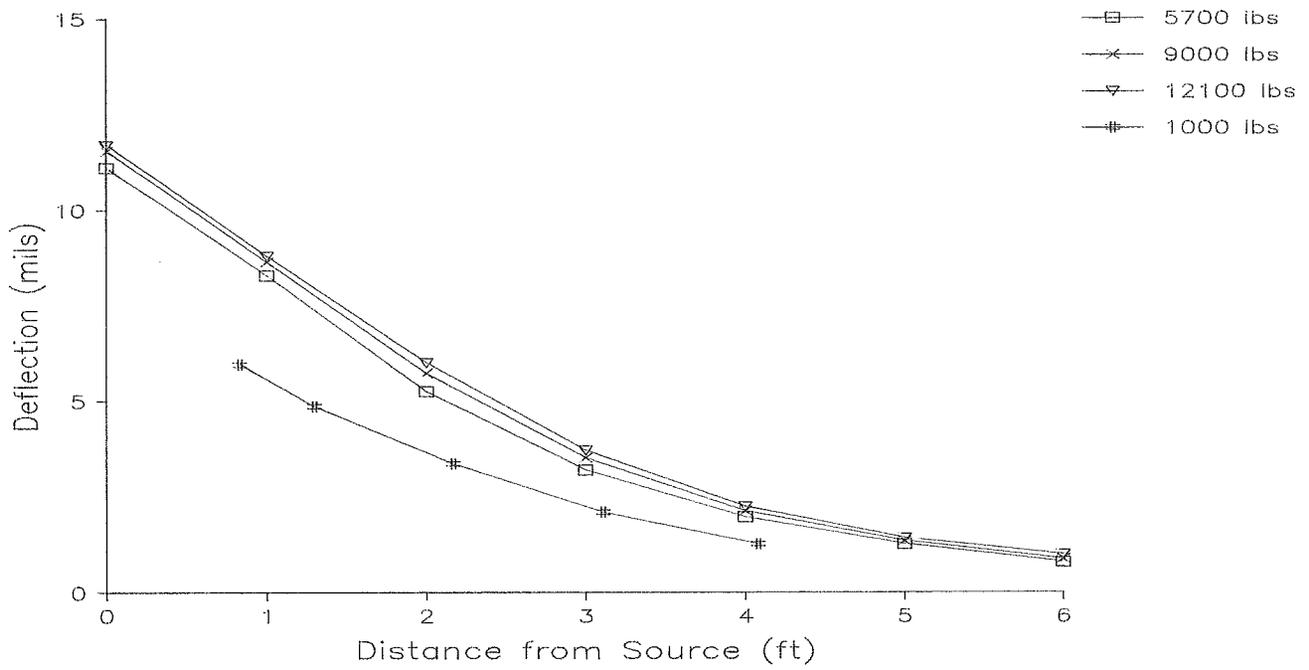


FIGURE A- 61. EQUIVALENT 9000 LB FWD DEFLECTIONS FOR SITE 9 STATION 10

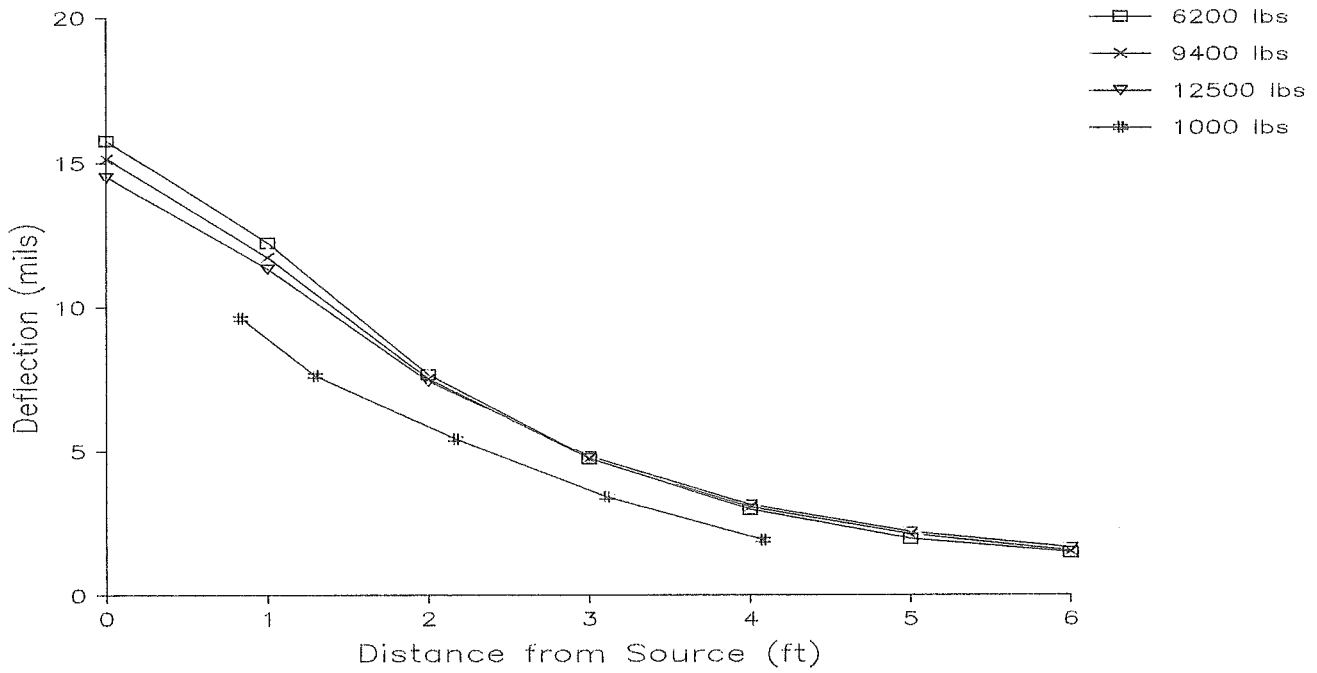


FIGURE A- 62. EQUIVALENT 9000 LB FWD DEFLECTIONS FOR SITE 10 STATION 1

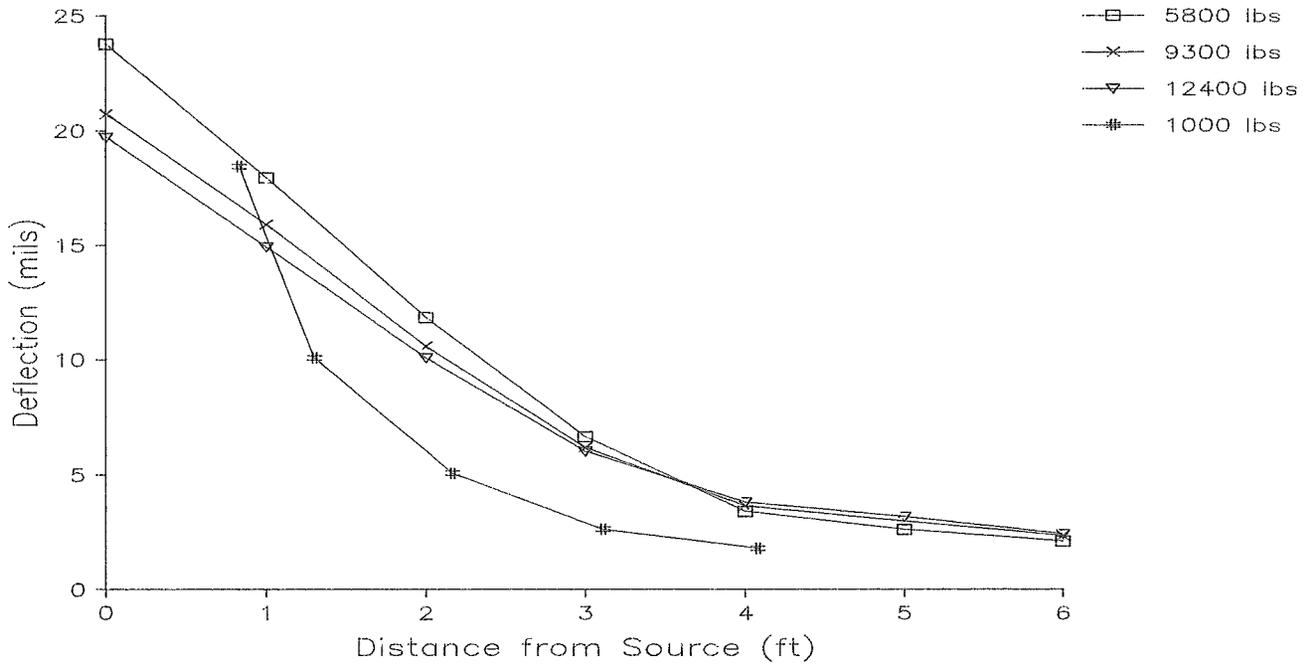


FIGURE A- 63. EQUIVALENT 9000 LB FWD DEFLECTIONS FOR SITE 10 STATION 5

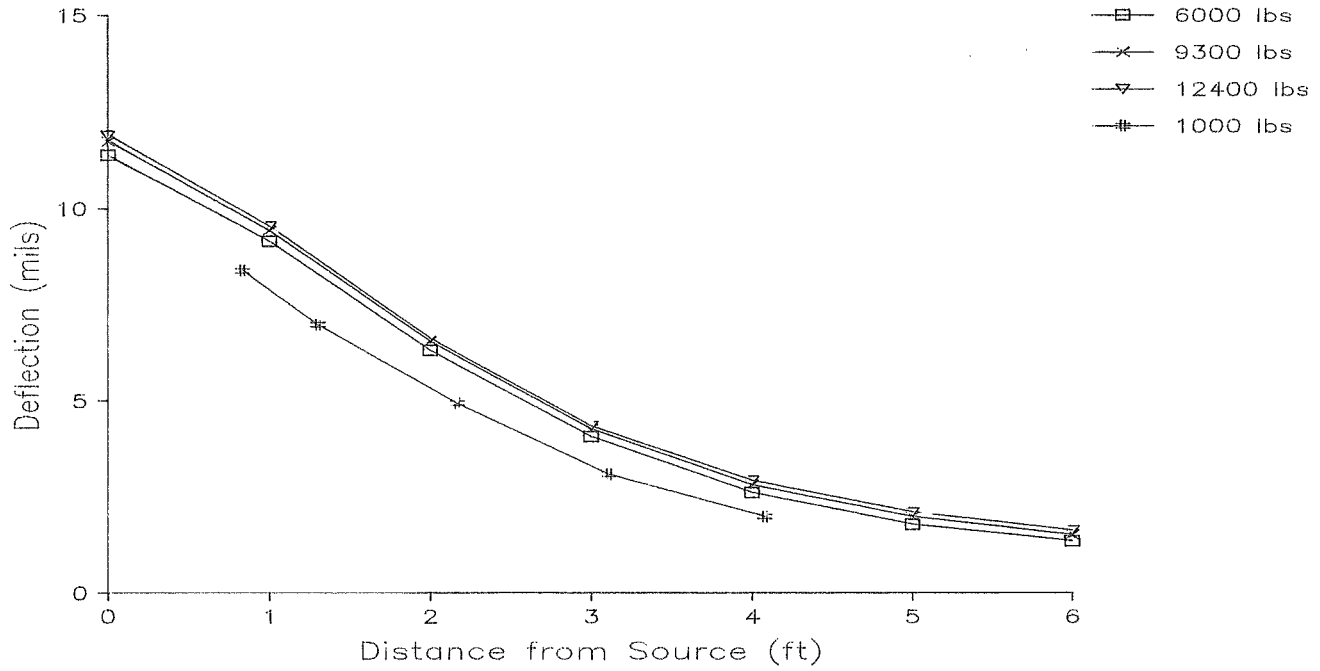


FIGURE A- 64. EQUIVALENT 9000 LB FWD DEFLECTIONS FOR SITE 10 STATION 10

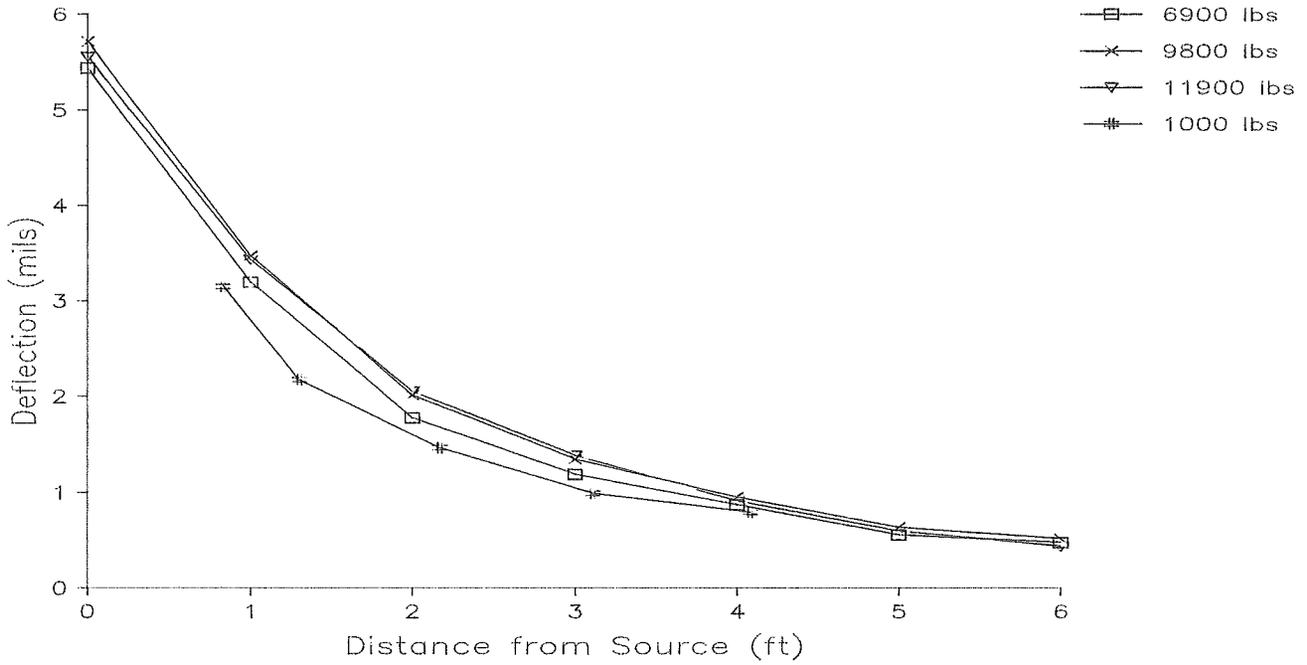


FIGURE A- 65. EQUIVALENT 9000 LB FWD DEFLECTIONS FOR SITE 11 STATION 1

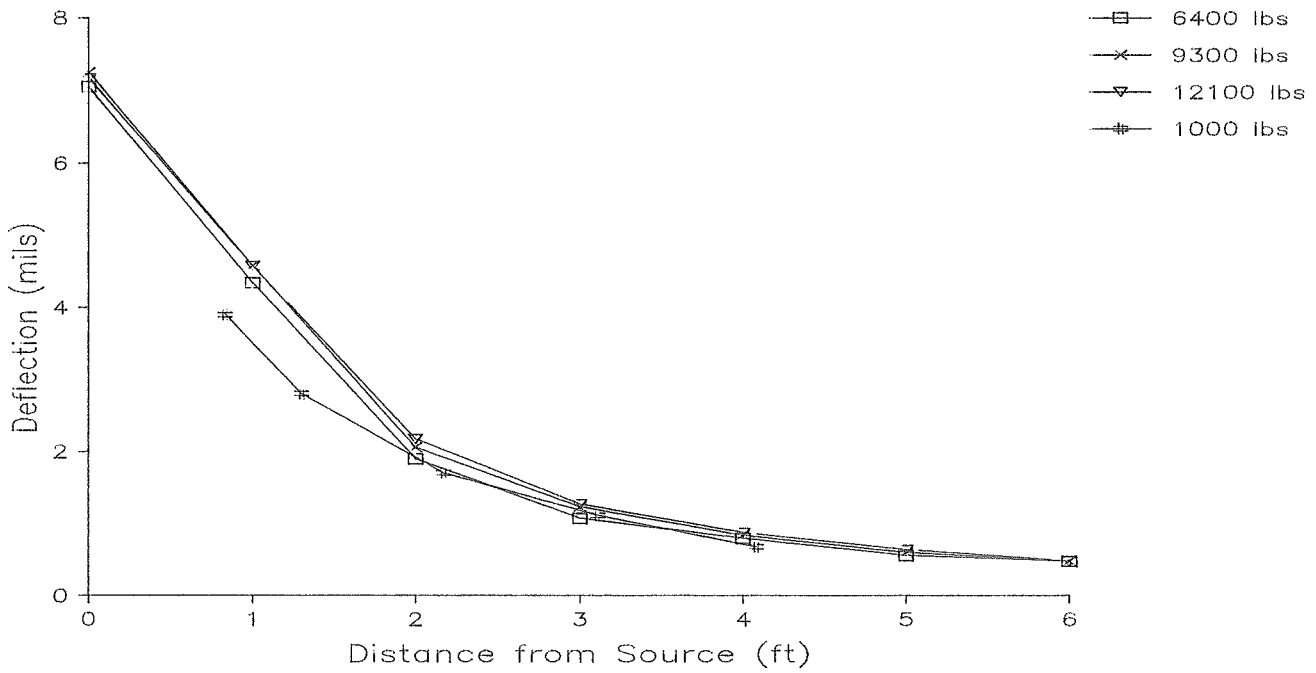


FIGURE A- 66. EQUIVALENT 9000 LB FWD DEFLECTIONS FOR SITE 11 STATION 5

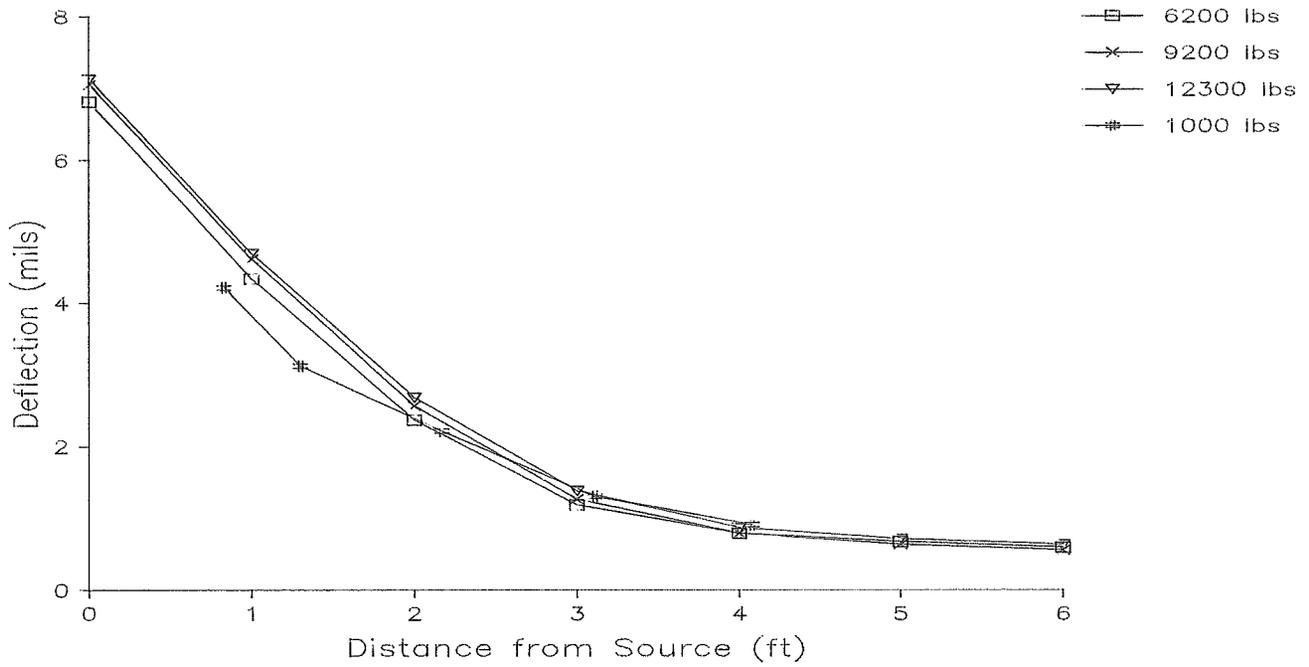


FIGURE A- 67. EQUIVALENT 9000 LB FWD DEFLECTIONS FOR SITE 11 STATION 10

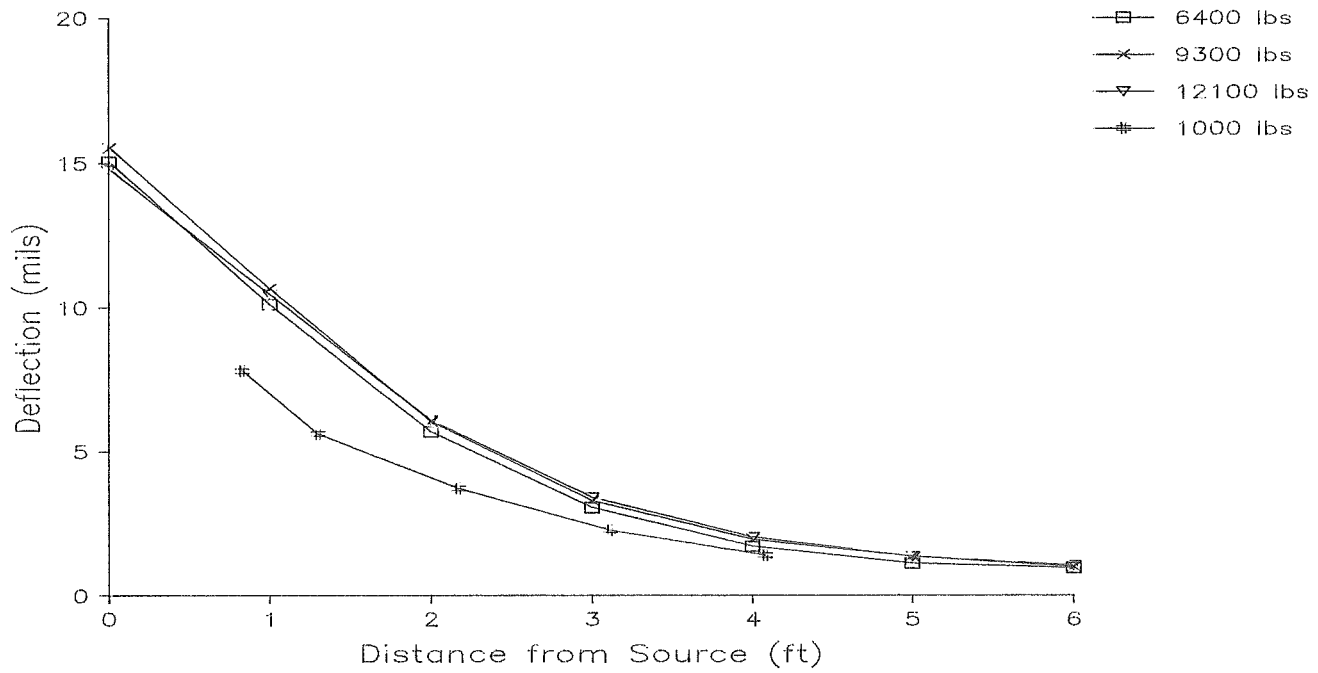


FIGURE A- 68. EQUIVALENT 9000 LB FWD DEFLECTIONS FOR SITE 12 STATION 1

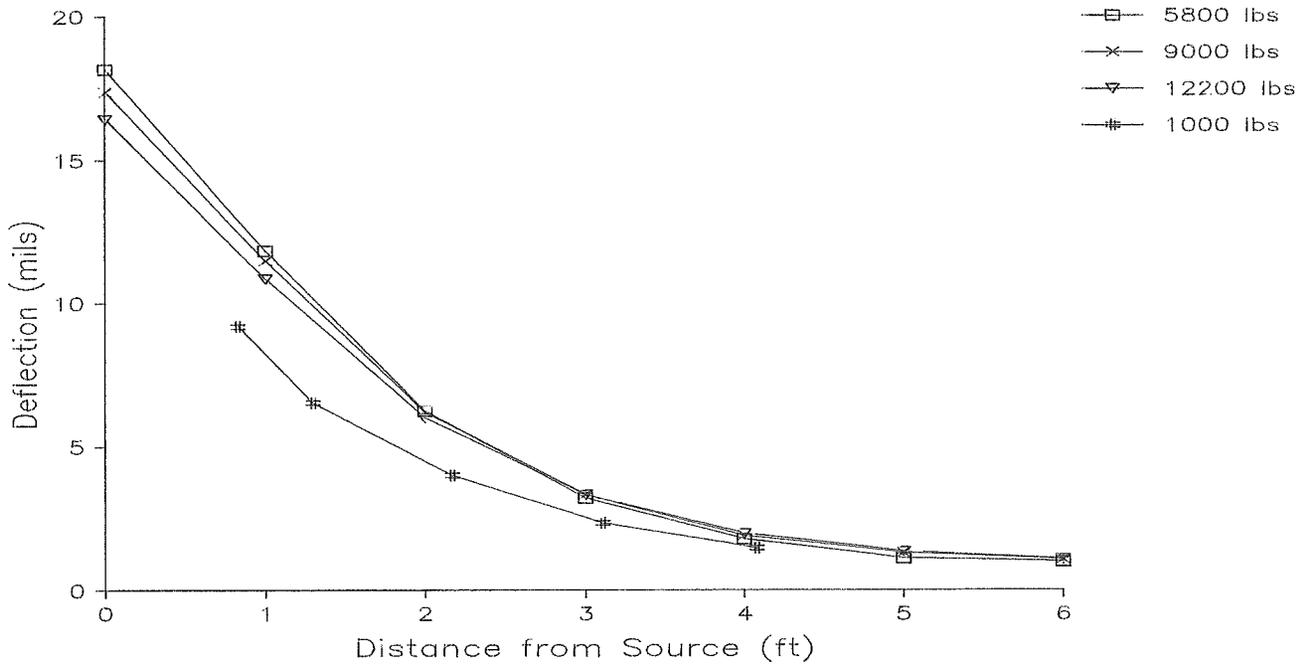


FIGURE A- 69. EQUIVALENT 9000 LB FWD DEFLECTIONS FOR SITE 12 STATION 5

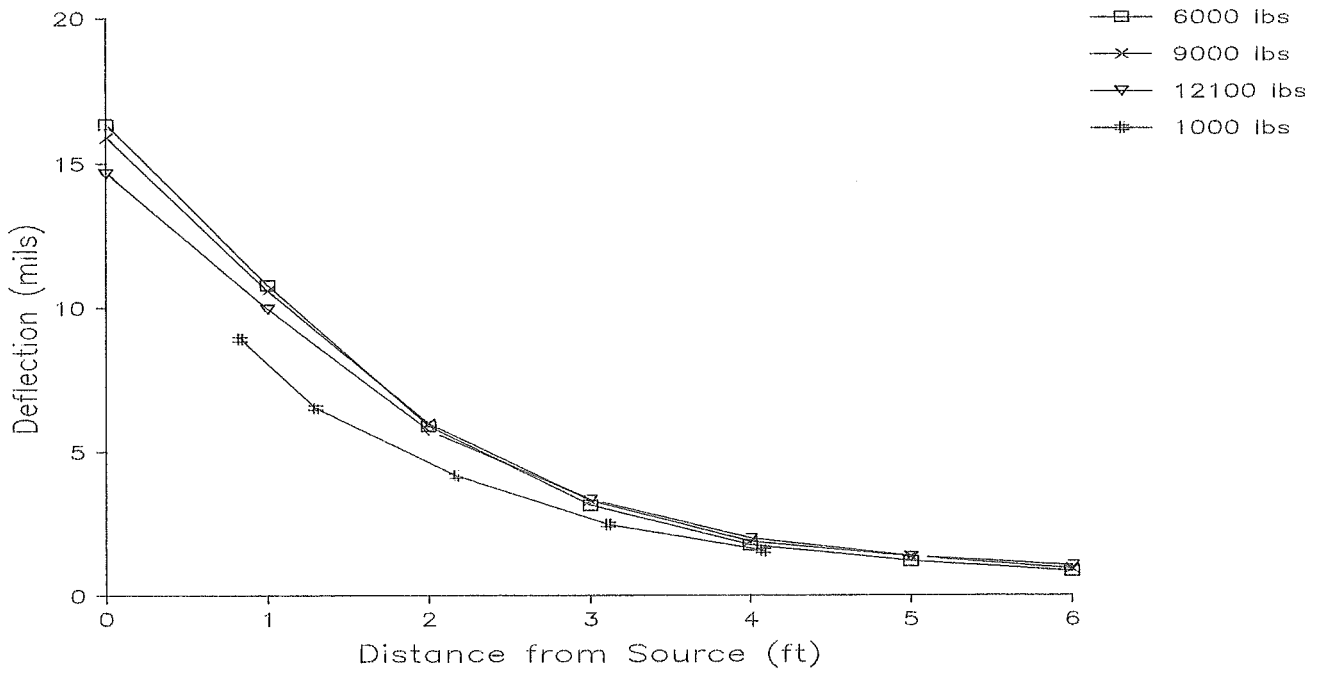


FIGURE A- 70. EQUIVALENT 9000 LB FWD DEFLECTIONS FOR SITE 12 STATION 10

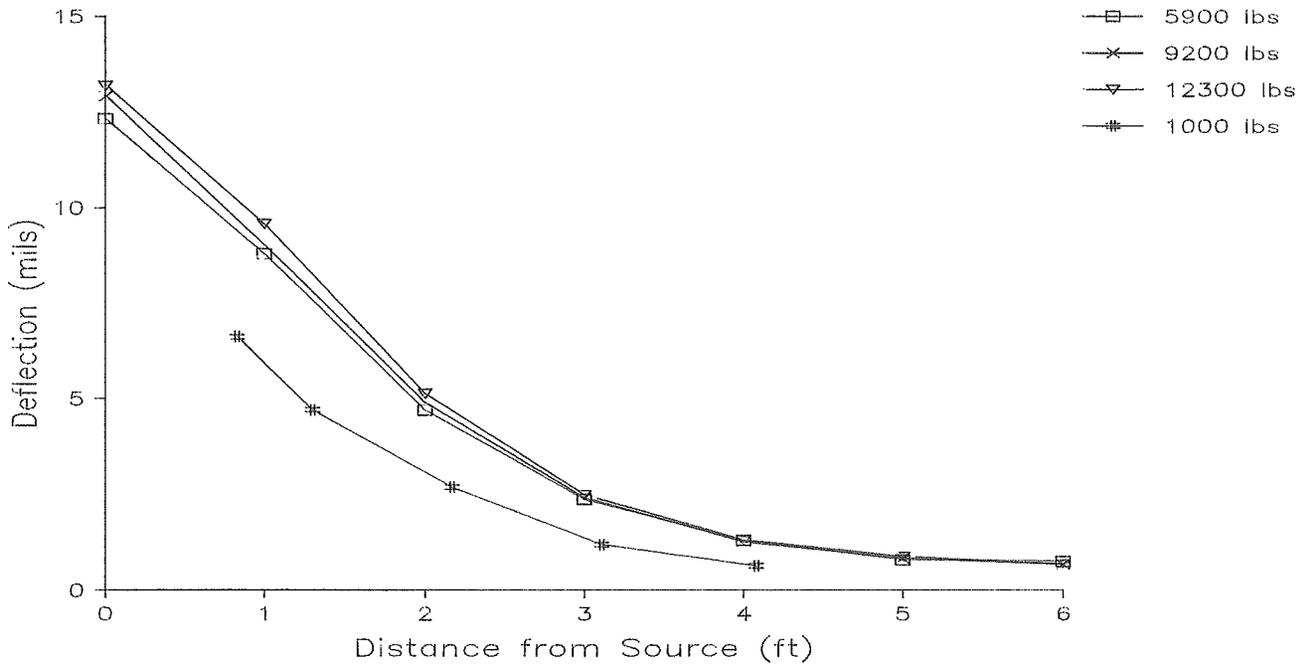


FIGURE A- 71. EQUIVALENT 9000 LB FWD DEFLECTIONS FOR SITE 13 STATION 1

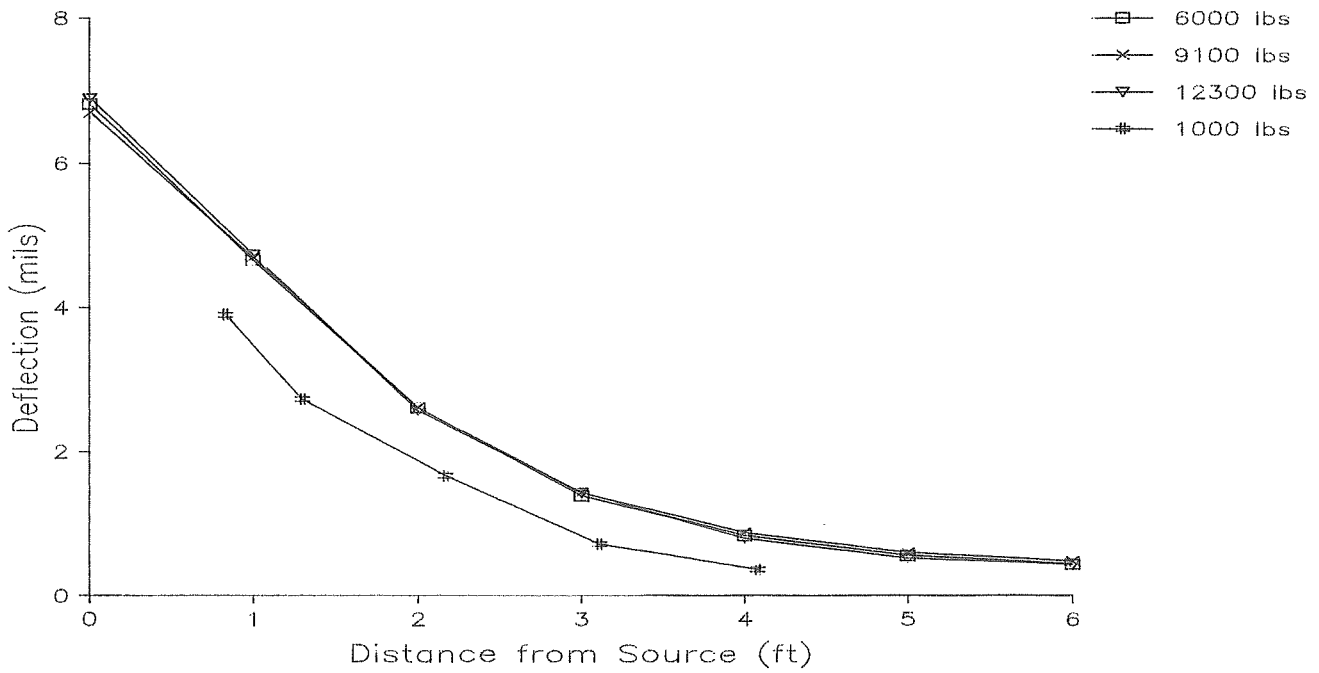


FIGURE A- 72. EQUIVALENT 9000 LB FWD DEFLECTIONS FOR SITE 13 STATION 5

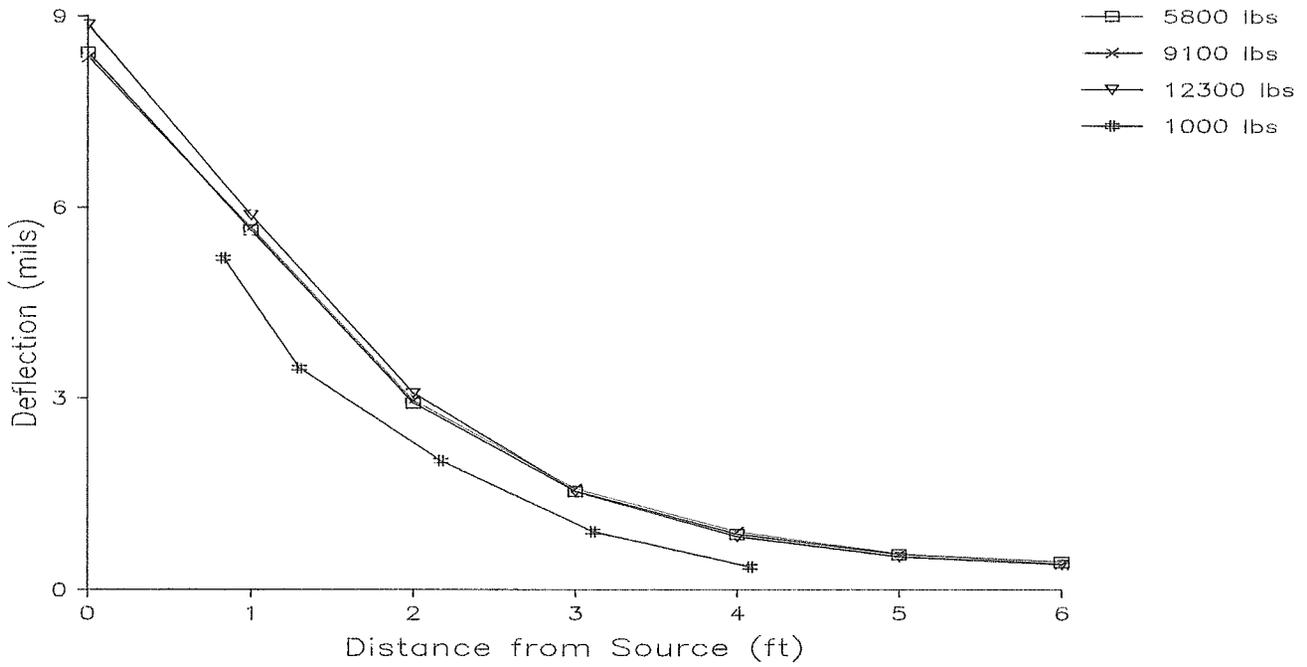


FIGURE A- 73. EQUIVALENT 9000 LB FWD DEFLECTIONS FOR SITE 13 STATION 10

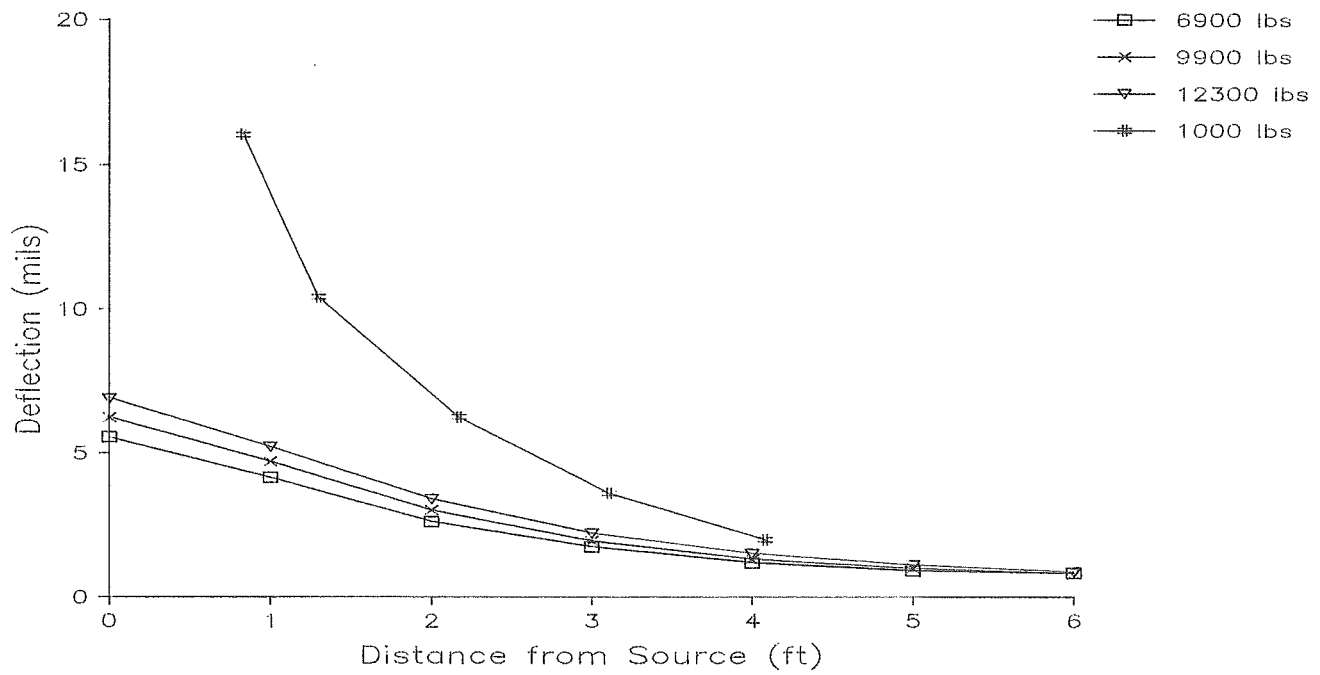


FIGURE A- 74. EQUIVALENT 9000 LB FWD DEFLECTIONS FOR SITE 15 STATION 1

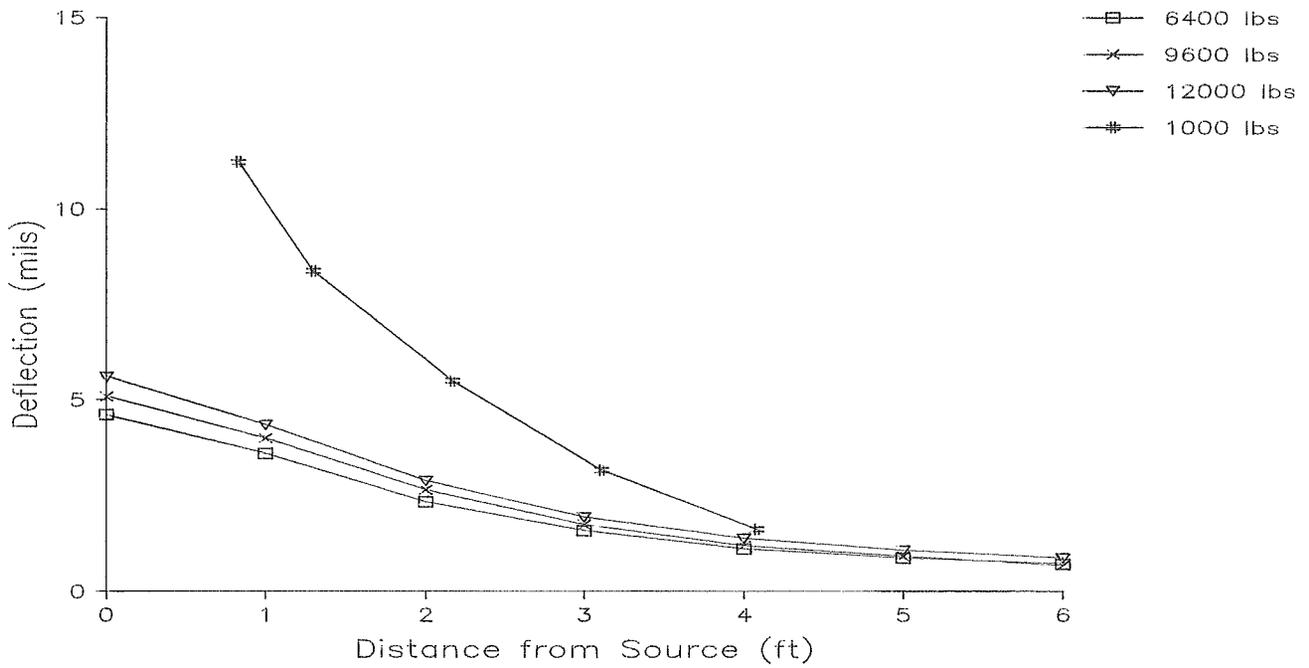


FIGURE A- 75. EQUIVALENT 9000 LB FWD DEFLECTIONS FOR SITE 15 STATION 5

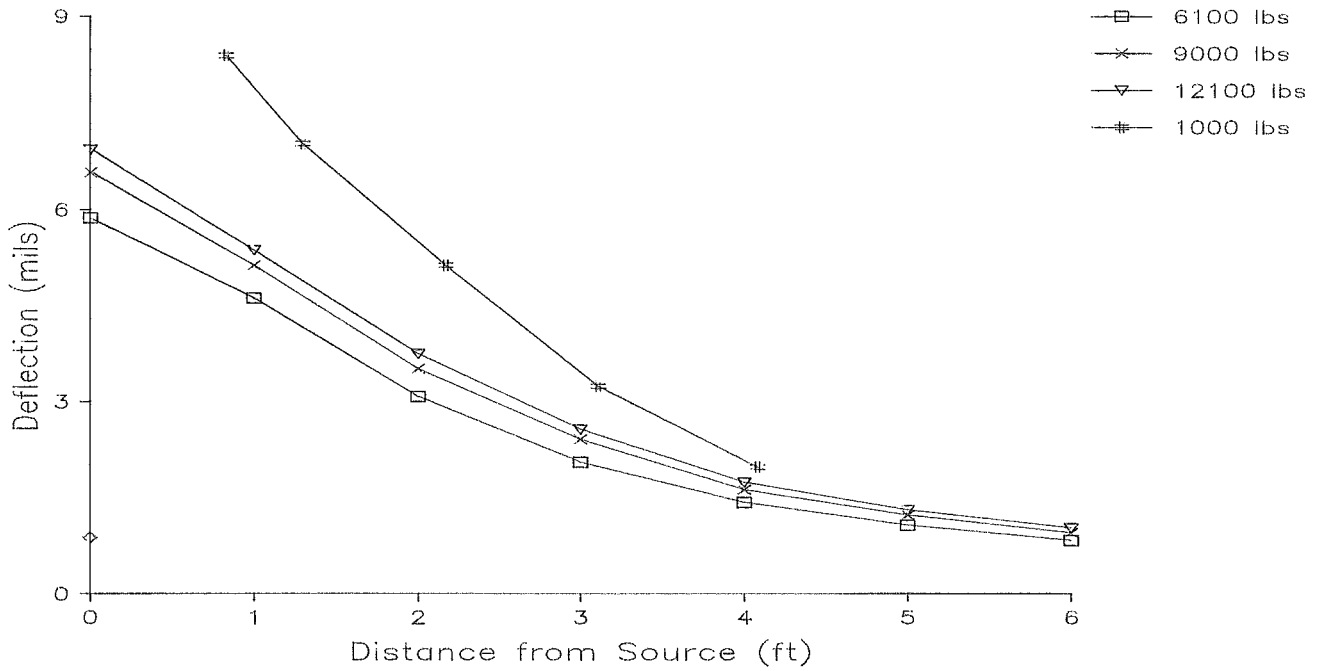


FIGURE A- 76. EQUIVALENT 9000 LB FWD DEFLECTIONS FOR SITE 15 STATION 10

APPENDIX B

TEST DRILLING EQUIPMENT AND PROCEDURES

DRILLING EQUIPMENT

Foree and Vann Geotechnical Inc. uses a 1986 model CME-55 drill capable of auger drilling to depths of 250 ft in tenacious southwestern soils. When core or rotary methods are employed this range may be extended to 1000 ft in depth. The drill is truck mounted for rapid, low cost mobilization to the jobsite and on the jobsite.

The CME-55 owned by this firm is powered by a 300 cubic inch, 6-cylinder Ford industrial engine that produces 124 horsepower. This energy is transmitted through a rugged mechanical drive that provides 7,000 ft-lbs of torque on the drillstring. Two 72 in. hydraulic cylinders develop 16,000 lbs of downward thrust and 24,000 lbs of retract force. Two hydraulic cable hoists and a mechanical cathead allow downhole sampling and testing at any depth to be accomplished with great speed and accuracy. the drill is mounted on a 1985, F-700 series Ford truck. For drilling operations the truck is stabilized with platform mounted vertical hydraulic jacks with stroke of 48 in.

The drill rig and the truck have been in service just over one year. The operation of nearly new equipment by an experienced crew allows Foree and Vann Geotechnical Inc. to complete any type of drilling job with minimum downtime and maximum efficiency.

Drilling through soil or softer rock is performed with 7 3/4 O.D., or 4 1/2 inch continuous flight auger. Carbide insert teeth are normally used on the auger bits so they can often penetrate rock or very strongly cemented soils which require blasting or very heavy equipment for excavation.

SAMPLING PROCEDURES

Dynamically driven tube samples are usually obtained at selected intervals in the borings by the ASTM D1586 procedure. In many cases, 2" O.D., 1 3/8" I.D. samplers are used to obtain the standard penetration resistance. "Undisturbed" samples of firmer soils are often obtained with 3" O.d. samplers lined with 2.42" I.D. brass rings. the driving energy is generally recorded as the number of blows of a 140 pound 30 inch free fall drop hammer required to advance the samplers in 6 inch increments. However, in stratified soils, driving resistance is sometimes recorded in 2 or 3 inch increments so that soil changes and the presence of scattered gravel or cemented layers can be readily detected and the realistic penetration values obtained for consideration in design. These values are expressed in blows per foot on the logs. "Undisturbed" sampling of softer soil is sometimes performed with thin walled Shelby tubes (ASTM D1587). where samples of rock are required, they are obtained by NX diamond core drilling (ASTM D2113). Tube samples are labeled and placed in watertight containers to maintain field moisture contents for testing. When necessary for testing, larger bulk samples are taken from auger cuttings.

CONTINUOUS PENETRATION TESTS

Continuous penetration tests are performed by driving a 2" O.D. blunt nosed penetrometer adjacent to or in the bottom of borings. The penetrometer is attached to 1 5/8" O.D. drill rods to provide clearance to minimize side friction so that penetration values are as nearly as possible a measure of end resistance. Penetration values are recorded as the number of blows of a 140 pound 30 inch free fall drop hammer required to advance the penetrometer in one foot increments or less.

As an alternate, Cone Penetration Testing soundings may be utilized in an effort to determine the point capacity of the cone tip, and skin friction measured on the cone sleeve.

BORING RECORDS

Drilling operations are directed by our field engineer or geologist who examines soil recovery and prepared boring logs. soils are visually classified in accordance with the Unified Soil Classification System (ASTM D2487) with appropriate group symbols being shown on the logs.

APPENDIX C

LABORATORY RESILIENT MODULUD DATA

OF ASPHALT CONCRETE CORES

TABLE C-1. LABORATORY RESILIENT MODULI OF ASPHALT CONCRETE SAMPLES AT 41F

| Site/ Station/ Sample no. | Height (in) | Inst. res. mod. pos.1 (ksi) | Inst. res. mod. pos.2 (ksi) | Total res. mod. pos.1 (ksi) | Total res. mod. pos.2 (ksi) | Avg. inst. res. mod. (ksi) | Avg. total res. mod. (ksi) |
|------------------------------------|----------------|---|---|---|---|--|--|
| 1/1/1 | 2.410 | -- | 1223 | | 1062 | 1223 | 1062 |
| 2/1/1 | 2.316 | 3653 | 2436 | 2436 | 1827 | 3045 | 2131 |
| 2/1/2 | 2.008 | 2928 | 3294 | 2635 | 2774 | 3111 | 2705 |
| 3/1/1 | 2.538 | 2076 | 4508 | 1683 | 3381 | 3292 | 2532 |
| 3/1/2 | 2.391 | 758 | 1376 | 607 | 1214 | 1067 | 910 |
| 3/7/1 | 2.470 | 6121 | 4633 | 4894 | 3241 | 5377 | 4067 |
| 4/1/1 | 2.393 | 3640 | 3637 | 2502 | 2357 | 3638 | 2430 |
| 4/1/2 | 2.391 | 2948 | 5084 | 1876 | 1937 | 4016 | 1906 |
| 5/4/1 | 1.569 | 2376 | 2516 | 2079 | 1793 | 2446 | 1936 |
| 5/4/2 | 1.574 | 1496 | 1297 | 1210 | 1178 | 1397 | 1194 |
| 6/1/1 | 2.514 | 1422 | 2844 | 1207 | 1593 | 2133 | 1400 |
| 6/1/2 | 2.136 | 1886 | 1864 | 321 | 1286 | 1875 | 804 |
| 6/1/3 | 1.826 | 1371 | 1382 | 945 | 1009 | 1376 | 977 |
| 7/4/2 | 2.215 | 1569 | 3099 | 1443 | 2146 | 2334 | 1794 |
| 8/1/1 | 2.381 | 628 | 1523 | 576 | 1066 | 1075 | 821 |
| 8/1/2 | 2.499 | 1563 | 1451 | 1129 | 1195 | 1507 | 1162 |
| 9/1/1 | 2.128 | 714 | 3002 | 497 | 1876 | 1858 | 1186 |
| 9/1/2 | 2.107 | 3959 | 3174 | 3394 | 2497 | 3567 | 2945 |
| 10/4/2 | 2.641 | 2325 | 3384 | 1533 | 2901 | 2855 | 2217 |
| 11/5/1 | 1.841 | 2827 | 4726 | 2121 | 3753 | 3776 | 2937 |
| 12/1/1 | 1.839 | 1814 | 2722 | 1183 | 1944 | 2268 | 1564 |
| 12/1/2 | 2.413 | 2963 | 6914 | 2183 | 2963 | 4939 | 2573 |
| 13/1/1 | 2.160 | 4075 | 3481 | 3398 | 2964 | 3778 | 3181 |
| 13/4/1 | 2.434 | 2381 | 2559 | 2123 | 2111 | 2470 | 2117 |
| 14/4/1 | 2.119 | 1153 | 1157 | 880 | 959 | 1155 | 920 |
| 15/4/1 | 2.585 | 3165 | 2593 | 2086 | 1652 | 2879 | 1869 |
| 15/4/2 | 1.944 | 3117 | 2731 | 2350 | 2080 | 2924 | 2215 |
| 16/1/1 | 2.341 | 3016 | 2970 | 2561 | 2617 | 2993 | 2589 |
| 17/1/1 | 2.025 | 1373 | 1481 | 1187 | 1110 | 1427 | 1148 |
| 18/1/1 | 2.368 | 2271 | 2901 | 1870 | 2684 | 2586 | 2277 |
| 19/4/1 | 2.454 | 1272 | 1358 | 1148 | 1204 | 1315 | 1176 |
| 19/4/2 | 2.293 | 749 | 1151 | 664 | 1020 | 950 | 842 |
| 20/1/1 | 2.016 | 3901 | 2464 | 3467 | 2104 | 3182 | 2786 |
| 20/1/2 | 2.337 | 3365 | 6335 | 2991 | 5051 | 4850 | 4021 |

APPENDIX D
LABORATORY RESILIENT MODULUS DATA
OF SUBGRADE MATERIALS

TABLE D-1

| Site/ Station | Sample Depth (in.) | Dry Density (pcf) | Water Content (%) | Confining Pressure (kPa) | Deviator Stress (kPa) | Resilient Modulus (MPa) | Resilient Modulus (ksi) |
|------------------|--------------------------|-------------------------|-------------------------|--------------------------------|-----------------------------|-------------------------------|-------------------------------|
| 1/1 | 25-32 | 122.1 | 5.28 | 14 | 93 | 75.2 | 10.9 |
| | | | | 22 | 56 | 69.35 | 10.05 |
| | | | | 31 | 28 | 98 | 14.2 |
| | | | | 14 | 50 | 59 | 8.55 |
| | | | | 22 | 26 | 72.1 | 10.45 |
| | | | | 14 | 18 | 57.95 | 8.4 |
| 2/1 | 19-25 | 118.6 | 7.09 | 17 | 69 | 80.7 | 11.7 |
| | | | | 23 | 48 | 83.1 | 12.05 |
| | | | | 30 | 22 | 111.8 | 16.2 |
| | | | | 17 | 45 | 81.4 | 11.8 |
| | | | | 20 | 31 | 85.6 | 12.4 |
| | | | | 23 | 18 | 109.7 | 15.9 |
| 2/7 | 38-45 | 111.6 | 7.83 | 23 | 27 | 89.7 | 13 |
| | | | | 21 | 20 | 116.6 | 16.9 |
| | | | | 20 | 38 | 92.5 | 13.4 |
| | | | | 27 | 18 | 129.4 | 18.75 |
| 3/7 | 27-34 | 112.4 | 12.4 | 14 | 86 | 39 | 5.65 |
| | | | | 22 | 53 | 40 | 5.8 |
| | | | | 31 | 26 | 64.2 | 9.3 |
| | | | | 14 | 46 | 36.9 | 5.35 |
| | | | | 22 | 24 | 47.6 | 6.9 |
| | | | | 14 | 18 | 39 | 5.65 |
| 4/1 | 25-32 | 111.8 | 10.4 | 24 | 84 | 59 | 8.55 |
| | | | | 32 | 55 | 65.9 | 9.55 |
| | | | | 41 | 23 | 82.8 | 12 |
| | | | | 21 | 50 | 55.2 | 8 |
| | | | | 31 | 24 | 65.9 | 9.55 |
| | | | | 17 | 31 | 54.5 | 7.9 |
| | | | | 17 | 21 | 64.2 | 9.3 |
| | | | | 22 | 20 | 68.3 | 9.9 |
| | 40 | 86 | 79.7 | 11.55 | | | |

TABLE D-1 (CONT.)

| Site/ Station | Sample Depth (in.) | Dry Density (pcf) | Water Content (%) | Confining Pressure (kPa) | Deviator Stress (kPa) | Resilient Modulus (MPa) | Resilient Modulus (ksi) |
|------------------|--------------------------|-------------------------|-------------------------|--------------------------------|-----------------------------|-------------------------------|-------------------------------|
| 5/4 | 20-27 | 119.9 | 12.4 | 20 | 62 | 58 | 8.4 |
| | | | | 27 | 39 | 85.9 | 12.45 |
| | | | | 33 | 21 | 99.7 | 14.45 |
| | | | | 20 | 38 | 74.2 | 10.75 |
| | | | | 25 | 21 | 96.3 | 13.95 |
| | | | | 20 | 19 | 104.5 | 15.15 |
| | | | | 20 | 39 | 70.4 | 10.2 |
| 7/1 | 27-34 | 118.1 | 10.6 | 20 | 75 | 64.8 | 9.4 |
| | | | | 15 | 45 | 53.1 | 7.7 |
| | | | | 27 | 45 | 68.4 | 9.9 |
| | | | | 35 | 19 | 122.9 | 17.8 |
| | | | | 25 | 19 | 111.1 | 16.1 |
| | | | | 15 | 19 | 74.95 | 10.85 |
| 7/4 | 27-34 | 120 | 9.03 | 21 | 77 | 71.7 | 10.4 |
| | | | | 77 | 48 | 76.5 | 11.1 |
| | | | | 35 | 21 | 112.4 | 16.3 |
| | | | | 15 | 48 | 56.9 | 8.25 |
| | | | | 26 | 21 | 87.9 | 12.75 |
| | | | | 16 | 19 | 64.5 | 9.35 |
| 8/1 | 31-38 | 112.8 | 11.1 | 21 | 47 | 48.3 | 7 |
| | | | | 25 | 35 | 58.3 | 8.45 |
| | | | | 29 | 19 | 61.4 | 8.9 |
| | | | | 21 | 19 | 48.3 | 7 |
| | | | | 21 | 29 | 53.1 | 7.7 |
| | | | | 26 | 19 | 61.4 | 8.9 |
| 9/1 | 50-57 | 104.2 | 22.8 | 26 | 71 | 103.5 | 15 |
| | | | | 31 | 42 | 106.95 | 15.5 |
| | | | | 26 | 30 | 112.5 | 16.3 |
| | | | | 26 | 19 | 109.4 | 15.85 |
| | | | | 31 | 19 | 124.5 | 18.05 |
| 10/4 | 44-51 | 97 | 25.9 | 25 | 49 | 73.5 | 10.65 |
| | | | | 29 | 33 | 81.8 | 11.85 |
| | | | | 33 | 21 | 88 | 12.7 |
| | | | | 25 | 31 | 84.2 | 12.2 |
| | | | | 29 | 21 | 97.3 | 14.1 |
| | | | | 25 | 22 | 92.1 | 13.35 |

TABLE D-1 (CONT.)

| Site/ Station | Sample Depth (in.) | Dry Density (pcf) | Water Content (%) | Confining Pressure (kPa) | Deviator Stress (kPa) | Resilient Modulus (MPa) | Resilient Modulus (ksi) |
|------------------|--------------------------|-------------------------|-------------------------|--------------------------------|-----------------------------|-------------------------------|-------------------------------|
| 11/1 | 12-19 | 122.8 | 2.21 | 31 | 80 | 94.5 | 13.7 |
| | | | | 37 | 55 | 97.3 | 14.1 |
| | | | | 48 | 23 | 123.9 | 17.95 |
| | | | | 26 | 57 | 90 | 13.05 |
| | | | | 34 | 25 | 92.5 | 13.4 |
| | | | | 20 | 30 | 77.6 | 11.25 |
| | | | | 24 | 19 | 90 | 13.05 |
| | | | | 16 | 19 | 70 | 10.15 |
| 12/1 | 32-39 | 120.3 | 8.56 | 15 | 58 | 46.6 | 67.5 |
| | | | | 16 | 49 | 50 | 7.25 |
| | | | | 21 | 31 | 50.7 | 7.35 |
| | | | | 21 | 18 | 48.6 | 7.05 |
| | | | | 25 | 19 | 59.7 | 8.65 |
| 13/4 | 13-20 | 110.4 | 8.81 | 15 | 65 | 97.3 | 14.1 |
| | | | | 20 | 46 | 100.4 | 14.55 |
| | | | | 25 | 31 | 123.9 | 17.95 |
| | | | | 18 | 33 | 91.4 | 13.25 |
| | | | | 13 | 55 | 90 | 13.05 |
| | | | | 22 | 20 | 108.7 | 15.75 |
| | | | | 12 | 31 | 81.4 | 11.8 |
| 14/4 | 12-19 | 101.7 | 15.4 | 12 | 58 | 82.5 | 11.95 |
| | | | | 17 | 42 | 88.7 | 12.85 |
| | | | | 22 | 22 | 82.1 | 11.9 |
| | | | | 11 | 40 | 65.6 | 9.5 |
| | | | | 16 | 21 | 64.9 | 9.4 |
| | | | | 9 | 19 | 47.6 | 6.9 |
| 16/1 | 17-24 | 117.7 | 7.9 | 15 | 61 | 61.55 | 8.9 |
| | | | | 20 | 40 | 64.35 | 9.35 |
| | | | | 25 | 26 | 73.75 | 10.7 |
| | | | | 13 | 52 | 56.65 | 8.2 |
| | | | | 18 | 31 | 63.64 | 9.25 |
| | | | | 22 | 20 | 88.85 | 12.85 |
| | | | | 12 | 29 | 54.1 | 7.85 |

TABLE D-1 (CONT.)

| Site/ Station | Sample Depth (in.) | Dry Density (pcf) | Water Content (%) | Confining Pressure (kPa) | Deviator Stress (kPa) | Resilient Modulus (MPa) | Resilient Modulus (ksi) |
|------------------|--------------------------|-------------------------|-------------------------|--------------------------------|-----------------------------|-------------------------------|-------------------------------|
| 17/1 | 20-26 | 104.9 | 17.8 | 15 | 57 | 28.85 | 4.2 |
| | | | | 25 | 21 | 43.65 | 6.35 |
| | | | | 17 | 43 | 28.35 | 4.1 |
| | | | | 20 | 31 | 33.05 | 4.8 |
| | | | | 20 | 20 | 37.4 | 5.4 |
| | | | | 12 | 26 | 27.9 | 4.05 |
| 19/1 | 23-30 | 104.2 | 22.7 | 15 | 55 | 66.15 | 9.6 |
| | | | | 27 | 20 | 98.7 | 14.3 |
| | | | | 17 | 41 | 73.1 | 10.6 |
| | | | | 20 | 29 | 81.6 | 11.8 |
| | | | | 20 | 20 | 94.8 | 13.75 |
| 19/4 | 31-38 | 96.3 | 28.9 | 15 | 53 | 111.4 | 16.15 |
| | | | | 27 | 19 | 113.8 | 16.5 |
| | | | | 17 | 39 | 90.05 | 13.05 |
| | | | | 20 | 29 | 106 | 15.2 |
| | | | | 15 | 28 | 119.2 | 17.3 |

APPENDIX E

DISCUSSION OF STRESS STATE

Since the subgrade materials are generally stress dependent, the resilient modulus varies at different stress states.

The moduli of the materials in the lab were determined at different confining pressures (σ_3) and deviator stresses ($\sigma_1 - \sigma_3$). In order to determine the specific modulus in the lab that corresponds to the in-situ condition, the state of stress of the sample in the lab has to match that in the field. For this purpose both octahedral normal stress and octahedral shear stress in the lab should be the same as those in the field. The octahedral normal and shear stresses (σ_{oct} and τ_{oct}) are defined as follows:

$$\sigma_{\text{oct}} = \frac{1}{3} (\sigma_1 + \sigma_2 + \sigma_3) \quad (\text{E-1})$$

$$\tau_{\text{oct}} = \frac{1}{3} \sqrt{(\sigma_1 - \sigma_2)^2 + (\sigma_1 - \sigma_3)^2 + (\sigma_2 - \sigma_3)^2} \quad (\text{E-2})$$

where σ_1 , σ_2 and σ_3 are the principal normal stresses.

To compute the octahedral normal and shear stresses in the field the Chevron multilayer elastic computer program was used (79). A standard wheel load (9000 lb) was applied at the surface of each pavement section and the stresses at the top of subgrade were computed.

For the lab triaxial conditions, $\sigma_2 = \sigma_3$ and $\sigma_d = \sigma_1 - \sigma_3$, where σ_d is the deviator stress. Therefore,

$$\sigma_{\text{oct}} = \frac{\sigma_d}{3} + \sigma_3, \text{ and} \quad (\text{E-3})$$

$$\tau_{\text{oct}} = \frac{\sqrt{2}}{3} \sigma_d \quad (\text{E-4})$$

Using Equations E-3 and E-4, σ_d and σ_3 in the lab can be computed by knowing σ_{oct} and τ_{oct} in the field.

The following figures explain the stress state conditions and some example computations:

- Figure E-1 - shows the 3-D stress space. In the upper diagram the view is down the hydrostatic axis. The lower diagram is a perspective view, showing that τ_{oct} is zero along the hydrostatic axis (H.A.).
- Figure E-2 - Shows two views of a typical failure surface for soil.
- Figure E-3 - Upper diagram shows the plane in which the triaxial stress conditions plot. The lower diagram depicts a surface which envelopes all the stress states ever imposed by traffic. Such a surface applied to only one point (depth) in the subgrade layer, of course.
- Figure E-4 - Depicts, in the octahedral plane, the desired limits for the lab testing program, which should correspond as closely as possible to the surface of maximum traffic loads shown in Figure E-3.
- Figure E-5 - Shows results an example computation of stress states for increasing wheel loads for three different depths. Results are plotted in terms of τ_{oct} and σ_{oct} for maximum generality.
- Figure E-6 - Shows a "stress triangle" (shaded) calculated for 25 inches depth as an example. The square data points show the prescribed stress states for the AASHTO Resilient Modulus test procedure. Although this is only an example, it is more or less typical, showing that the prescribed stress states for lab testing exceed the stress states due traffic loading significantly.

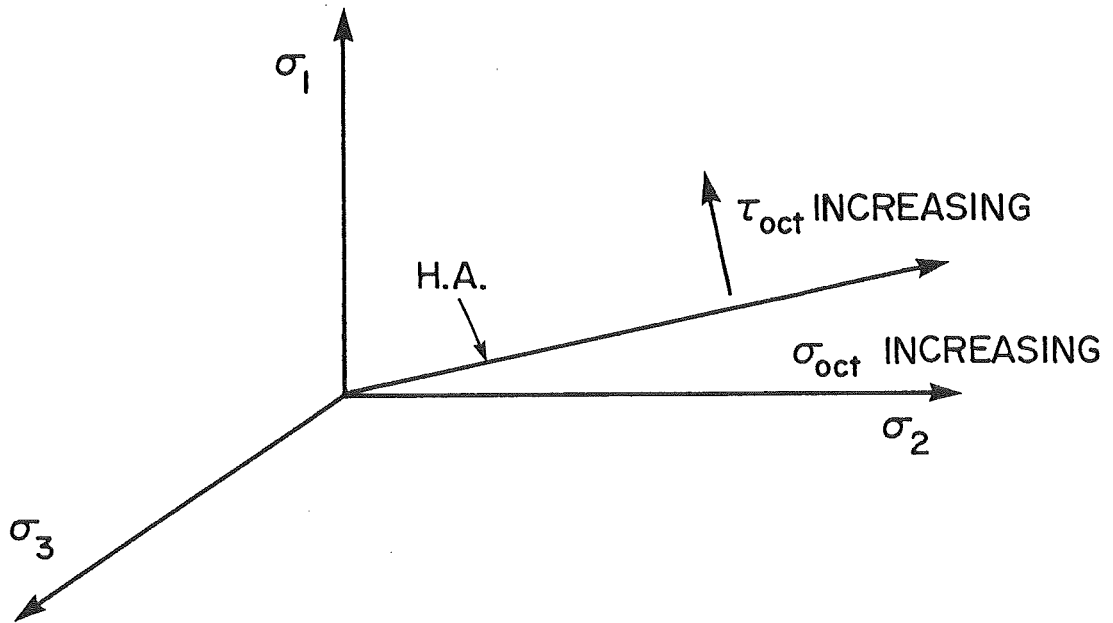
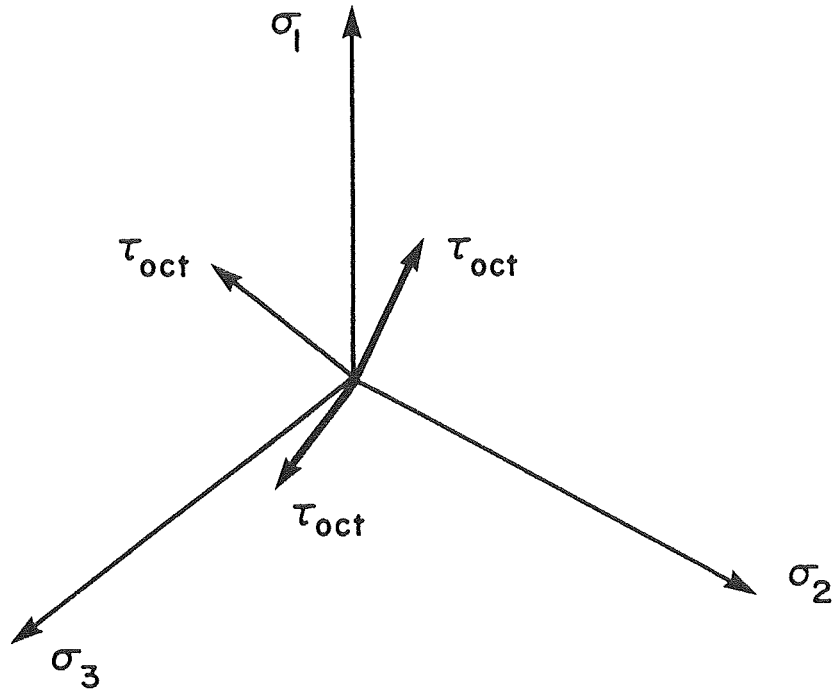


FIGURE E-1

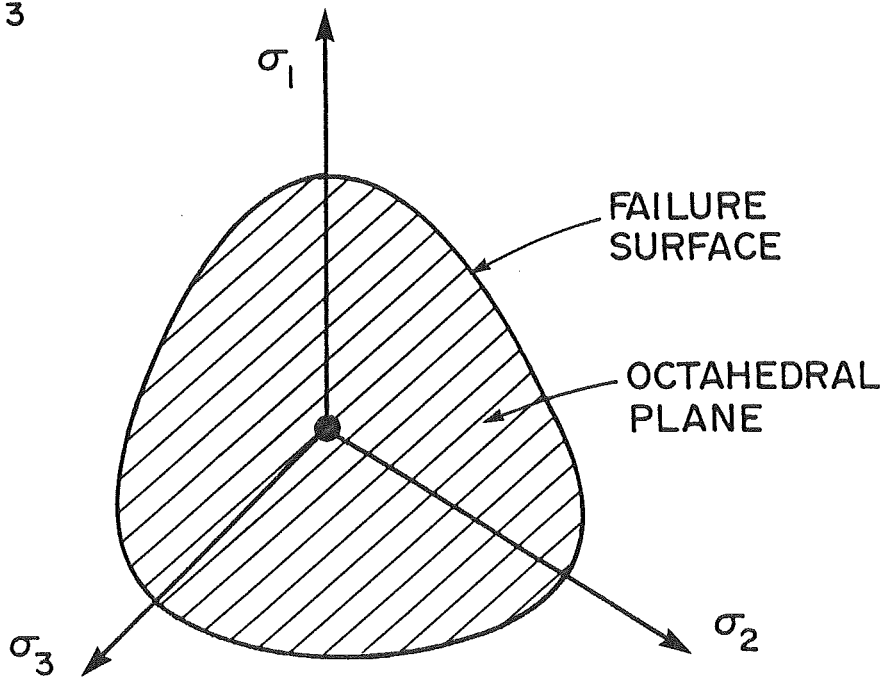
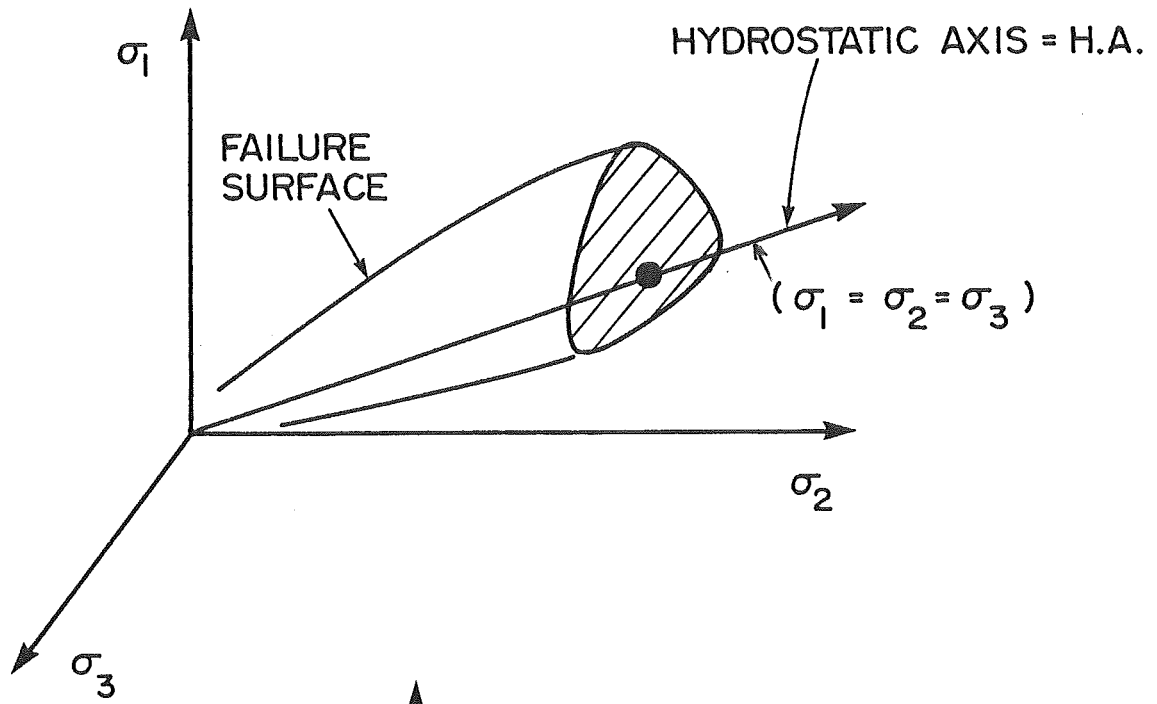


FIGURE E-2

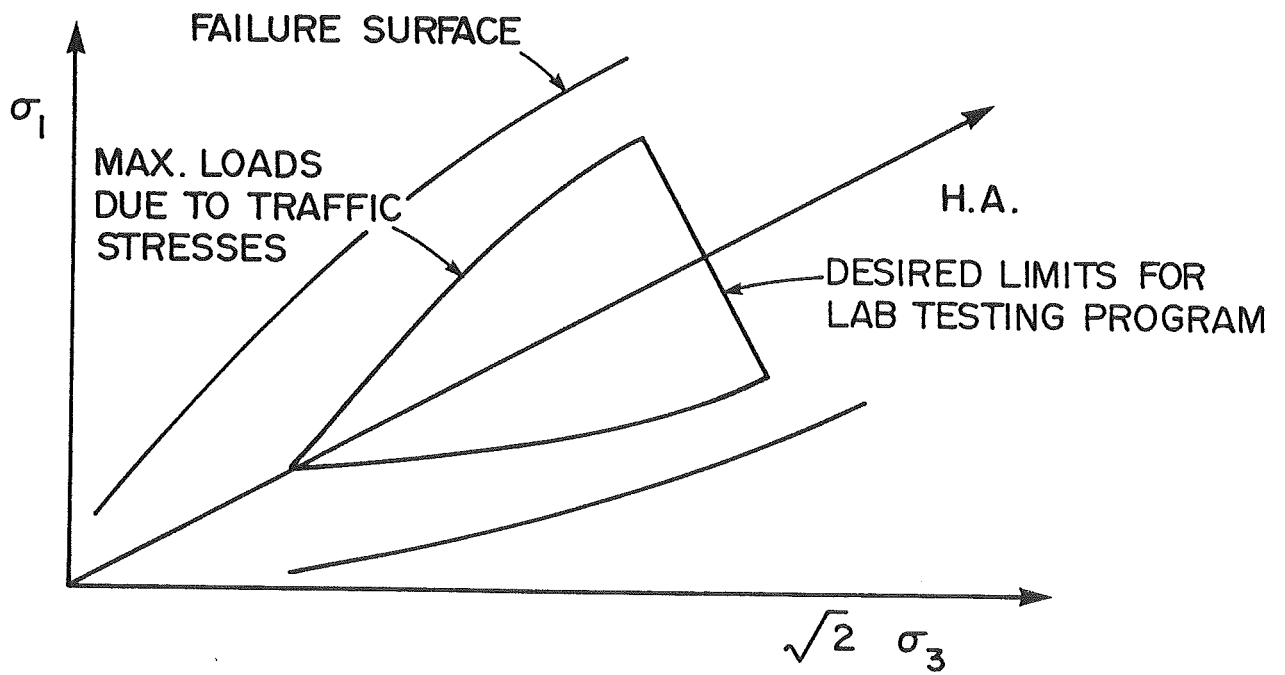
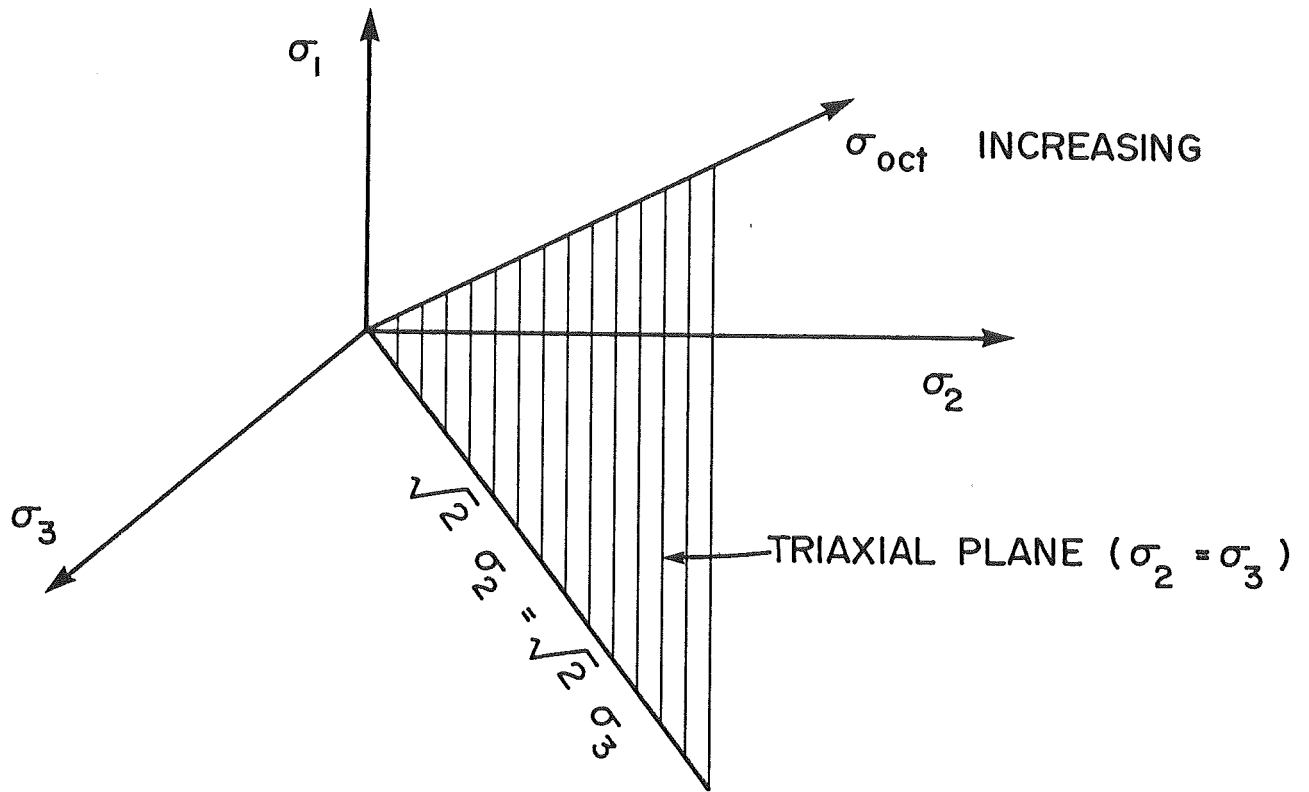


FIGURE E-3

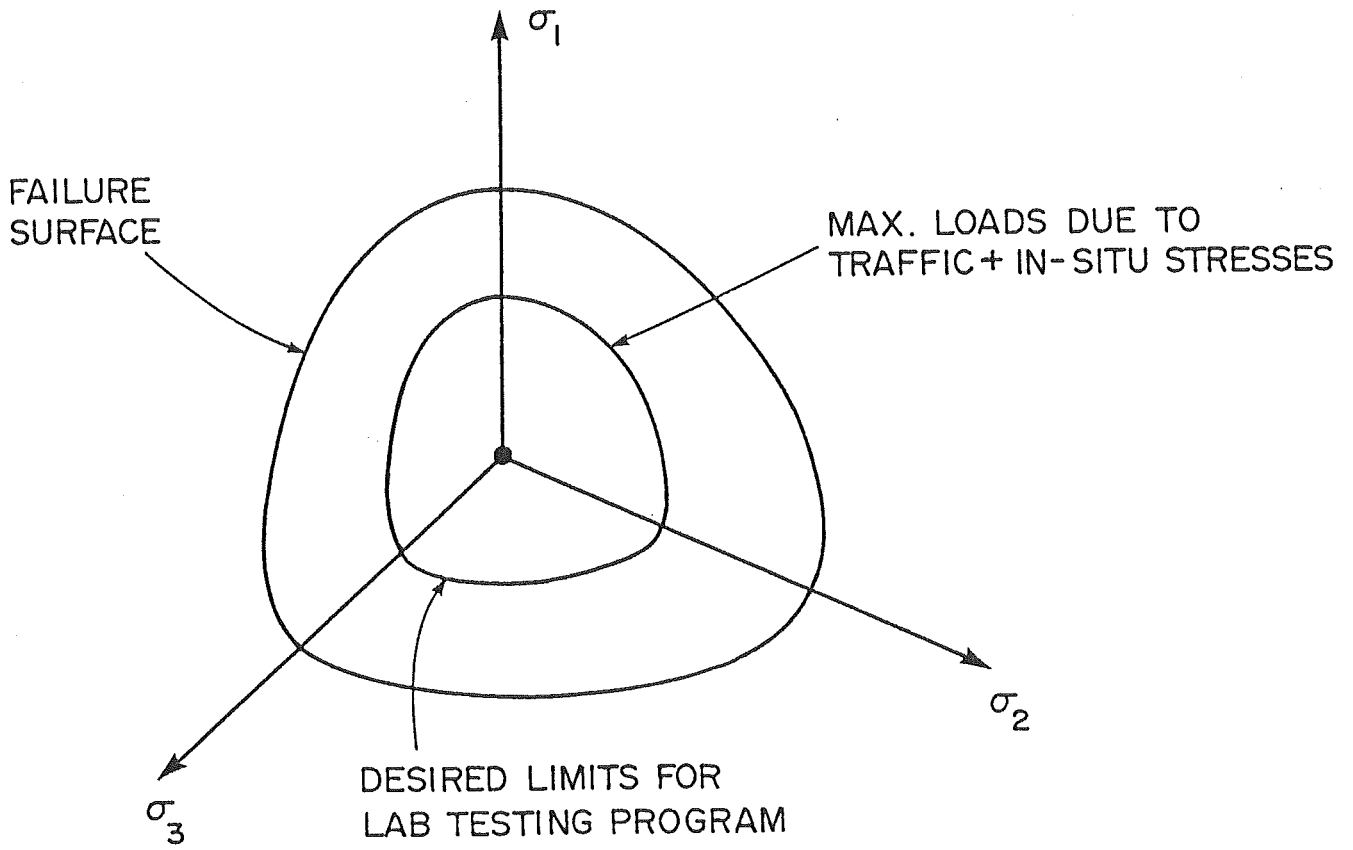


FIGURE E-4

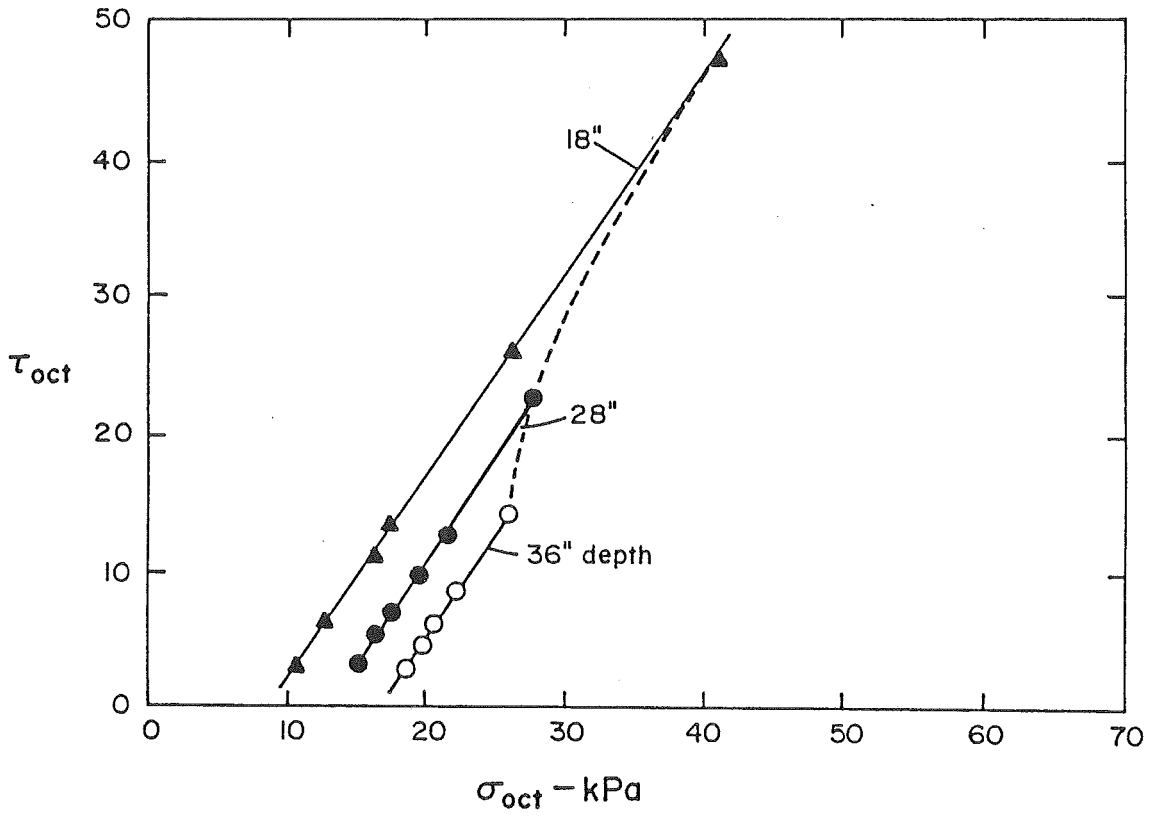


FIGURE E-5

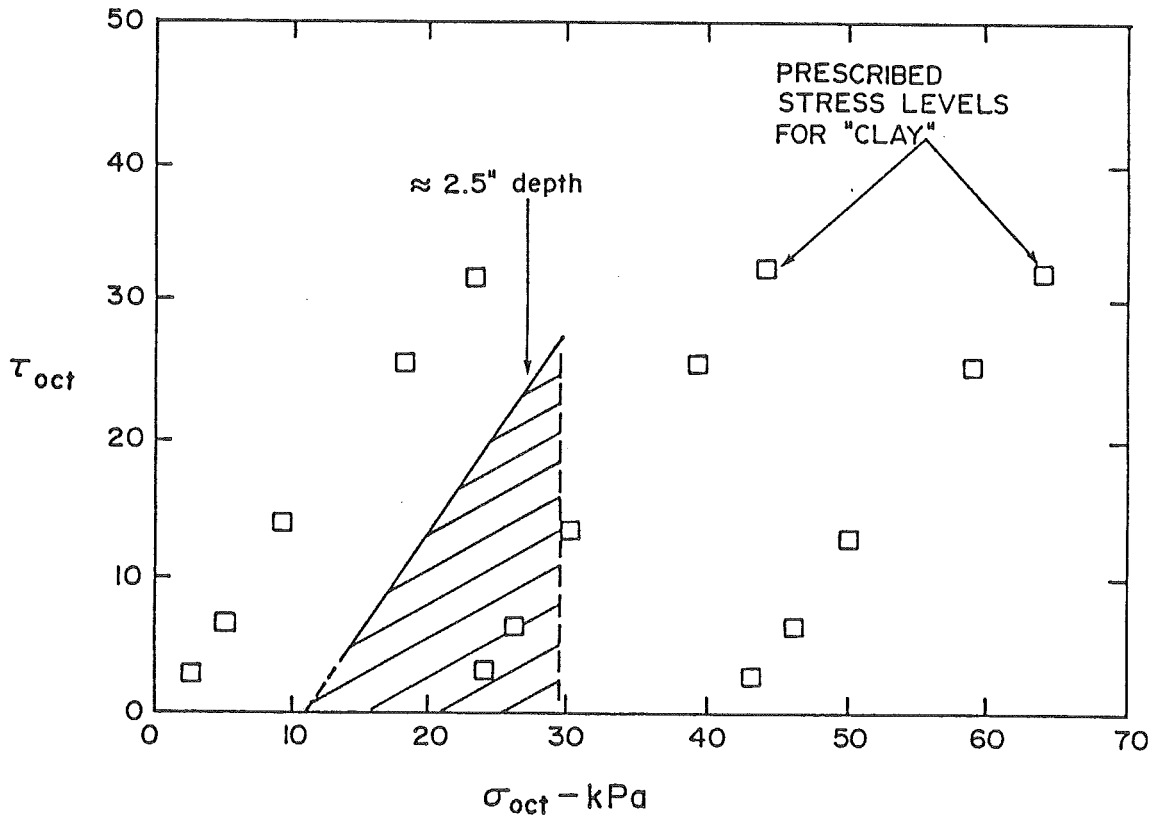


FIGURE E-6